Resolving the variable sky of gamma-rays at one Giga electron Volt with the Cherenkov-plenoscope

Sebastian Achim Mueller

Max-Planck-Institute
for Nuclear Physics

sebastian-achim.mueller@mpi-hd.mpg.de

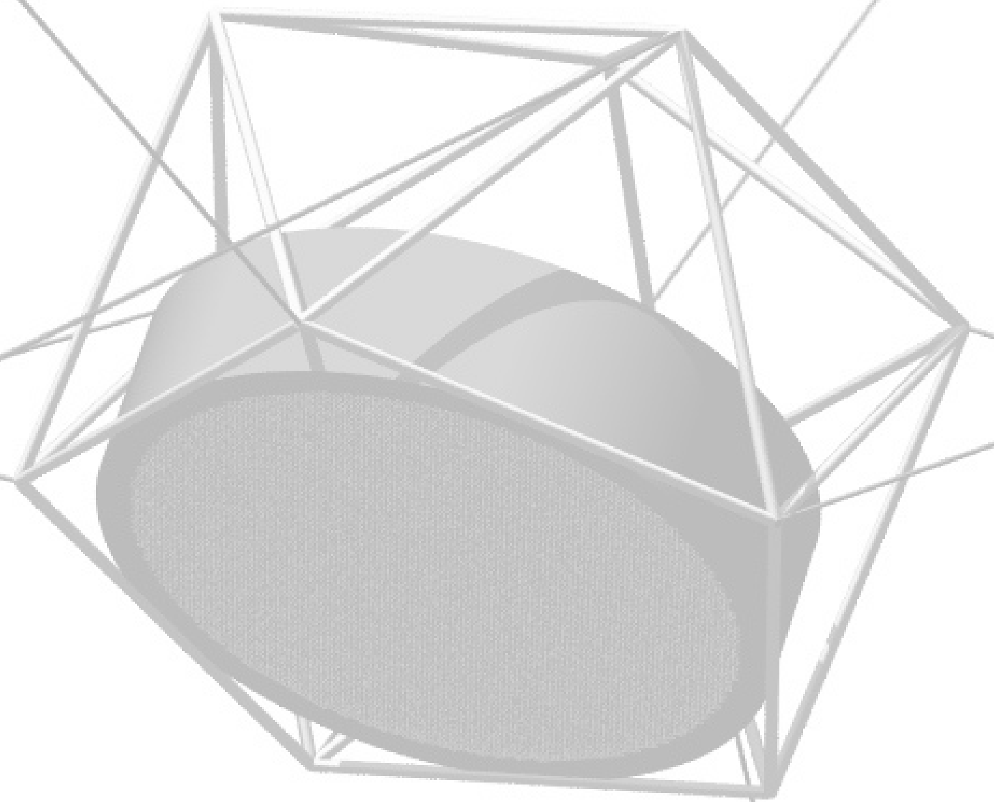

The Variable Multi-Messenger Sky

WE-Heraeus-Seminar
07 Nov - 10 Nov 2022
Cracow, Przegorzaly, Poland

Resolving variability

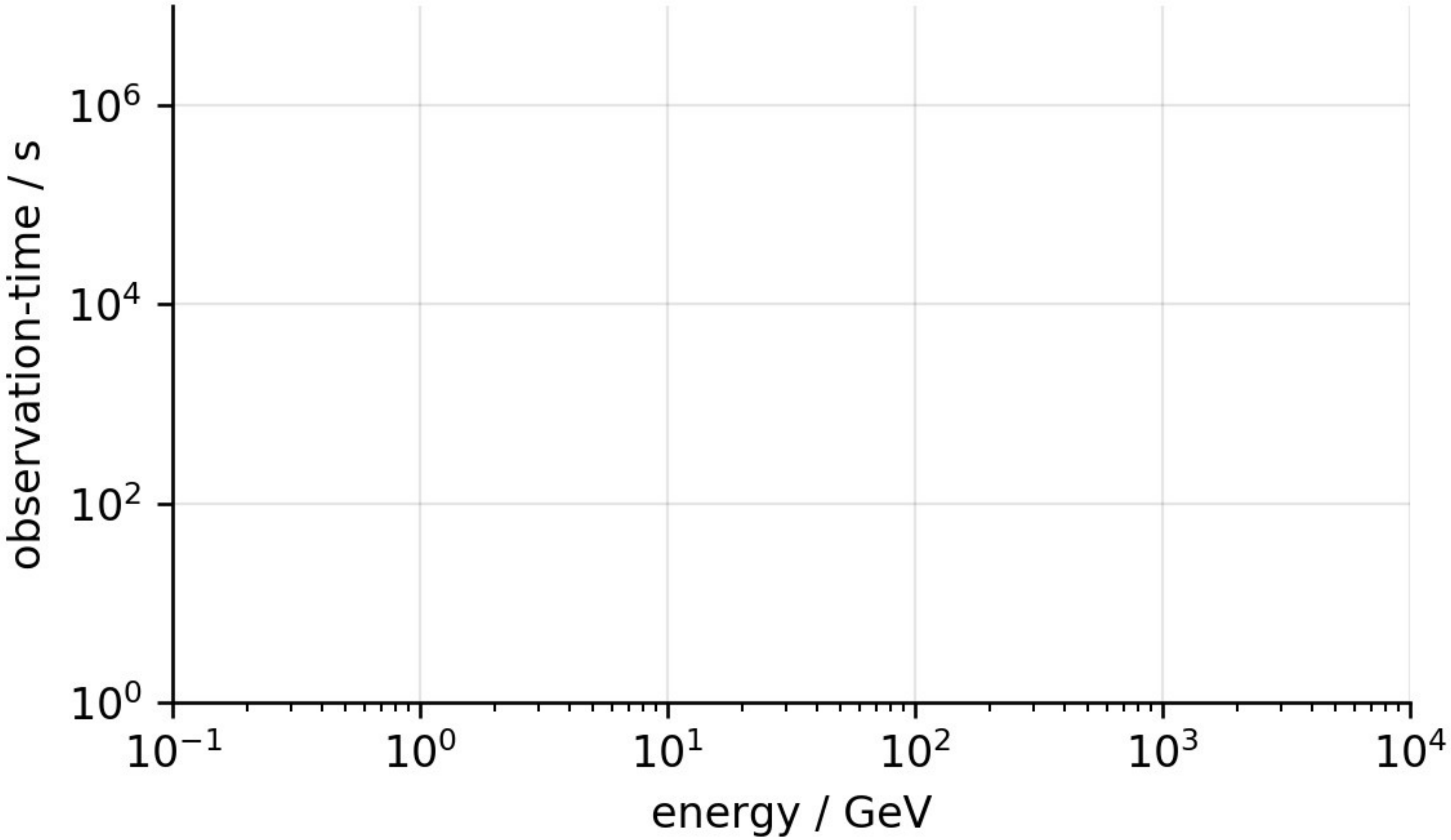

Resolving variability

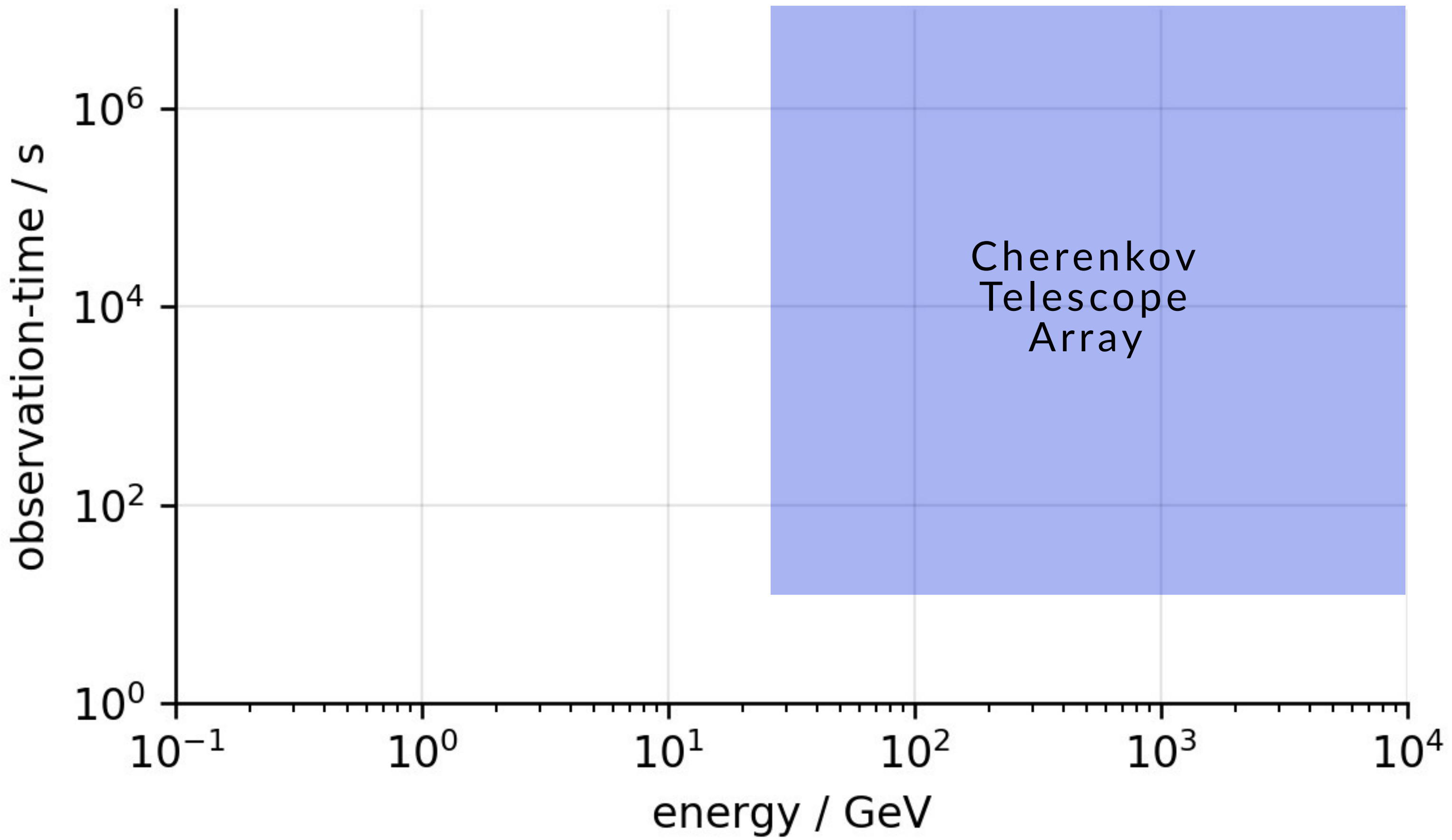

Resolving variability

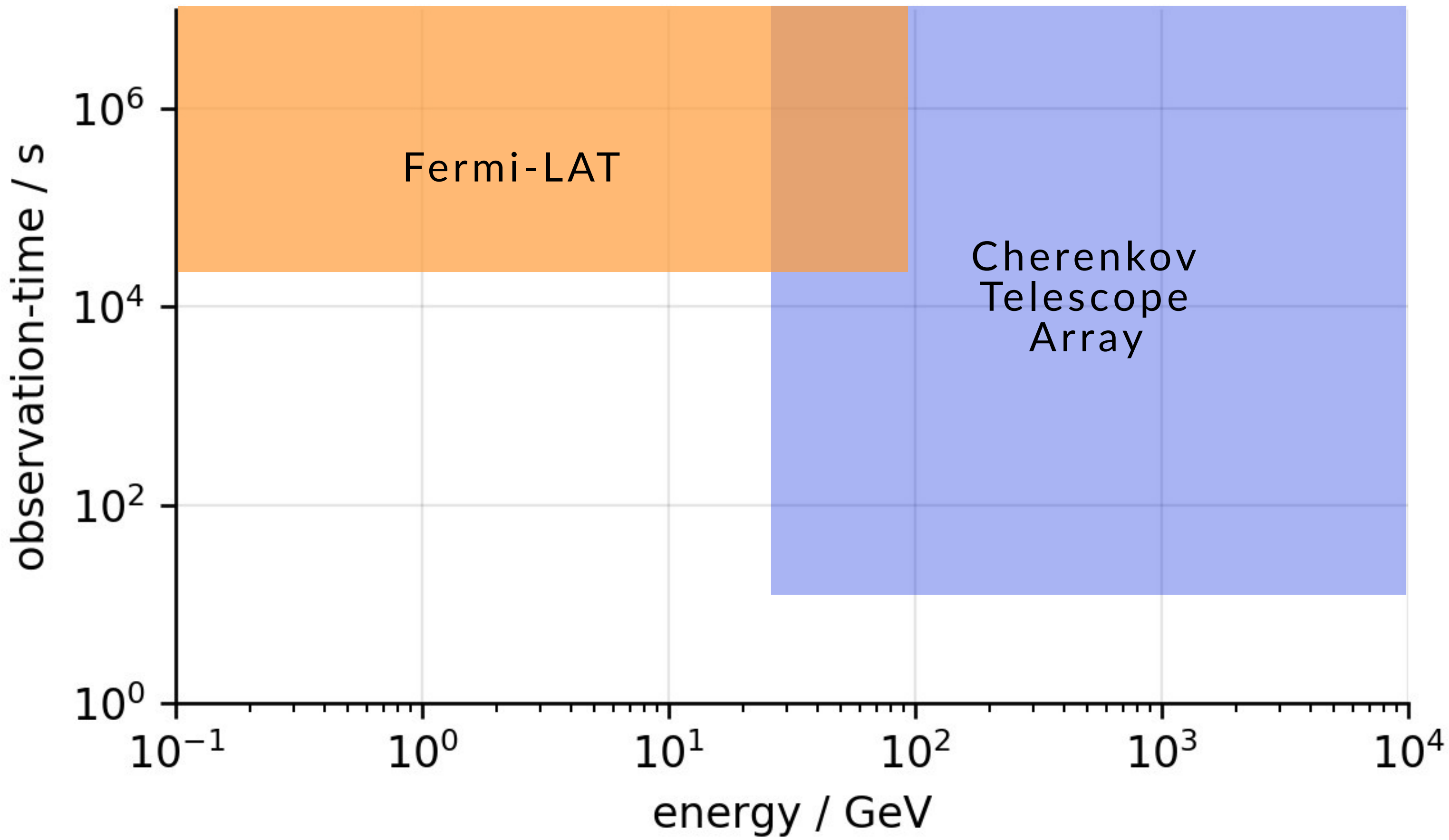

Resolving variability

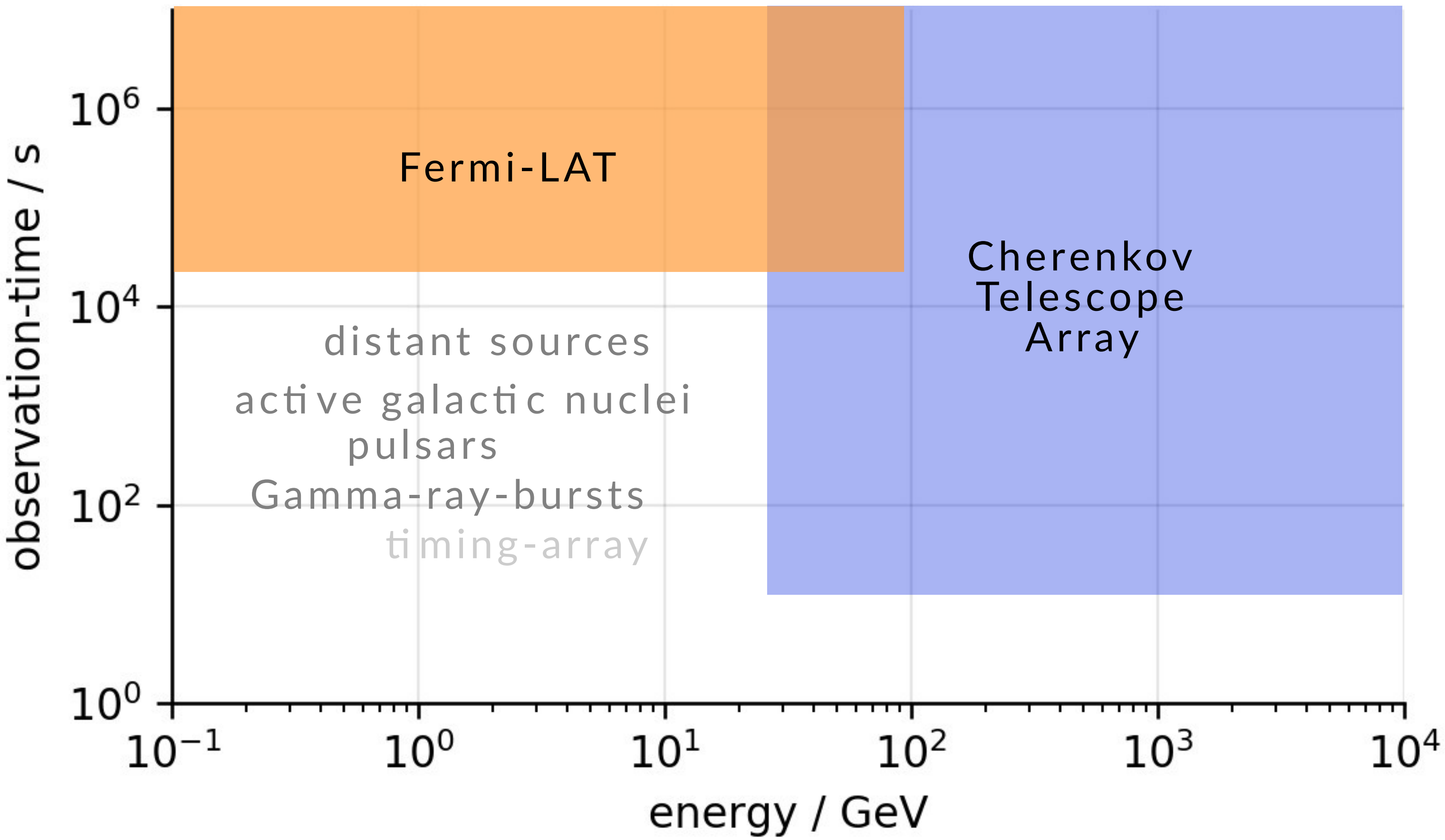

Resolving variability

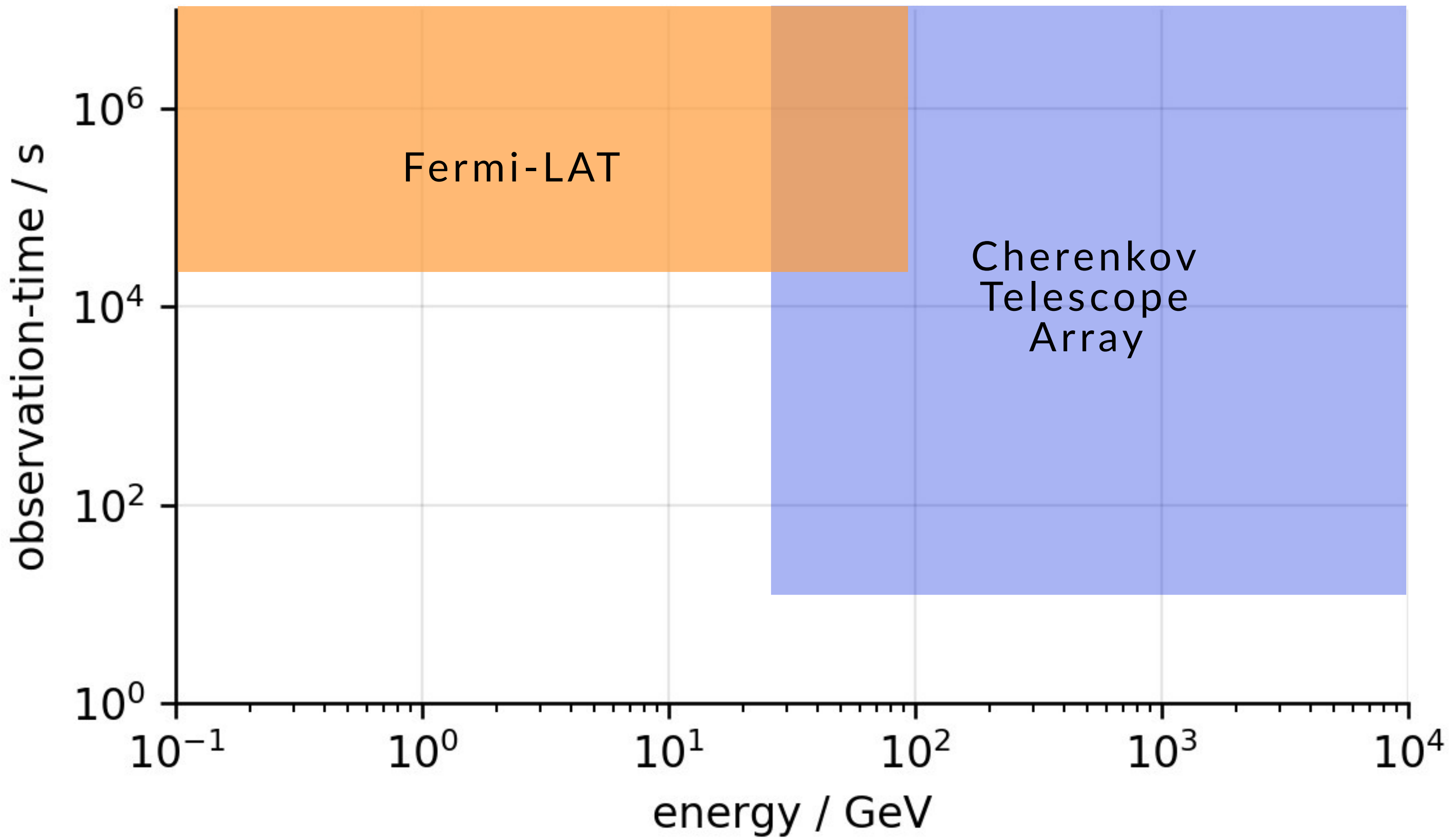

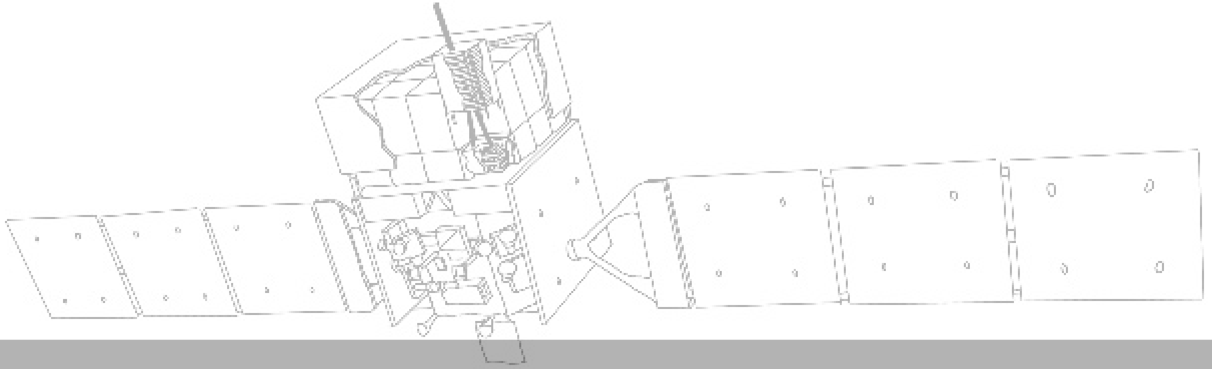

Today

Credit: https://www.mpi-hd.mpg.de/hfm/HESS/

Directly in Space

Credit: https://fermi.gsfc.nasa.gov/

Directly in Space

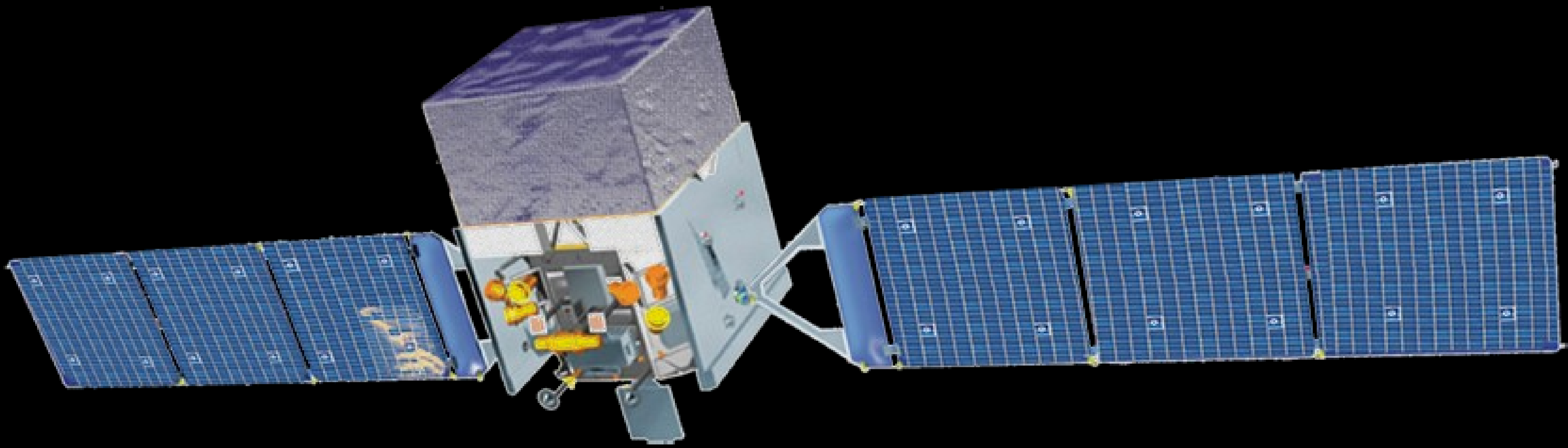

Credit: https://fermi.gsfc.nasa.gov/

Directly in Space

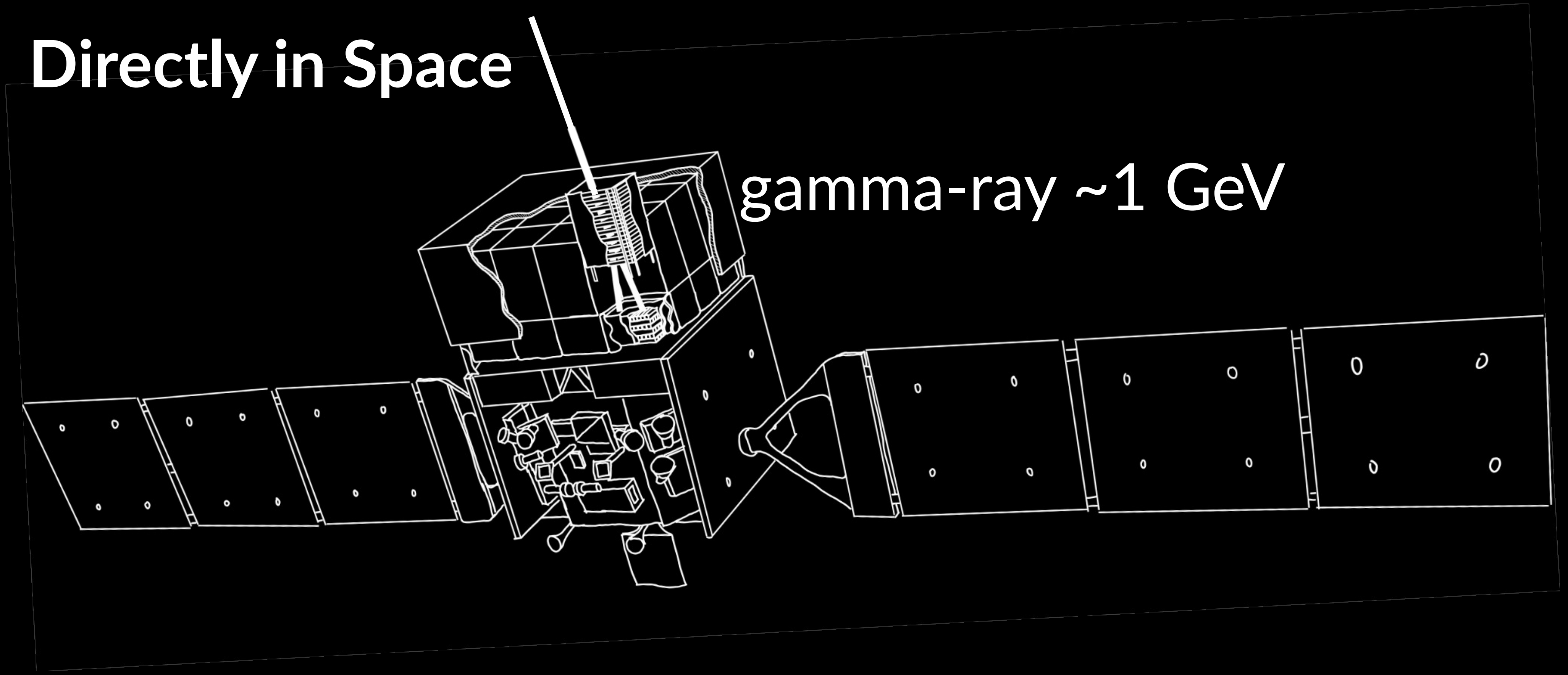

Directly in Space

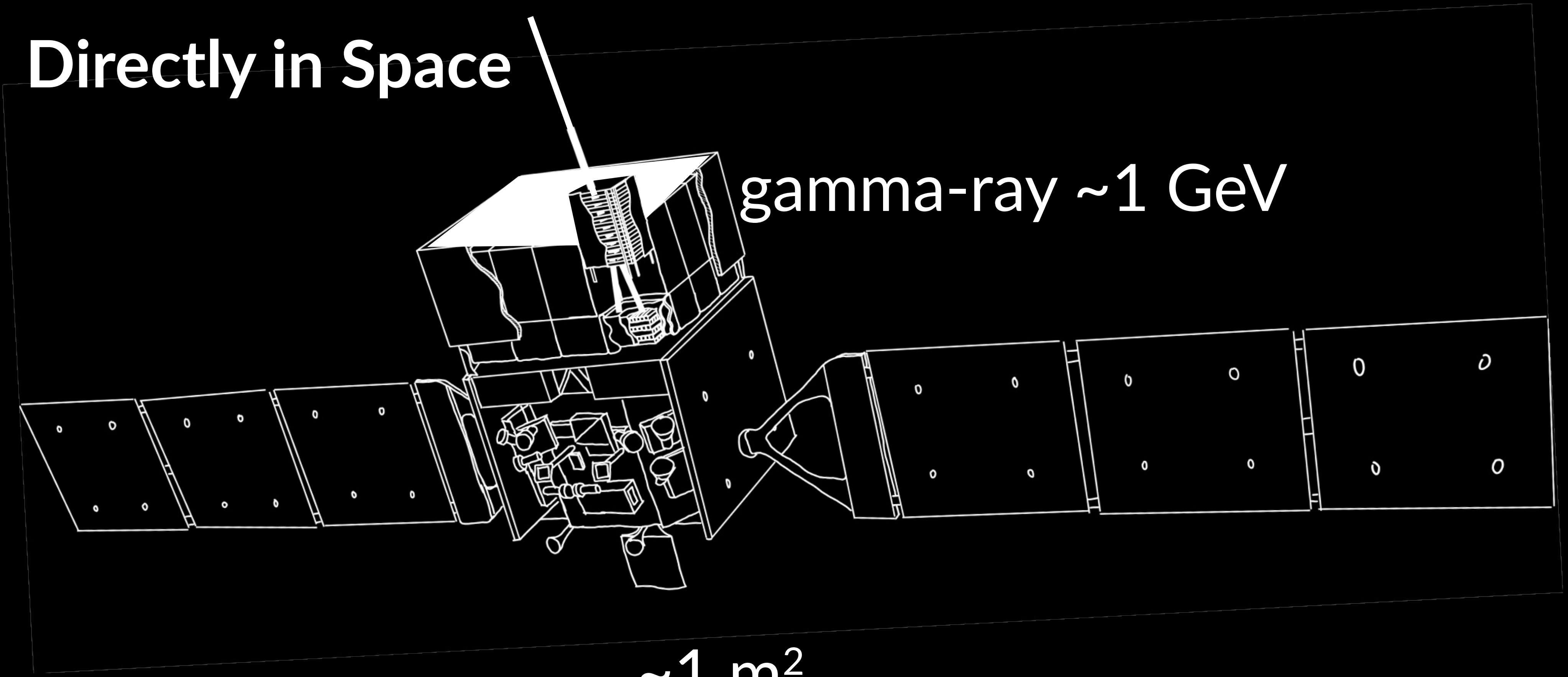

Indirectly in Atmosphere

Credit: https://www.mpi-hd.mpg.de/hfm/HESS/

Indirectly in Atmosphere

gamma-ray ~100 GeV

Credit: https://www.mpi-hd.mpg.de/hfm/HESS/

Indirectly in Atmosphere

gamma-ray ~100 GeV

Credit: https://www.mpi-hd.mpg.de/hfm/HESS/

Indirectly in Atmosphere

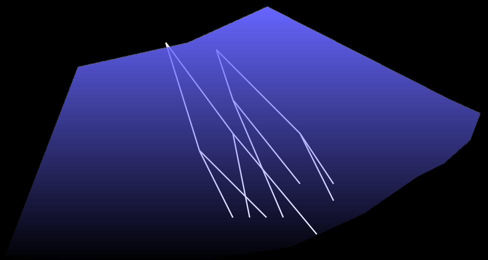

gamma-ray ~100 GeV

Credit: https://www.mpi-hd.mpg.de/hfm/HESS/

Indirectly in Atmosphere

gamma-ray ~100 GeV

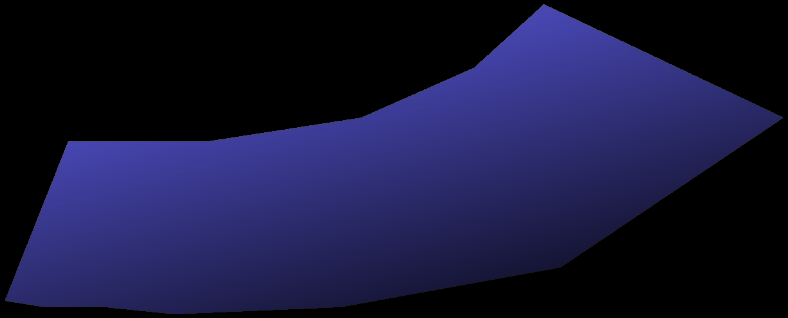

Credit: https://www.mpi-hd.mpg.de/hfm/HESS/

Indirectly in Atmosphere

gamma-ray ~100 GeV

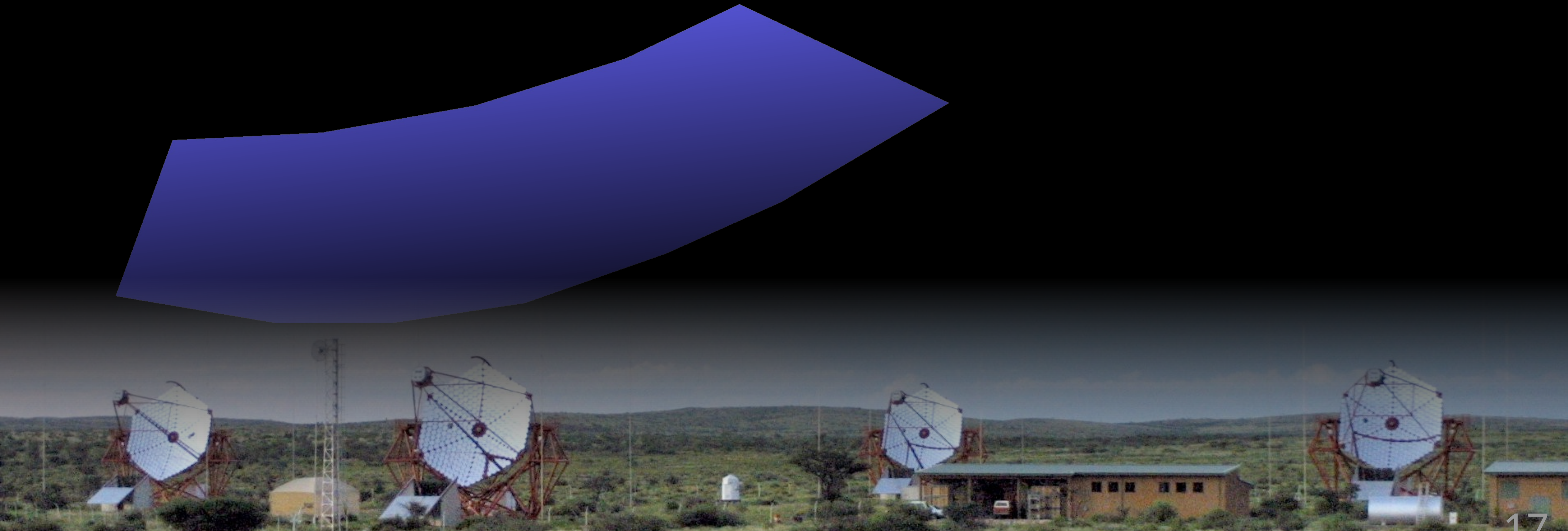

Credit: https://www.mpi-hd.mpg.de/hfm/HESS/

Indirectly in Atmosphere

gamma-ray ~100 GeV

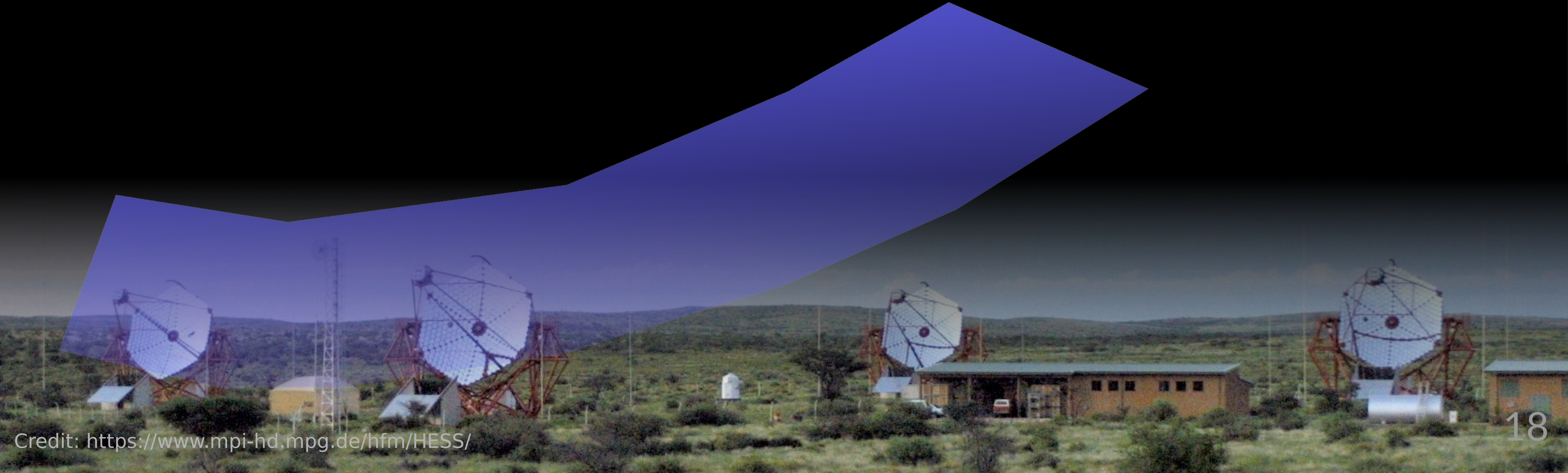

Credit: https://www.mpi-hd.mpg.de/hfm/HESS/

Indirectly in Atmosphere

gamma-ray ~100 GeV

Credit: https://www.mpi-hd.mpg.de/hfm/HESS/

Indirectly in Atmosphere

gamma-ray ~100 GeV

Credit: https://www.mpi-hd.mpg.de/hfm/HESS/

Indirectly in Atmosphere

gamma-ray ~100 GeV

Credit: https://www.mpi-hd.mpg.de/hfm/HESS/

Indirectly in Atmosphere

gamma-ray ~100 GeV

Credit: https://www.mpi-hd.mpg.de/hfm/HESS/

Indirectly in Atmosphere

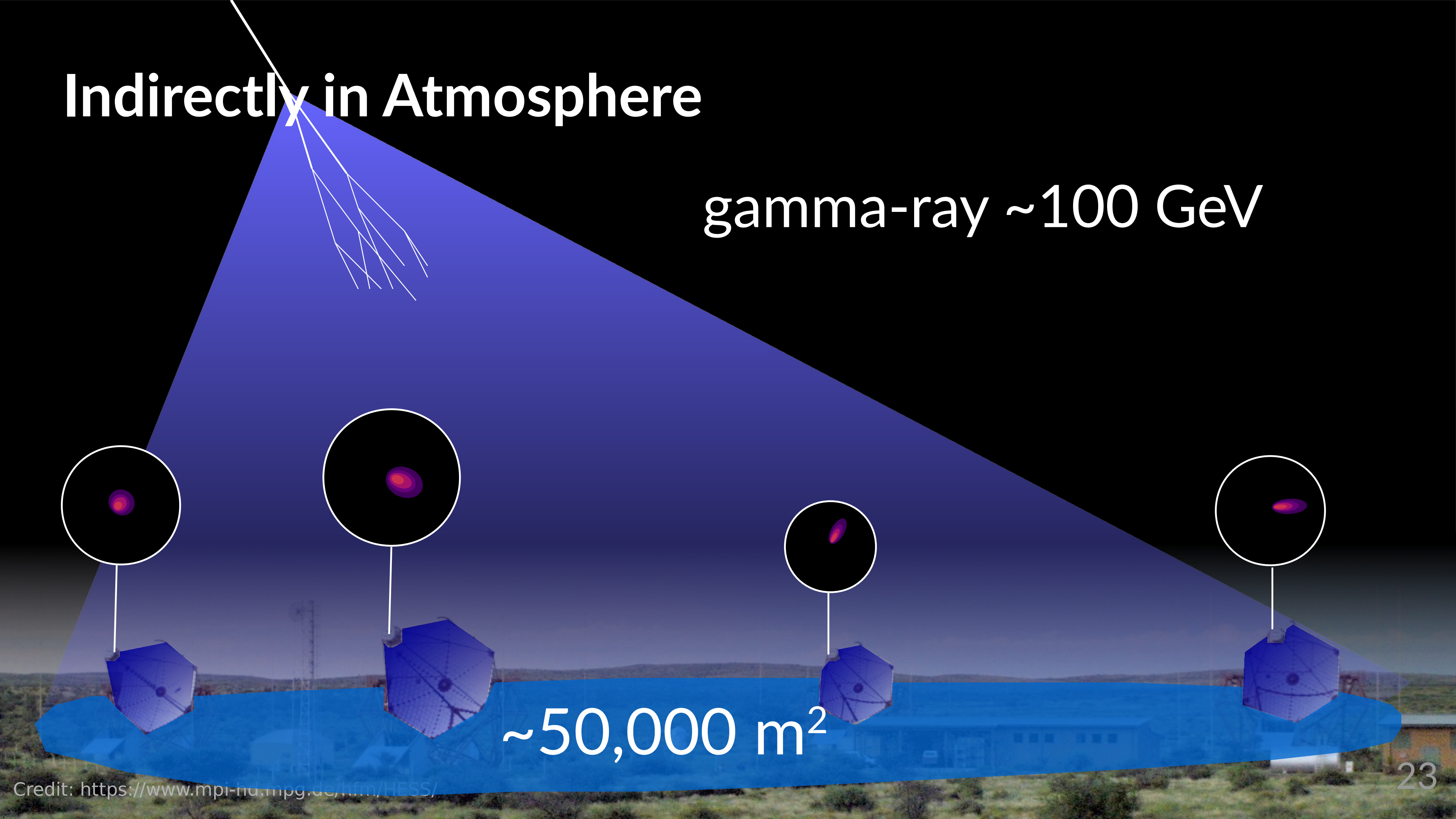

Credit: https://www.mpi-hd.mpg.de/hfm/HESS/

Indirectly in Atmosphere

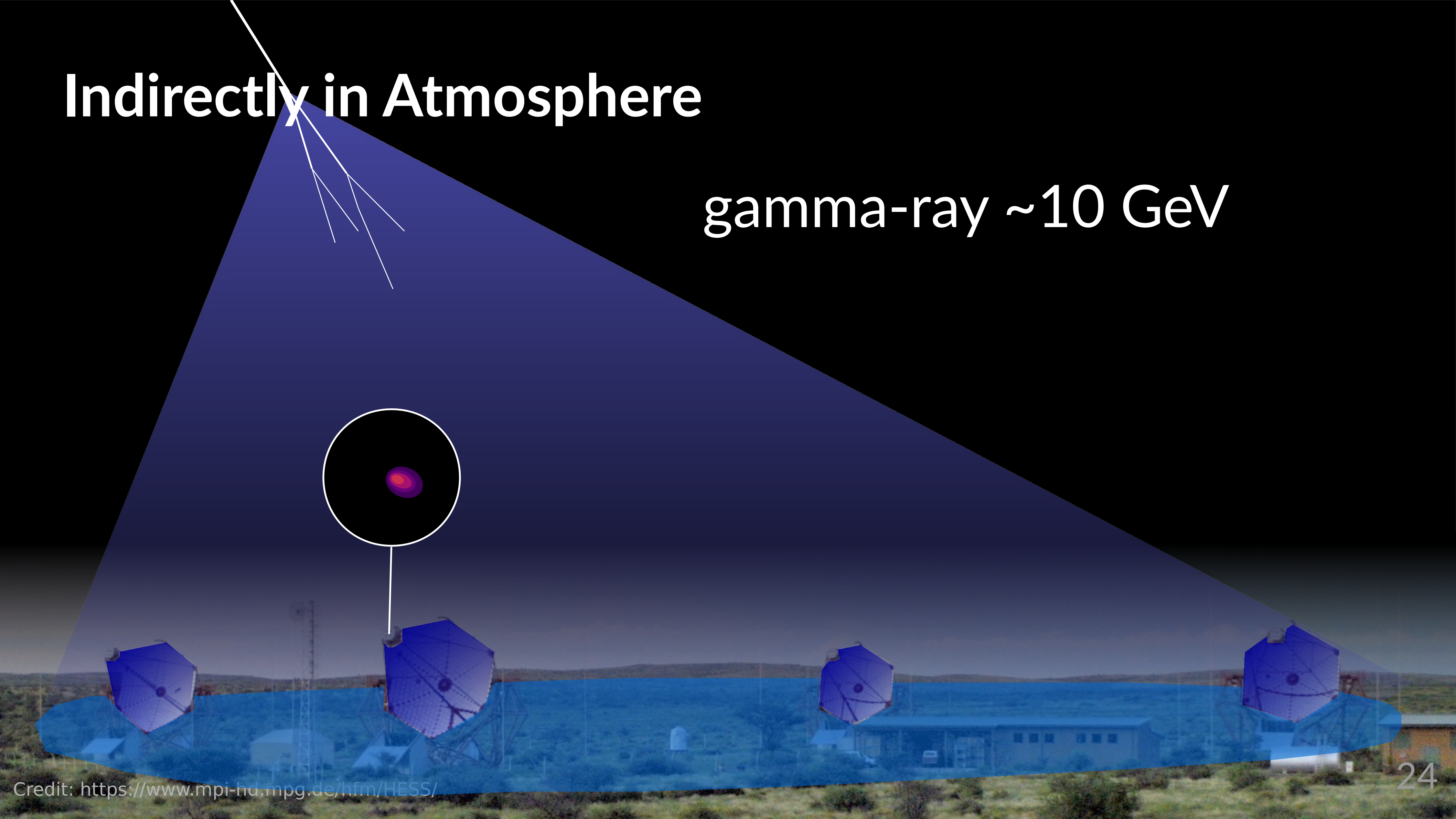

Credit: https://www.mpi-hd.mpg.de/hfm/HESS/

Indirectly in Atmosphere

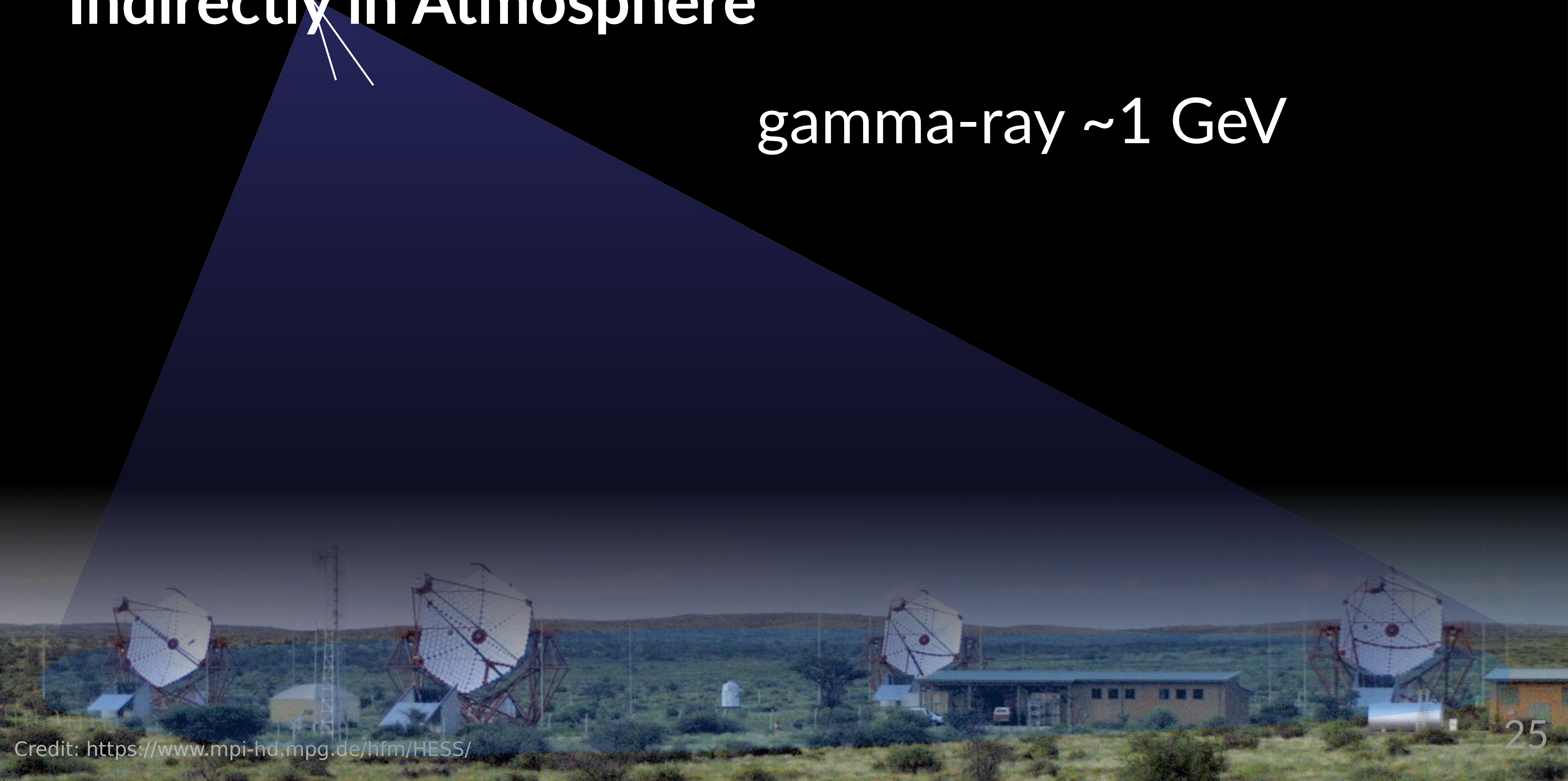

Credit: https://www.mpi-hd.mpg.de/hfm/HESS/

Centralized Trigger

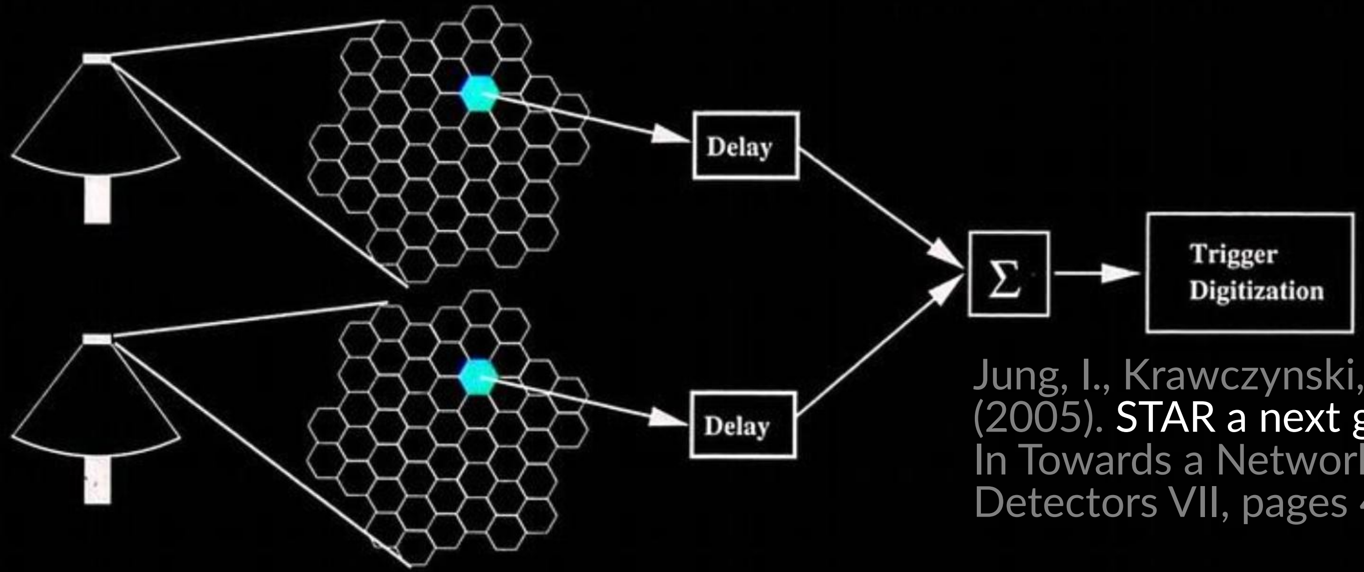

Jung, I., Krawczynski, H., Buckley, J., and Falcone, A. (2005). STAR a next generation Cherenkov telescope. In Towards a Network of Atmospheric Cherenkov Detectors VII, pages 463–6.

Credit: https://www.mpi-hd.mpg.de/hfm/HESS/

Centralized Trigger

López-Coto, R., Mazin, D., Paoletti, R., Bigas, O. B., and Cortina, J. (2016).
The Topo-Trigger: A new concept of stereo trigger system for imaging atmospheric Cherenkov telescopes.
Journal of Instrumentation, 11(04):P04005.

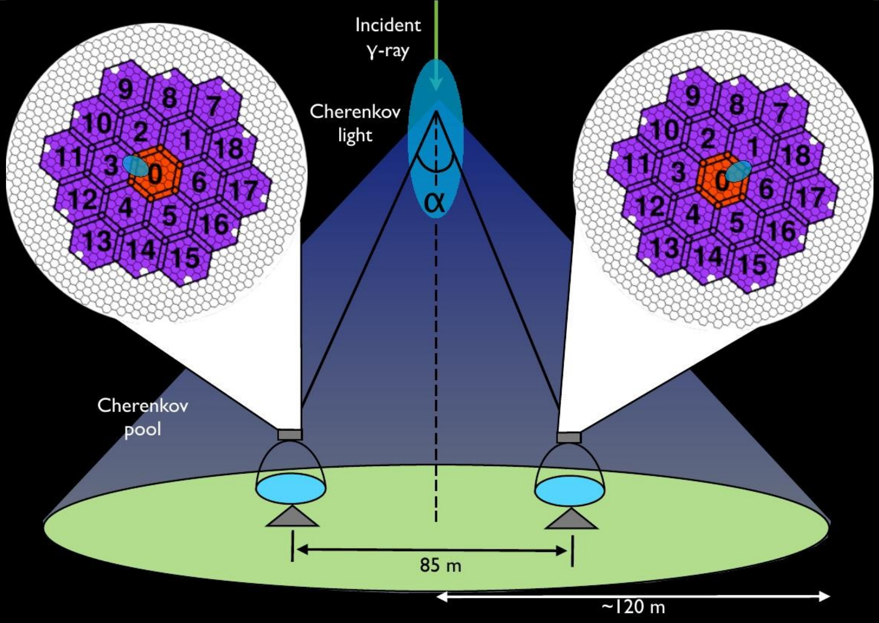

Credit: Thomas Kraehenbuehl

Large Telescope

Credit: Tomohiro Inada

Large Telescope

Credit: Tomohiro Inada

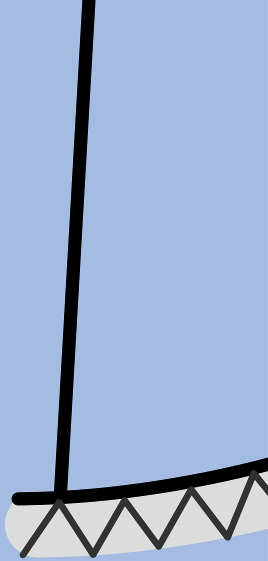

Large Telescope

Credit: Tomohiro Inada

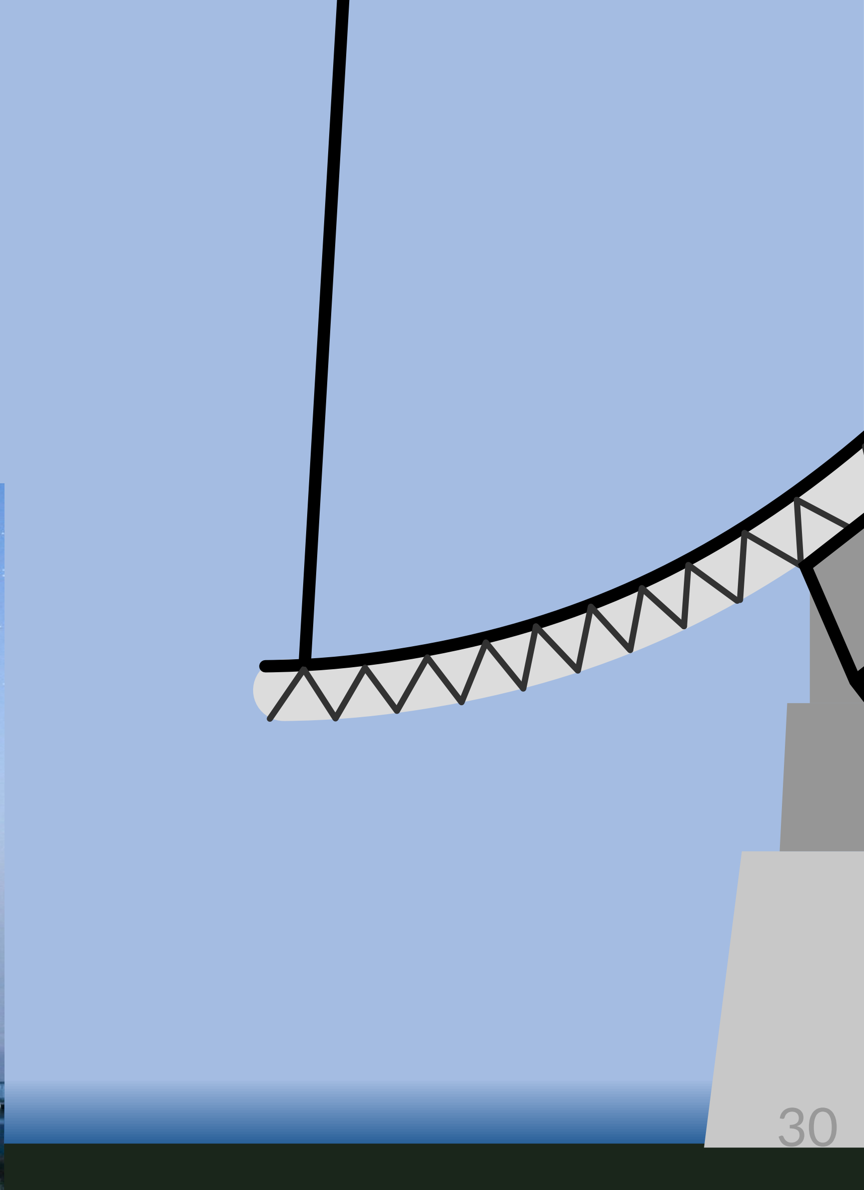

Large Telescope

square-cube-law

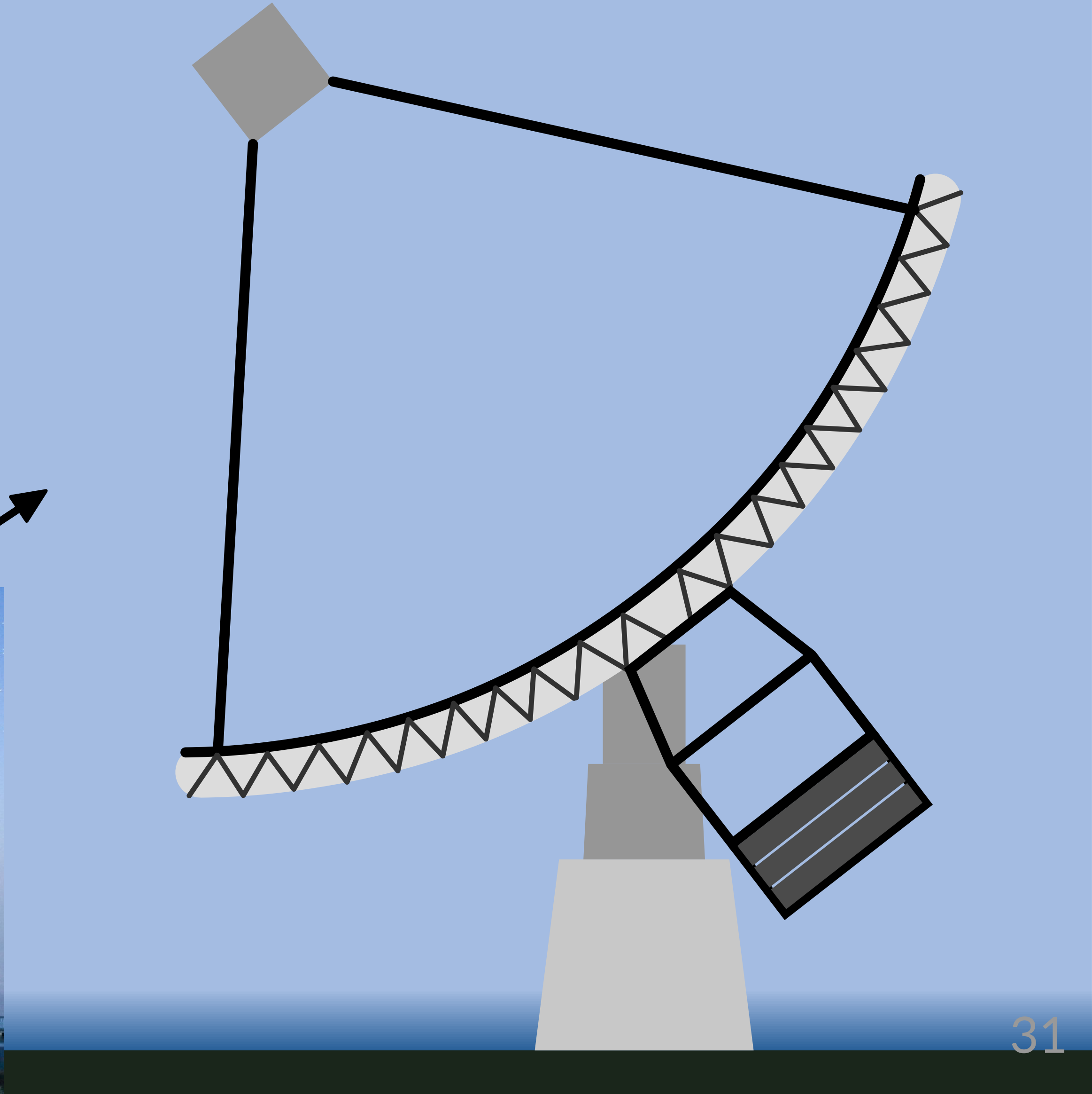

Large Telescope

square-cube-law

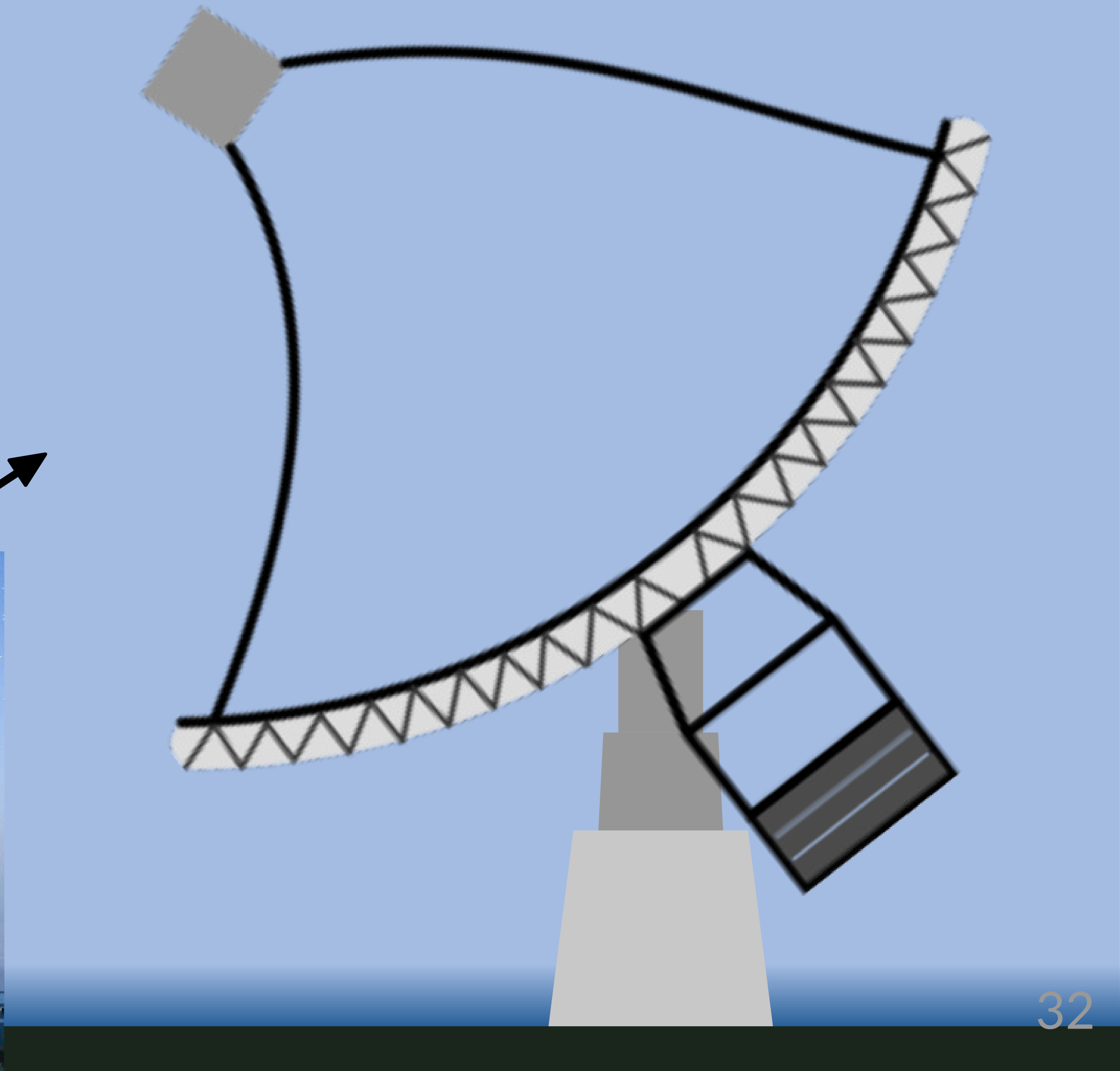

Large Telescope

square-cube-law

"... a problem with large telescopes ... is the very limited depth-of-field [Hofmann, W. 2001] ...

Bernlohr, K. et al. (2013).
Monte Carlo design studies for the Cherenkov Telescope Array.
Astroparticle Physics, 43:171–188.

Hofmann, W. (2001).
How to focus a Cherenkov telescope.
Journal of Physics G: Nuclear and Particle Physics, 27(4):933–939.

Credit: Tomohiro Inada

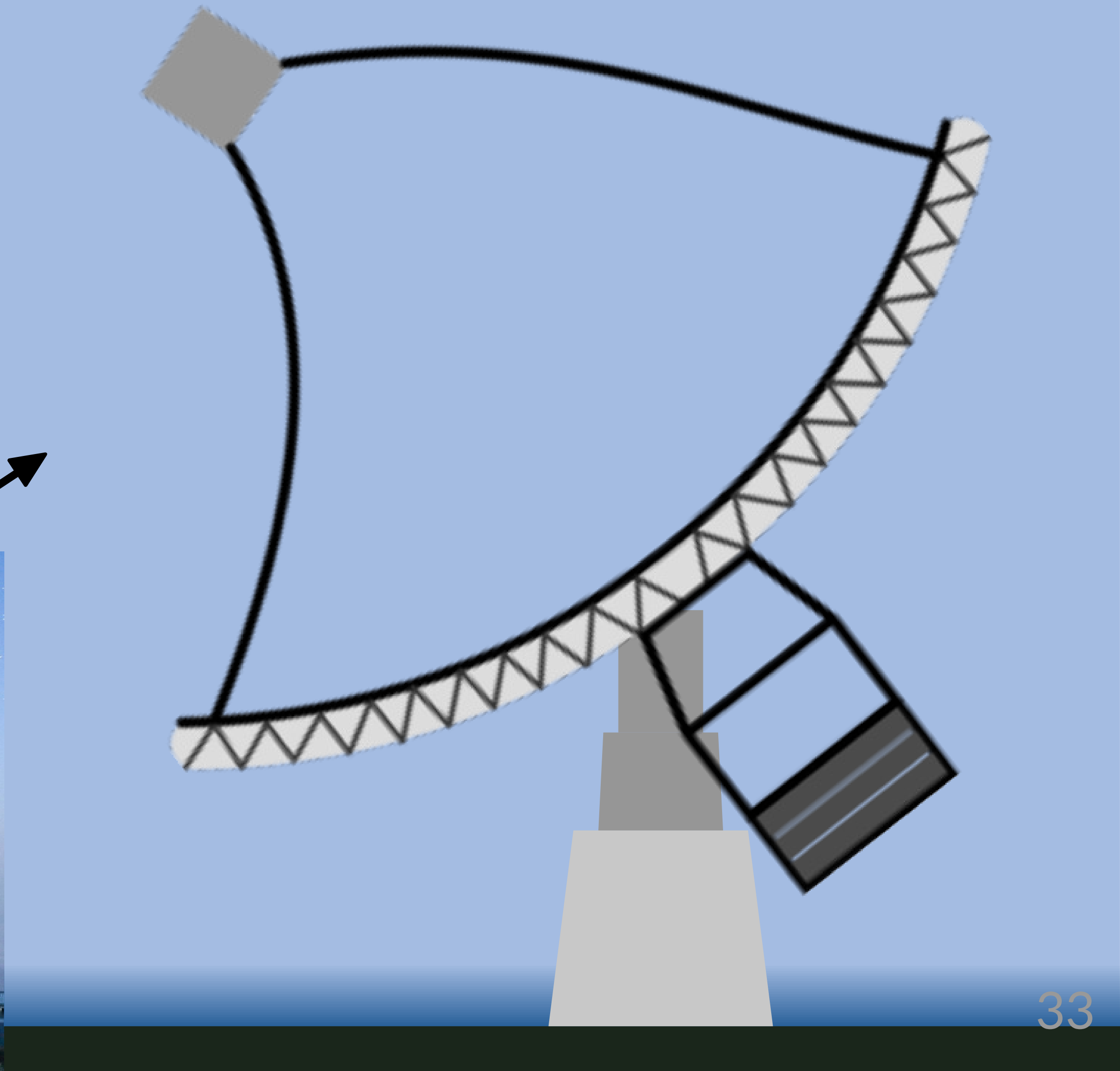

Large Telescope

square-cube-law

very limited depth-of-field


Credit: Tomohiro Inada

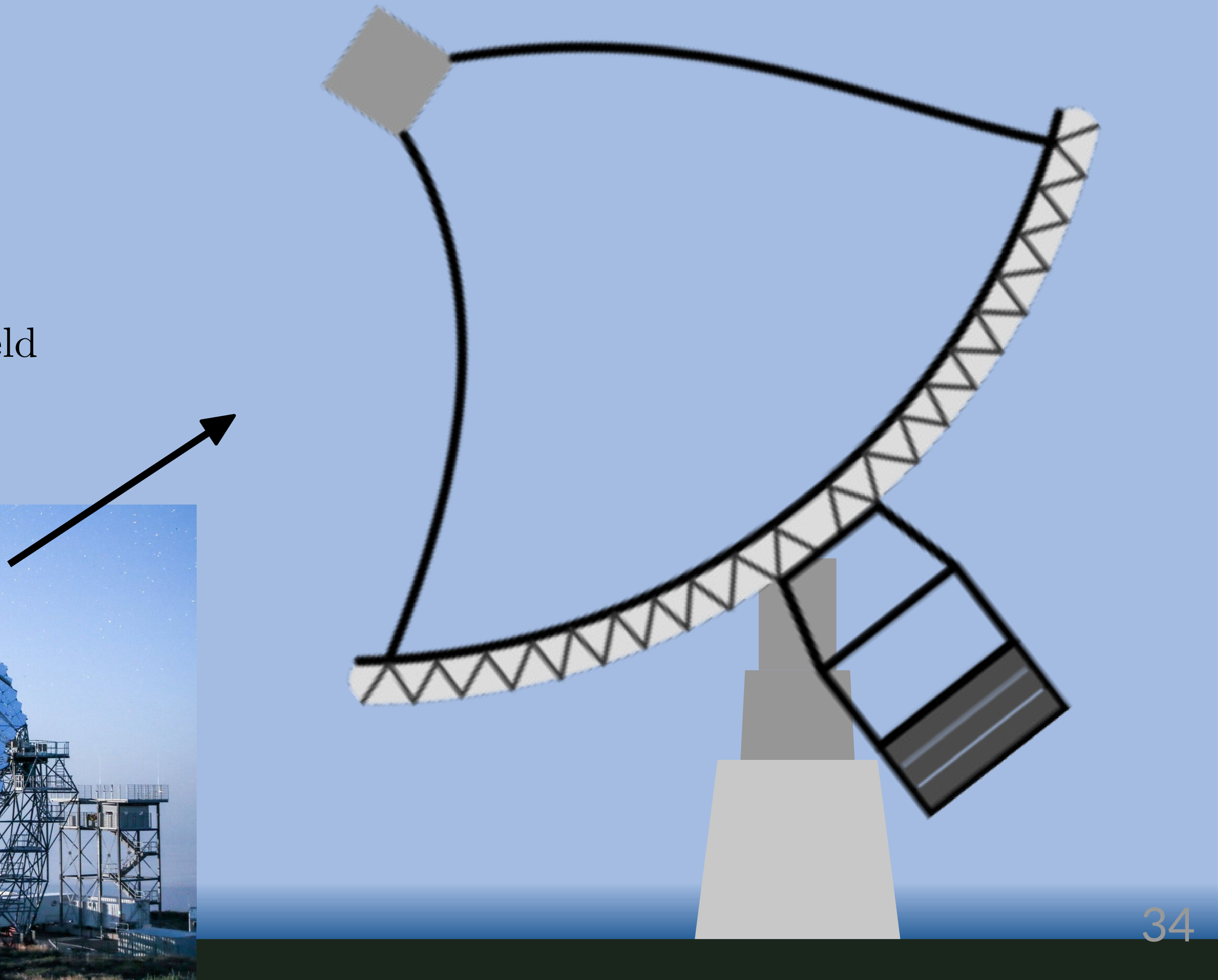

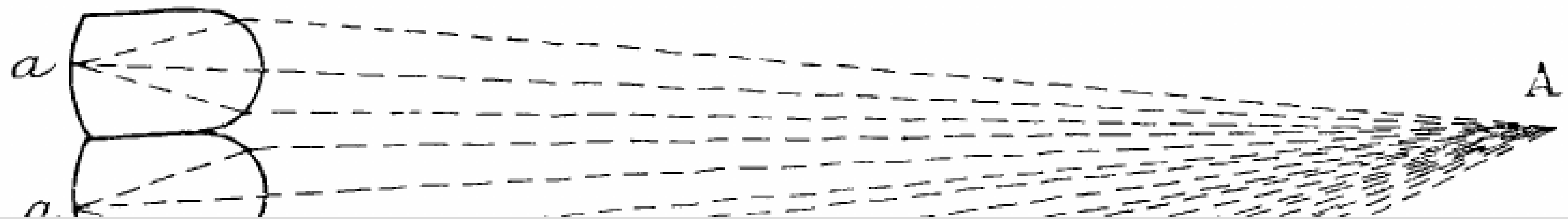

Plenoptics

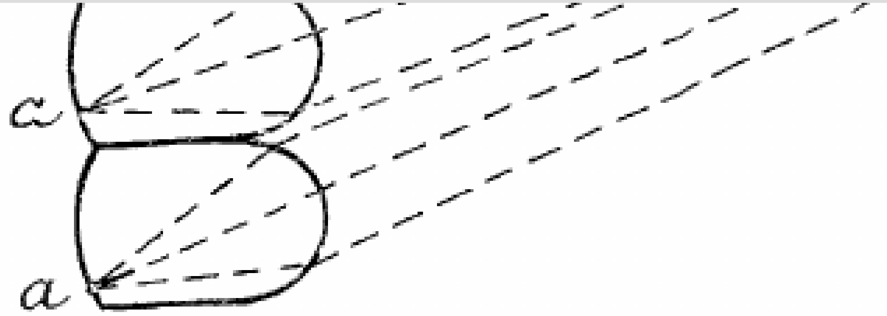

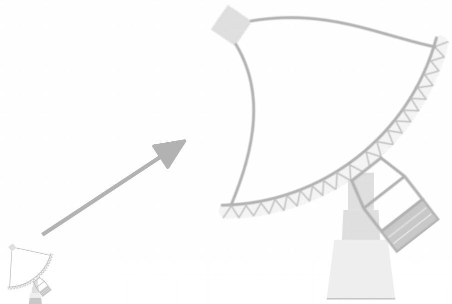

Plenoptics

Plenoptics

Plenoptics

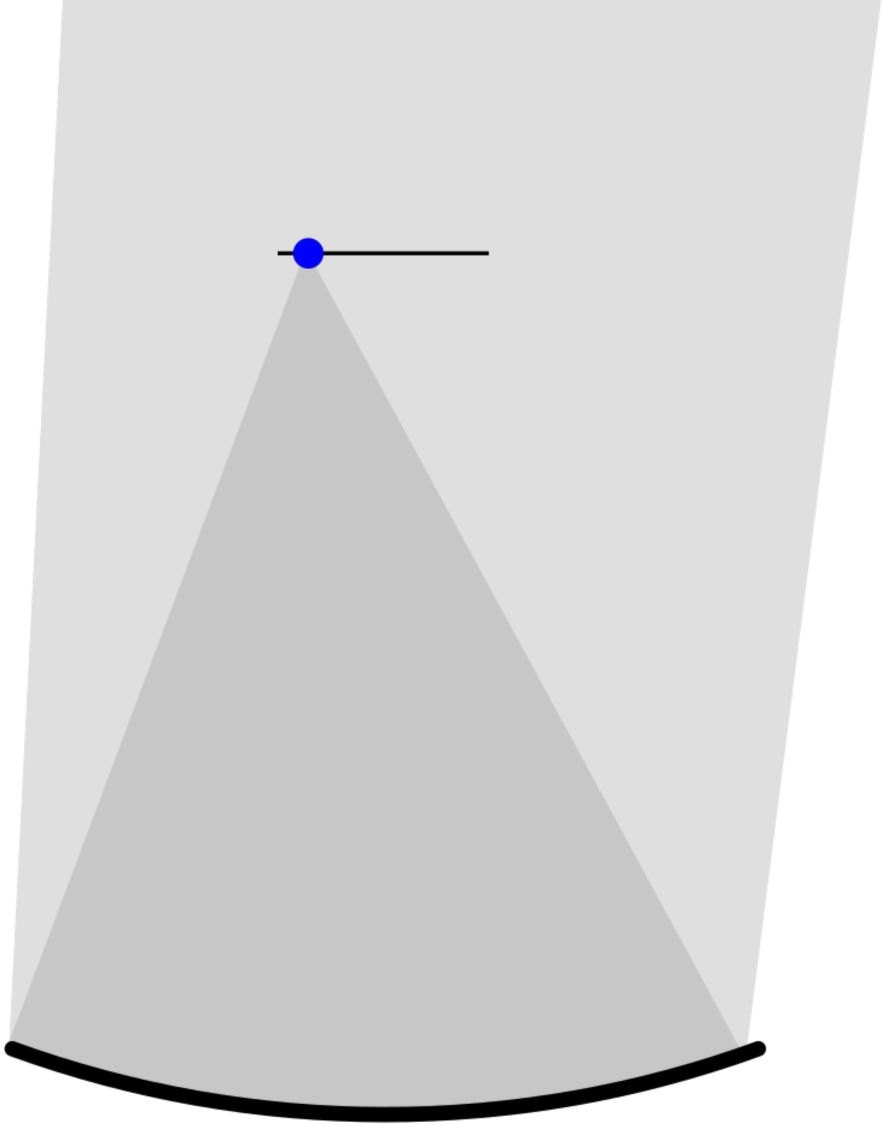

Plenoptics

Plenoptics

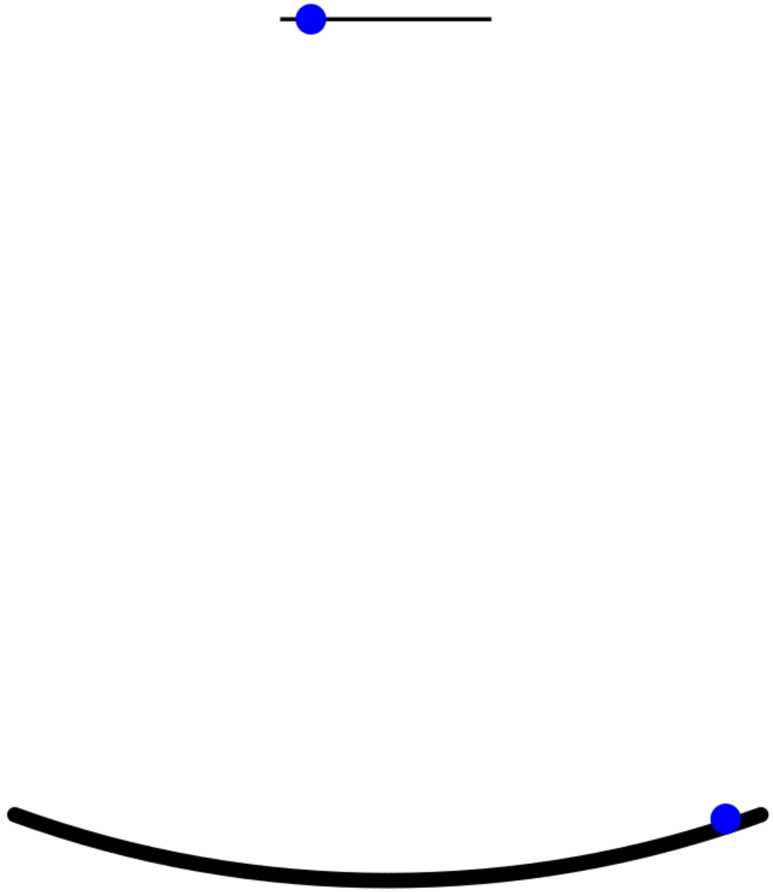

Plenoptics

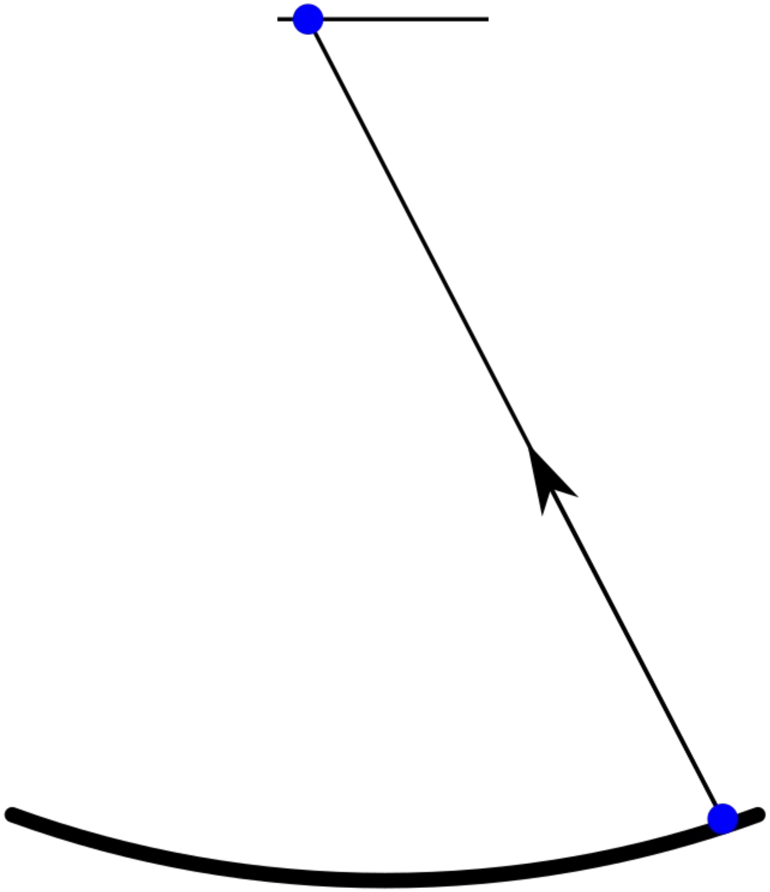

Plenoptics

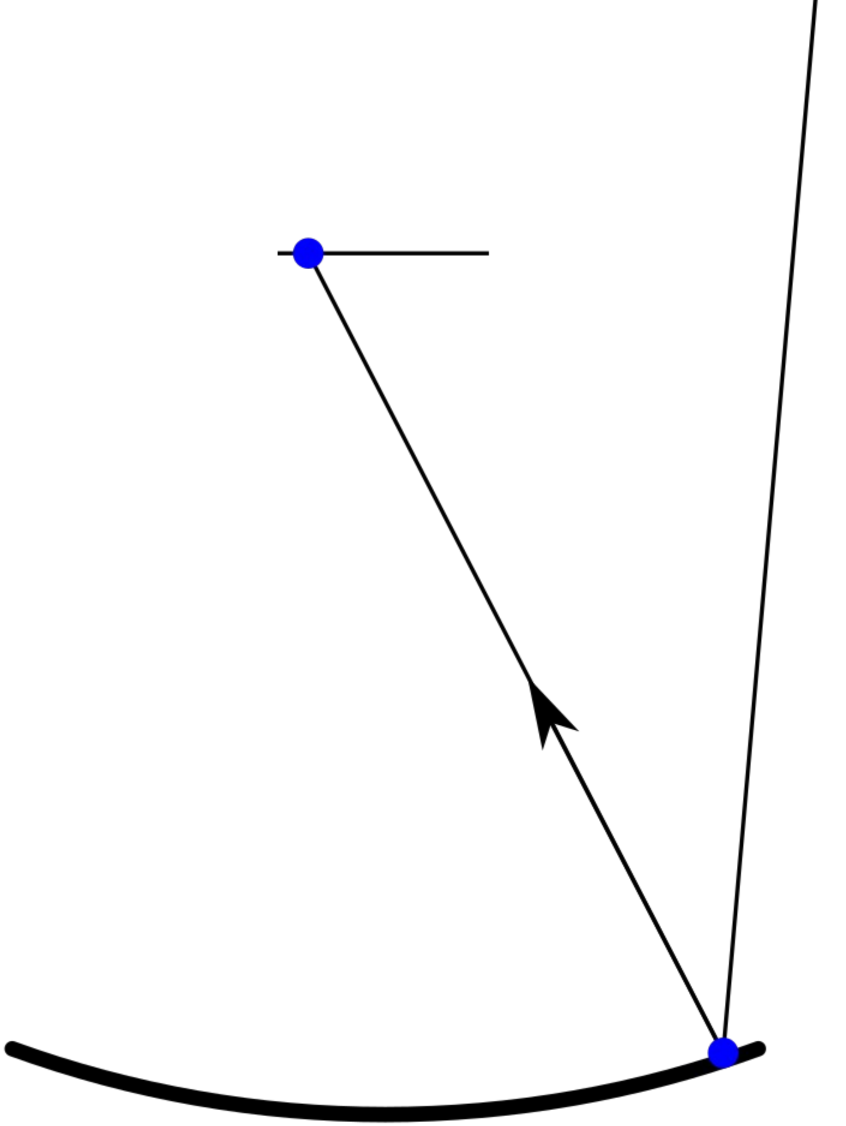

Plenoptics

Thin-Lens-Model

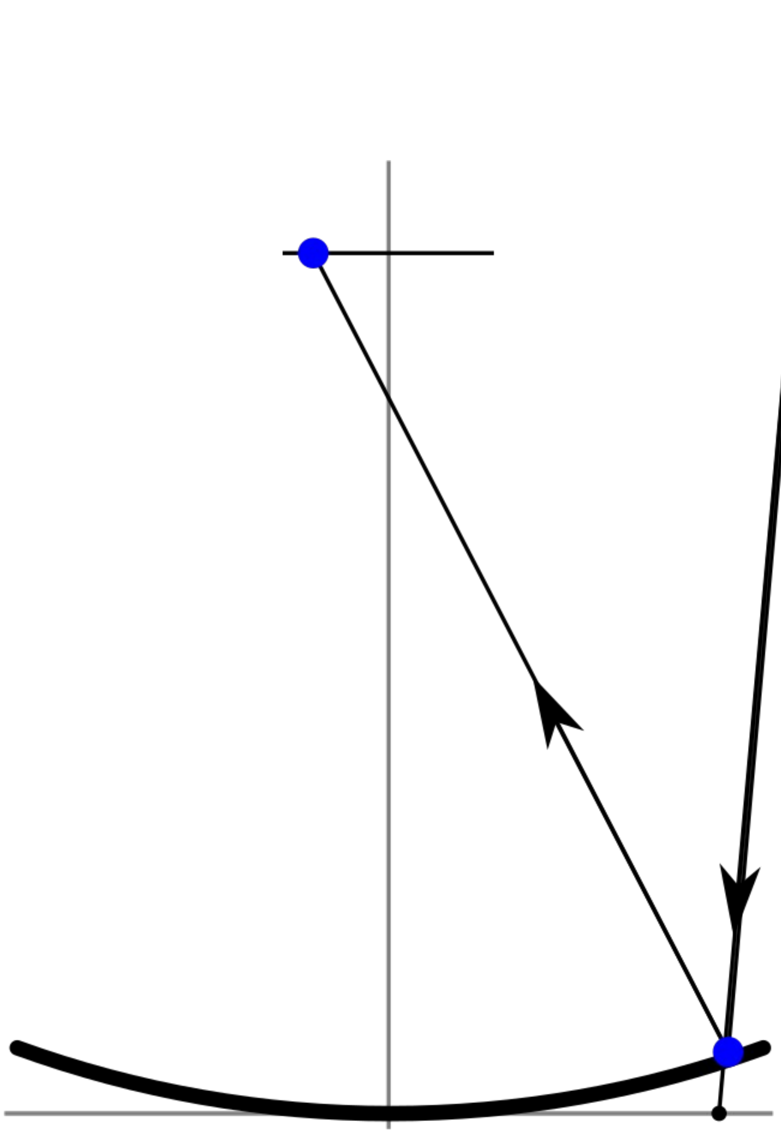

Plenoptics

Thin-Lens-Model

$$\frac{1}{f} = \frac{1}{\text{depth}} + \frac{1}{b}$$

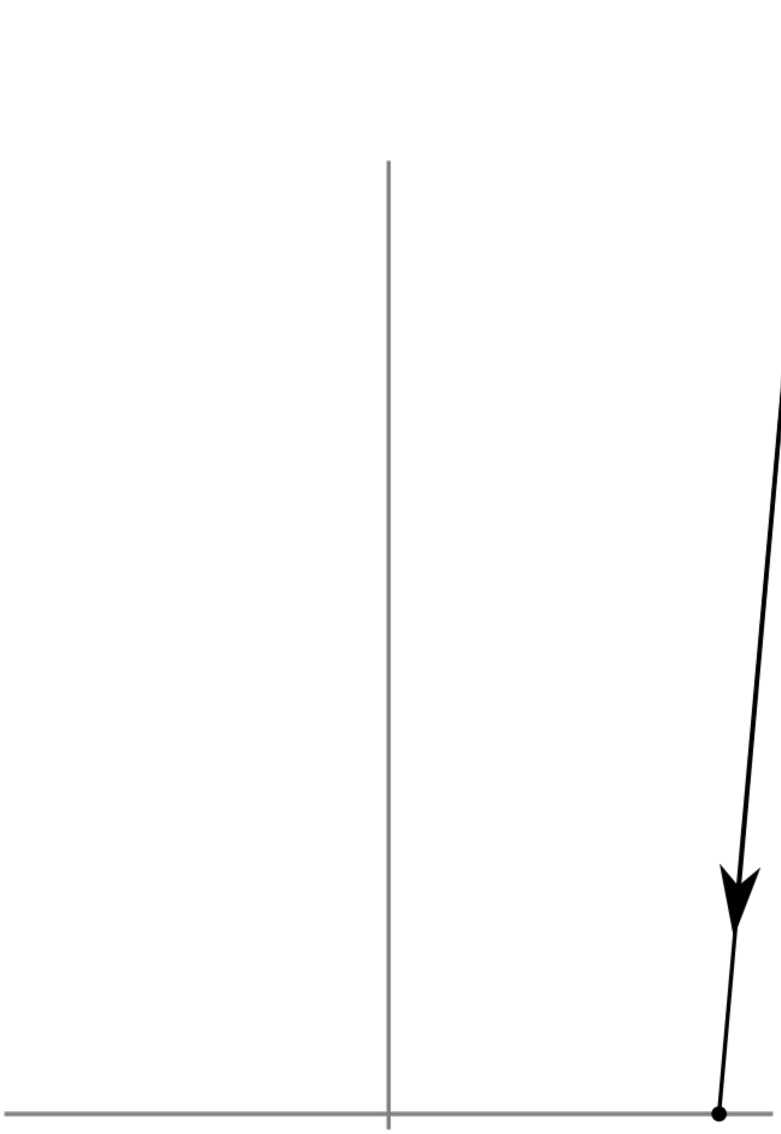

Plenoptics

Thin-Lens-Model

$$\frac{1}{f} = \frac{1}{\text{depth}} + \frac{1}{b}$$

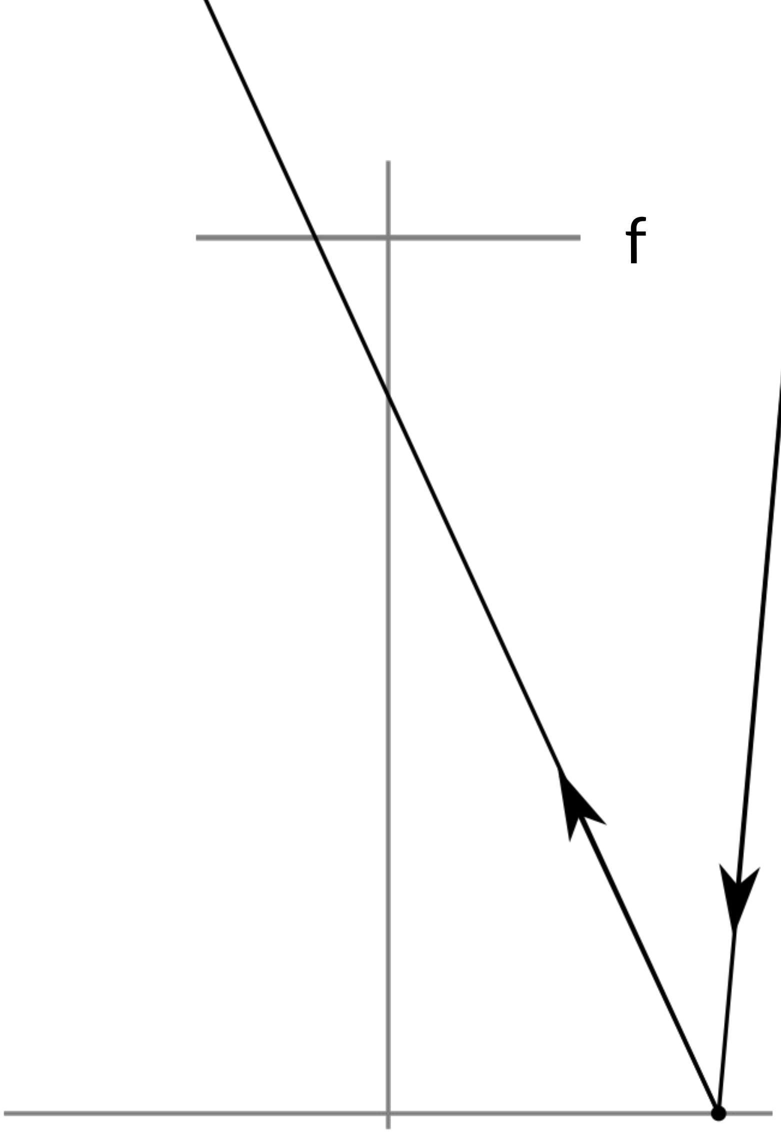

Plenoptics

Thin-Lens-Model

$$\frac{1}{f} = \frac{1}{\text{depth}} + \frac{1}{b}$$

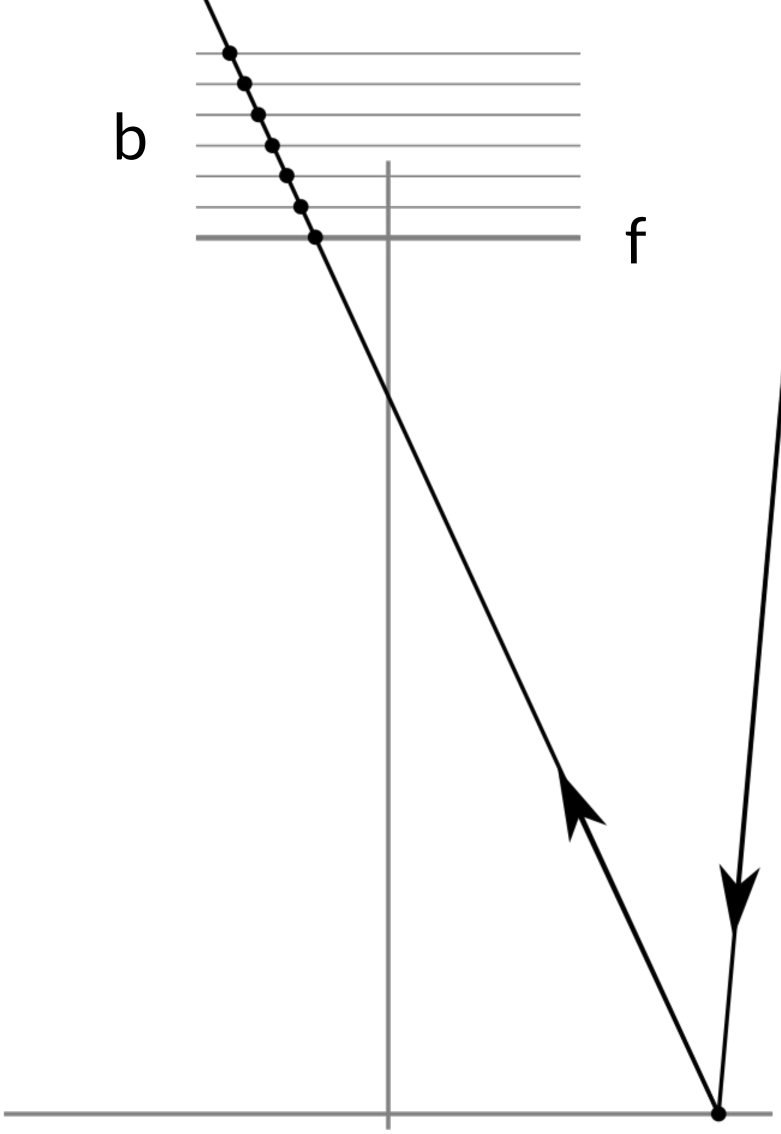

Plenoptics

Thin-Lens-Model

$$\frac{1}{f} = \frac{1}{\text{depth}} + \frac{1}{b}$$

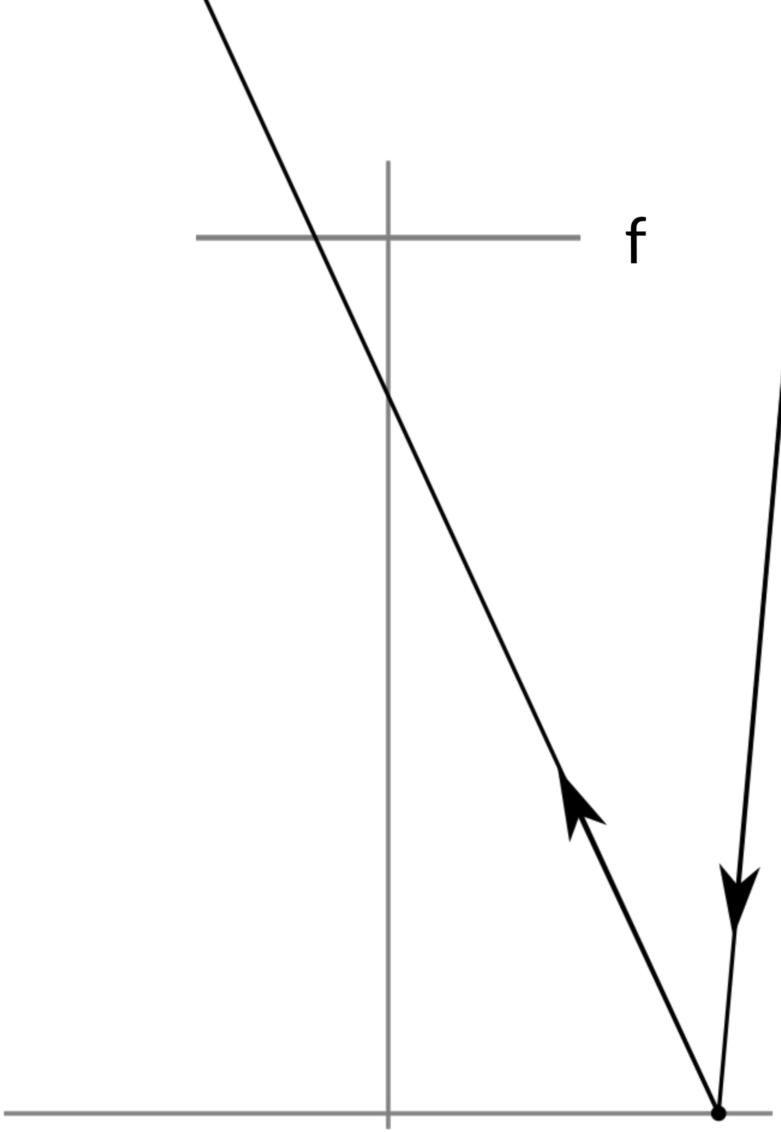

Plenoptics

Thin-Lens-Model

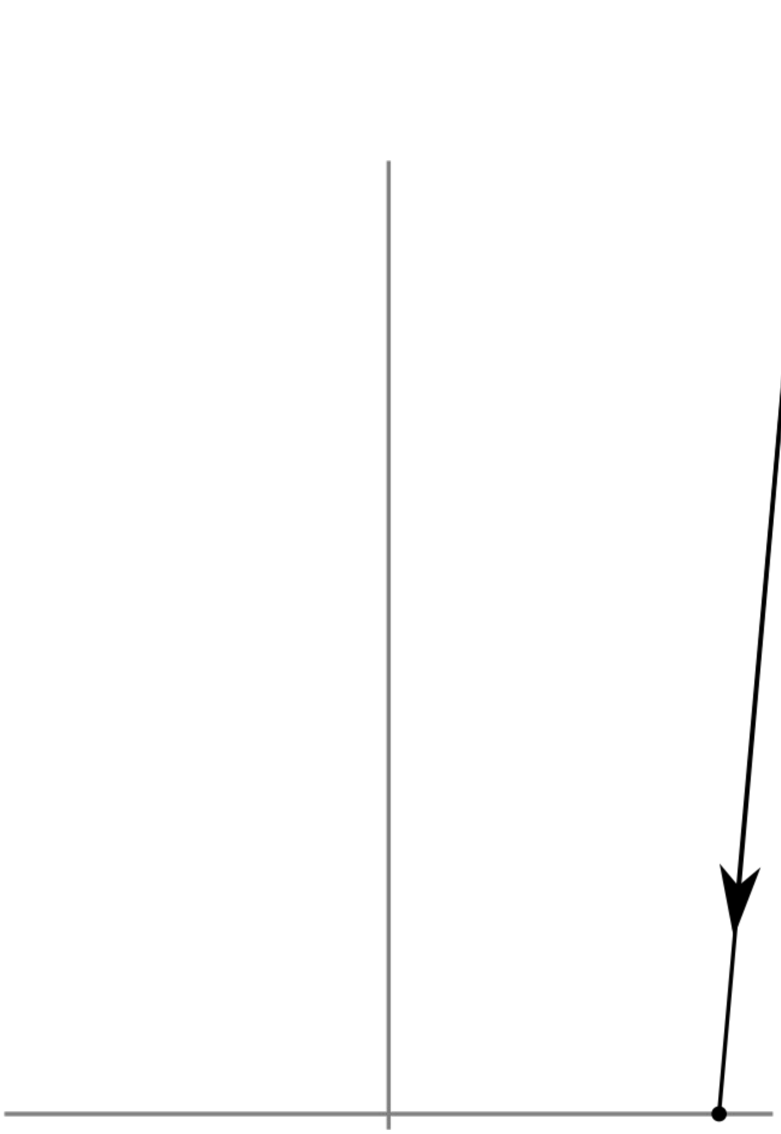

Plenoptics

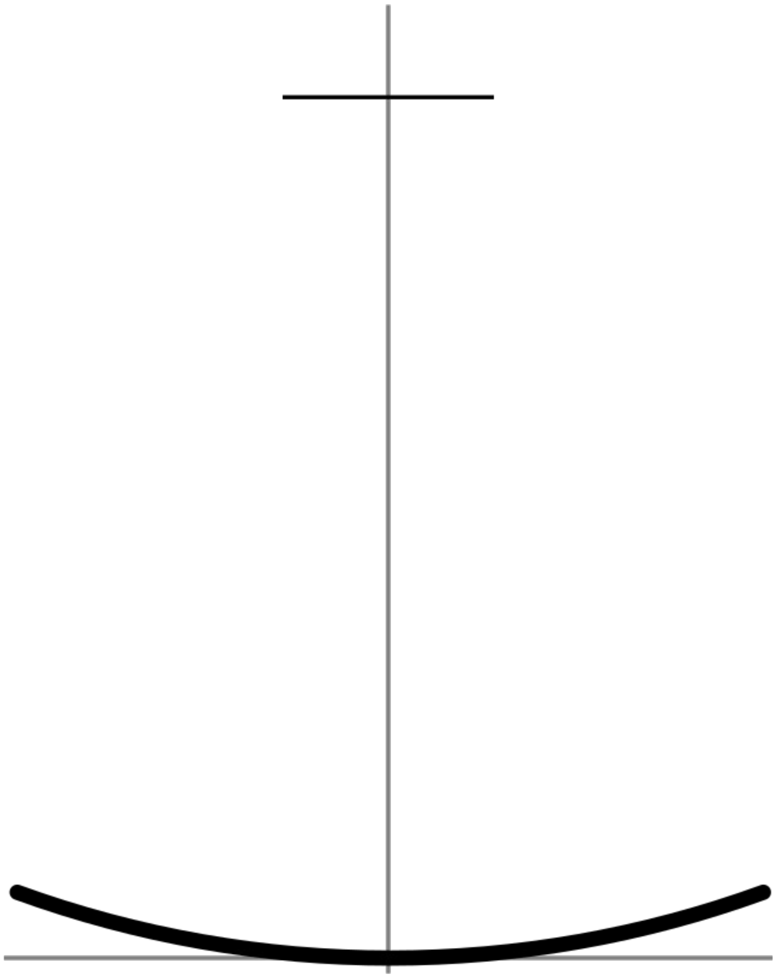

Plenoptics

Misalignment

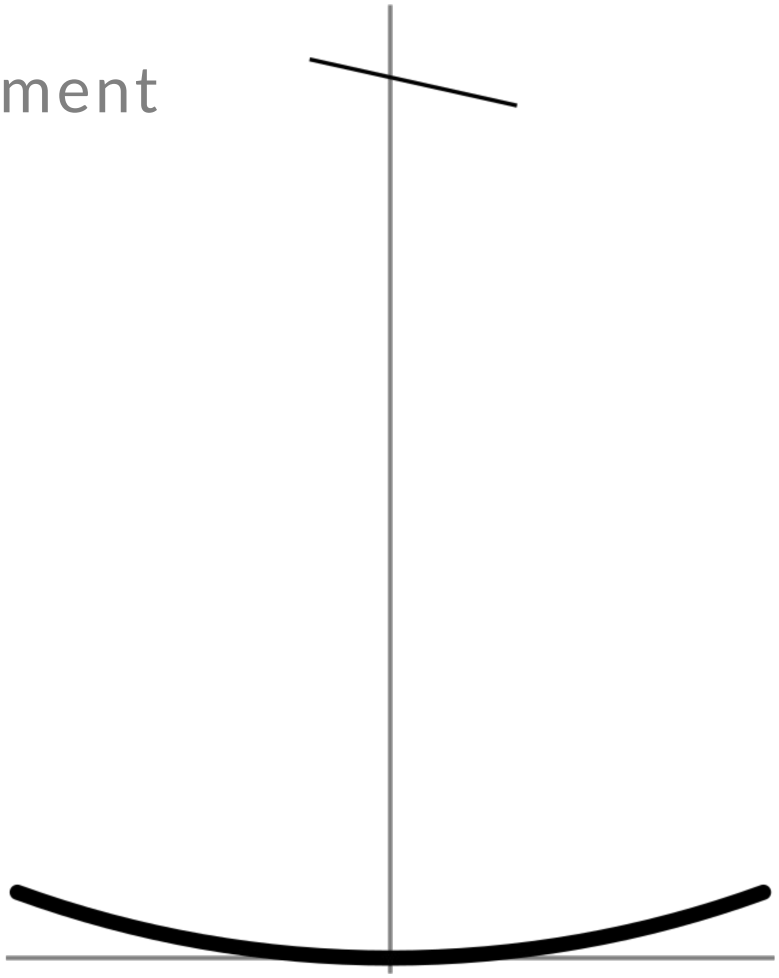

Plenoptics

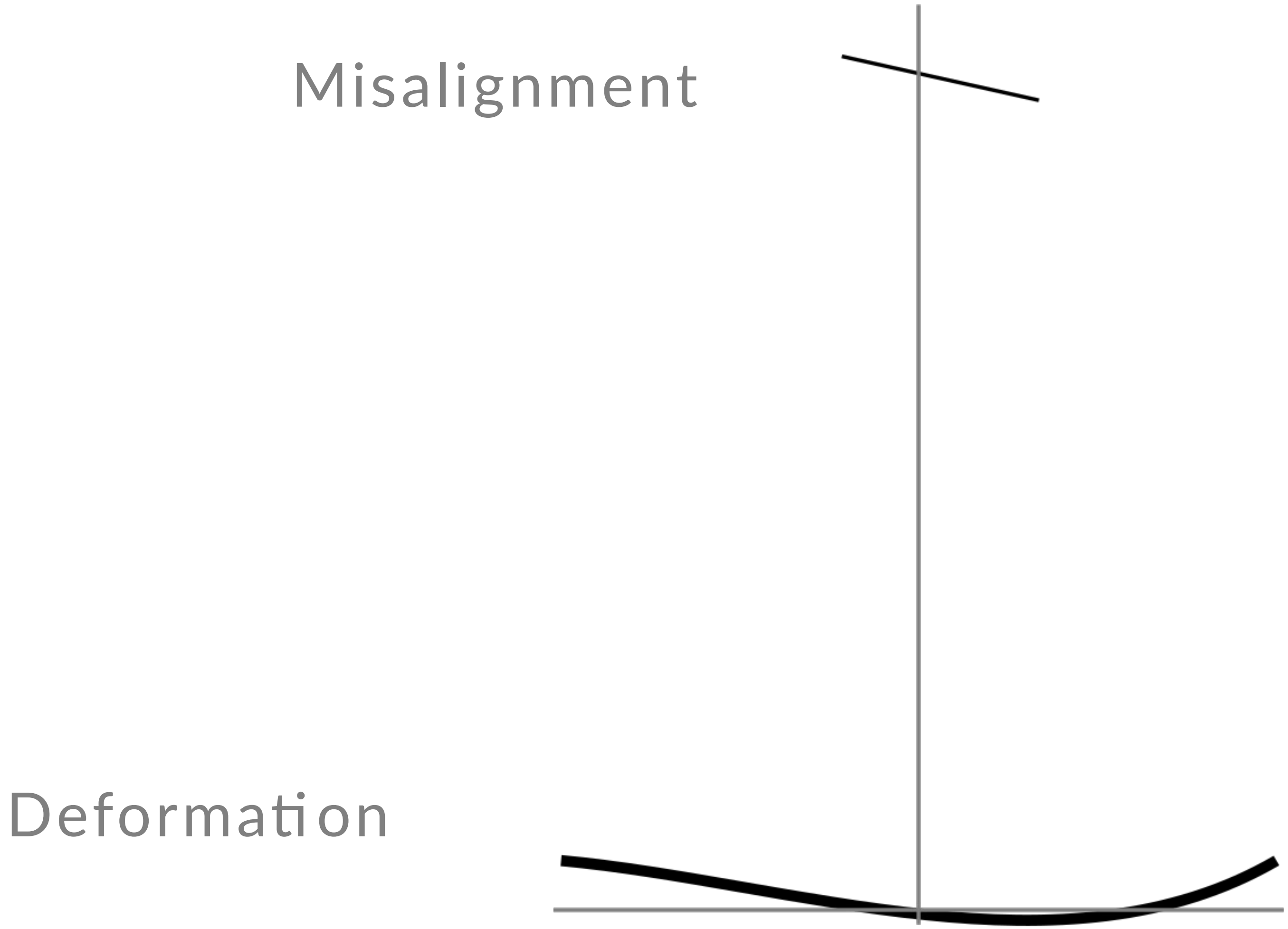

Plenoptics

Misalignment

Deformation

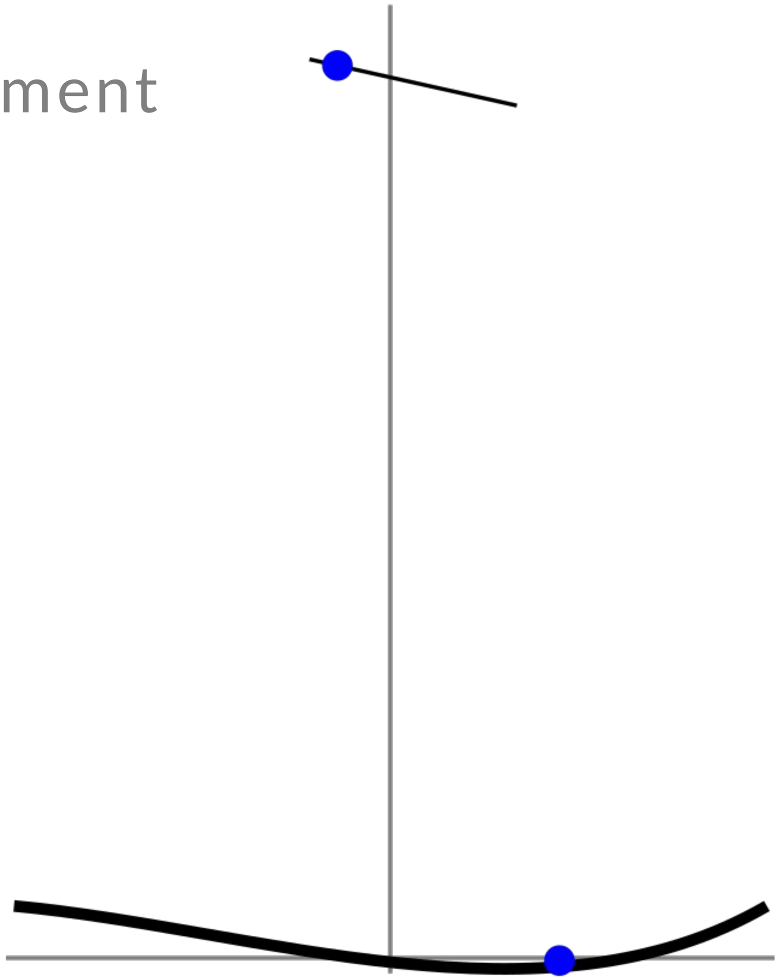

Plenoptics

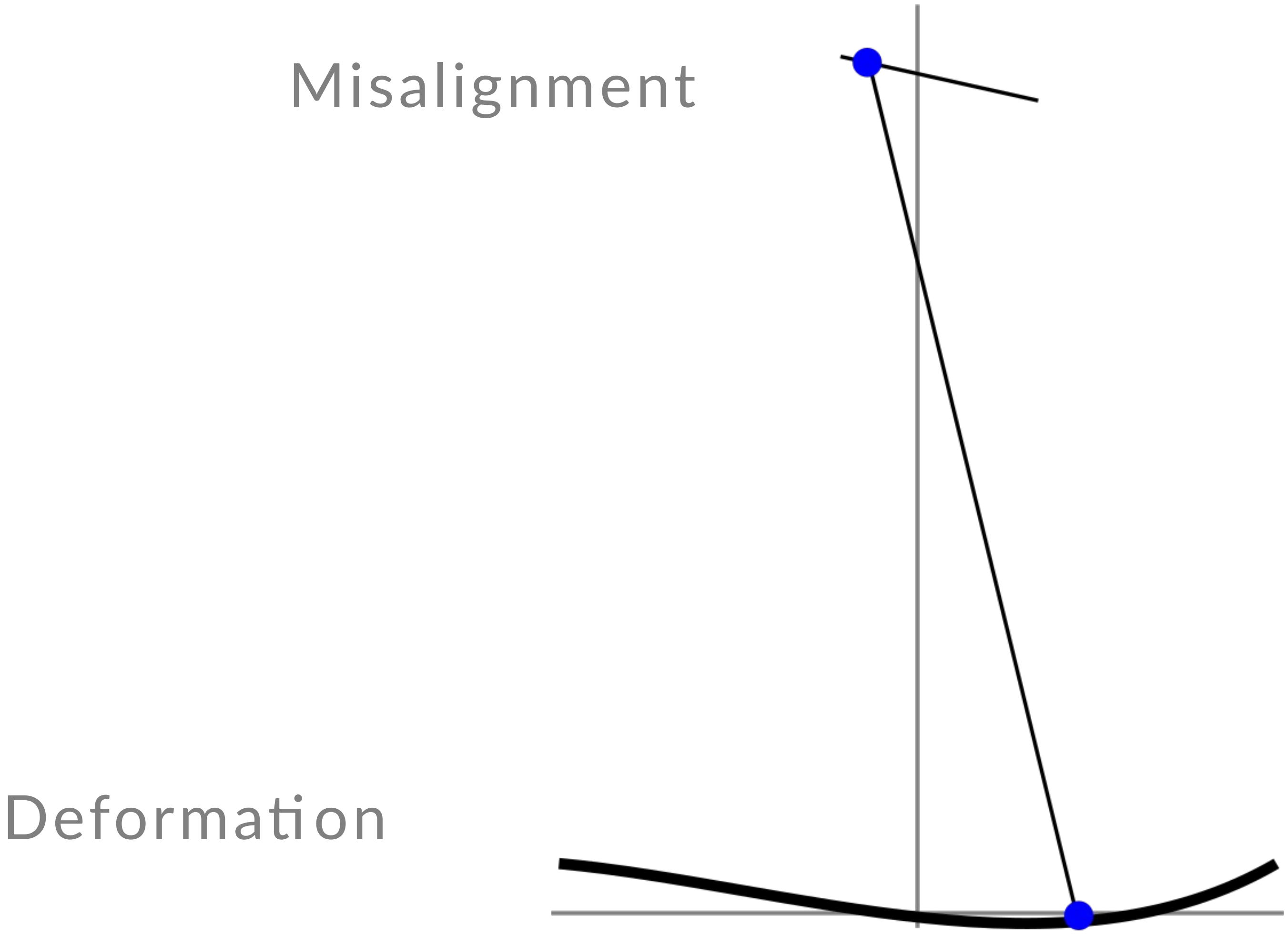

Plenoptics

Misalignment

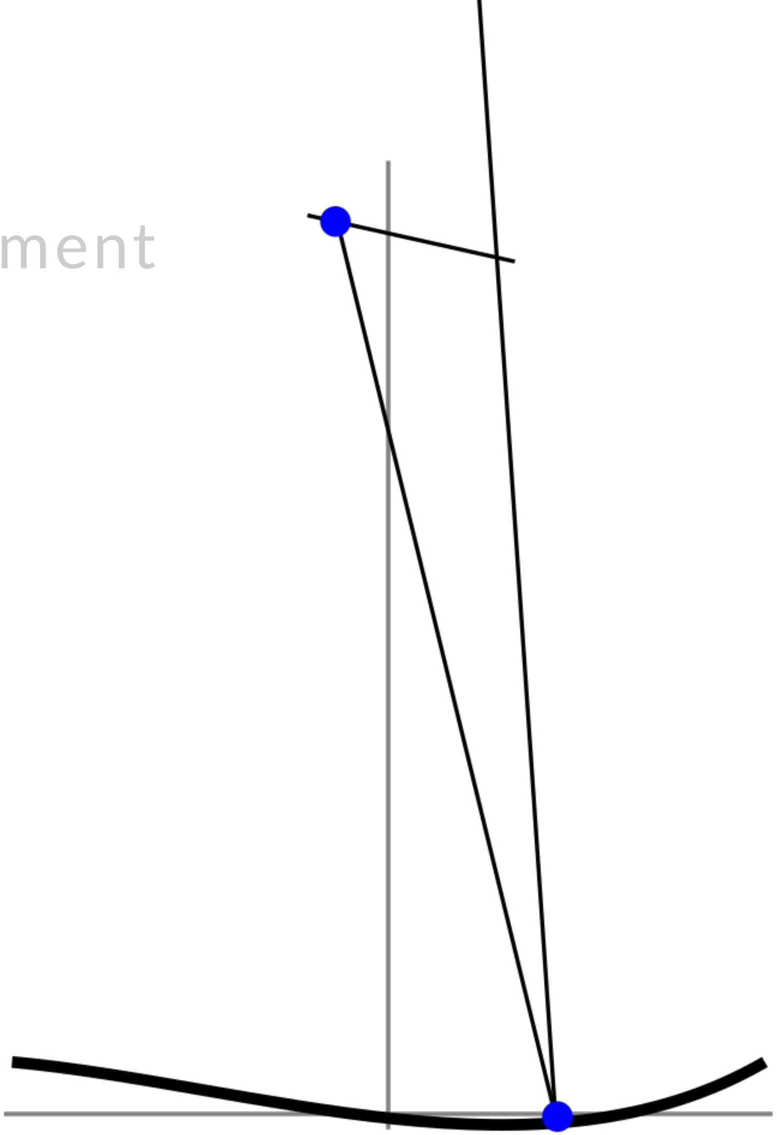

Deformation

Plenoptics

Thin-Lens-Model

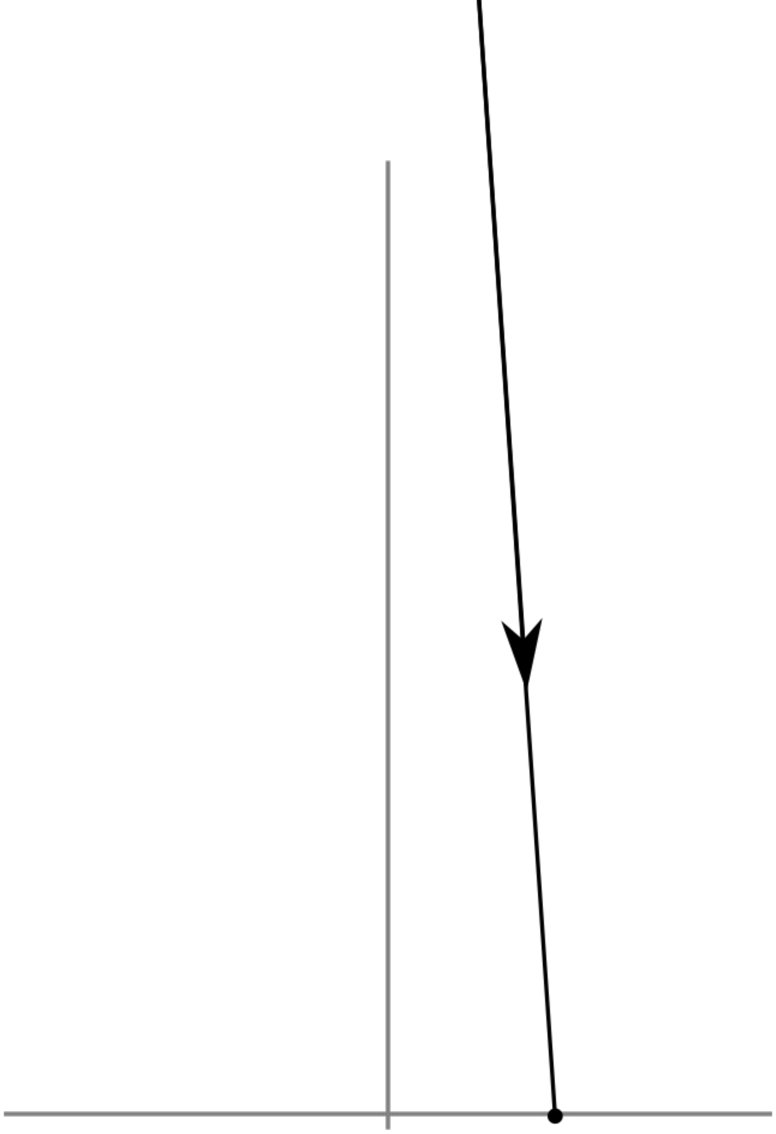

Plenoptics

Thin-Lens-Model

$$\frac{1}{f} = \frac{1}{\text{depth}} + \frac{1}{b}$$

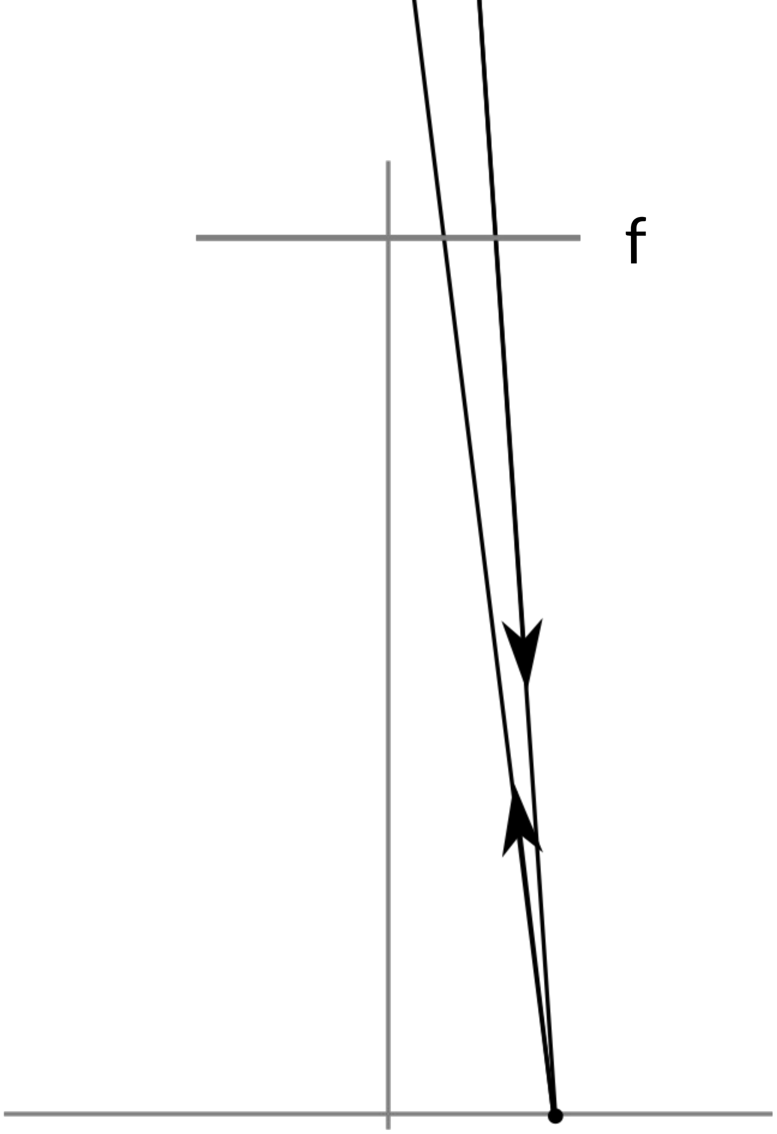

Plenoptics

Thin-Lens-Model

$$\frac{1}{f} = \frac{1}{\text{depth}} + \frac{1}{b}$$

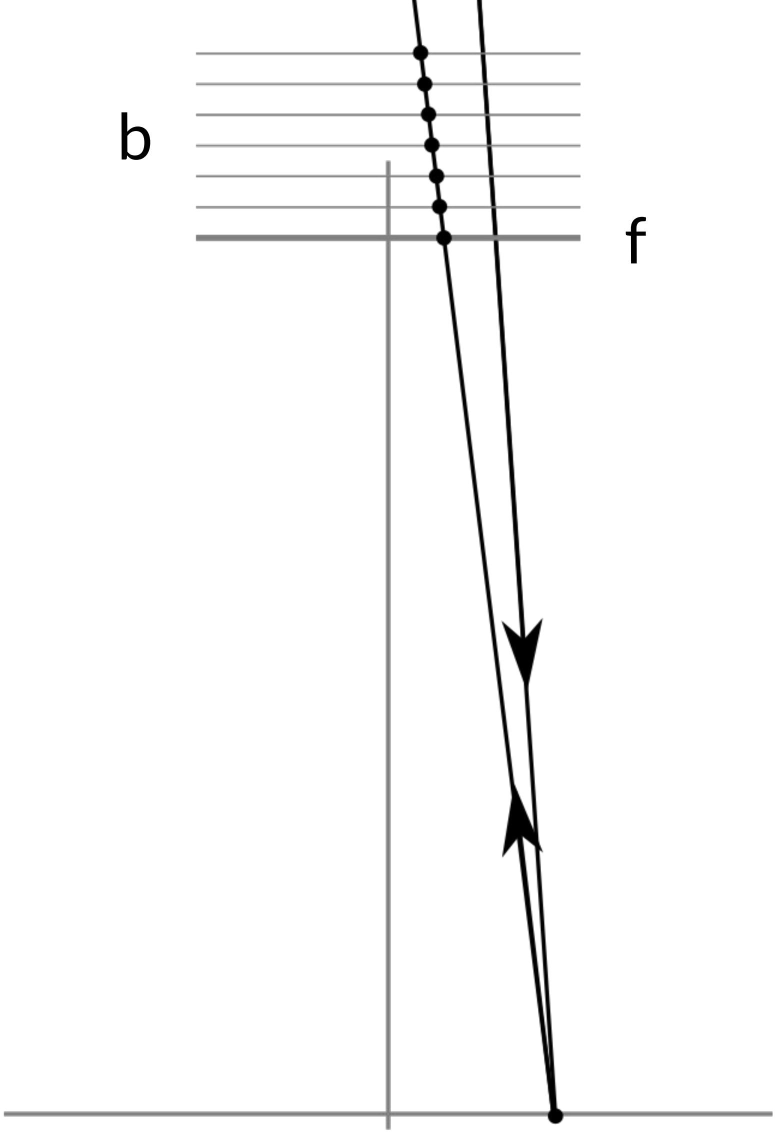

Implementation

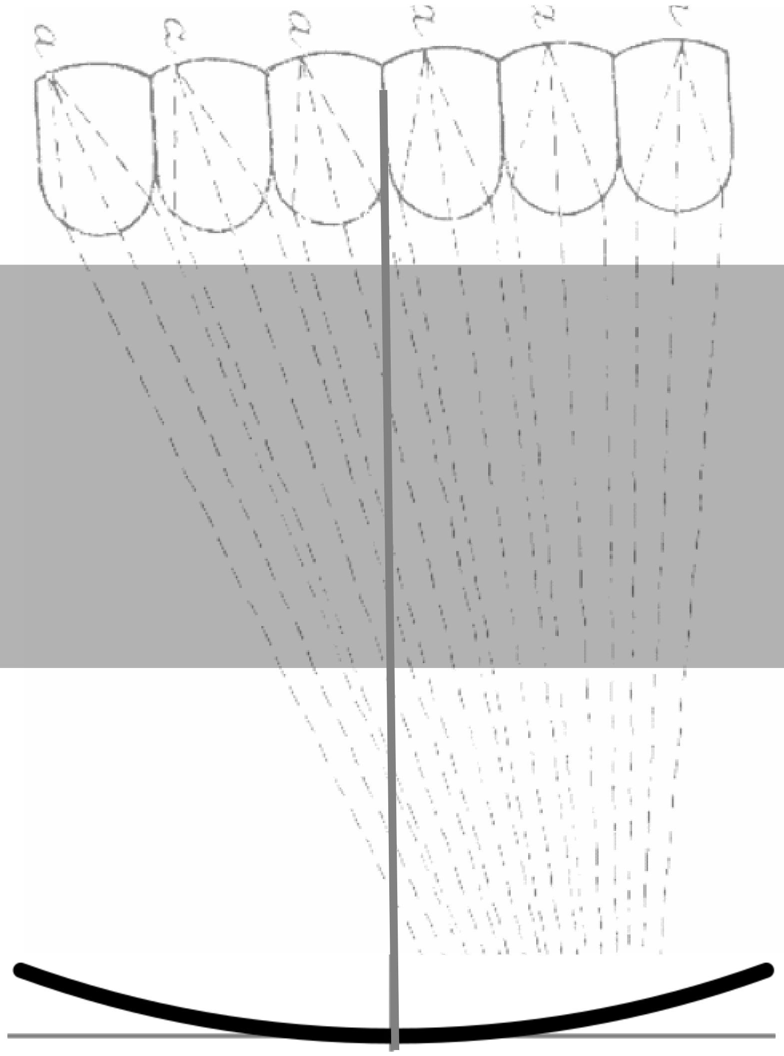

Plenoptics

Telescope

Plenoptics

Telescope

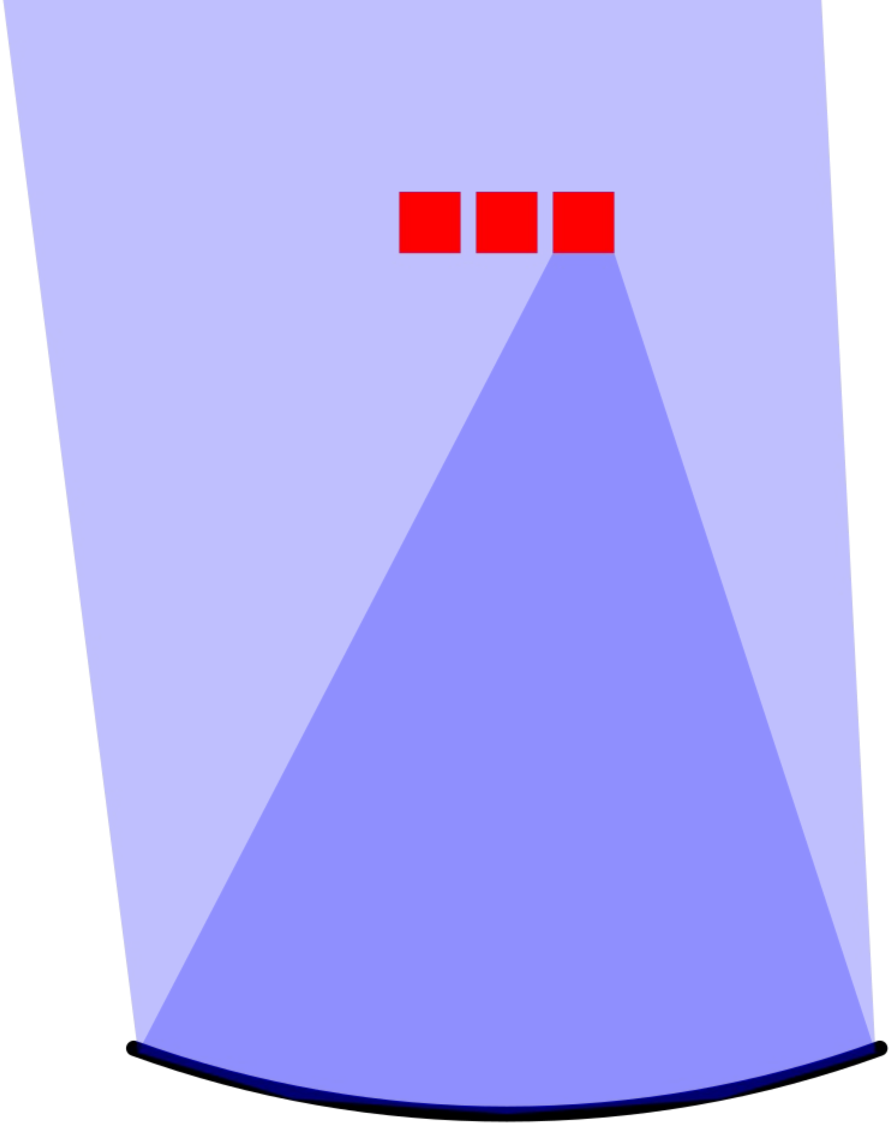

Plenoptics

Telescope

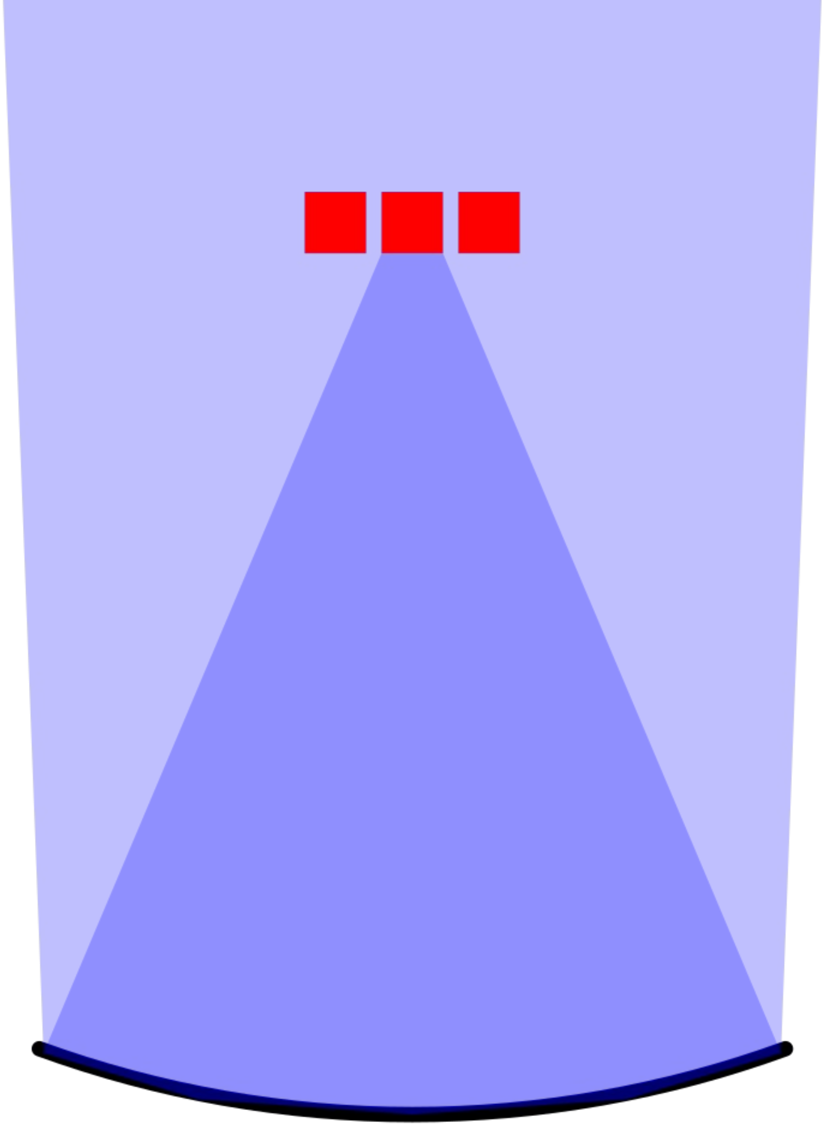

Plenoptics

Telescope

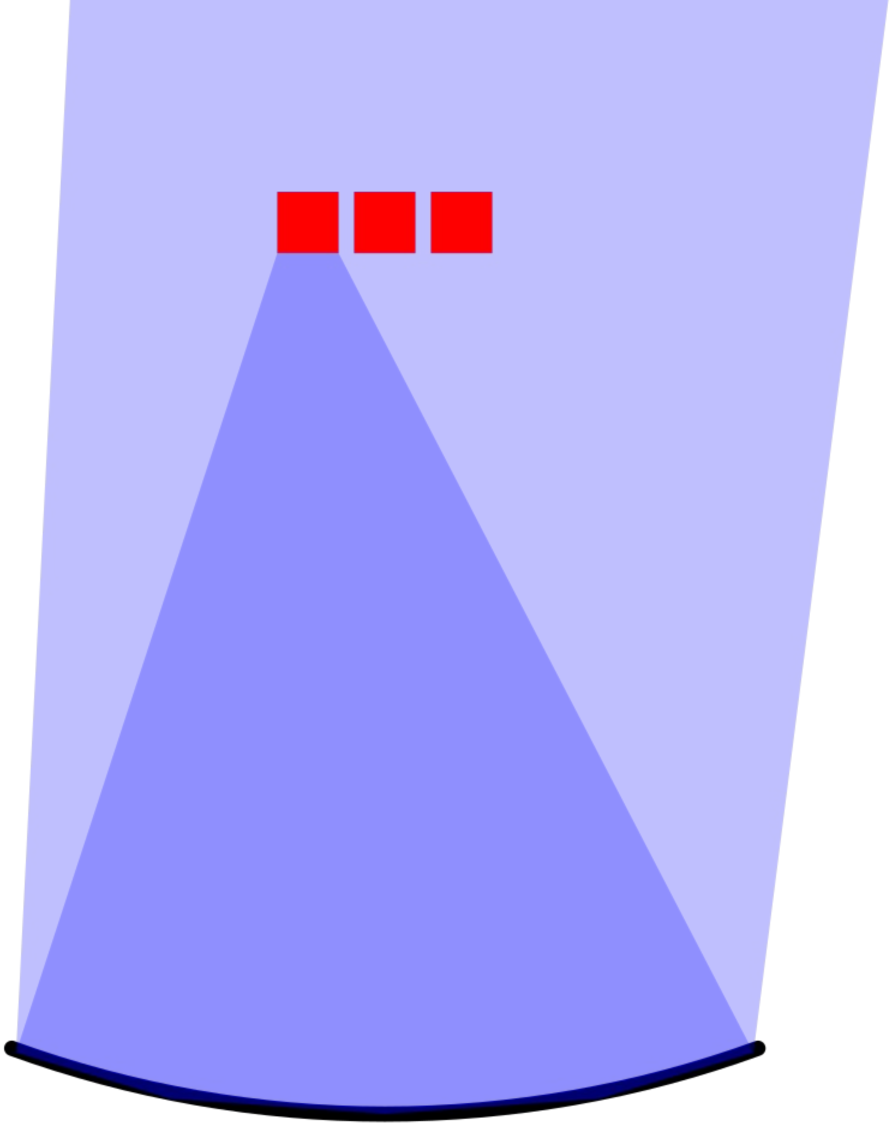

Plenoptics

Telescope

Plenoptics

Telescope

Plenoscope

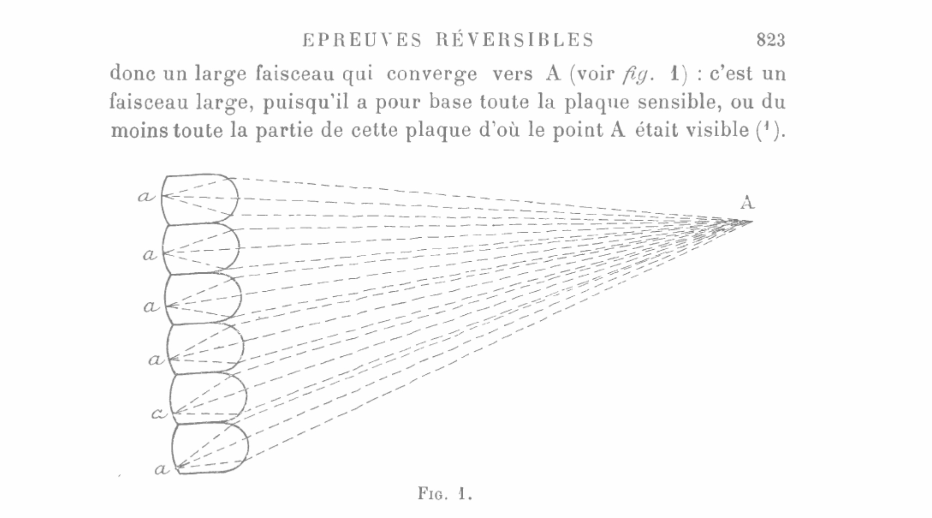

EPREUVES RÉVERSIBLES 823

donc un large faisceau qui converge vers A (voir *fig.* 1) : c'est un faisceau large, puisqu'il a pour base toute la plaque sensible, ou du moins toute la partie de cette plaque d'où le point A était visible (1).

Fig. 1.

Par M. G. Lippmann, (**1908**),
Epreuves reversibles donnant la sensation du relief,
Phys. Theor. Appl. 7, p.821-825

Plenoptics

Plenoscope

EPREUVES RÉVERSIBLES 823

donc un large faisceau qui converge vers A (voir *fig.* 1) : c'est un faisceau large, puisqu'il a pour base toute la plaque sensible, ou du moins toute la partie de cette plaque d'où le point A était visible (1).

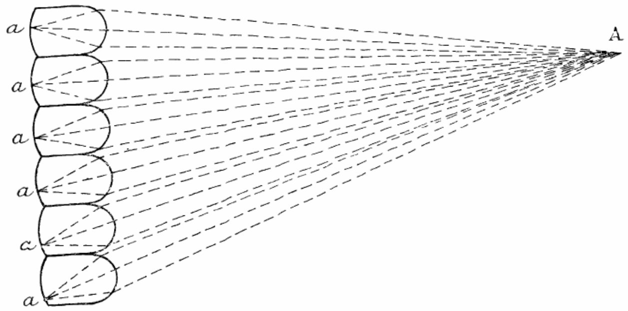

FIG. 1.

Par M. G. Lippmann, (**1908**),
Epreuves reversibles donnant la sensation du relief,
Phys. Theor. Appl. 7, p.821-825

Plenoptics

Plenoscope

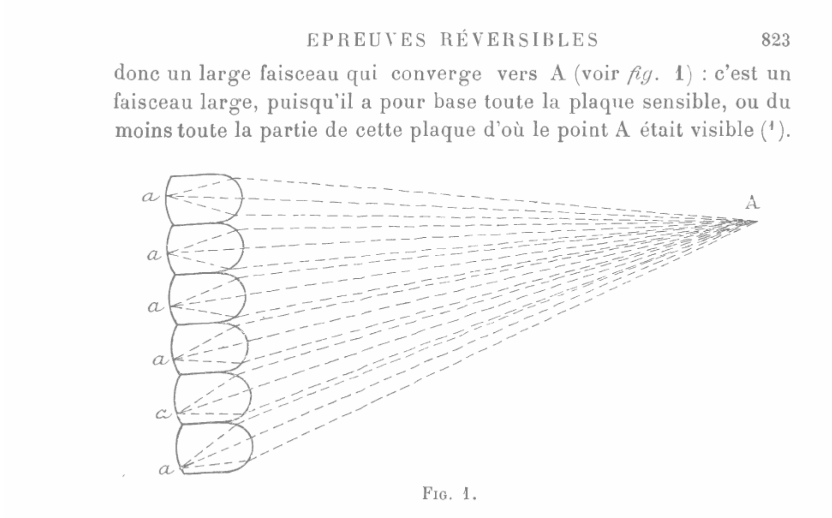

EPREUVES RÉVERSIBLES 823

donc un large faisceau qui converge vers A (voir *fig.* 1) : c'est un faisceau large, puisqu'il a pour base toute la plaque sensible, ou du moins toute la partie de cette plaque d'où le point A était visible [1].

Fig. 1.

Par M. G. Lippmann, (**1908**),
Epreuves reversibles donnant la sensation du relief,
Phys. Theor. Appl. 7, p.821-825

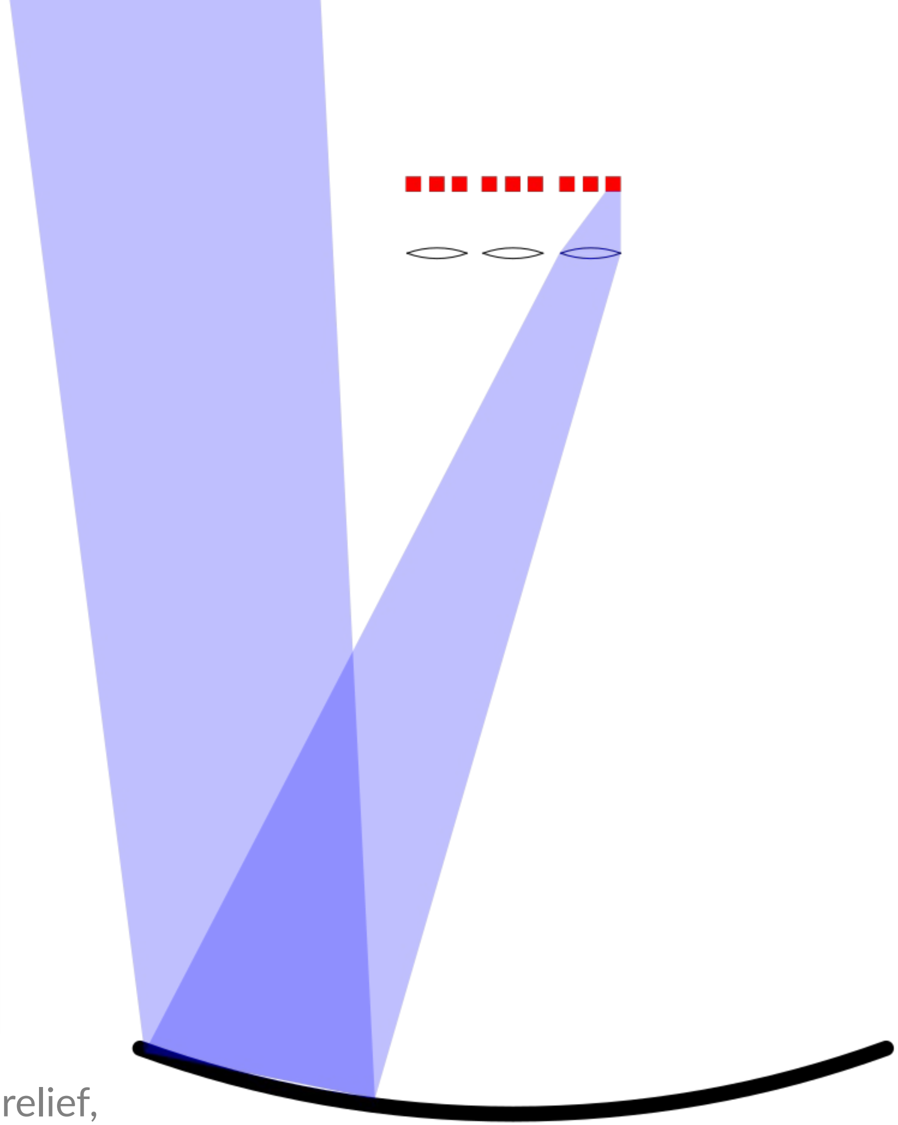

Plenoptics

Plenoscope

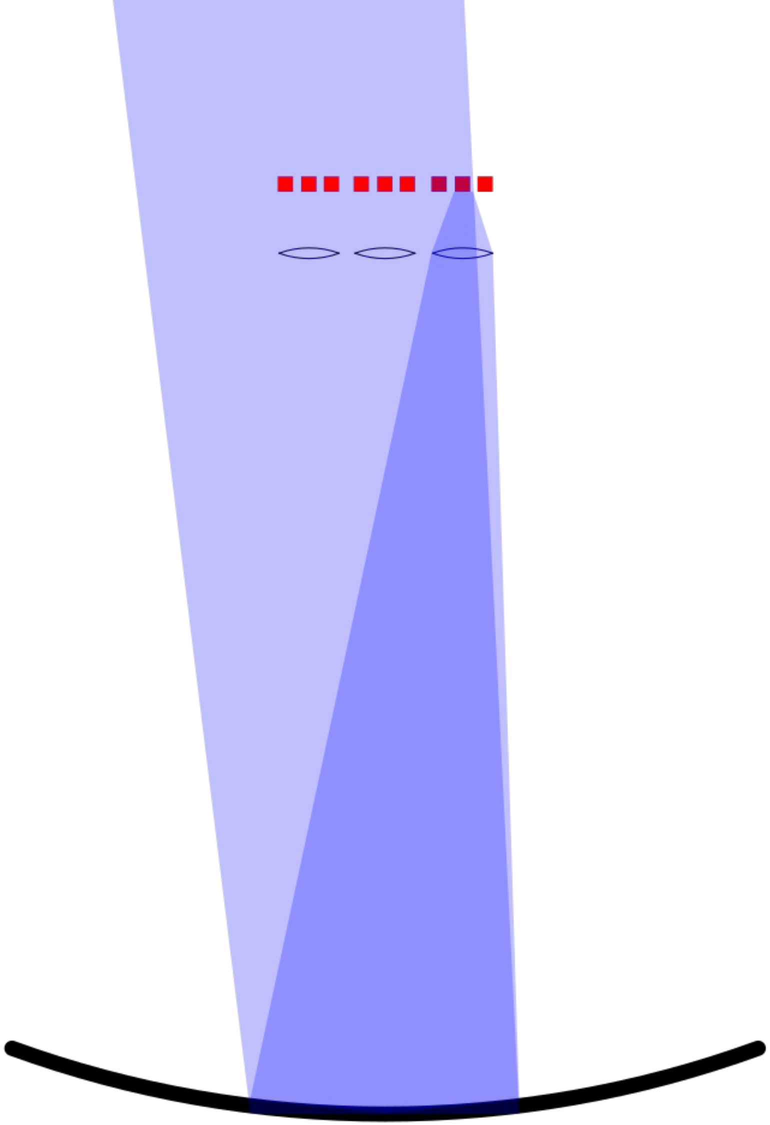

Plenoptics

Plenoscope

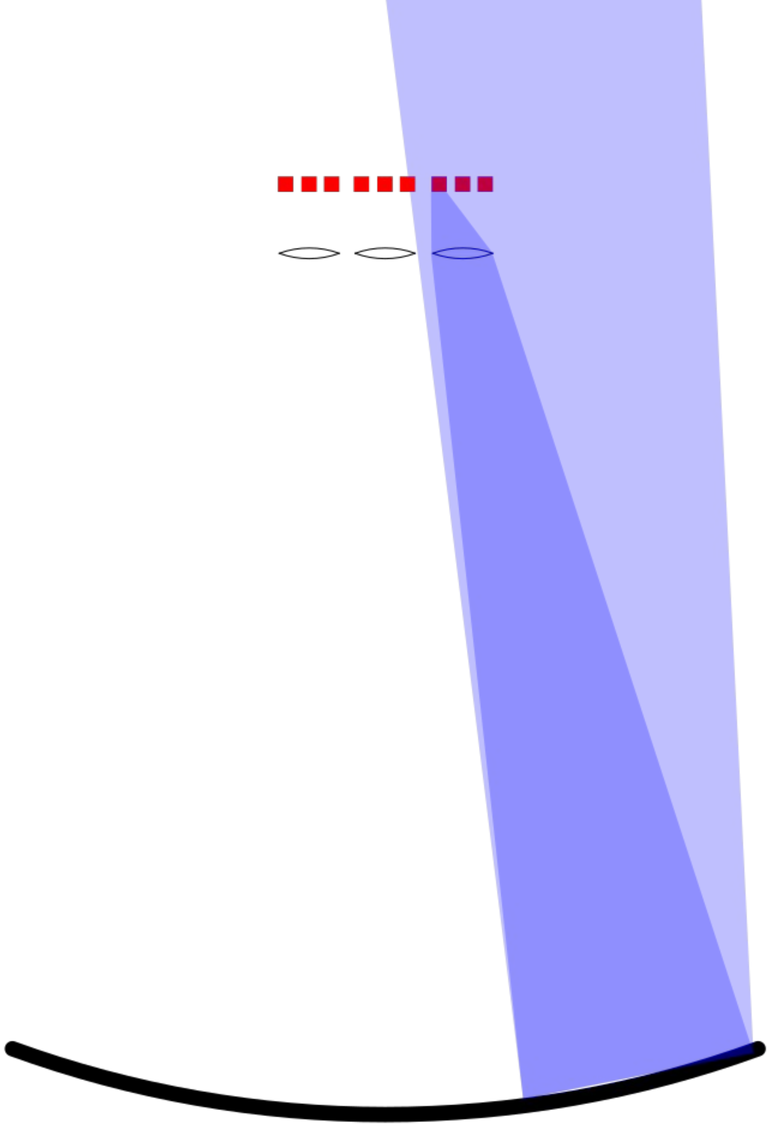

Plenoptics

Plenoscope

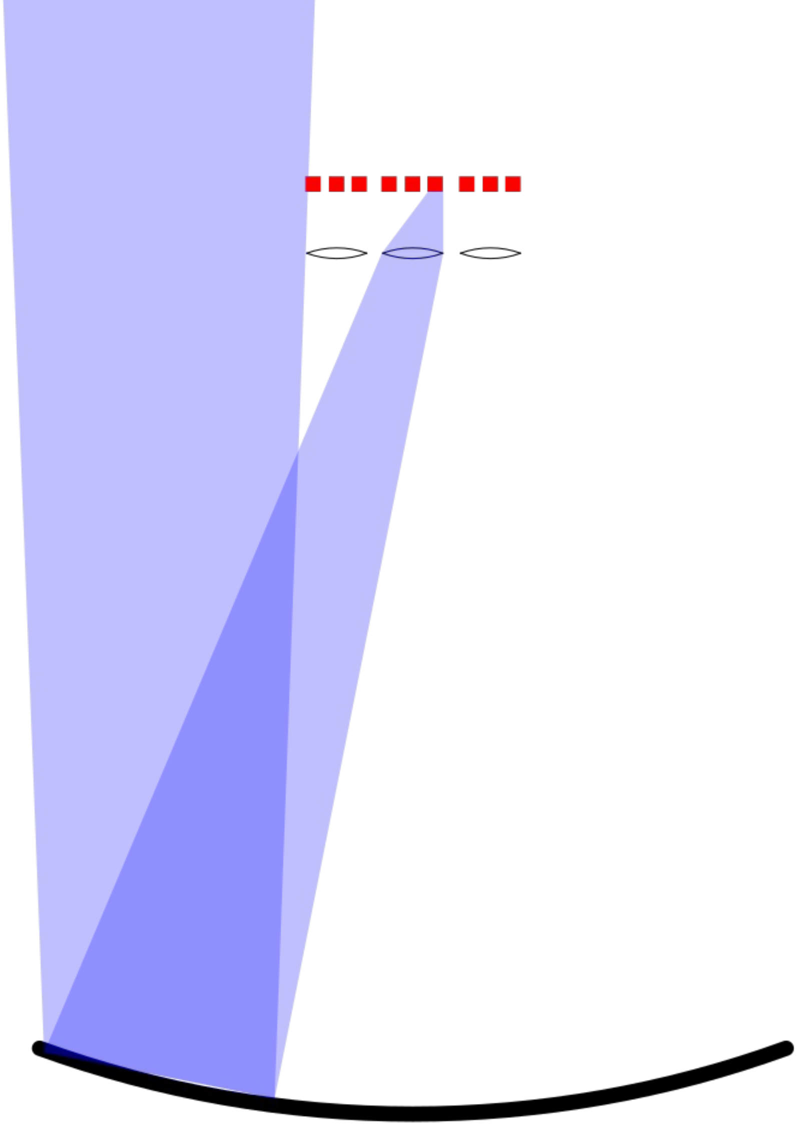

Plenoptics

Plenoscope

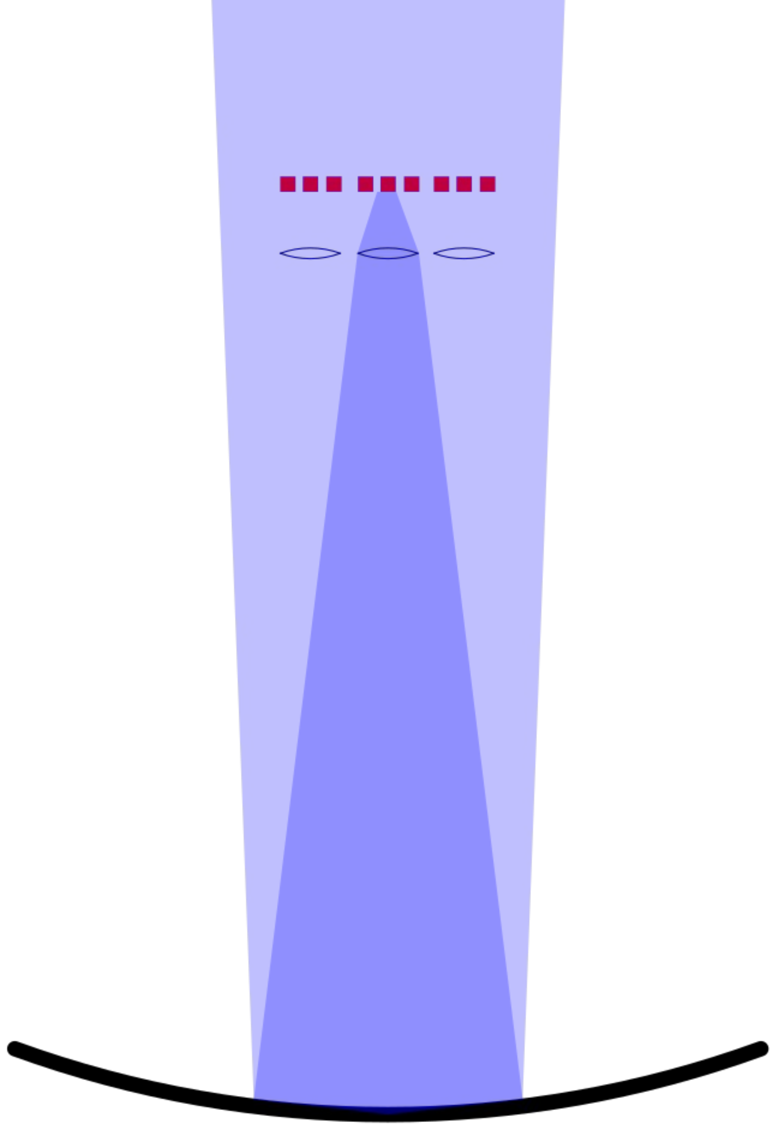

Plenoptics

Plenoscope

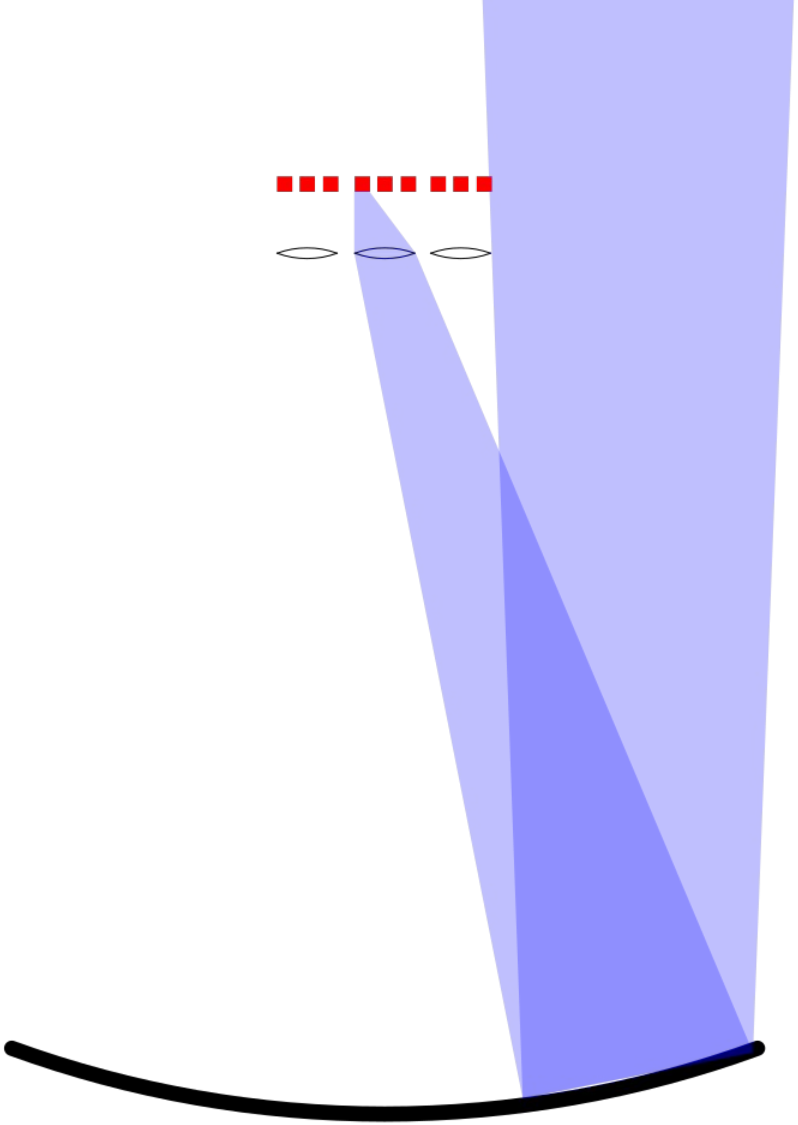

Plenoptics

Plenoscope

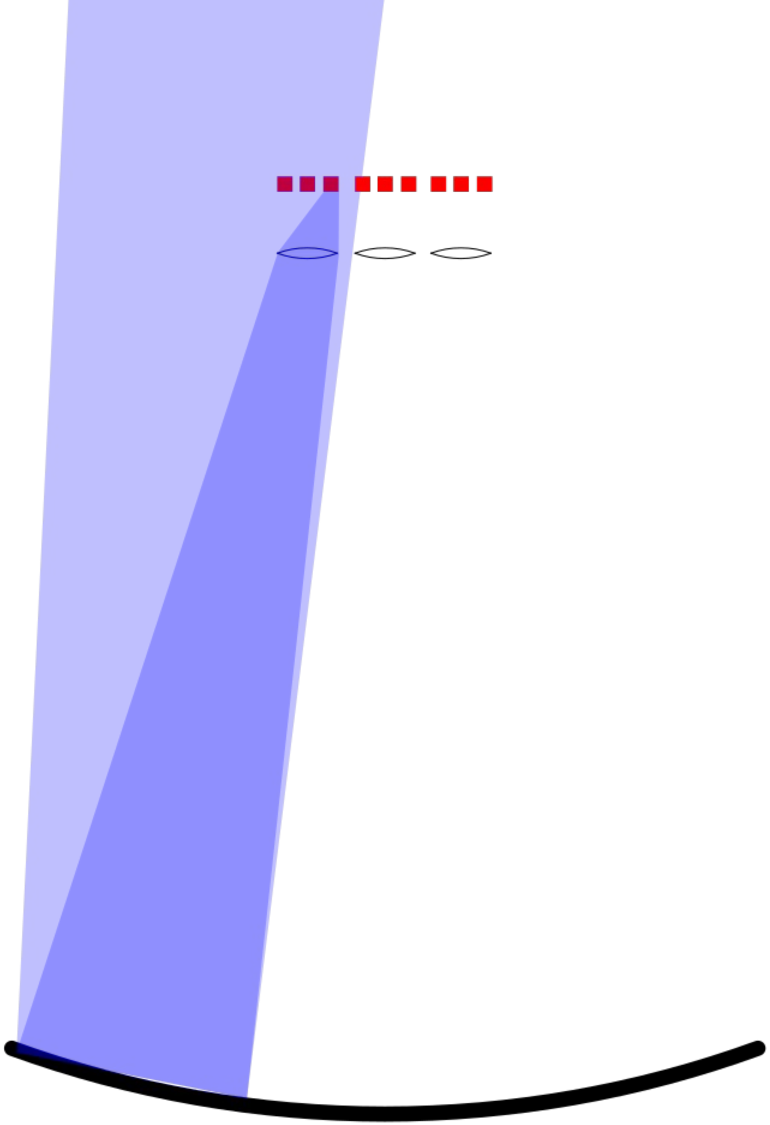

Plenoptics

Plenoscope

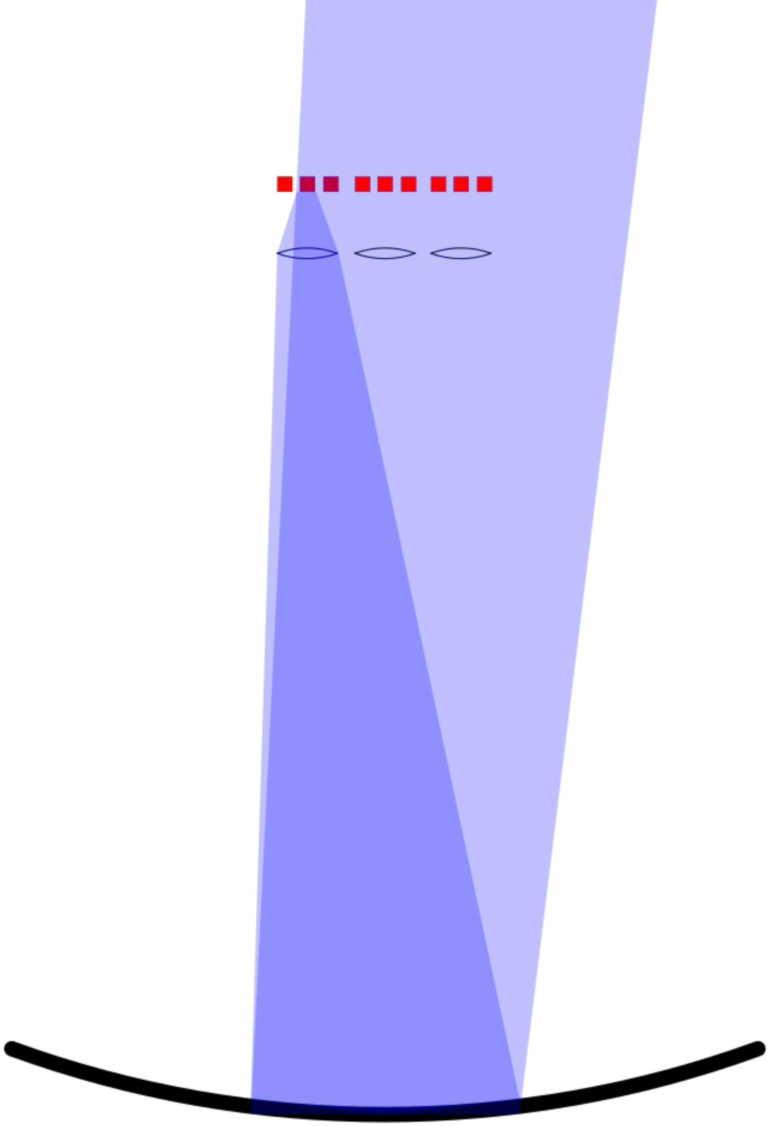

Plenoptics

Plenoscope

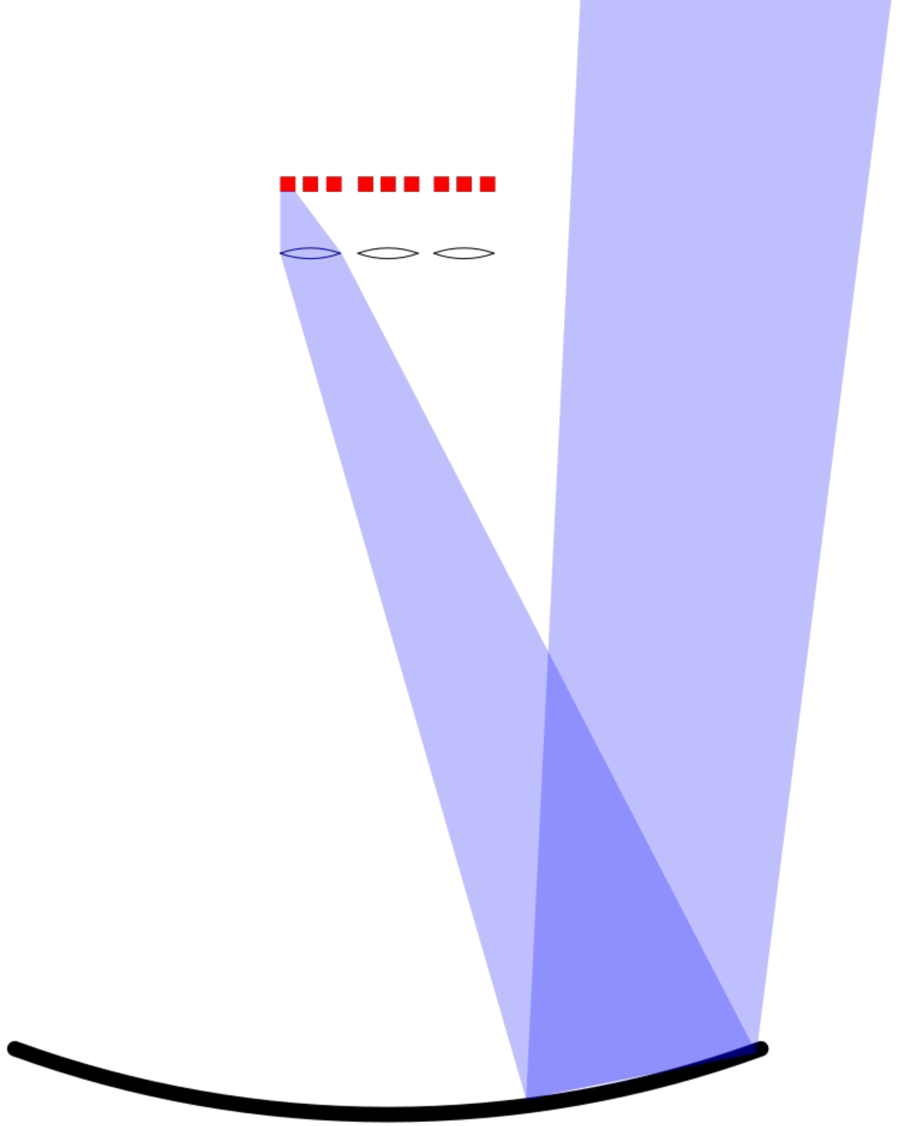

Plenoptics

Plenoscope

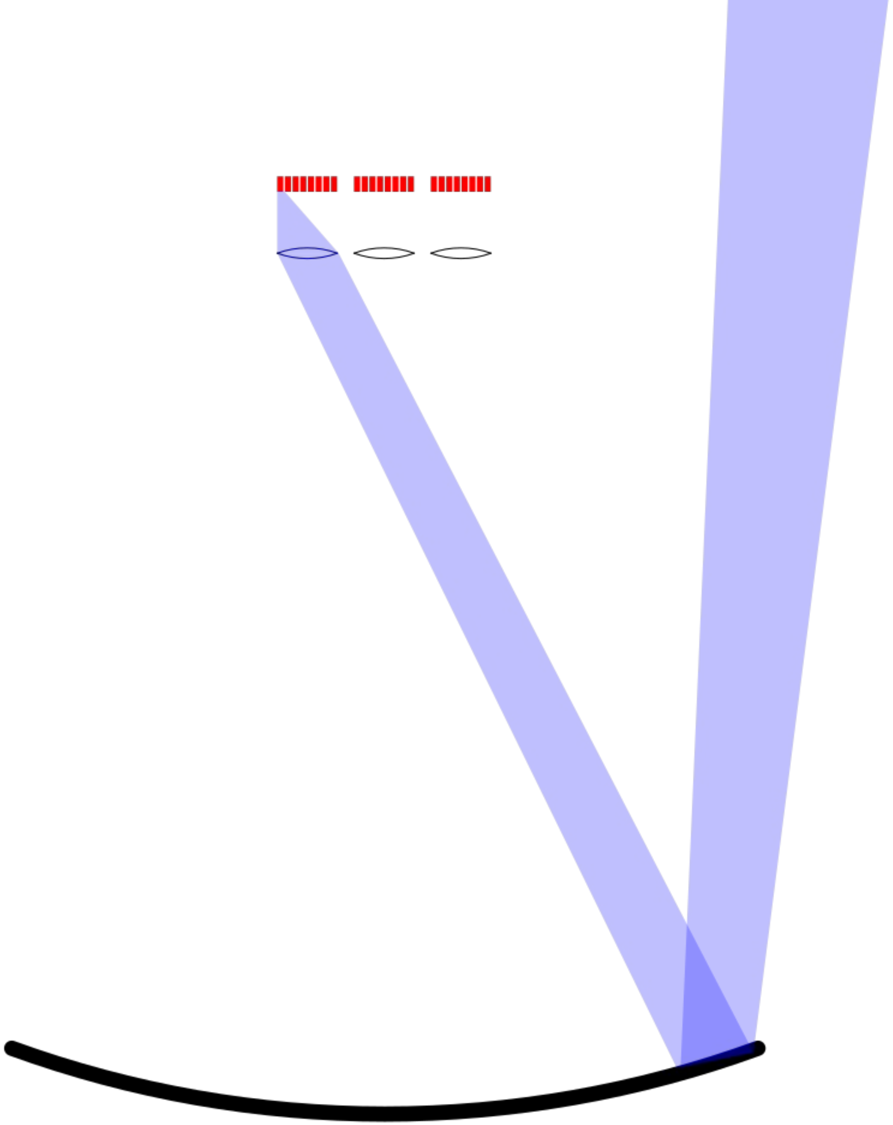

Plenoptics

Plenoscope

Thin-Lens-Model

$$\frac{1}{f} = \frac{1}{\text{depth}} + \frac{1}{b}$$

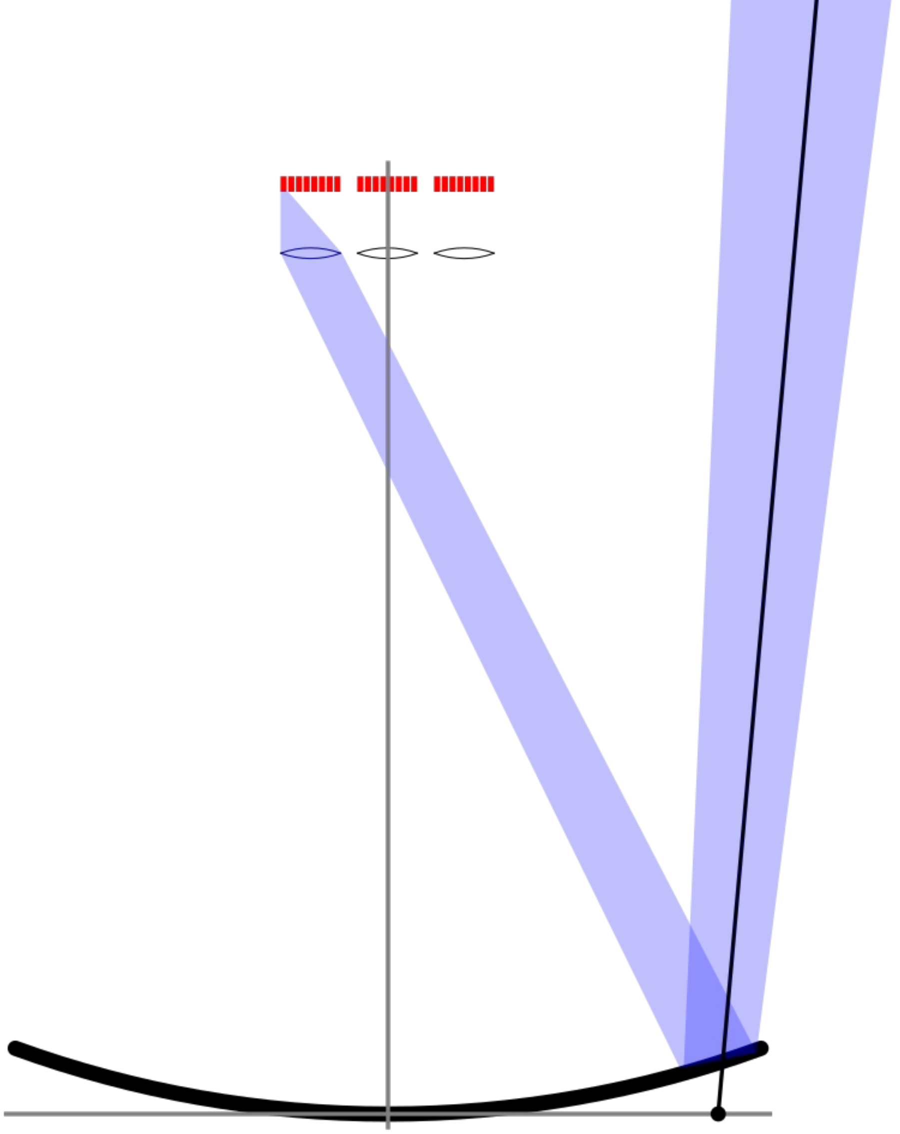

Plenoptics

Plenoscope

Thin-Lens-Model

$$\frac{1}{f} = \frac{1}{\text{depth}} + \frac{1}{b}$$

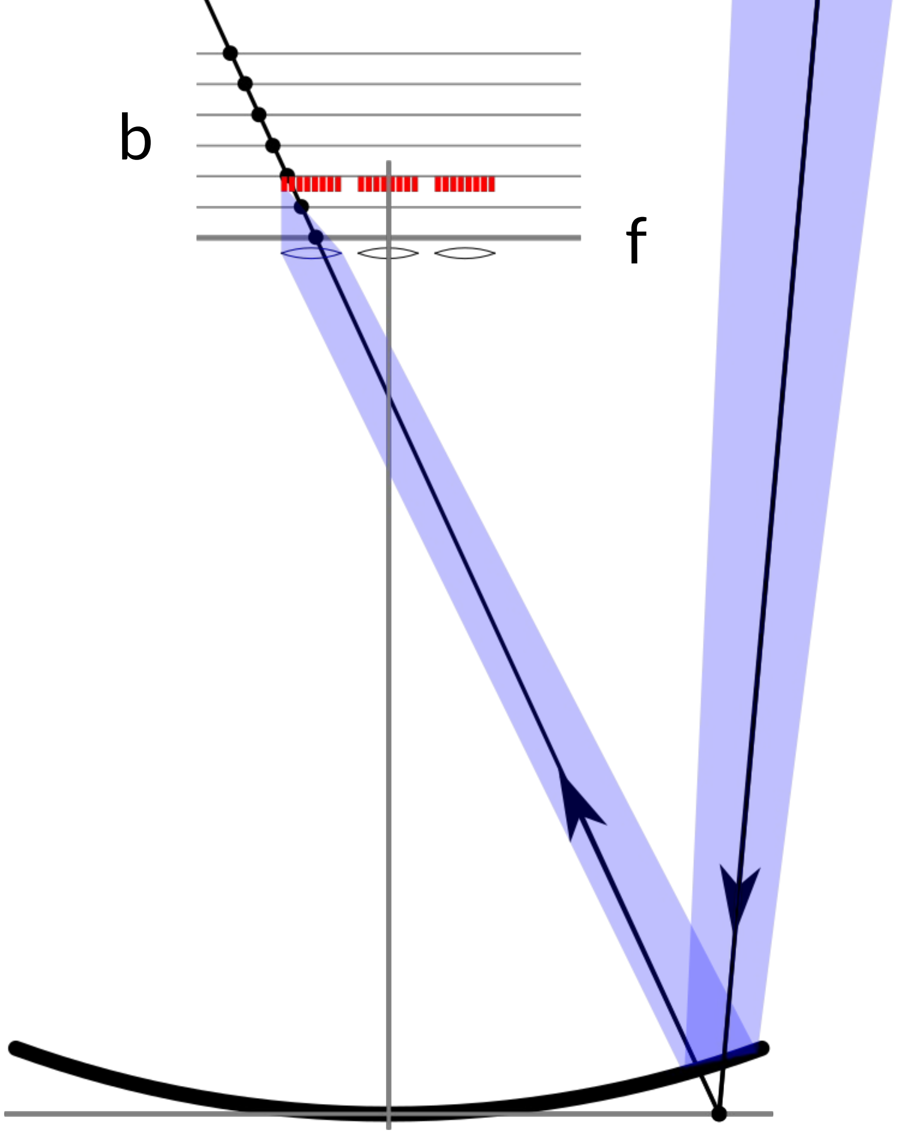

Plenoptics

Plenoscope

Thin-Lens-Model

$$\frac{1}{f} = \frac{1}{\text{depth}} + \frac{1}{b}$$

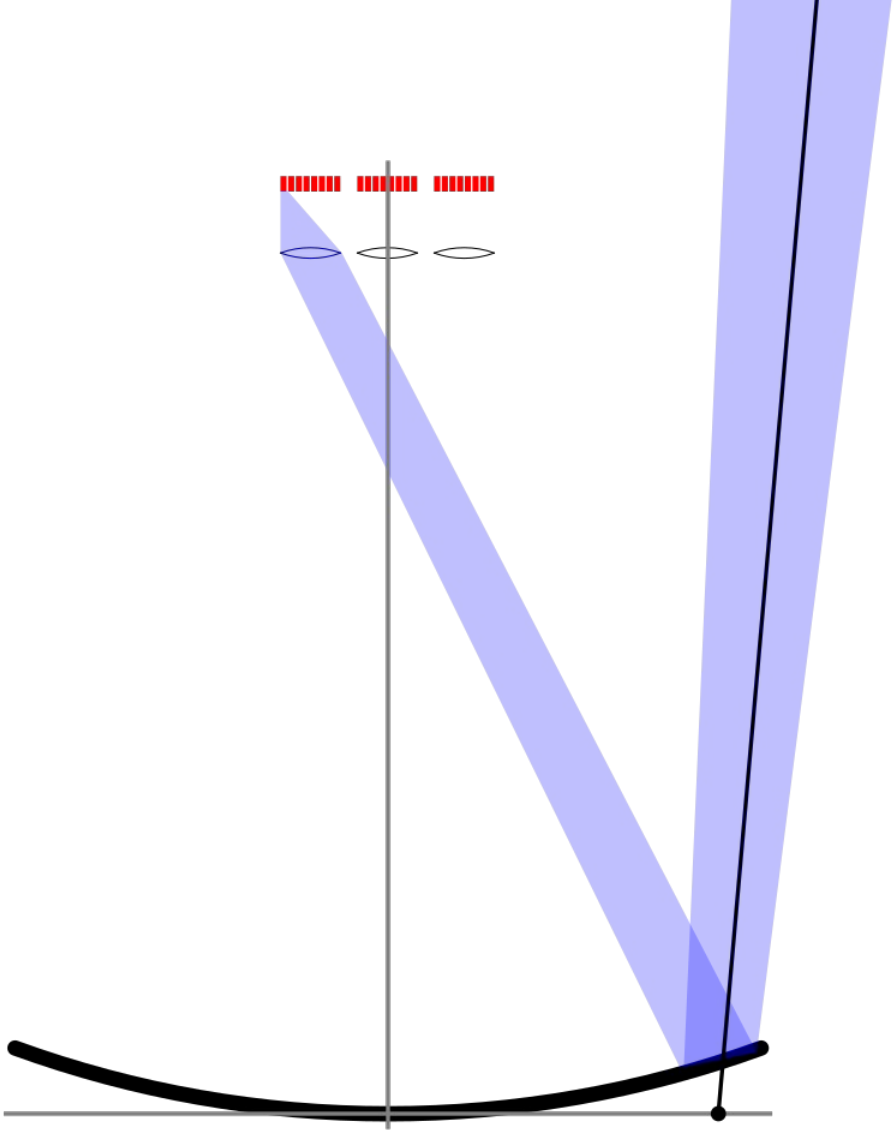

Plenoptics

Plenoscope

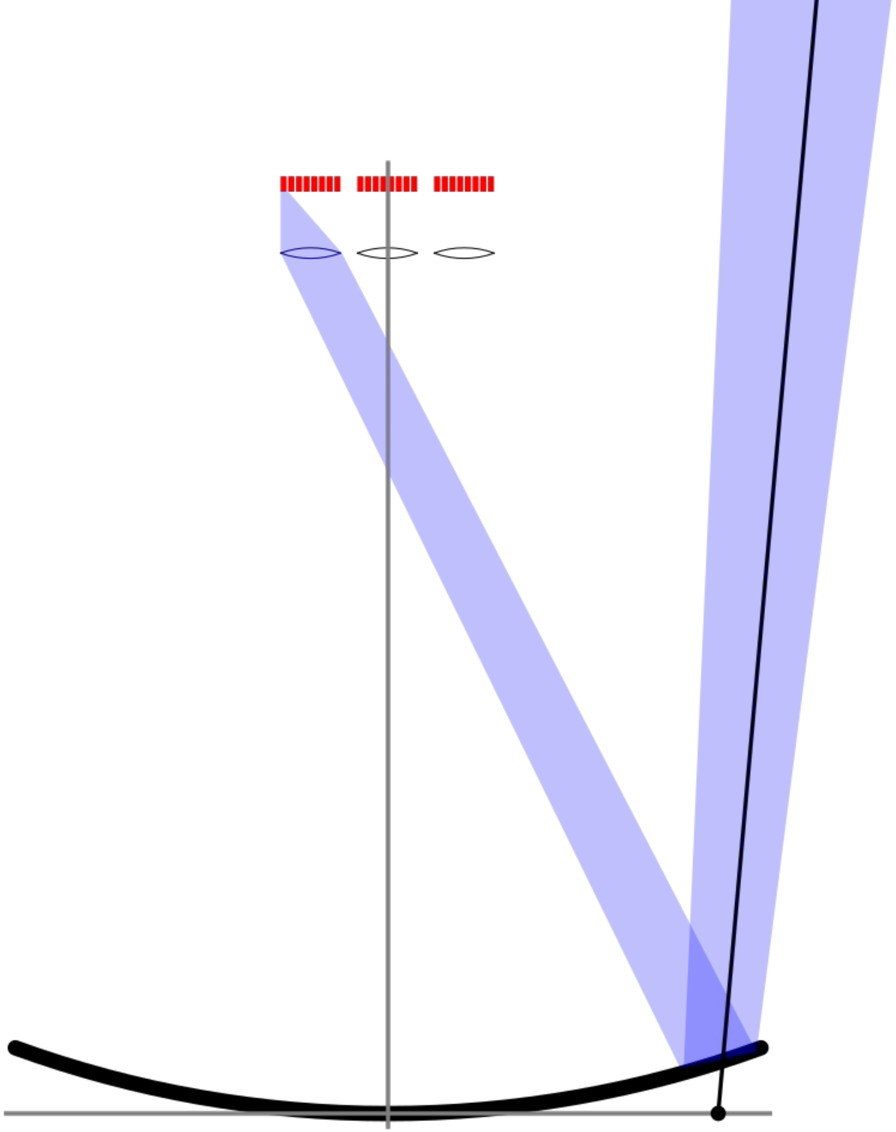

Plenoptics

Plenoscope

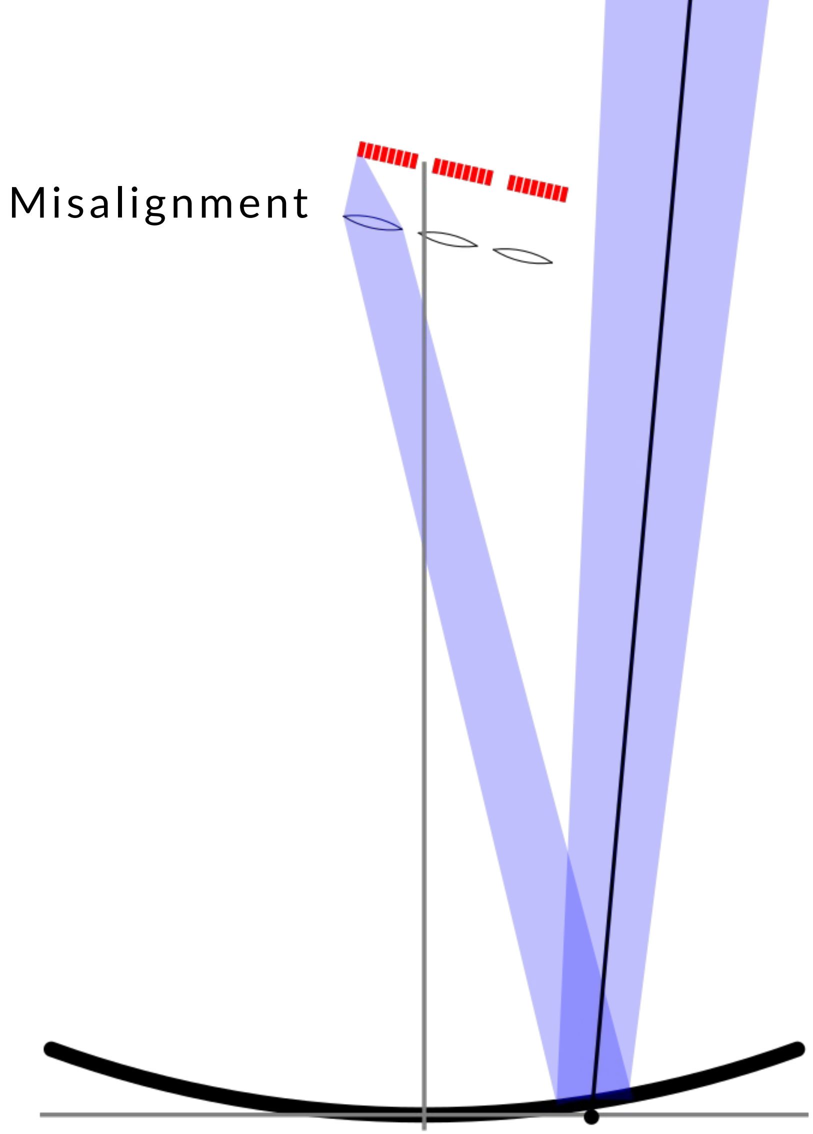

Plenoptics

Plenoscope

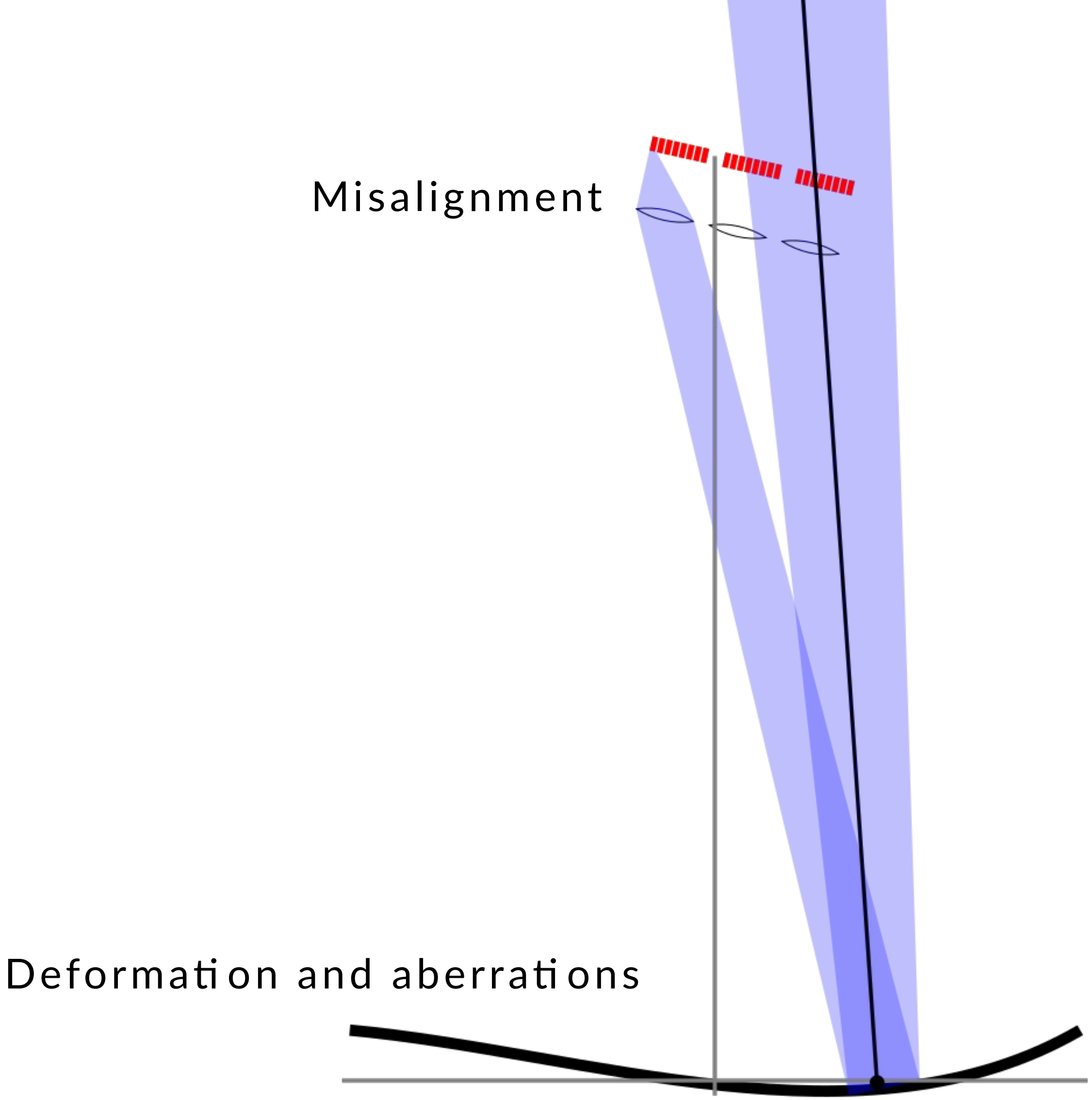

Plenoptics

Plenoscope

Thin-Lens-Model

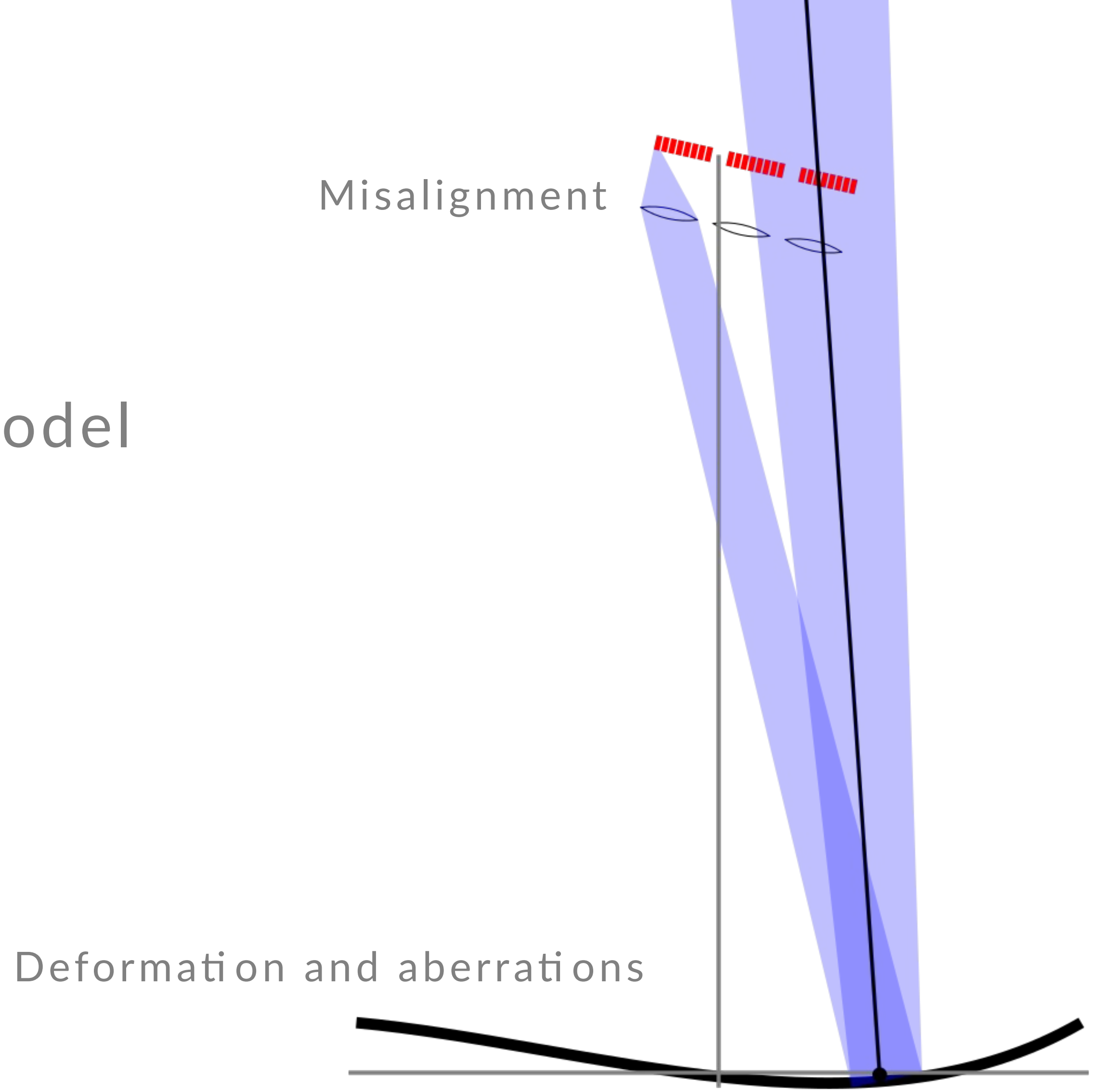

Plenoptics

Thin-Lens-Model

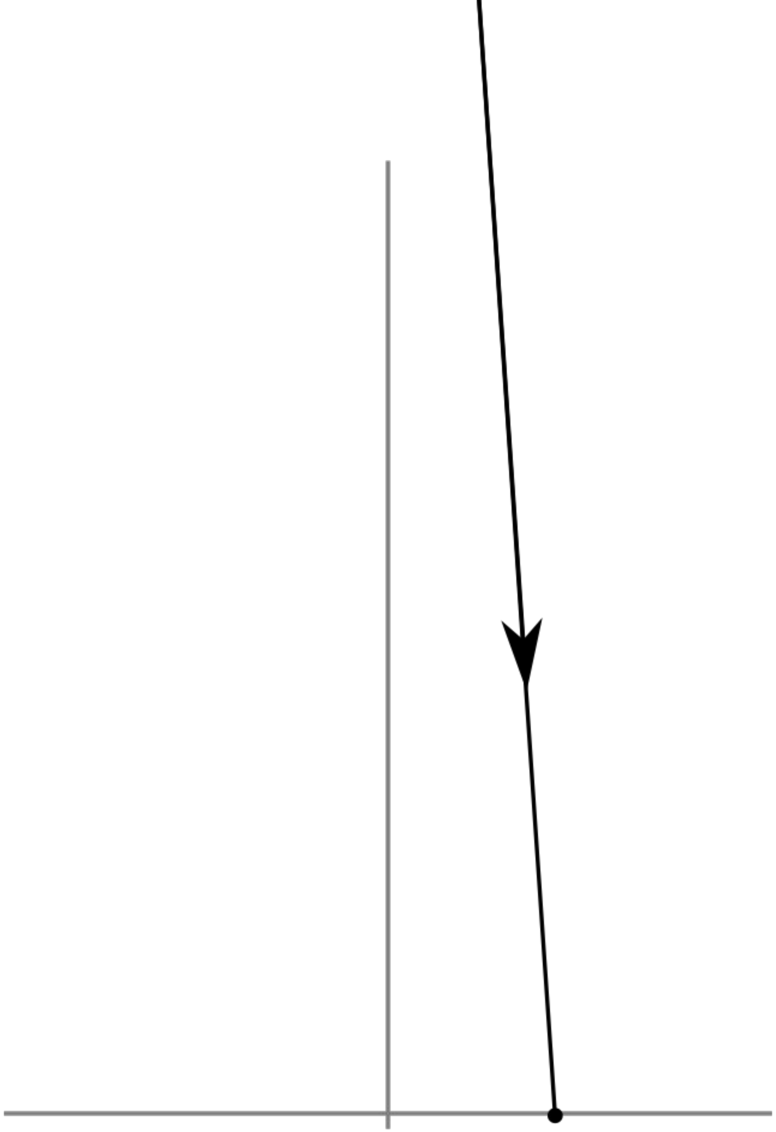

Plenoptics

Thin-Lens-Model

$$\frac{1}{f} = \frac{1}{\text{depth}} + \frac{1}{b}$$

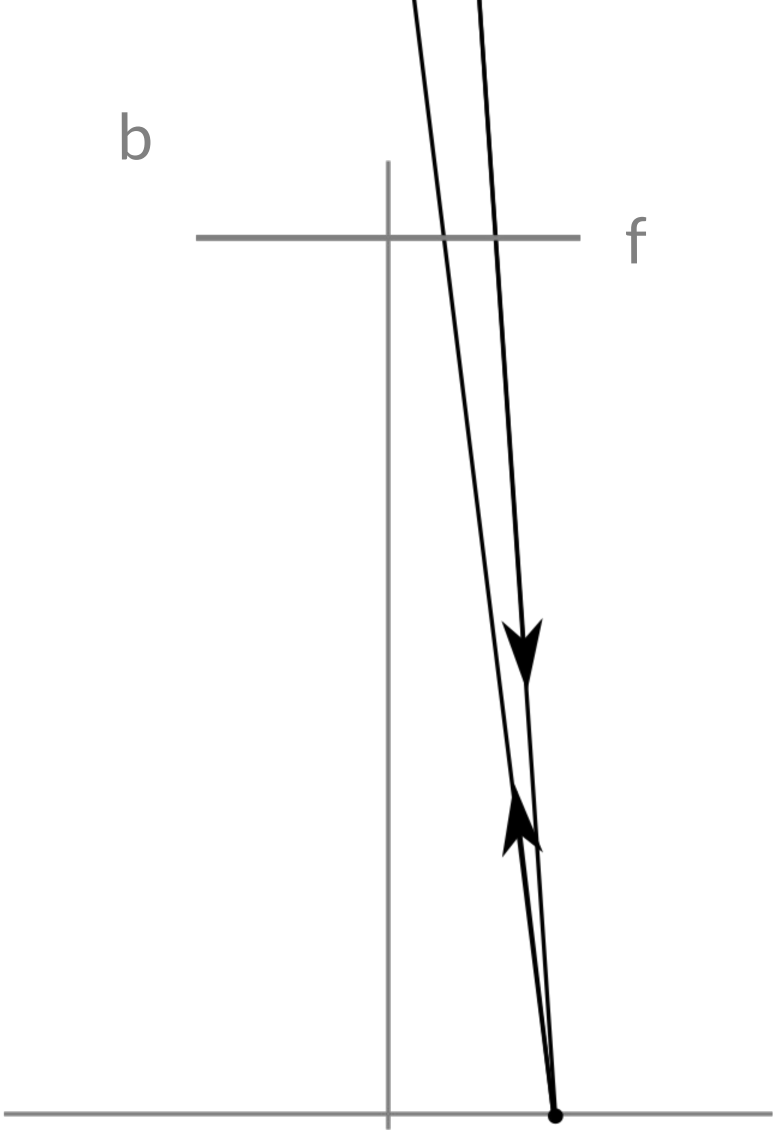

Plenoptics

Thin-Lens-Model

$$\frac{1}{f} = \frac{1}{\text{depth}} + \frac{1}{b}$$

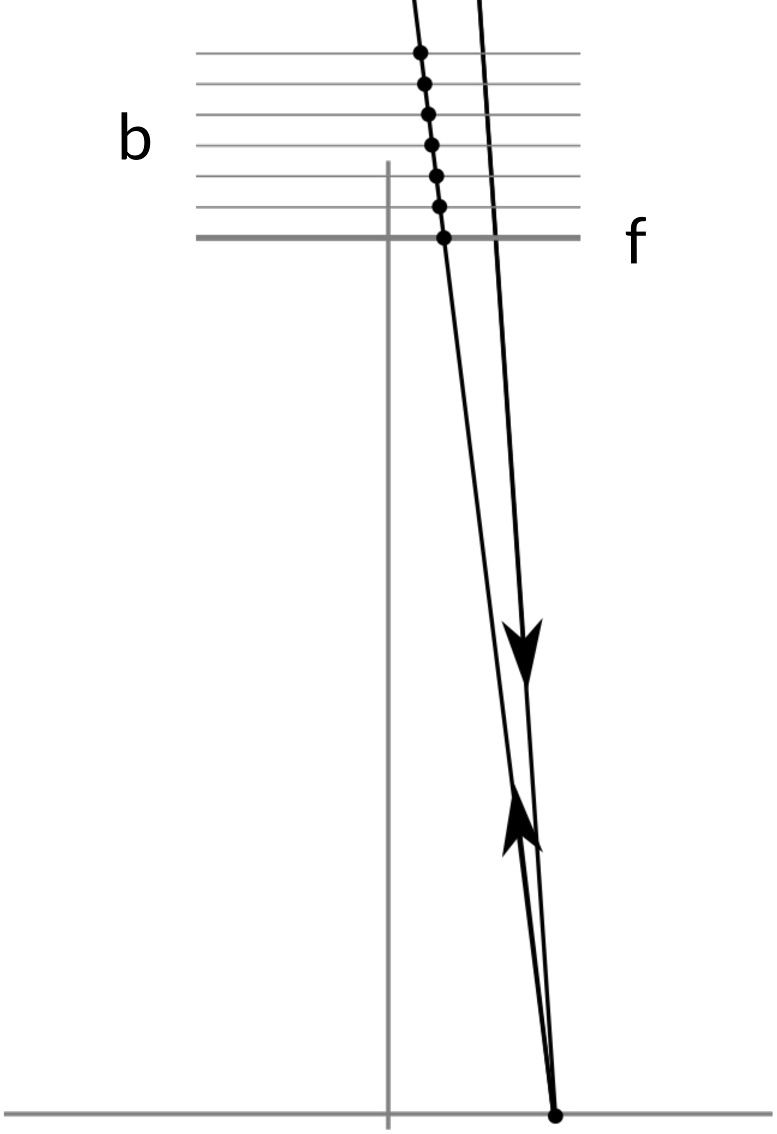

Plenoptics

Plenoscope

Thin-Lens-Model

$$\frac{1}{f} = \frac{1}{\text{depth}} + \frac{1}{b}$$

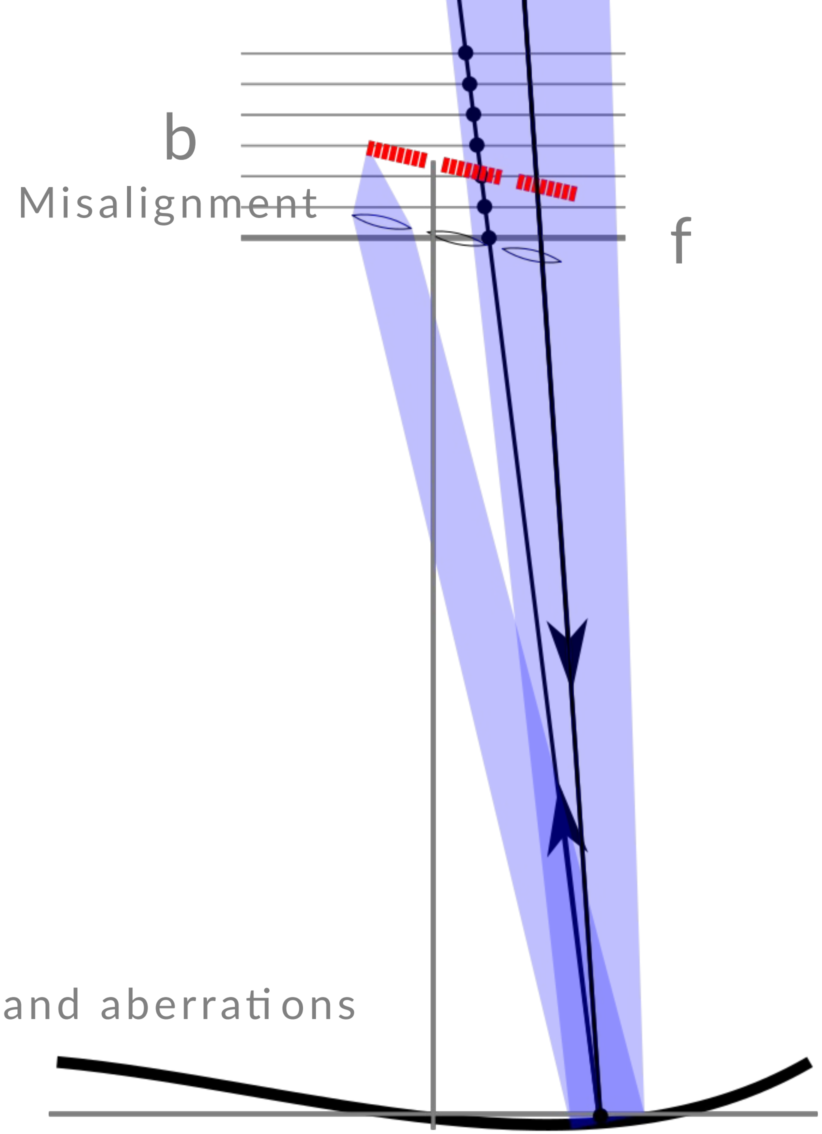

Plenoptics

Plenoscope

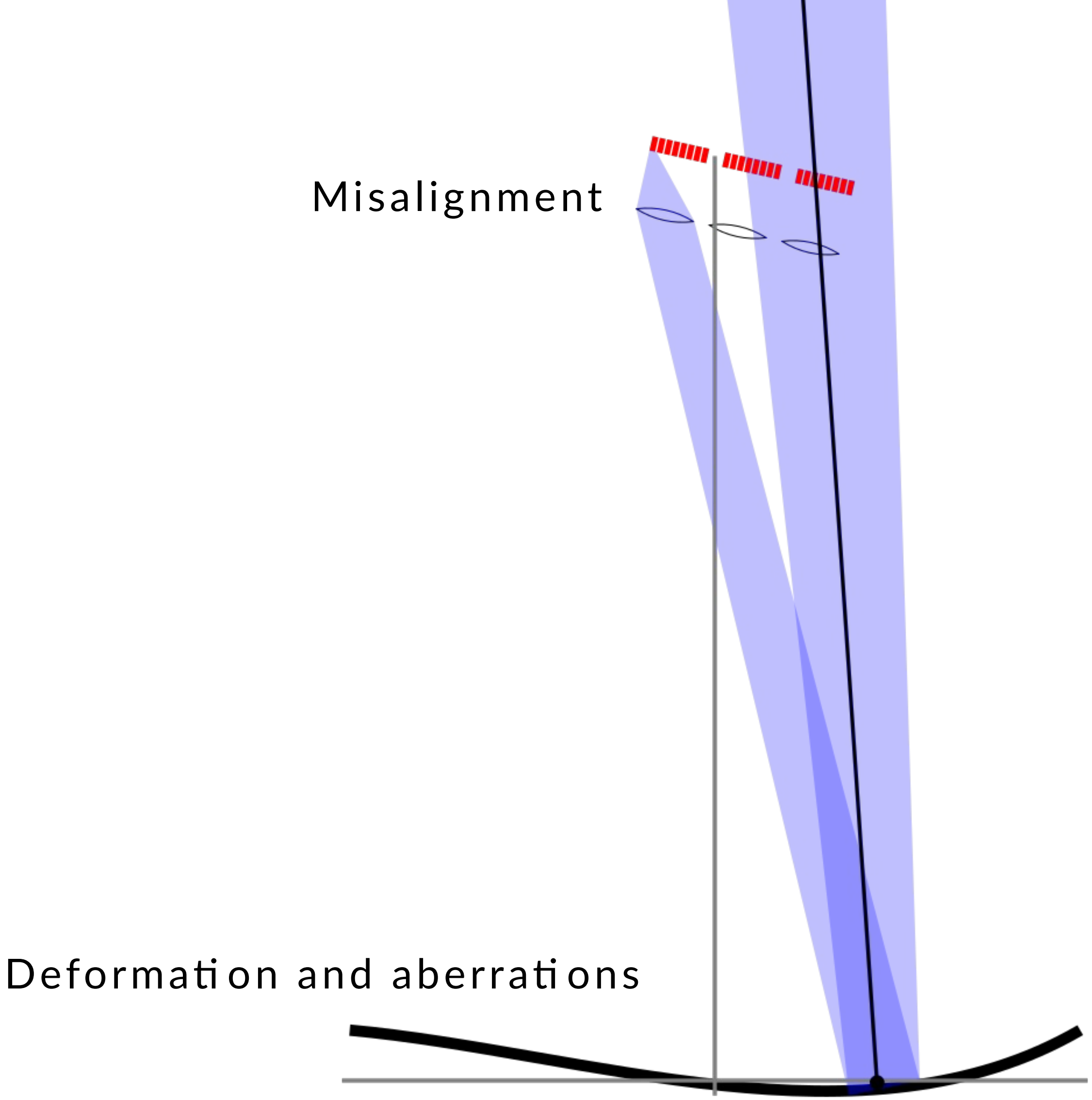

Plenoptics

Plenoscope

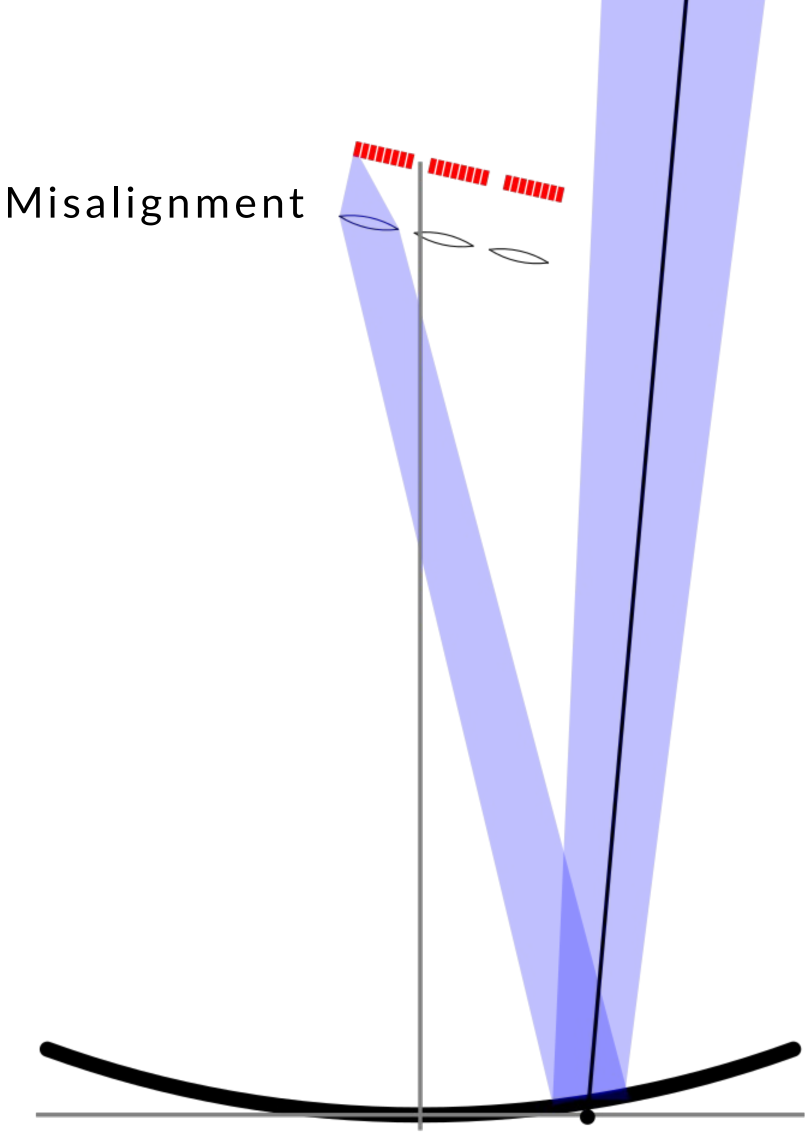

Plenoptics

Plenoscope

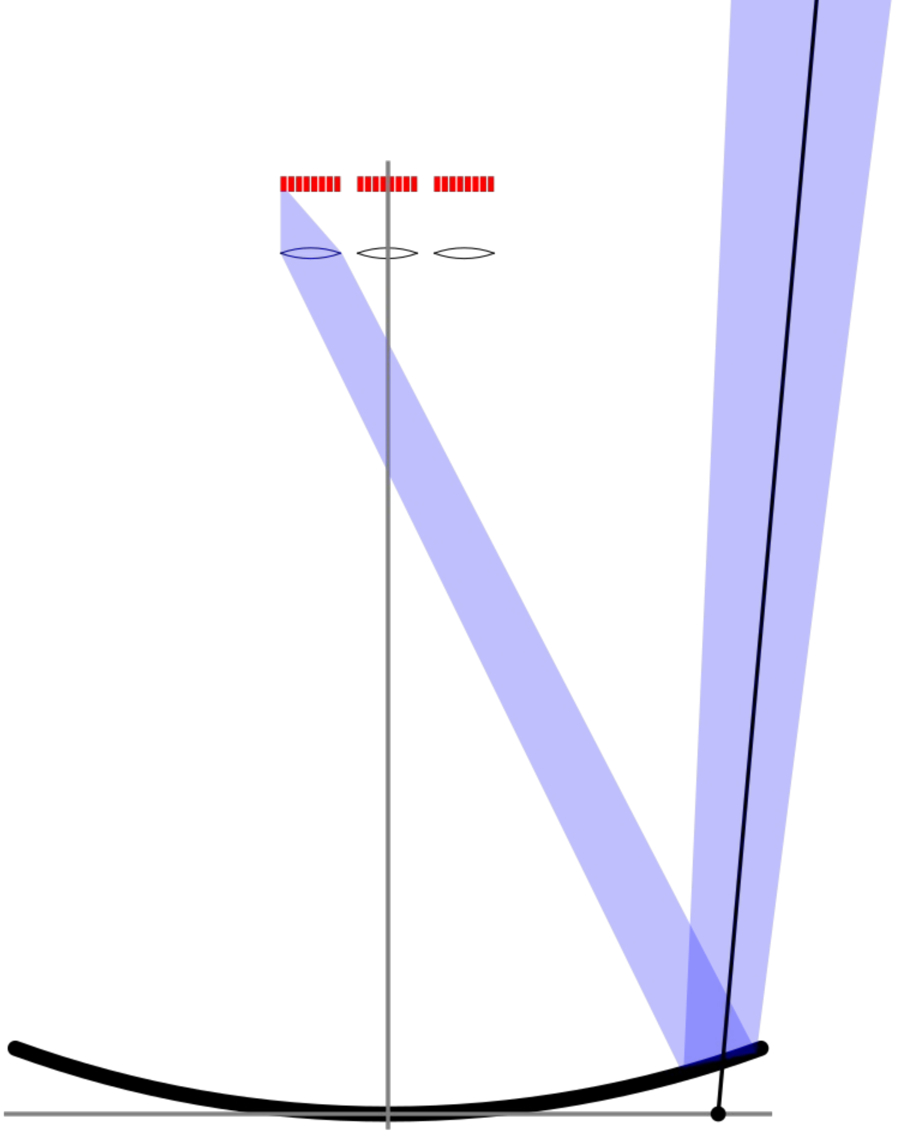

CHERENKOV-PLENOSCOPE

ETH zürich

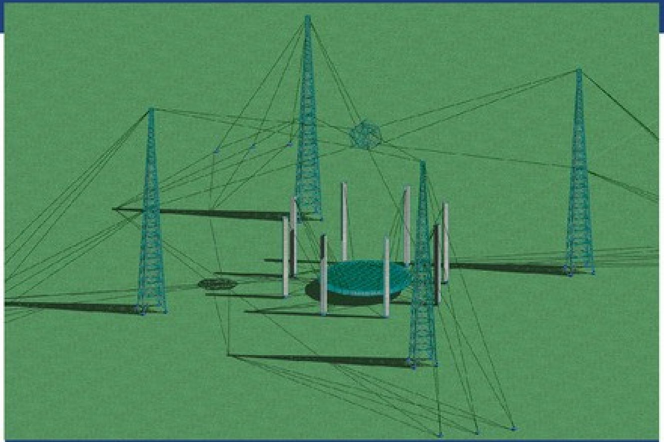

Design of a light weight supporting structure for next generation telescopes

Semester Project Report Spring 2016

Supervision: Professor Chatzi Eleni

Assistants: Egger Adrian, Martín-Sanz Henar

Georgios Zinas and Spyridon Daglas
Report (2016)

Structural Optimization of a Next Generation Gamma-Ray Telescope

Spyridon Daglas

A thesis presented for the degree of:
Master of Science ETH in Bauingenieurwissenschaften
Master of Science ETH in Civil Engineering

Spyridon Daglas
Master-thesis (2017)
in **Civil Engineering**

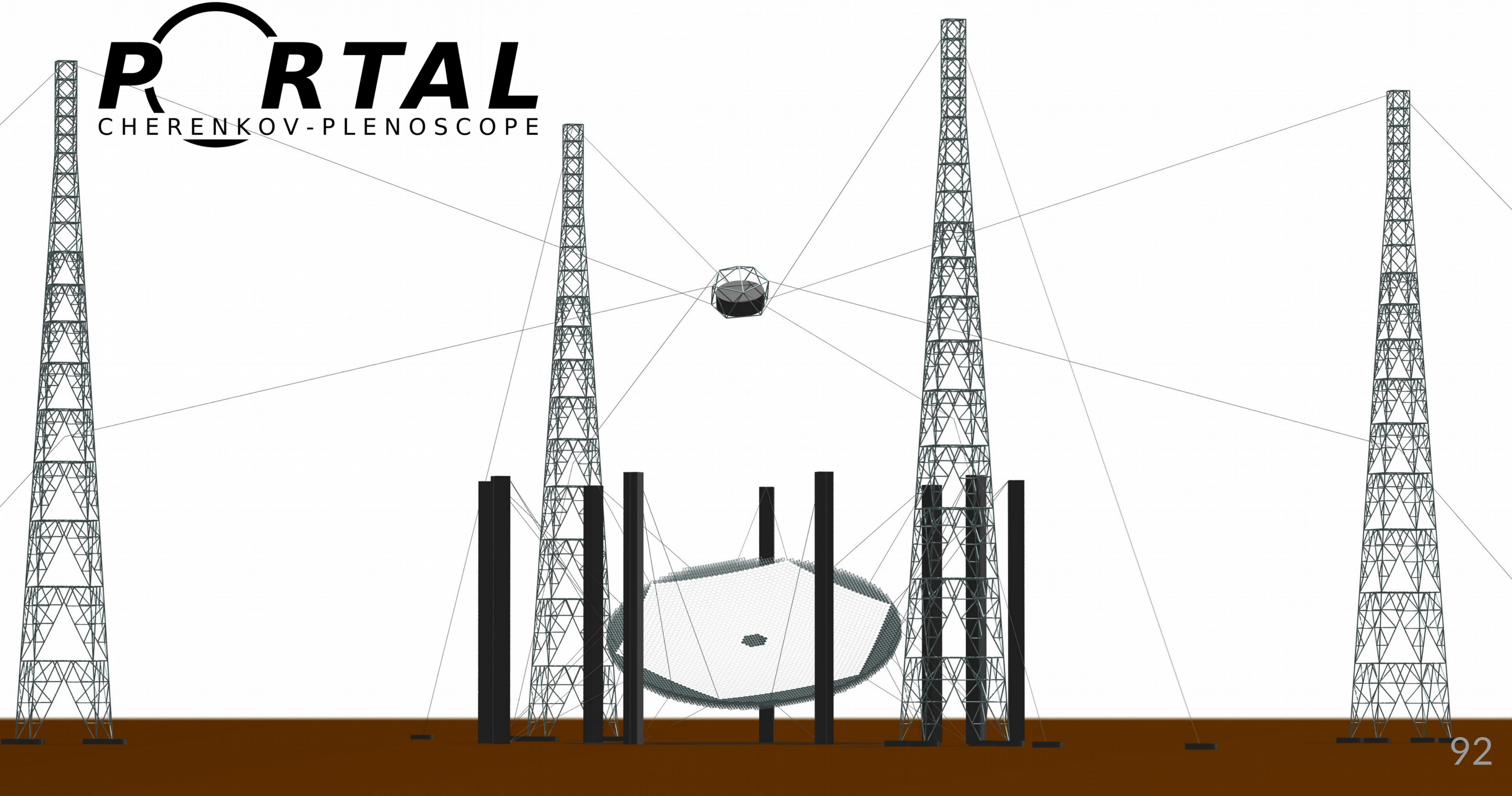
PORTAL
CHERENKOV-PLENOSCOPE

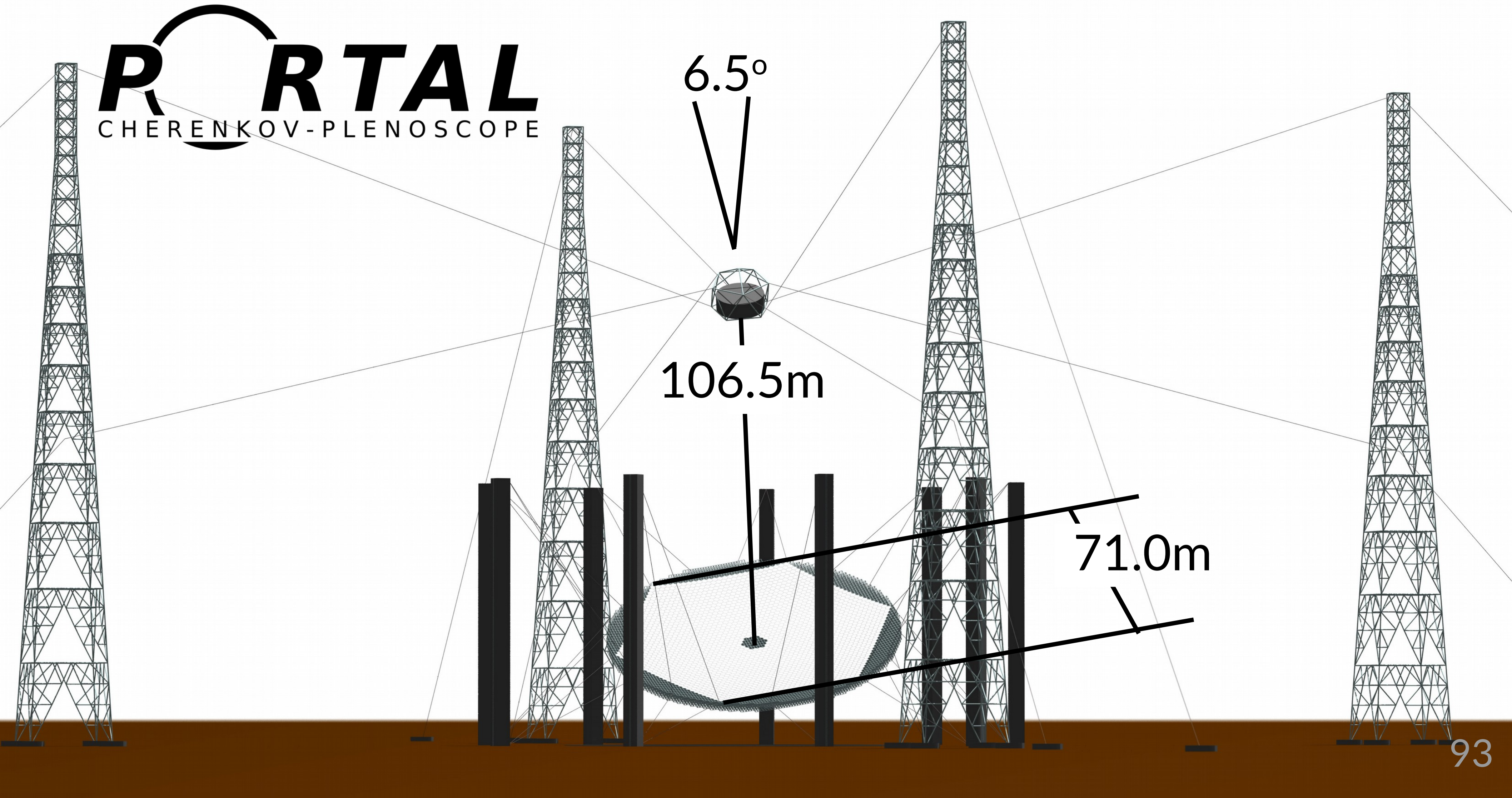
PORTAL
CHERENKOV-PLENOSCOPE
6.5°
106.5m
71.0m

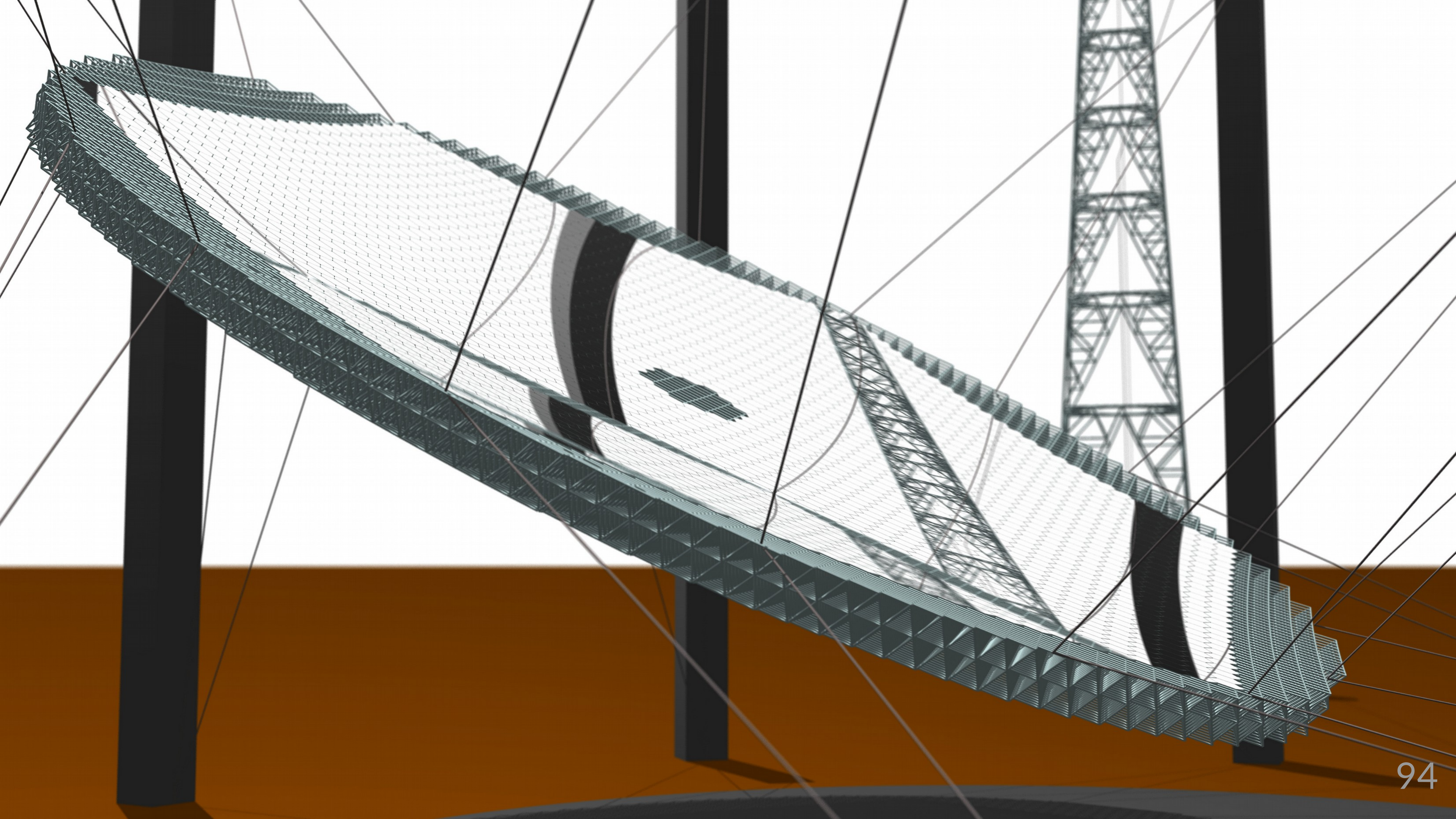

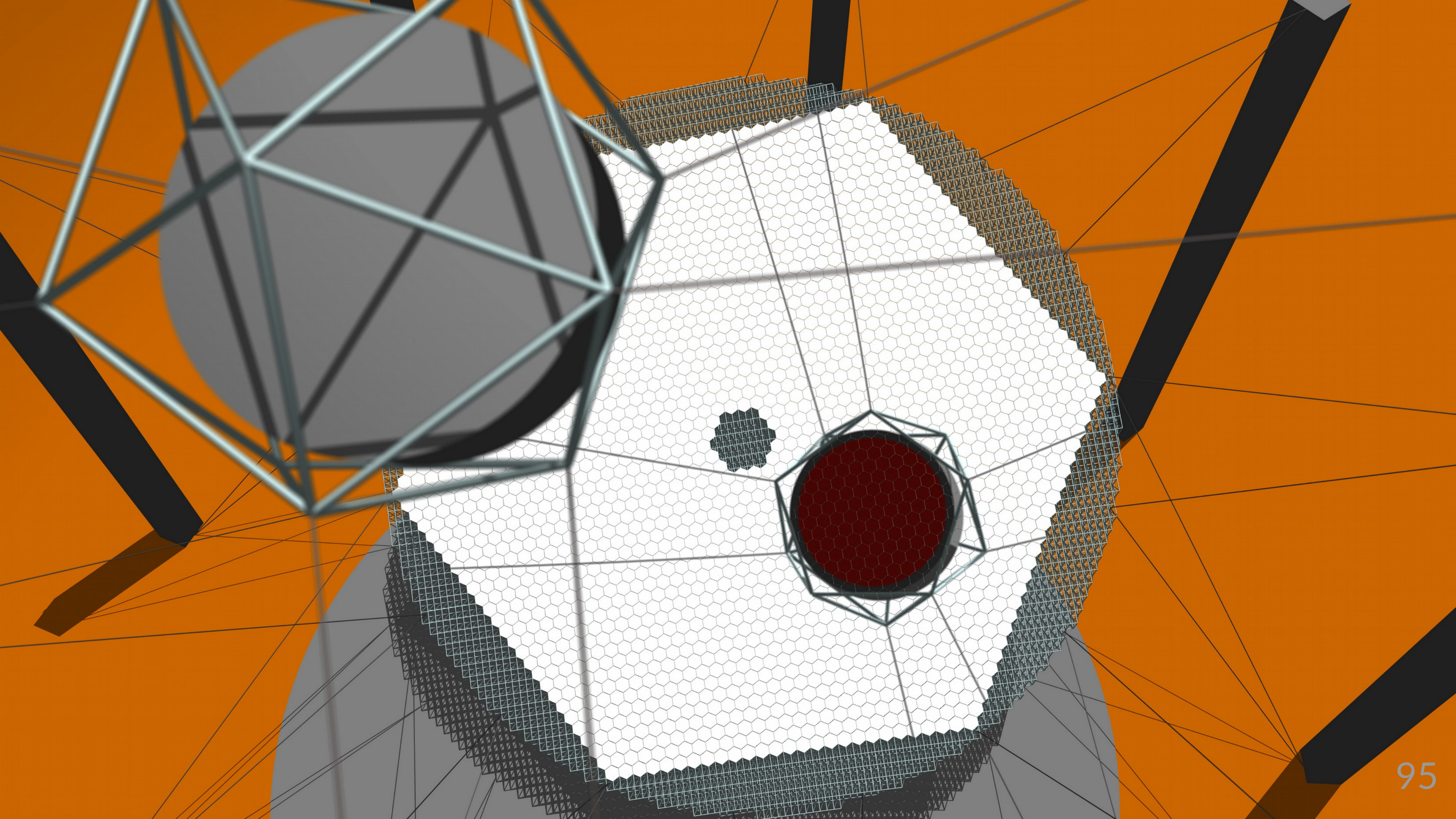

Miermeister, P., et al. (2016). The CableRobot Simulator: Large Scale Motion Platform Based on Cable Robot Technology. In IEEE/RSJ International Conference on Intelligent Robots and Systems.

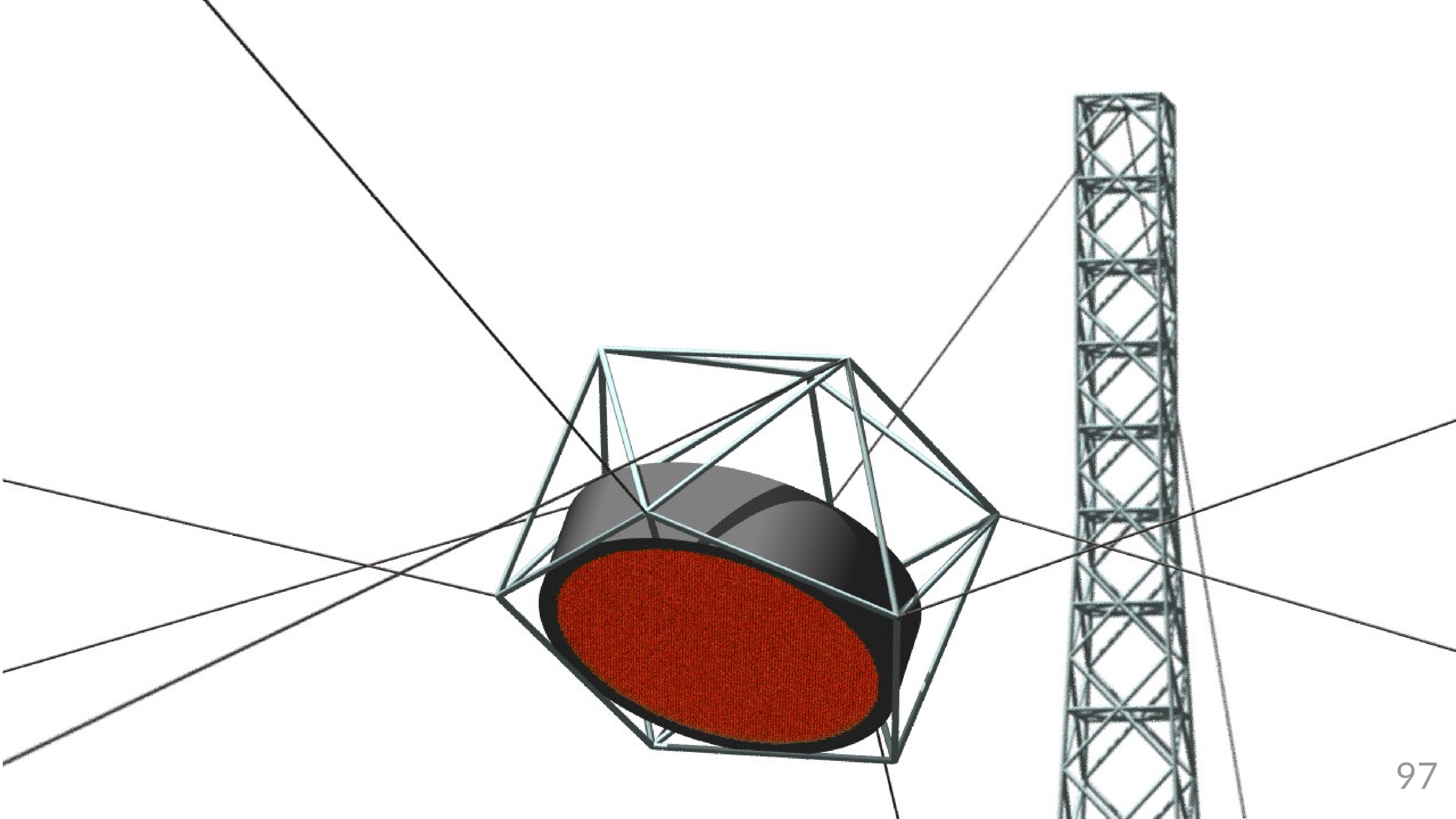

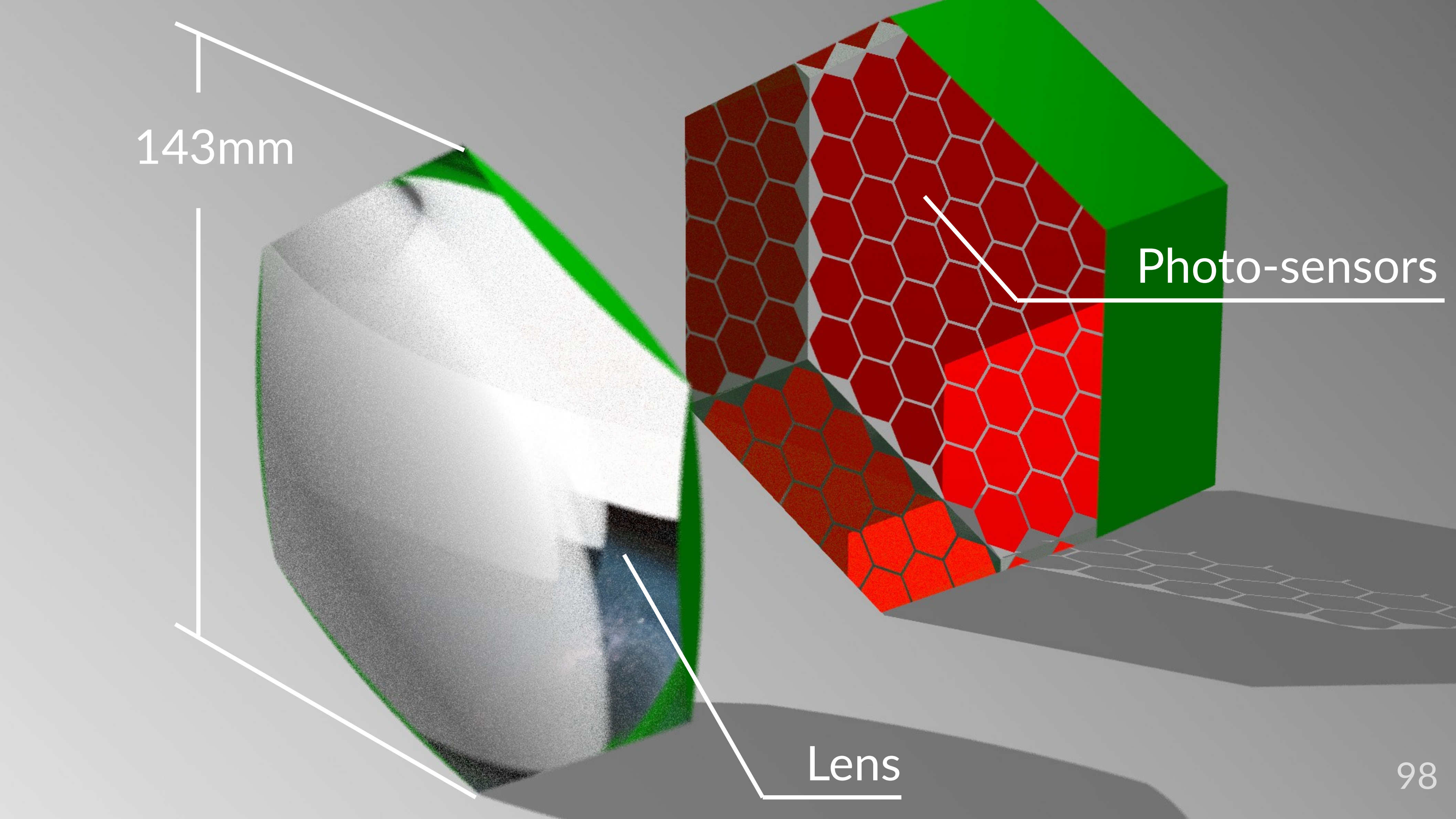
143mm
Photo-sensors
Lens

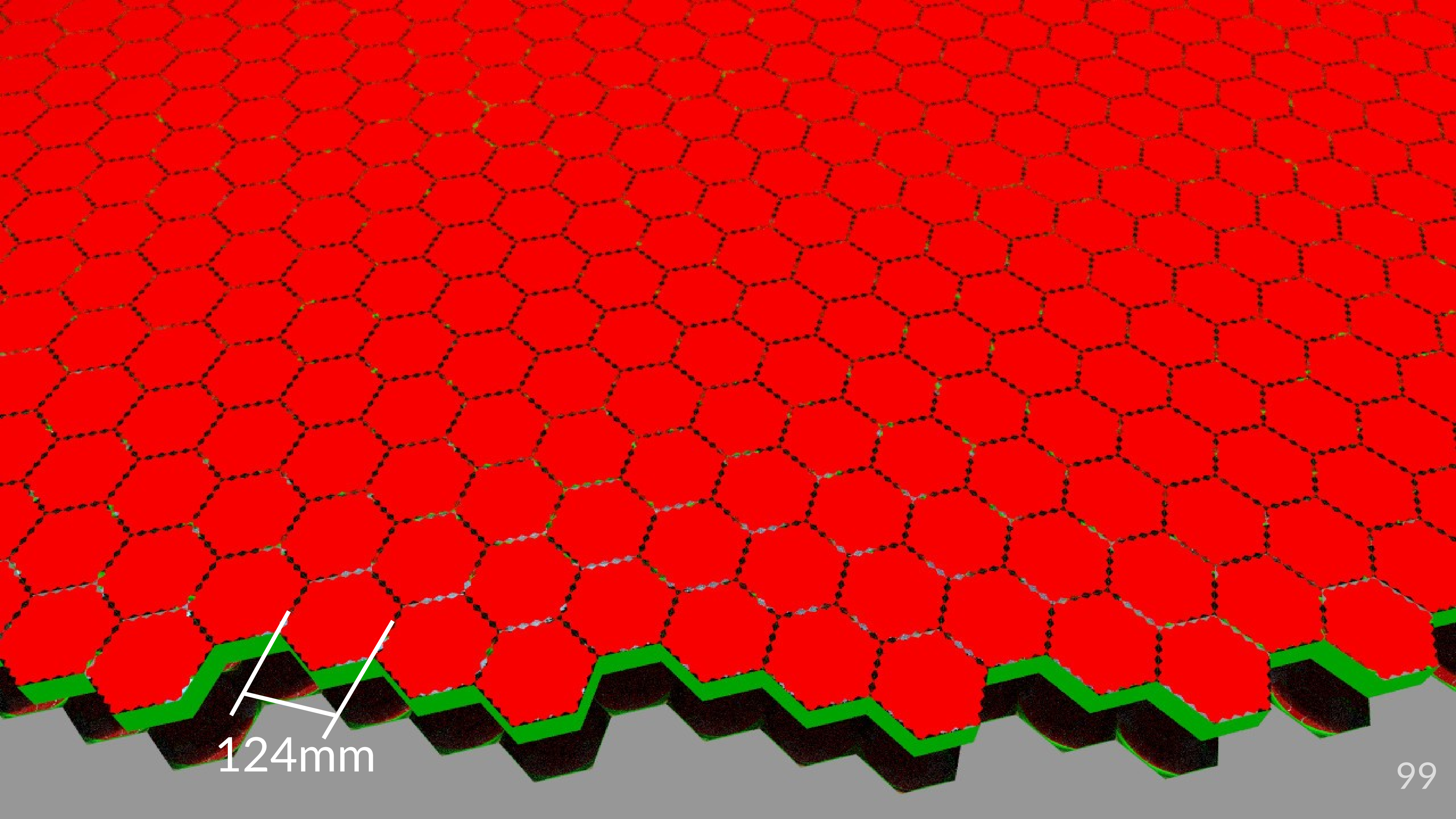
124mm

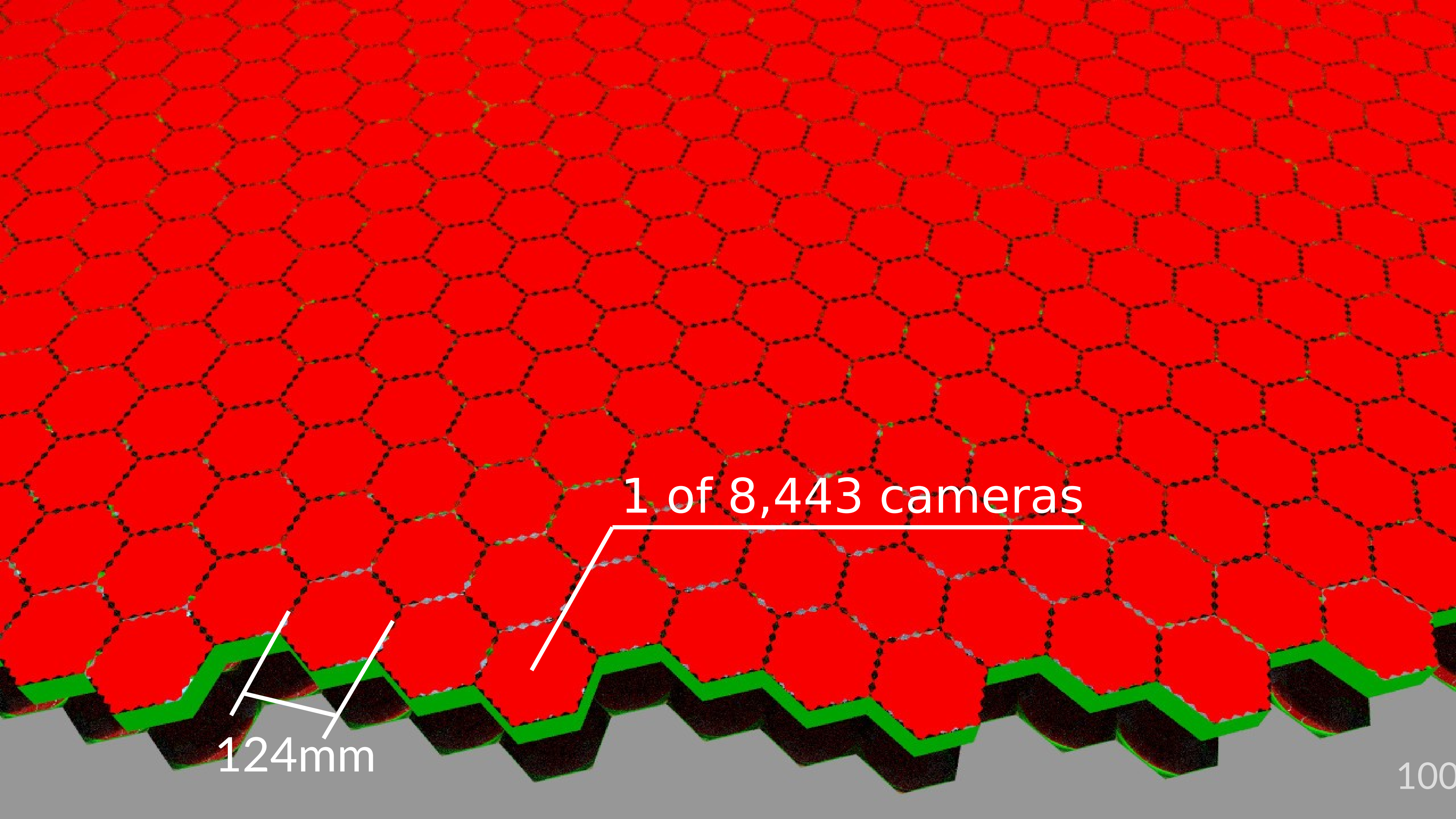
1 of 8,443 cameras
124mm

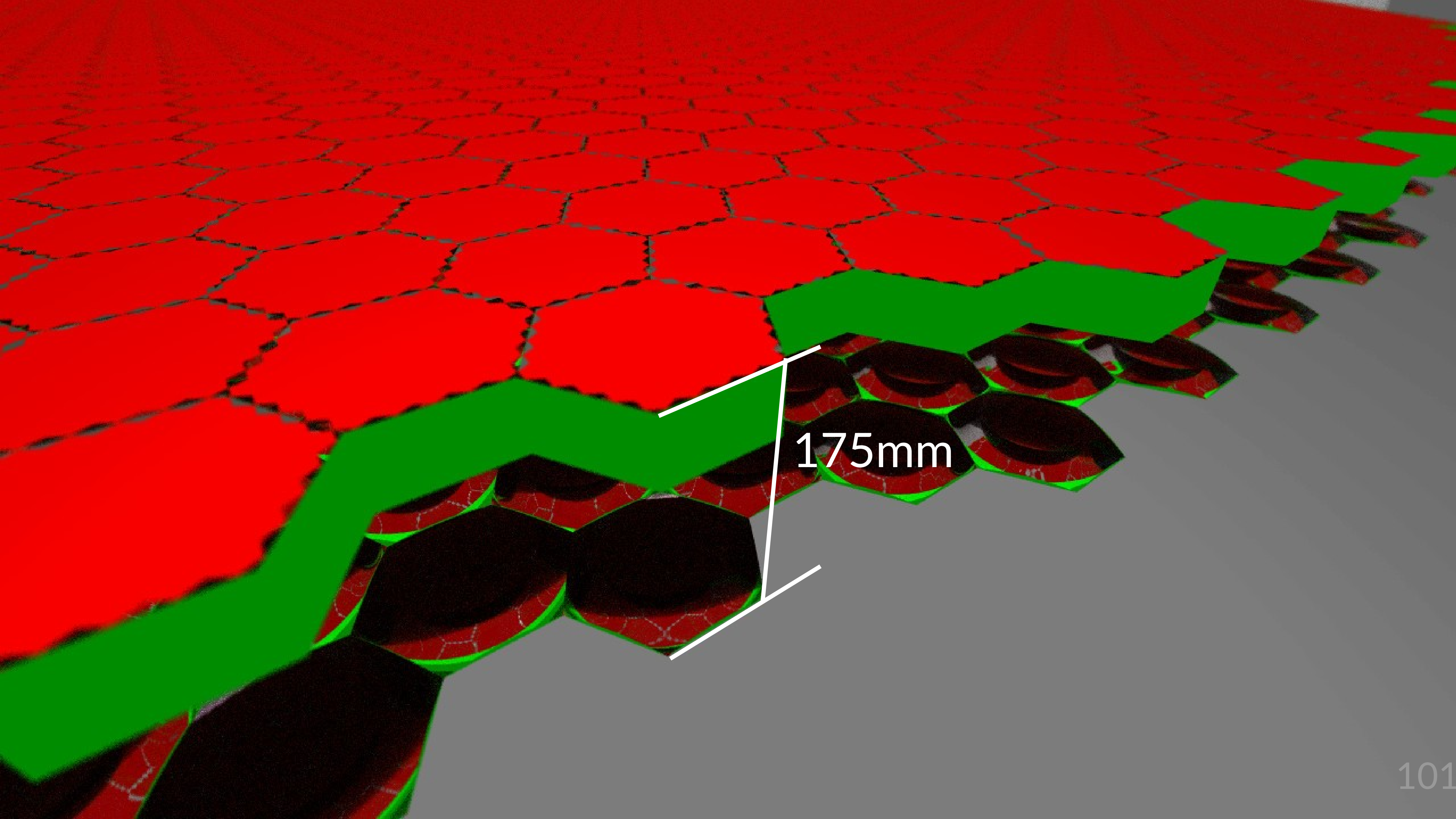
175mm

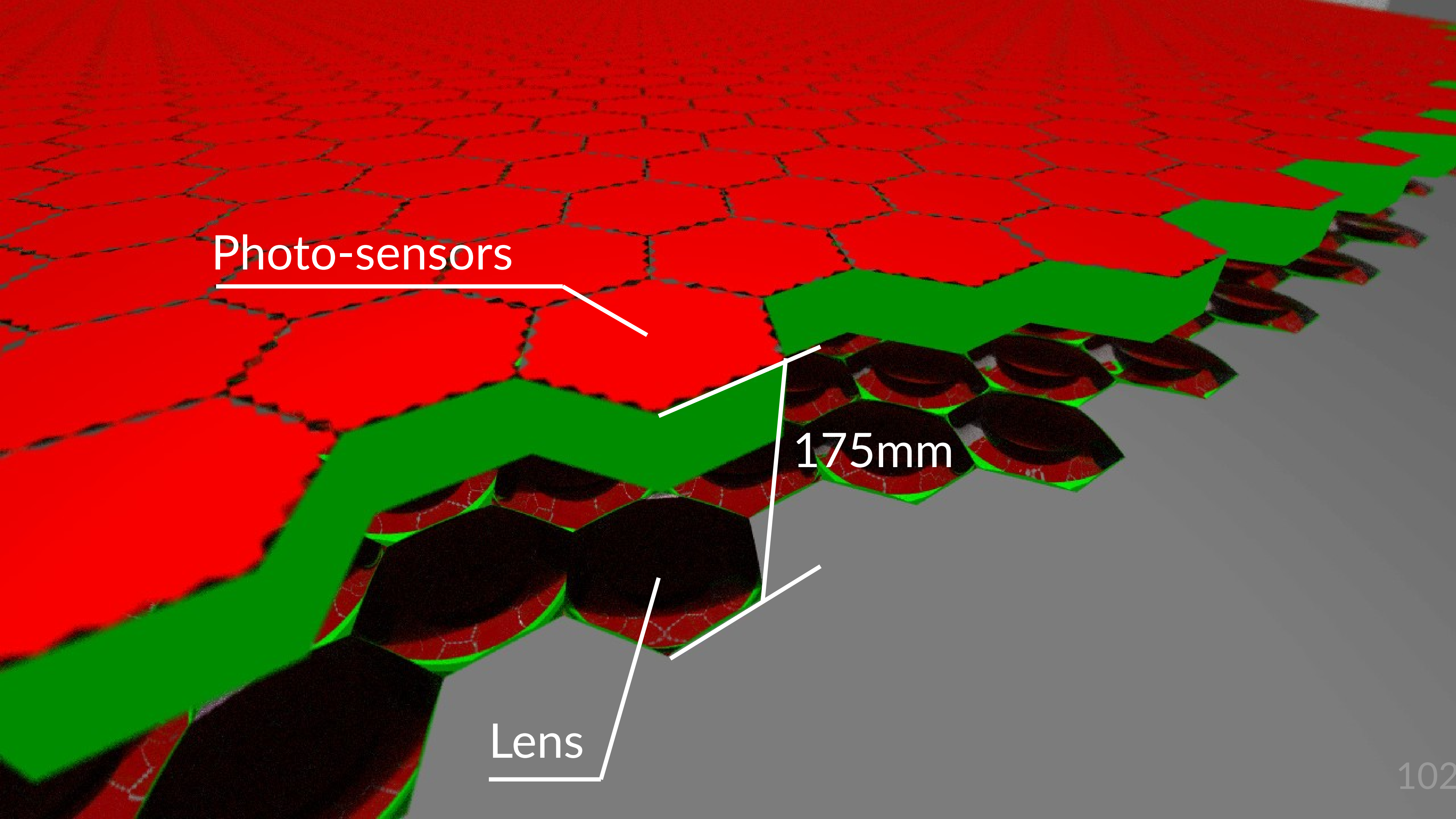
Photo-sensors
175mm
Lens

Pointing

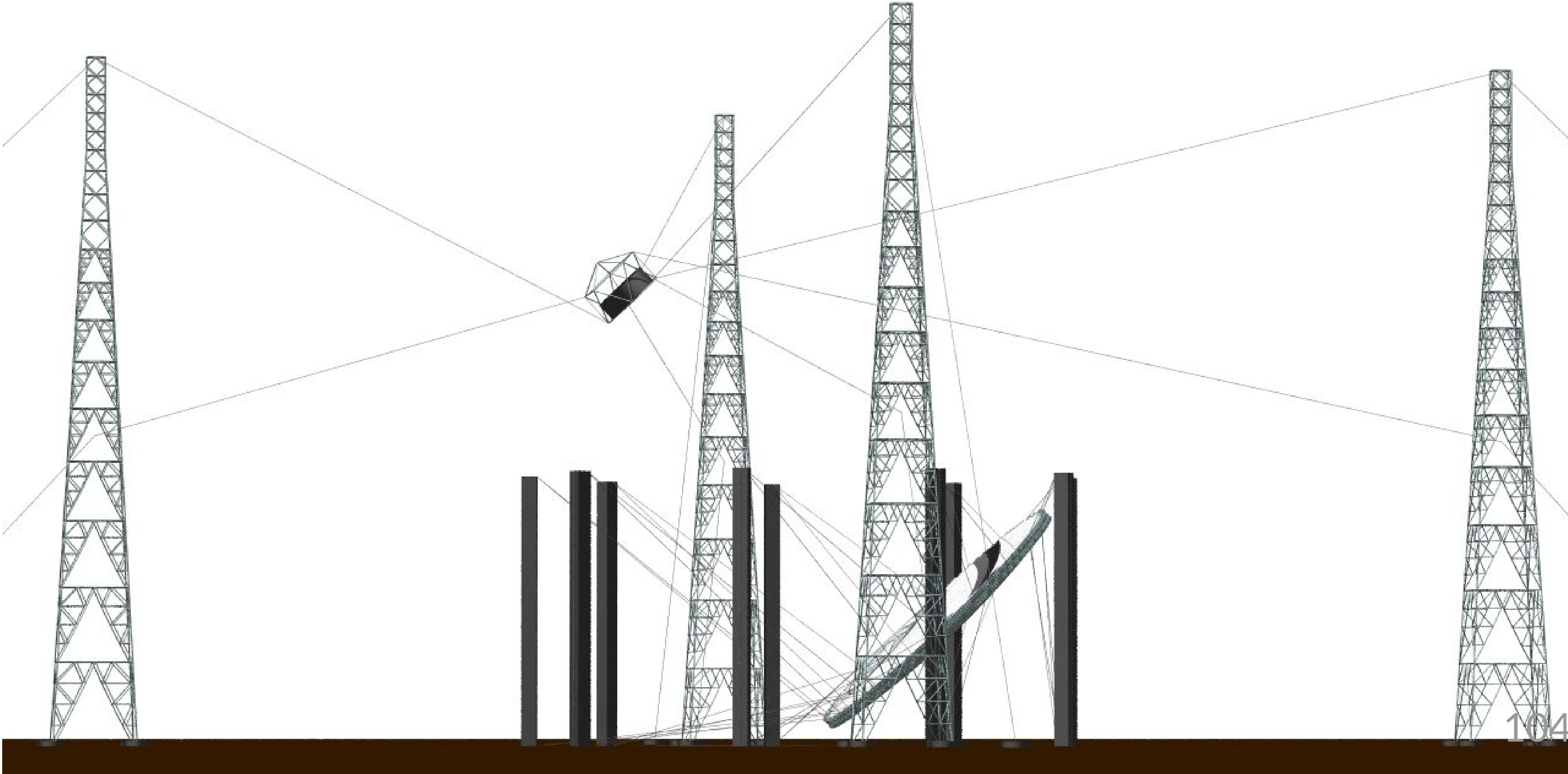

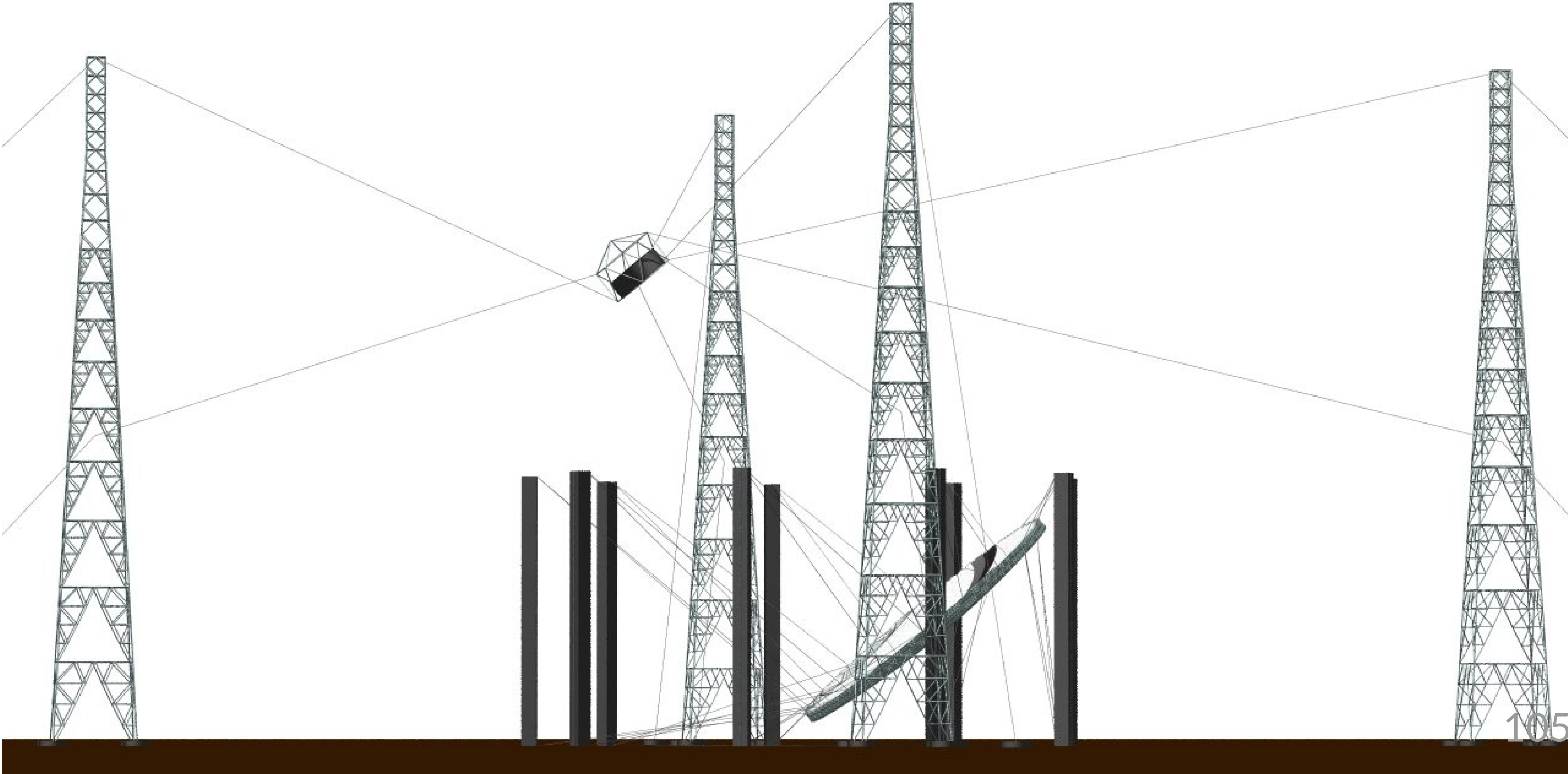

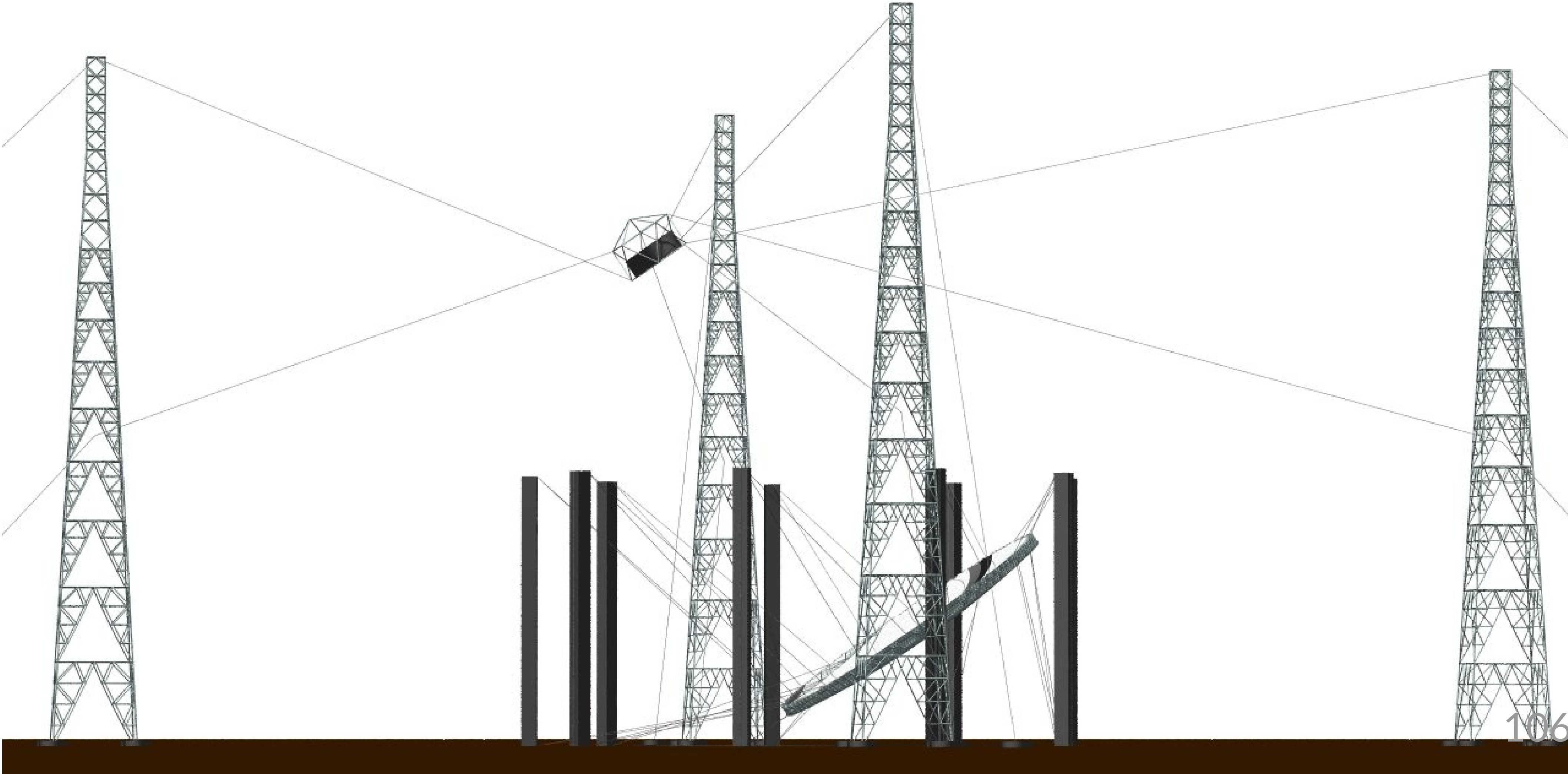

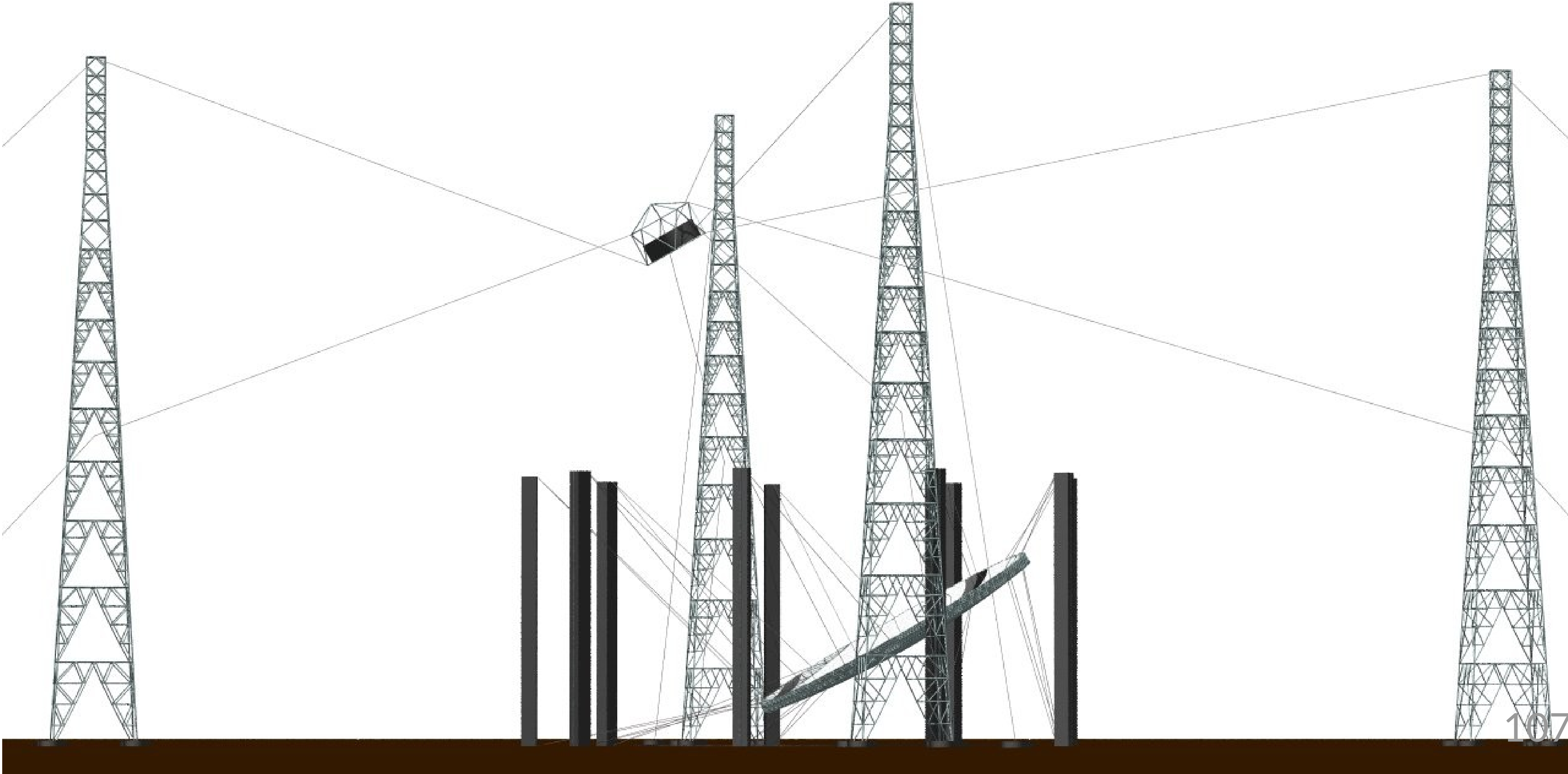

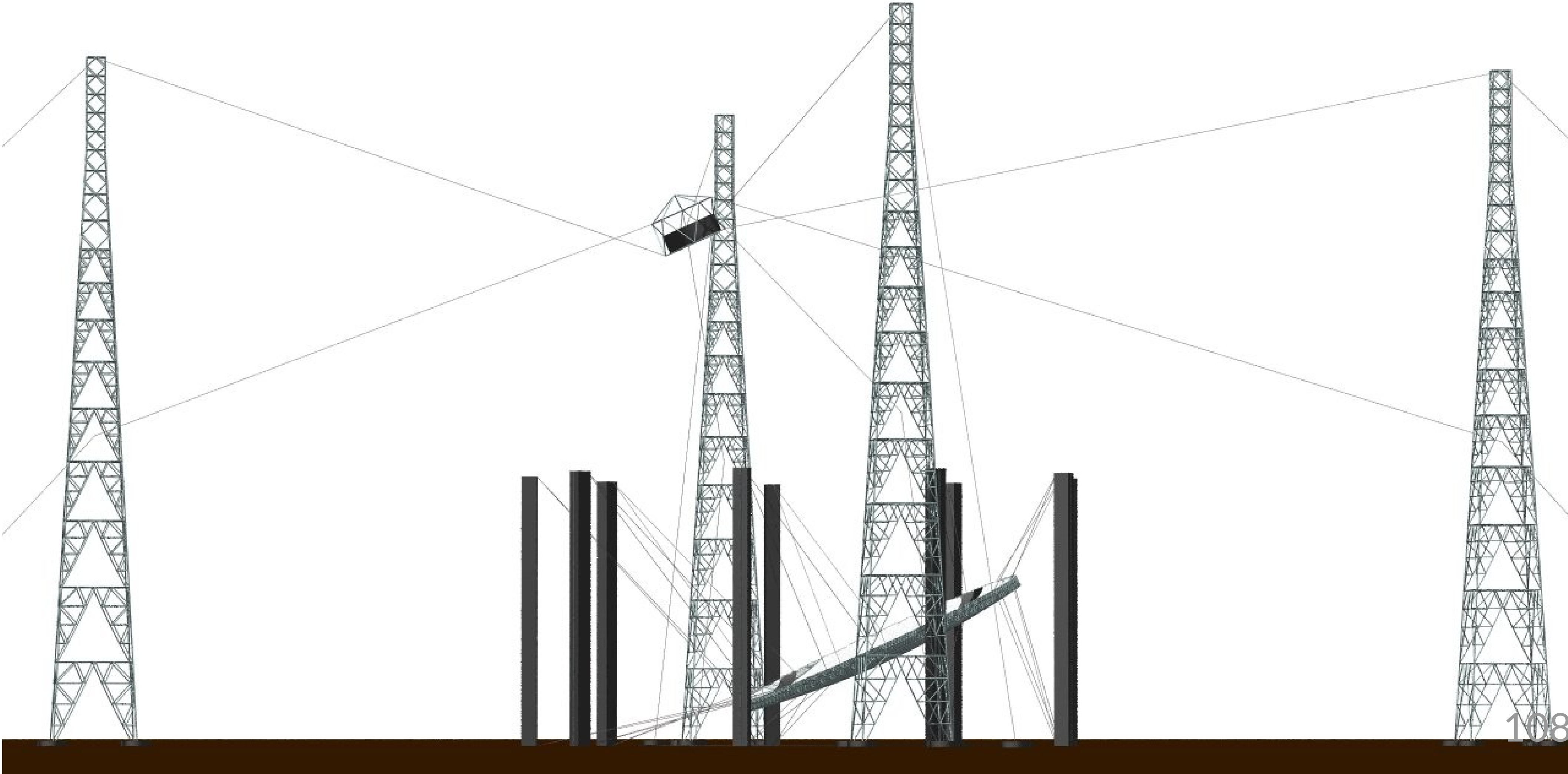

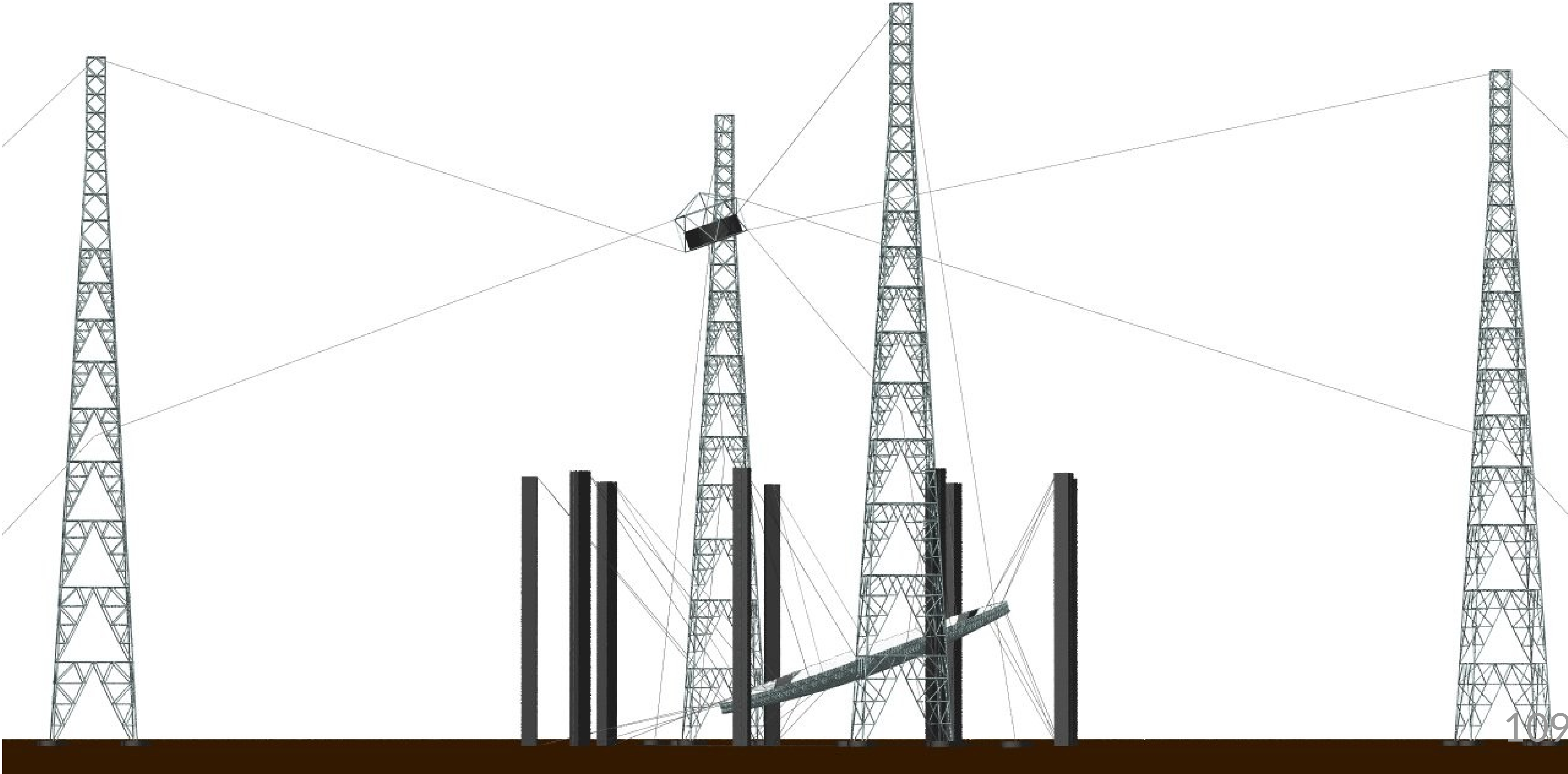

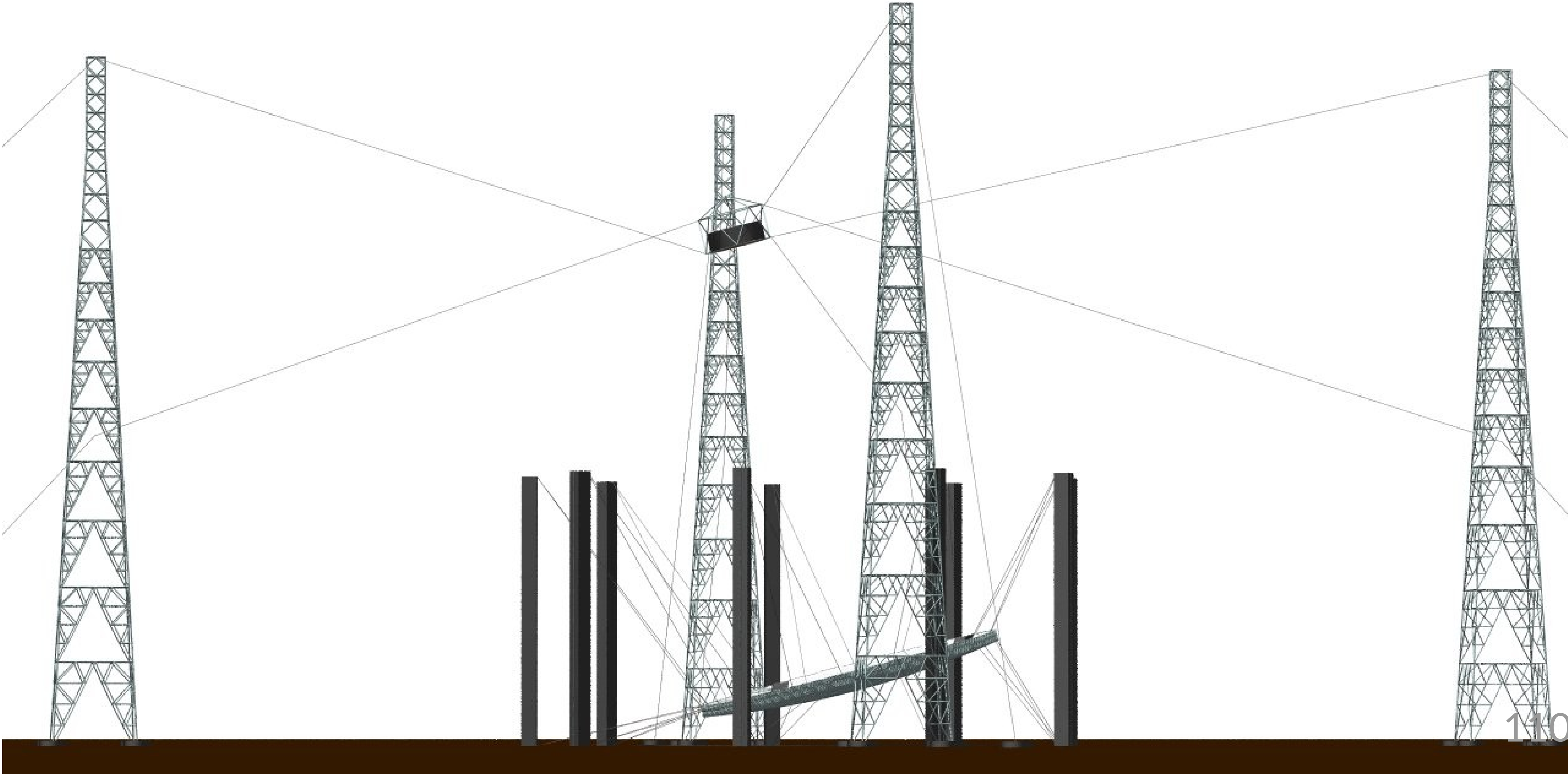

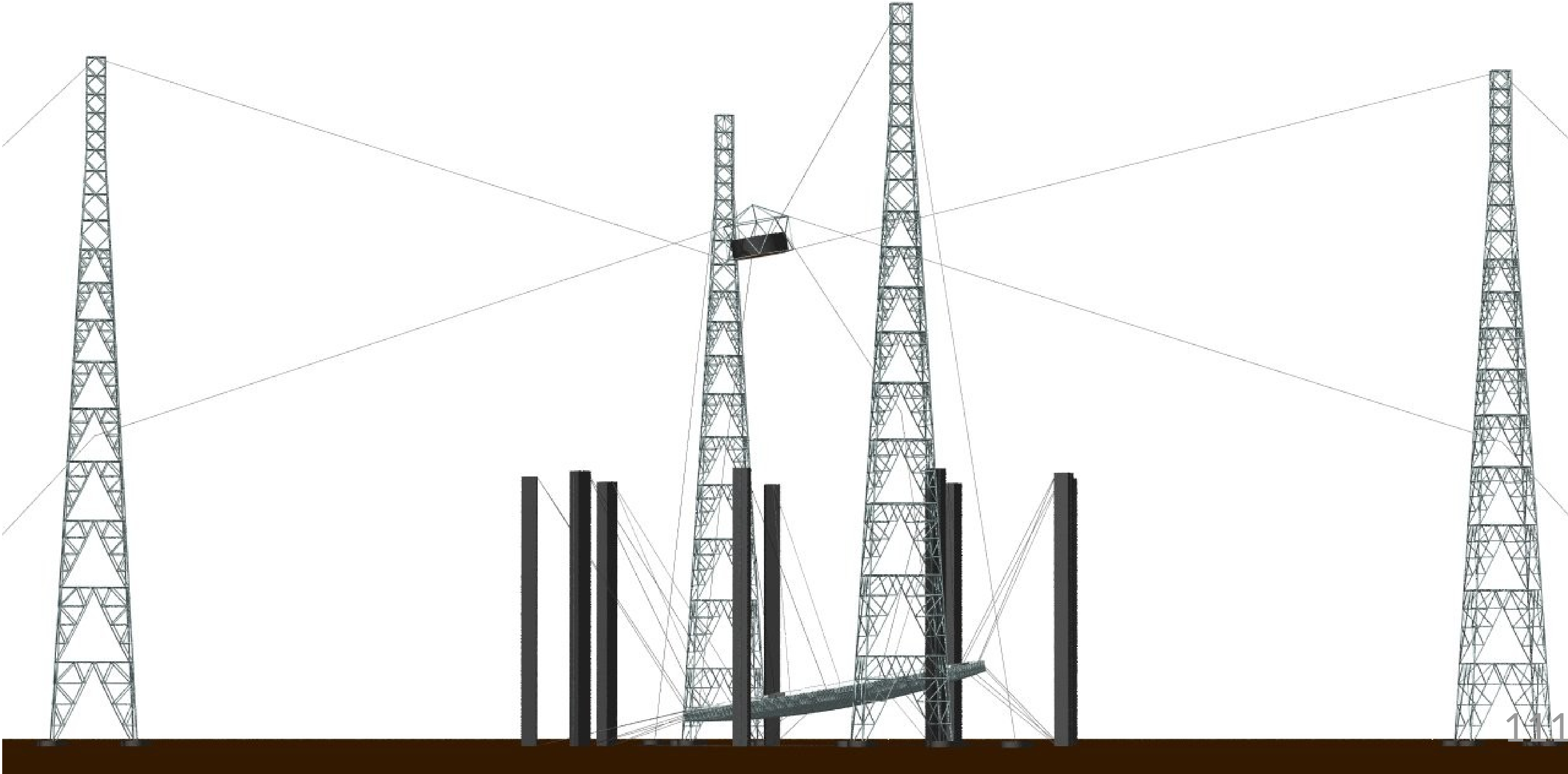

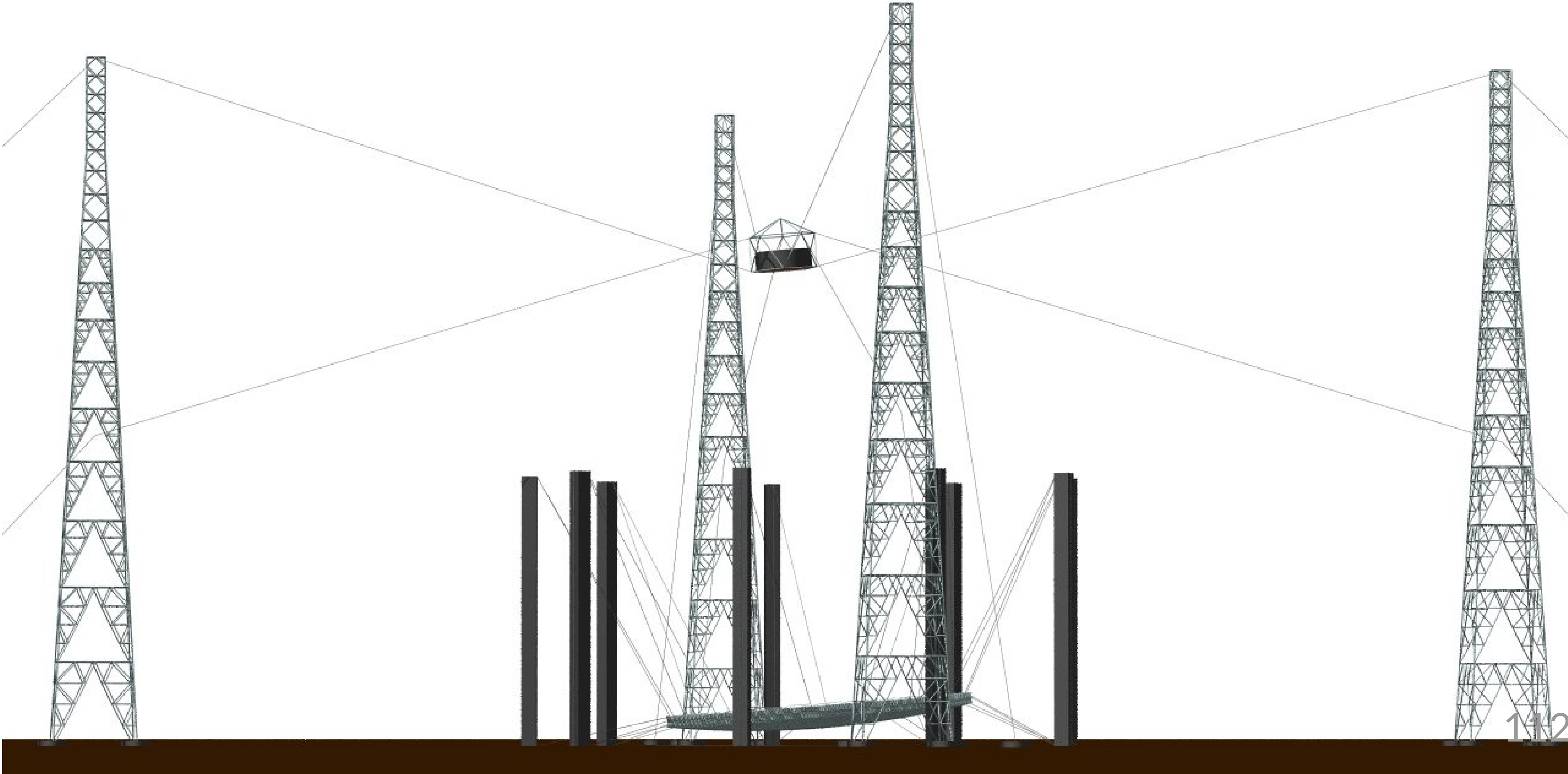

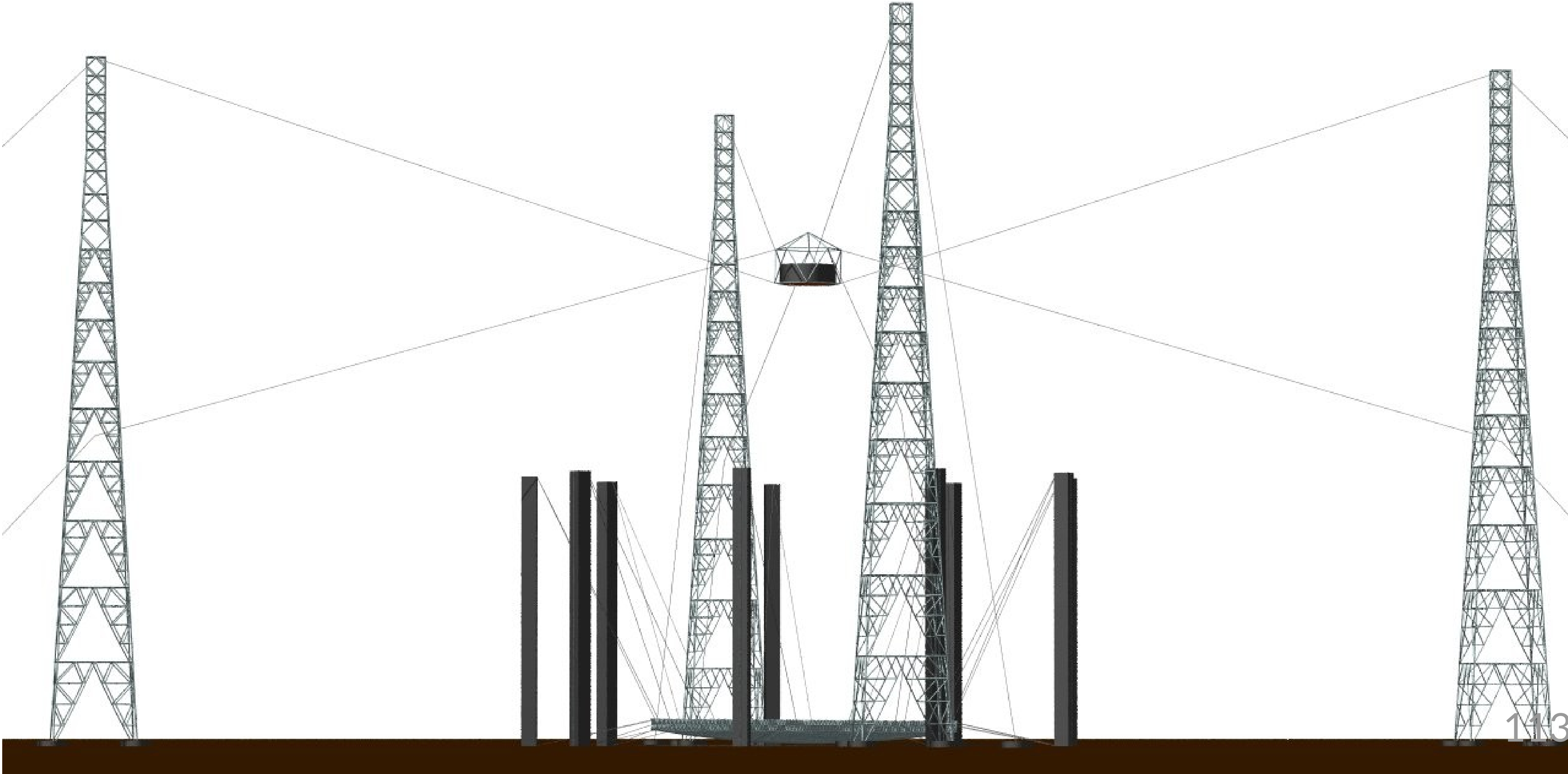

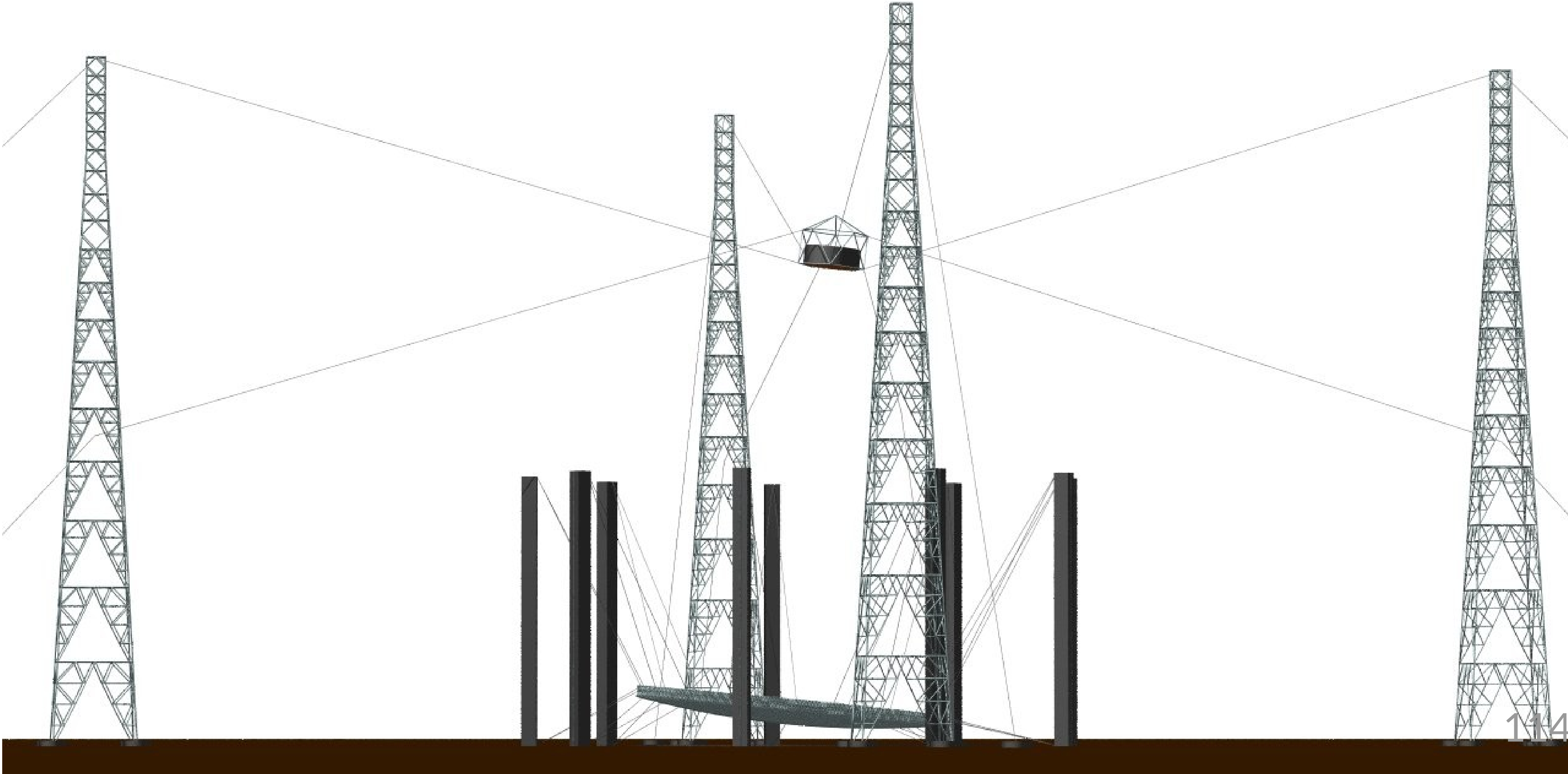

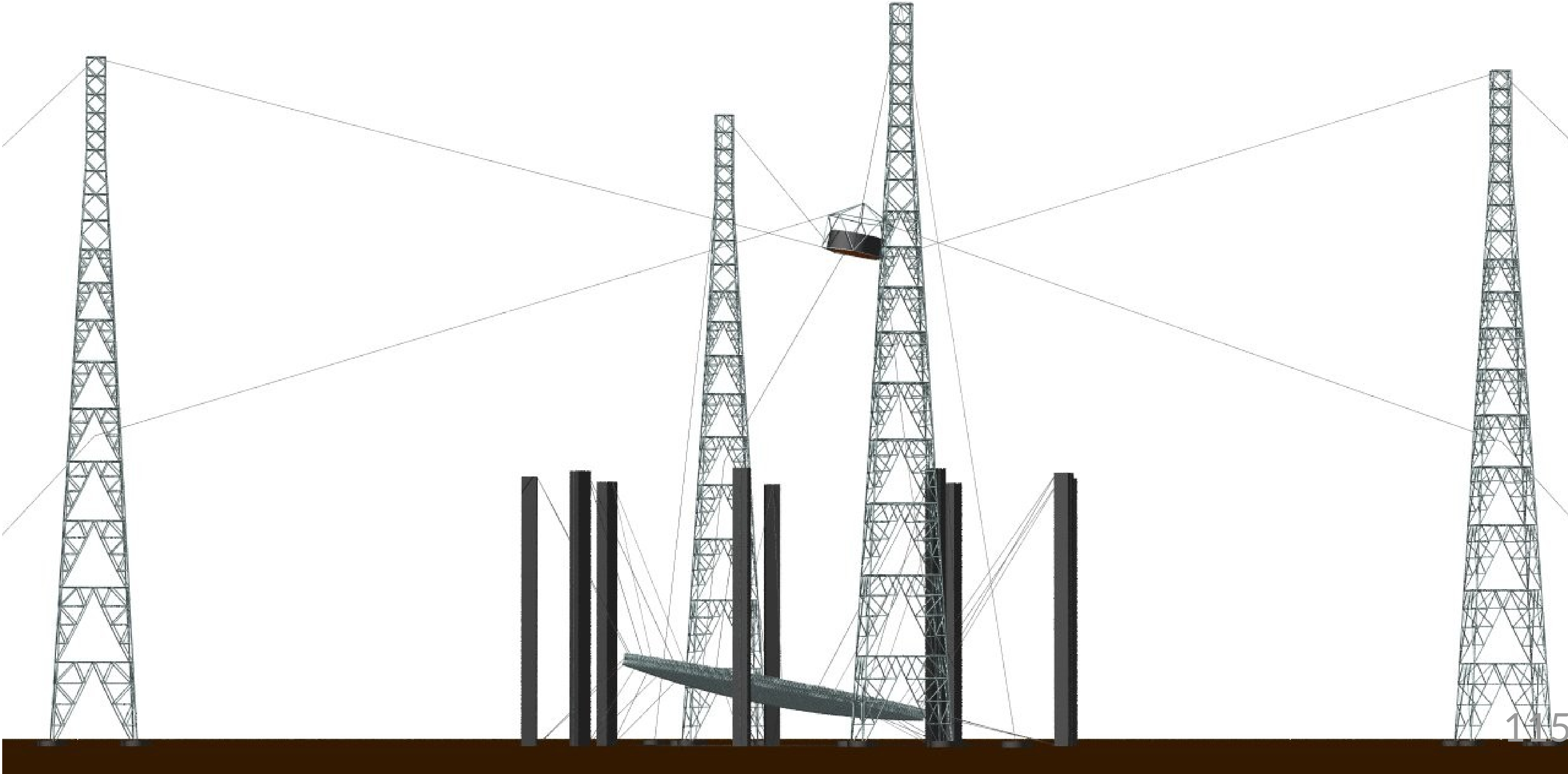

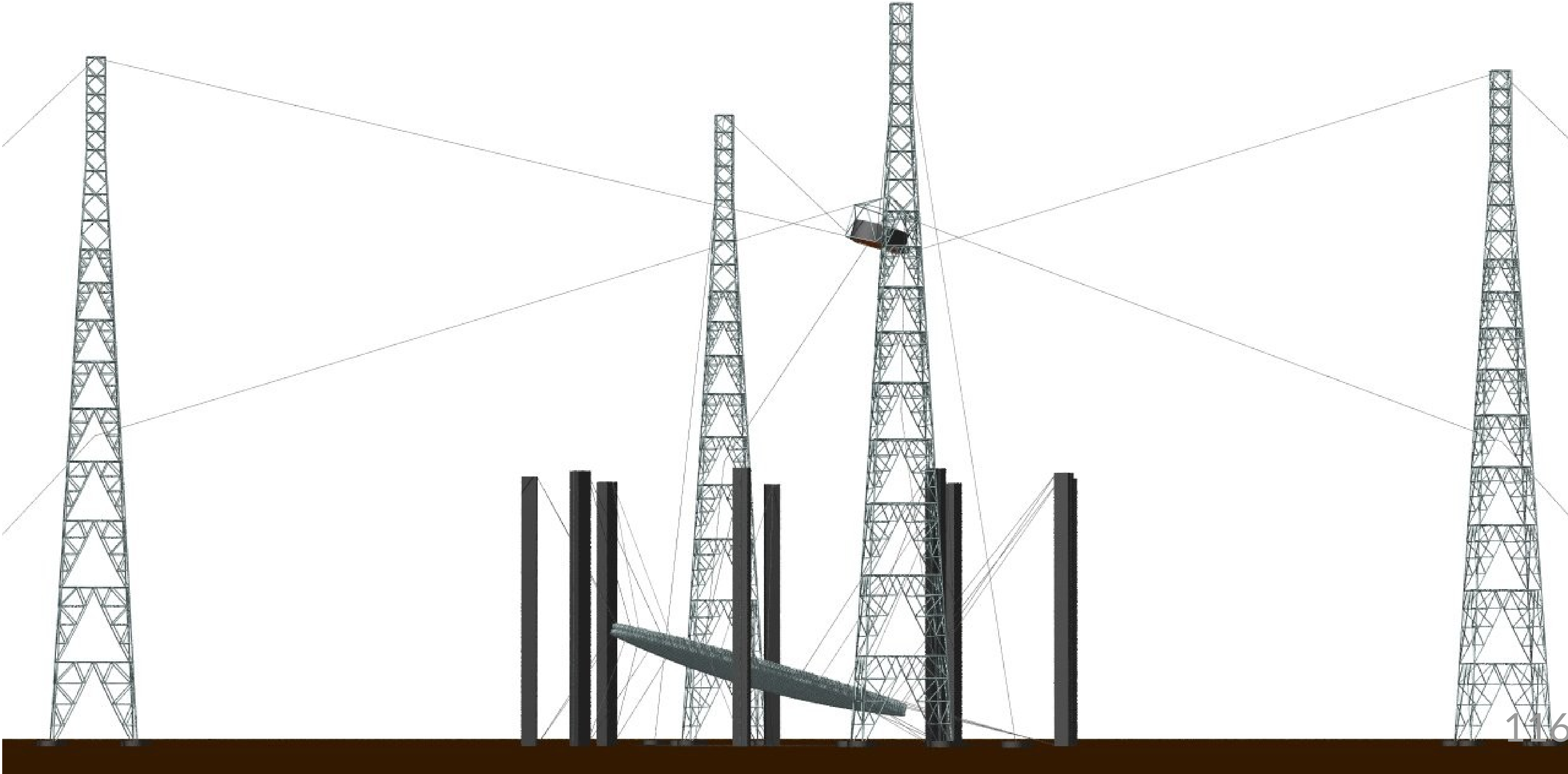

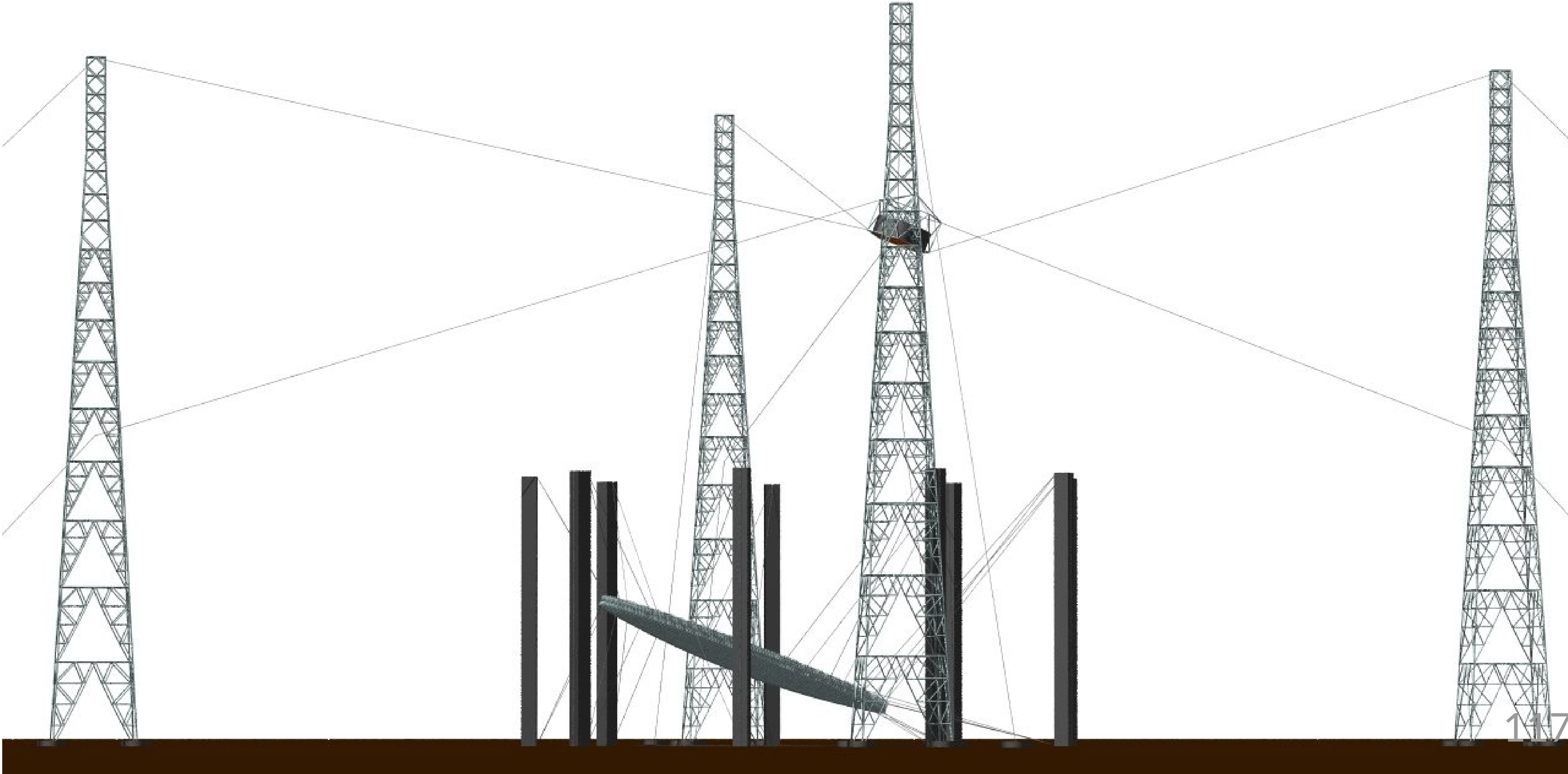

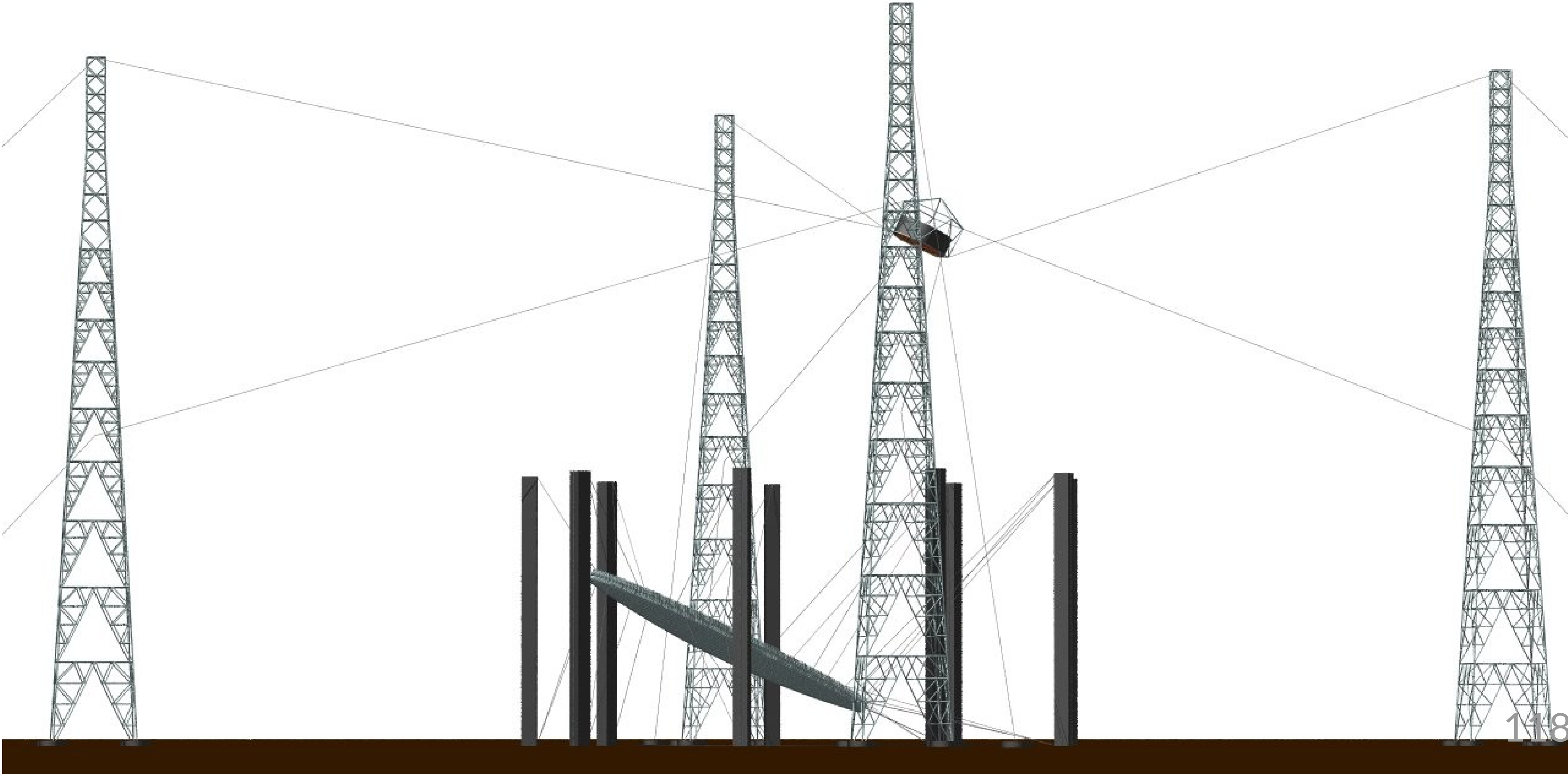

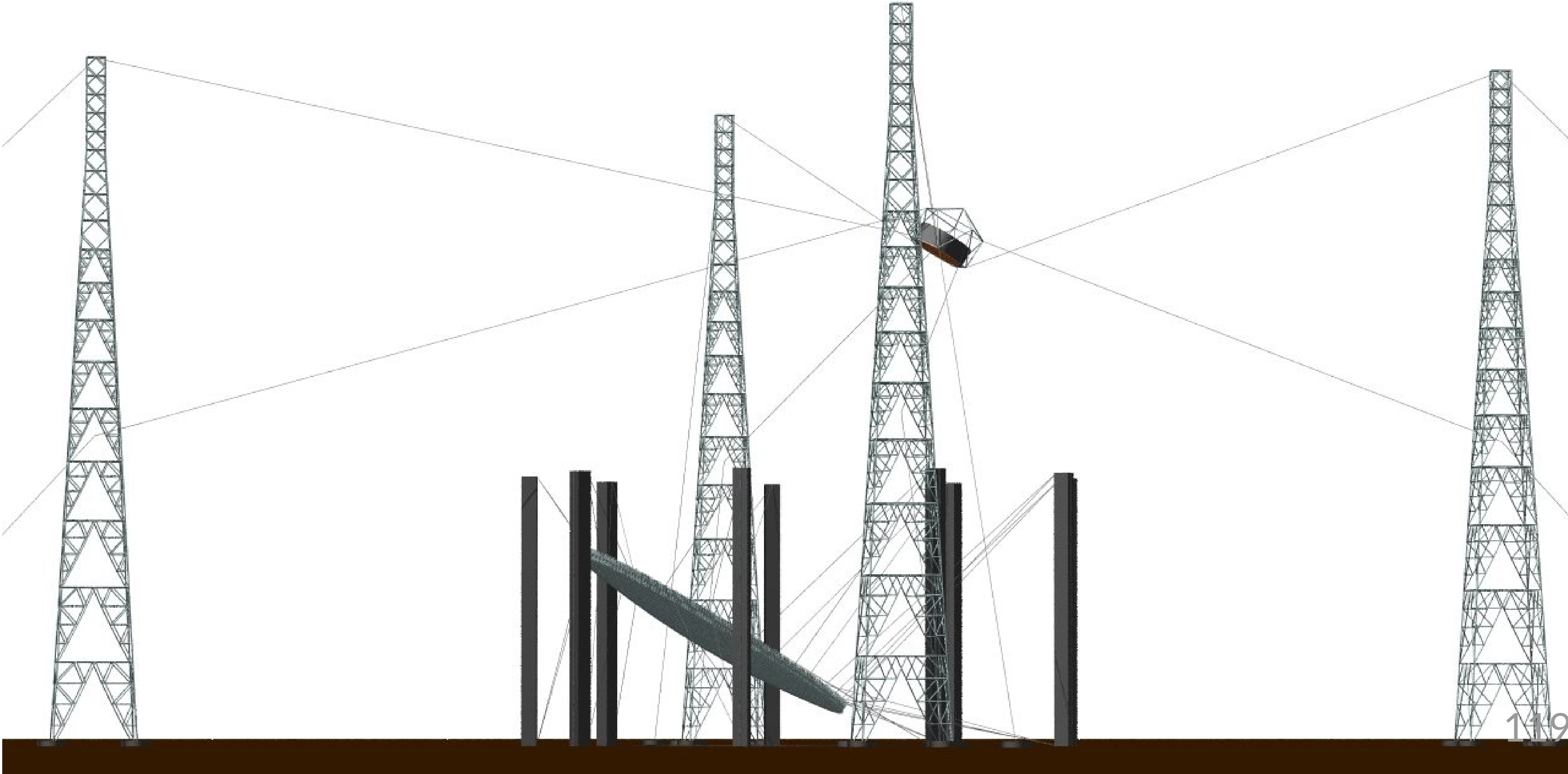

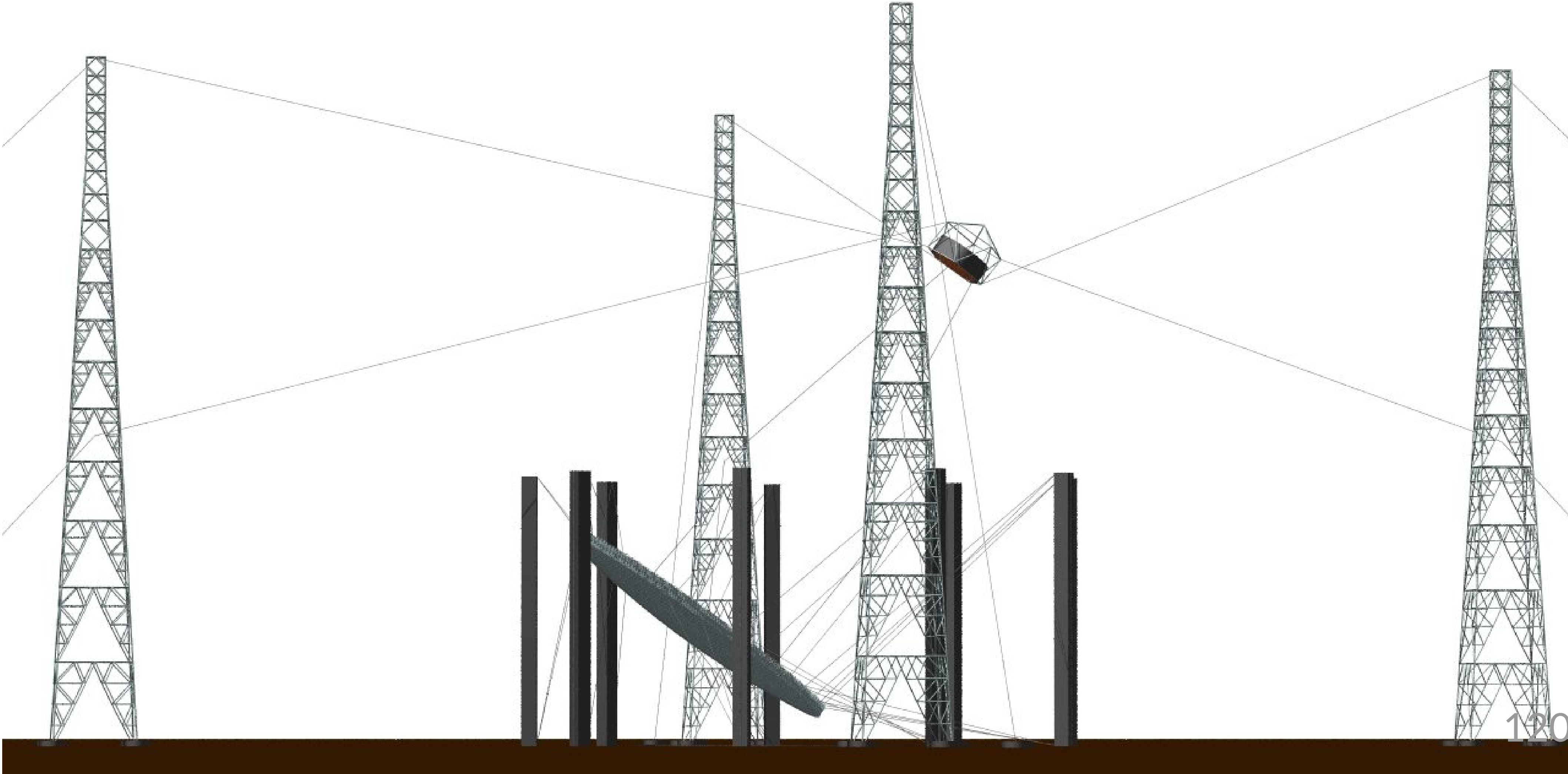

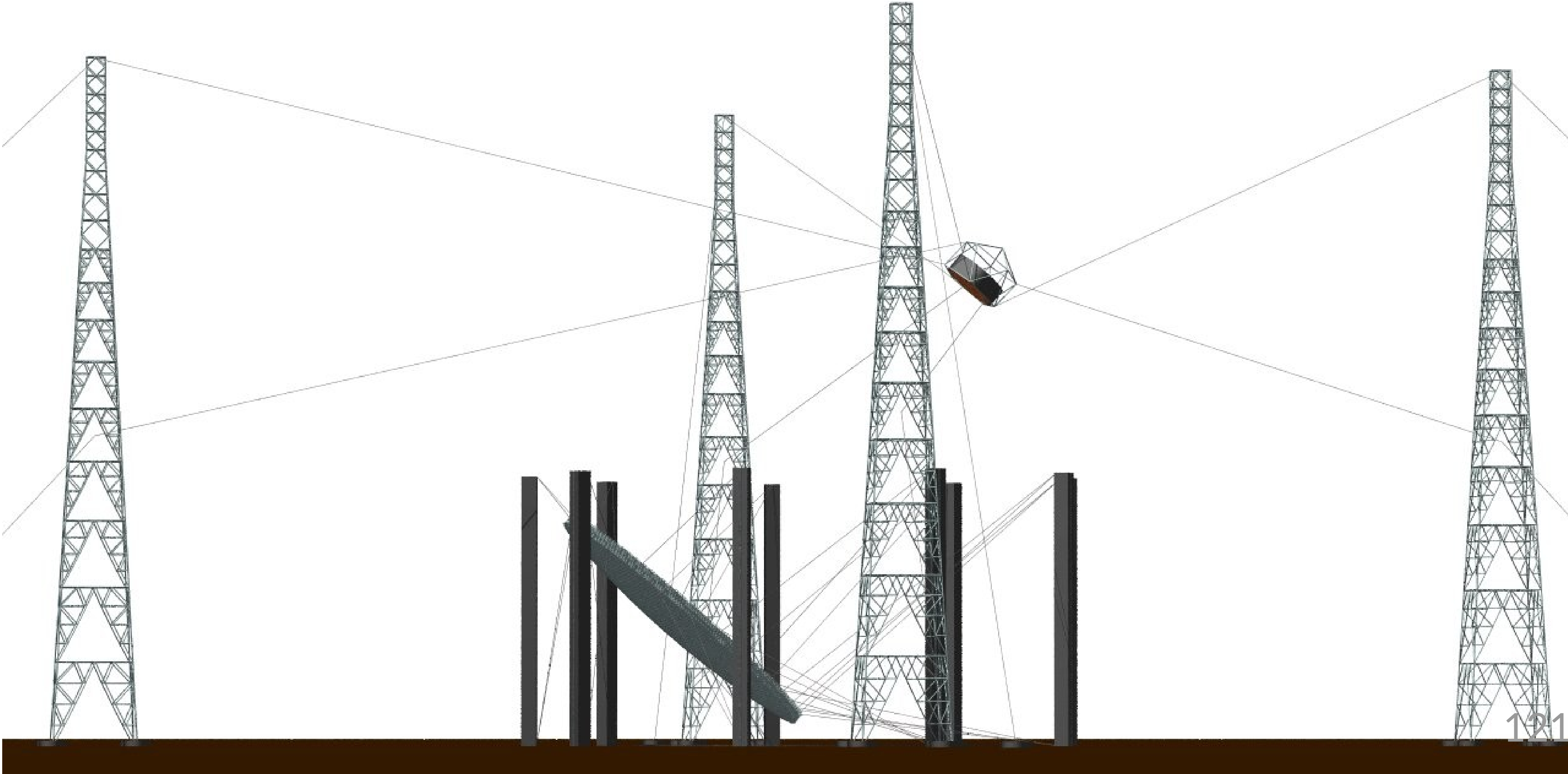

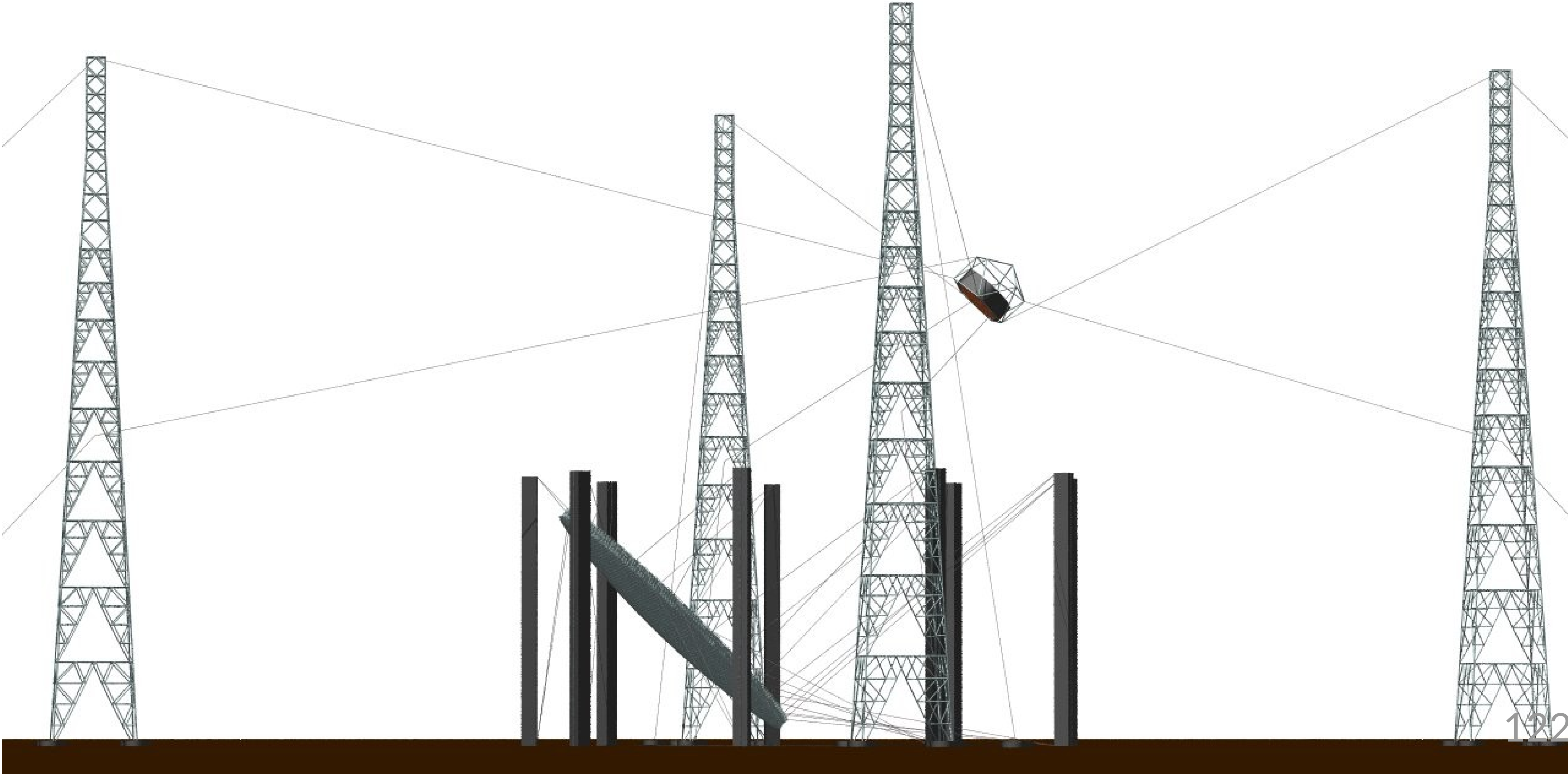

Phantom-Source

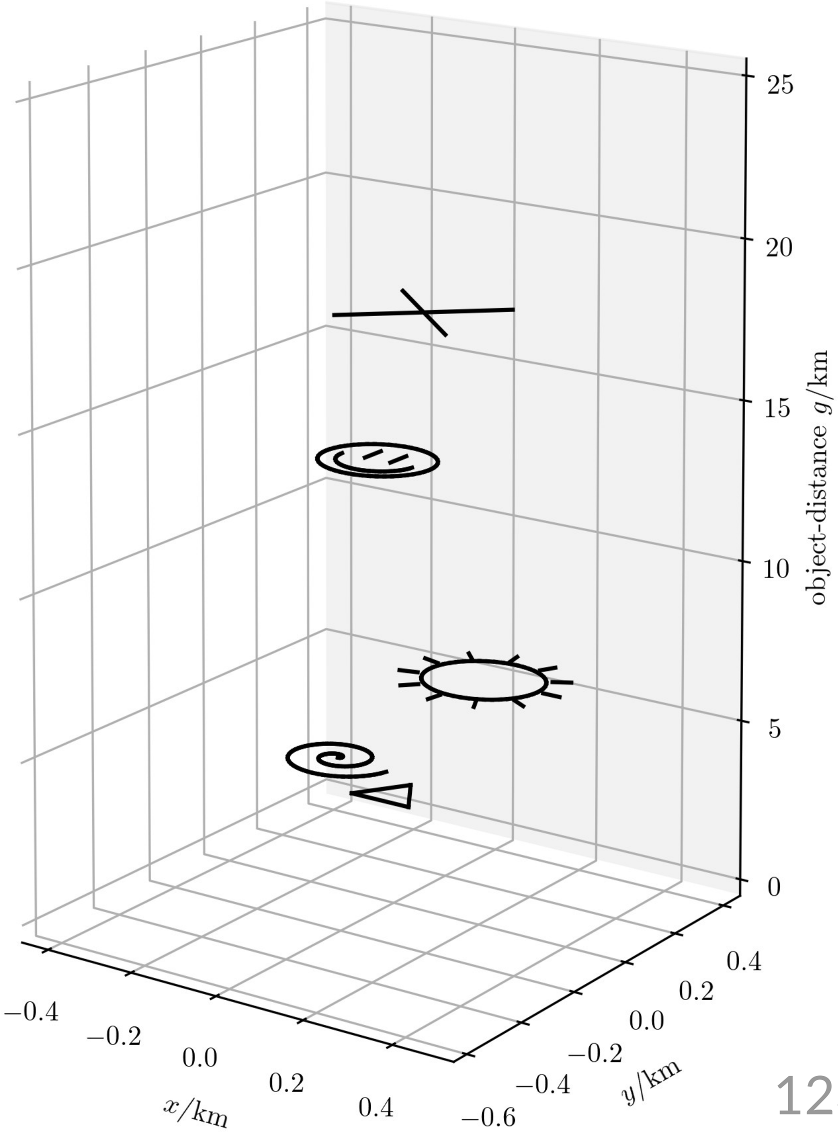

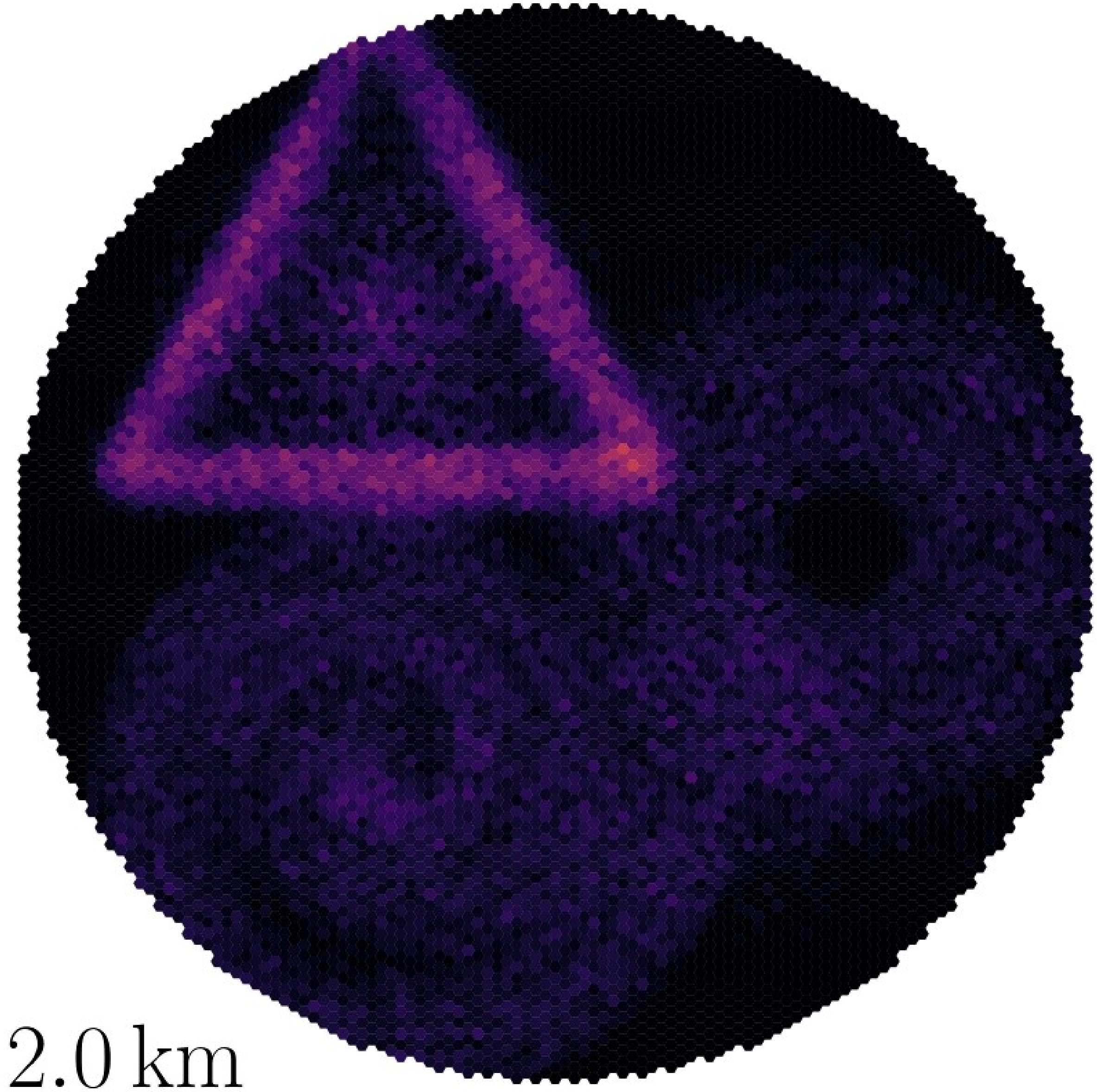
2.0 km

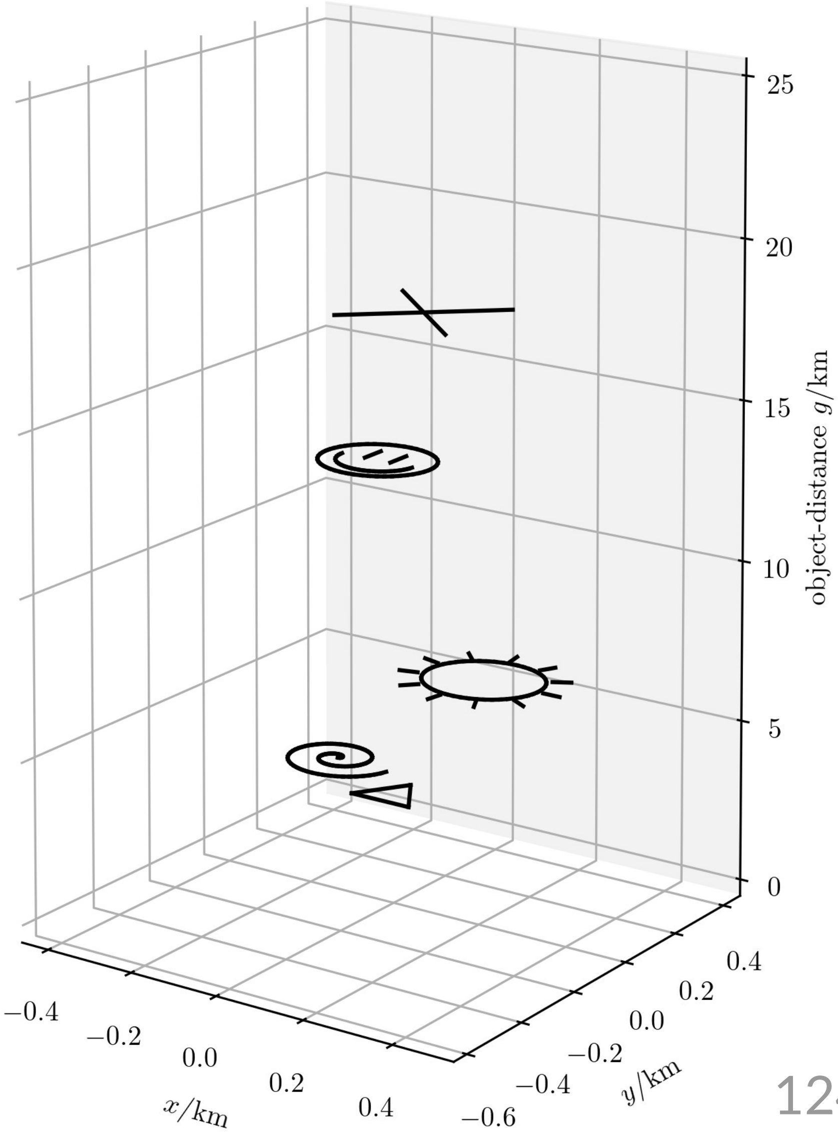
25
20
15
10
5
0
object-distance g/km
−0.4
−0.2
0.0
0.2
0.4
x/km
0.4
0.2
0.0
−0.2
−0.4
−0.6
y/km

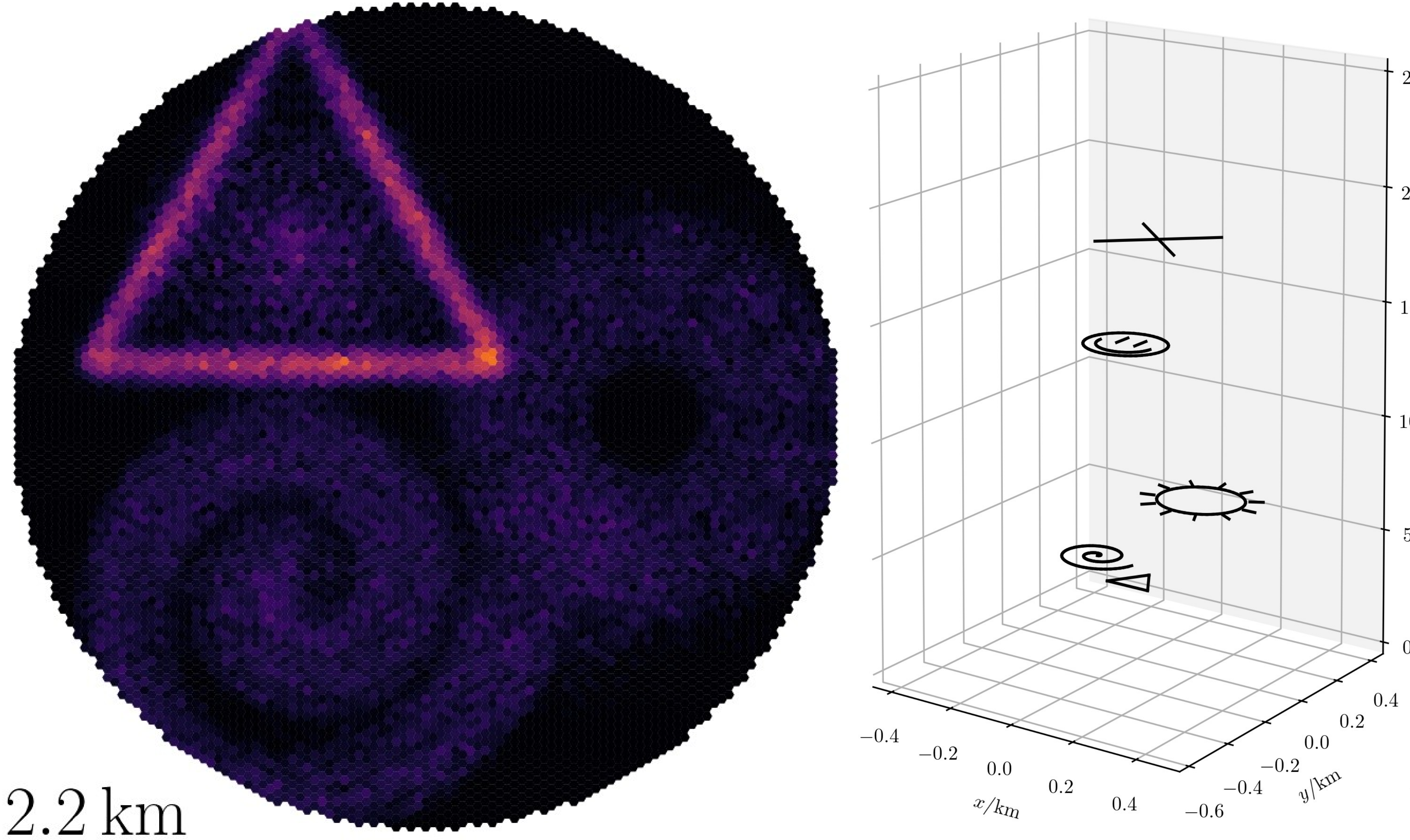
2.2 km
object-distance g/km
25
20
15
10
5
0
−0.4
−0.2
0.0
0.2
0.4
x/km
0.4
0.2
0.0
−0.2
−0.4
−0.6
y/km

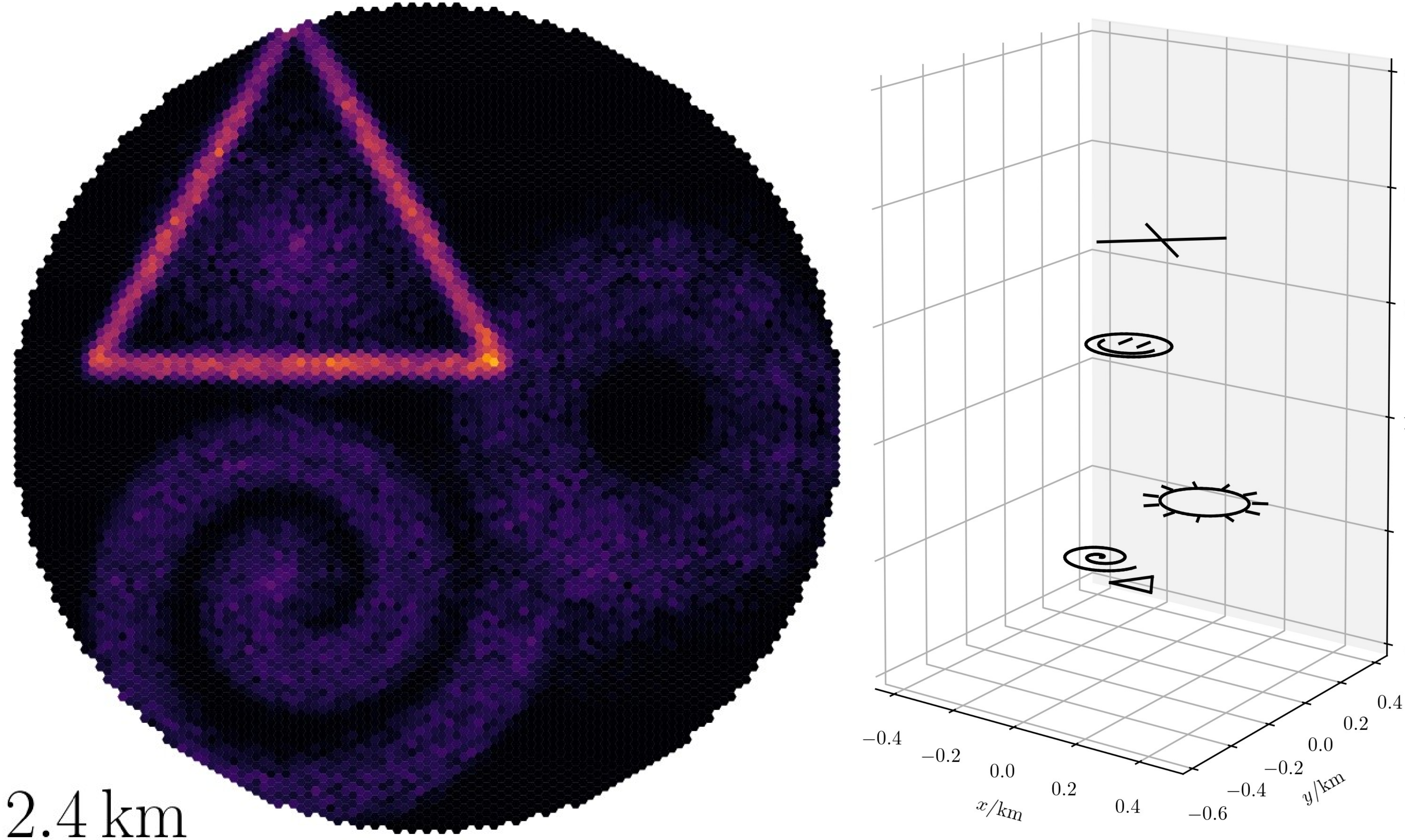

2.4 km
object-distance g/km
0
5
10
15
20
25
x/km
−0.4
−0.2
0.0
0.2
0.4
y/km
−0.6
−0.4
−0.2
0.0
0.2
0.4

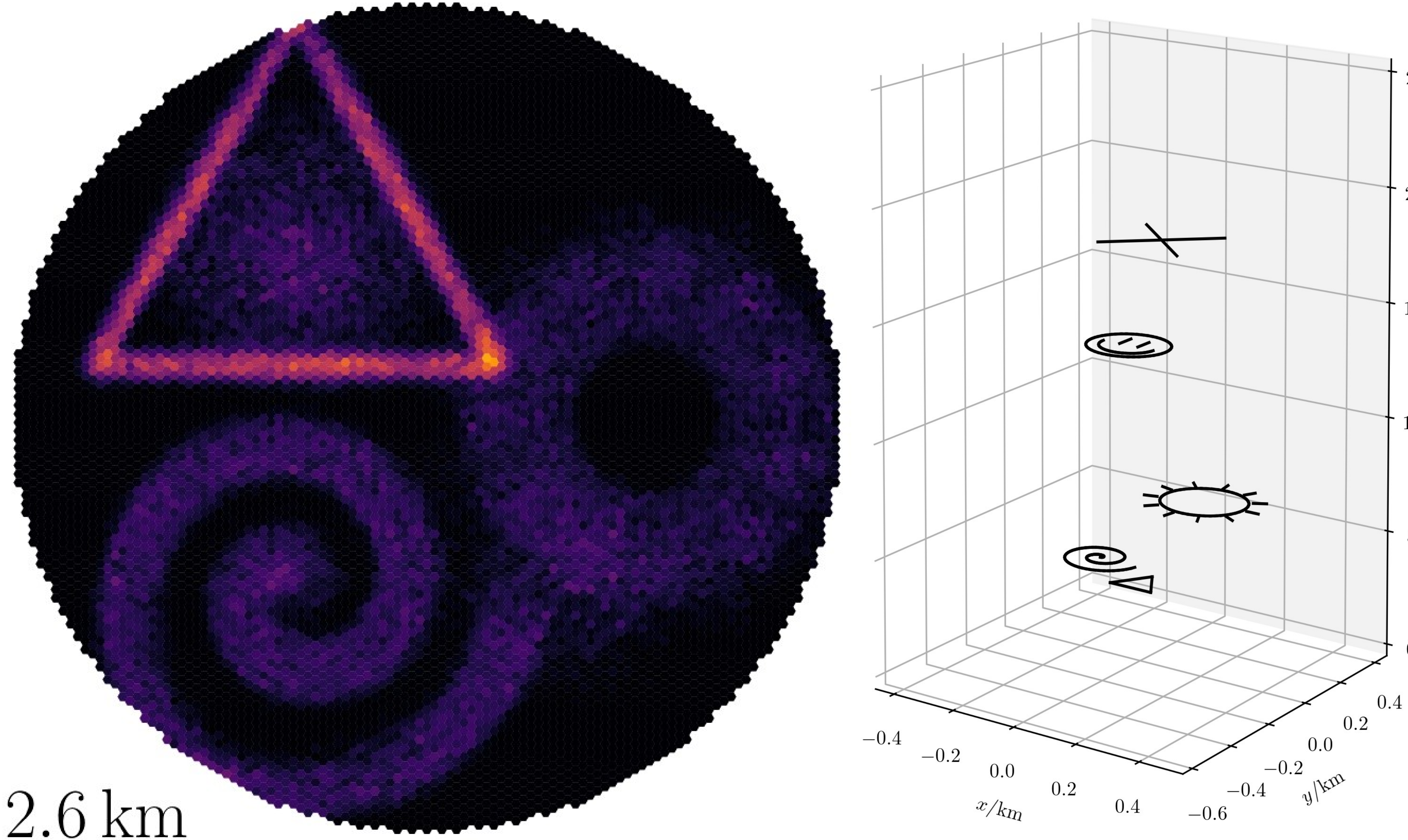
2.6 km
object-distance g/km
0
5
10
15
20
25
x/km
−0.4
−0.2
0.0
0.2
0.4
y/km
−0.6
−0.4
−0.2
0.0
0.2
0.4

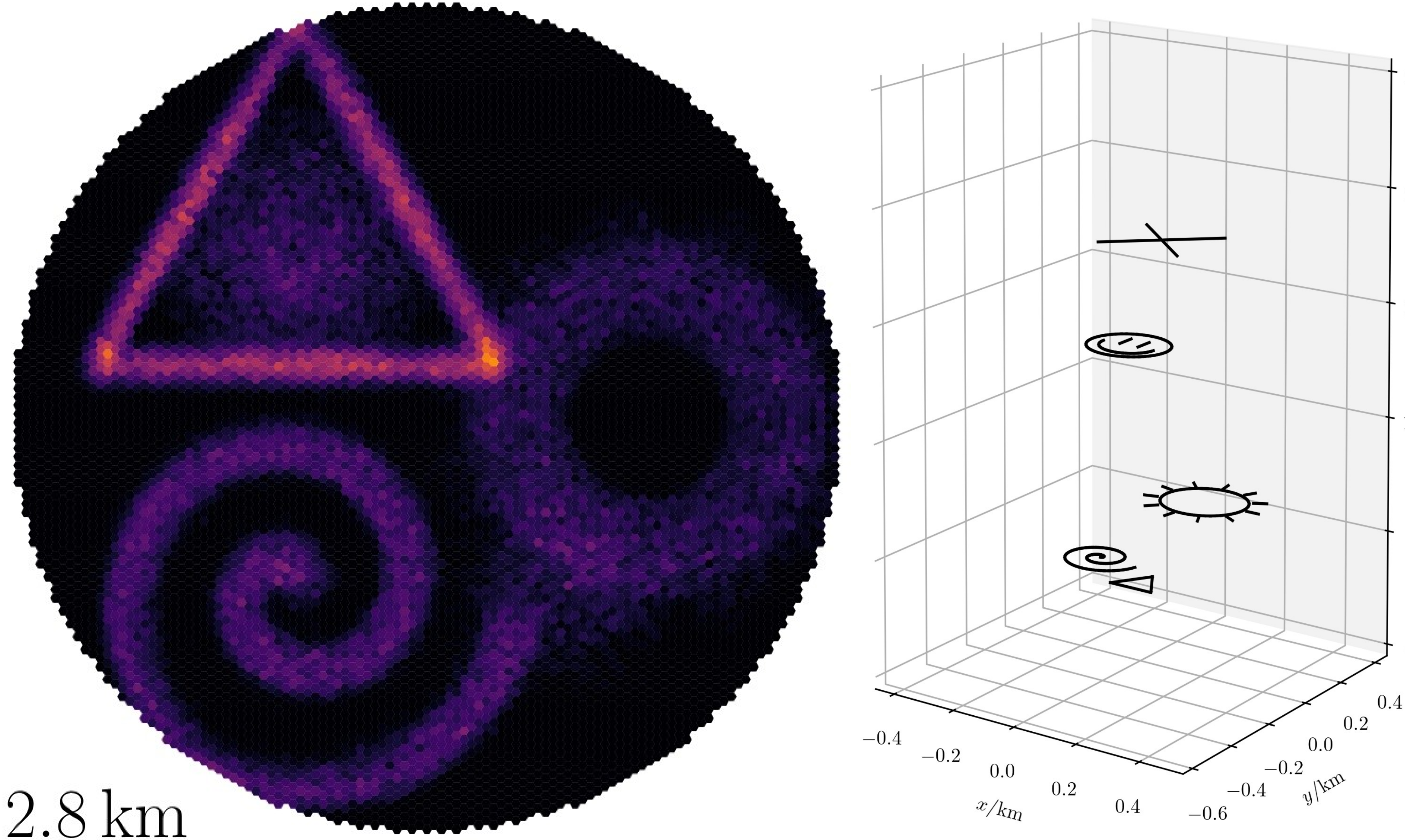

2.8 km
object-distance g/km
x/km
y/km
0
5
10
15
20
25
−0.4
−0.2
0.0
0.2
0.4
−0.6
−0.4
−0.2
0.0
0.2
0.4

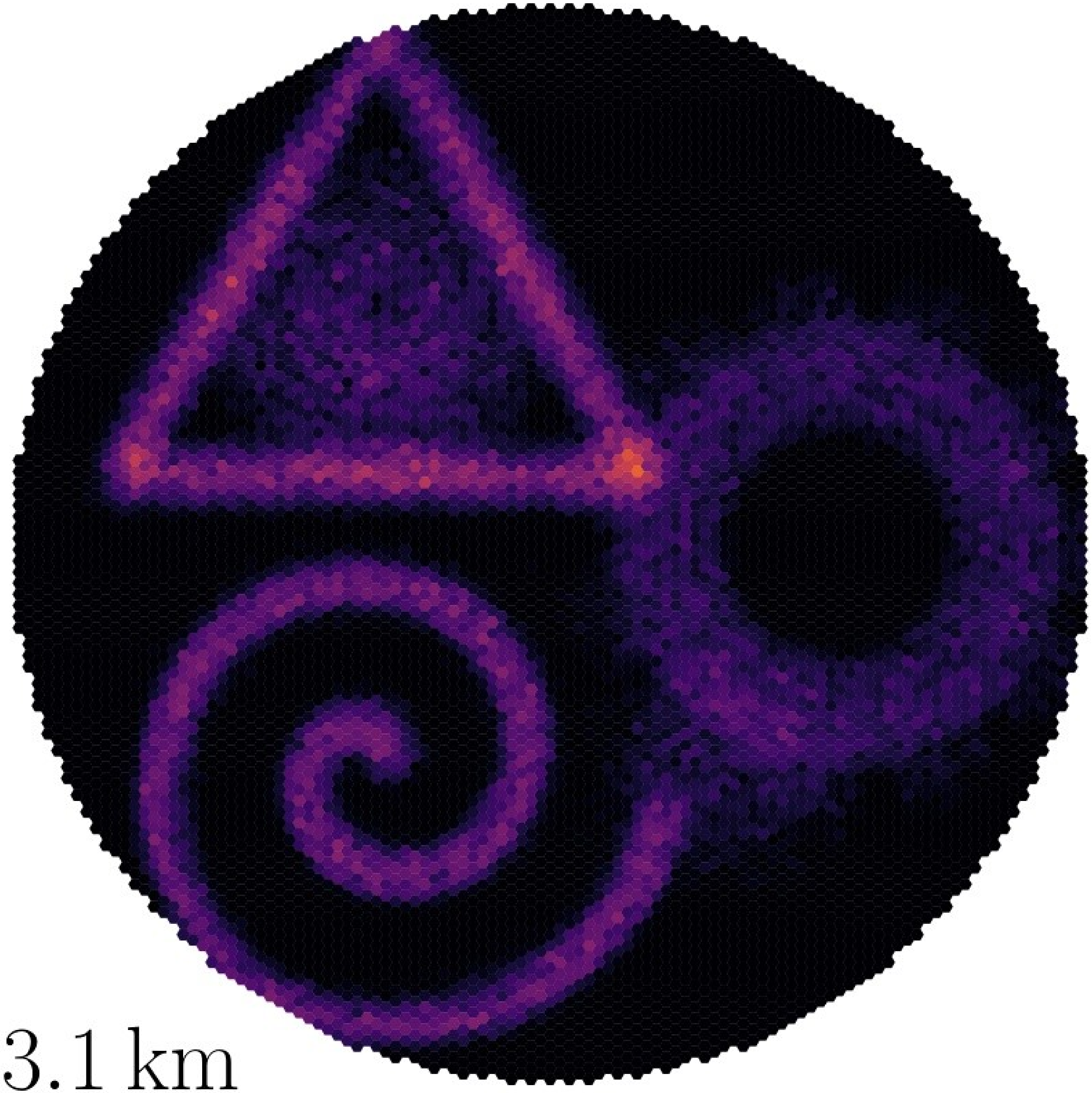

3.1 km

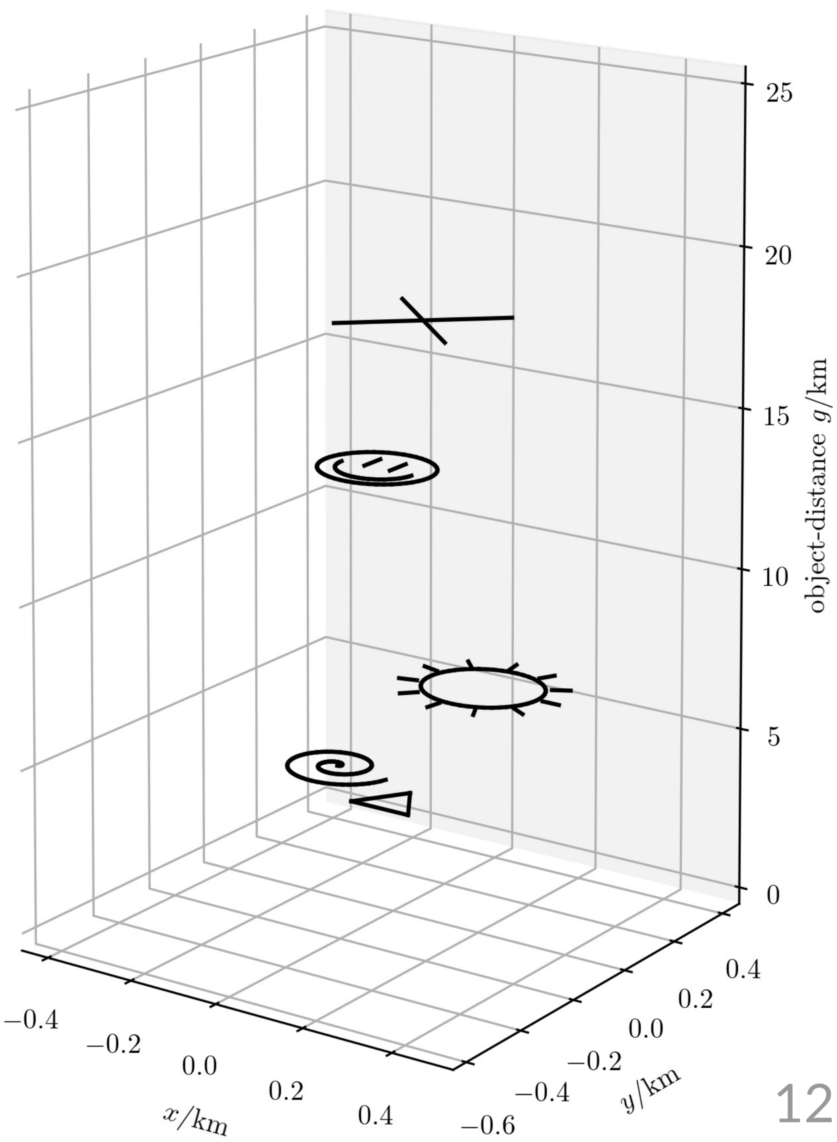
object-distance g/km
25
20
15
10
5
0
−0.4
−0.2
0.0
0.2
0.4
x/km
−0.6
−0.4
−0.2
0.0
0.2
0.4
y/km

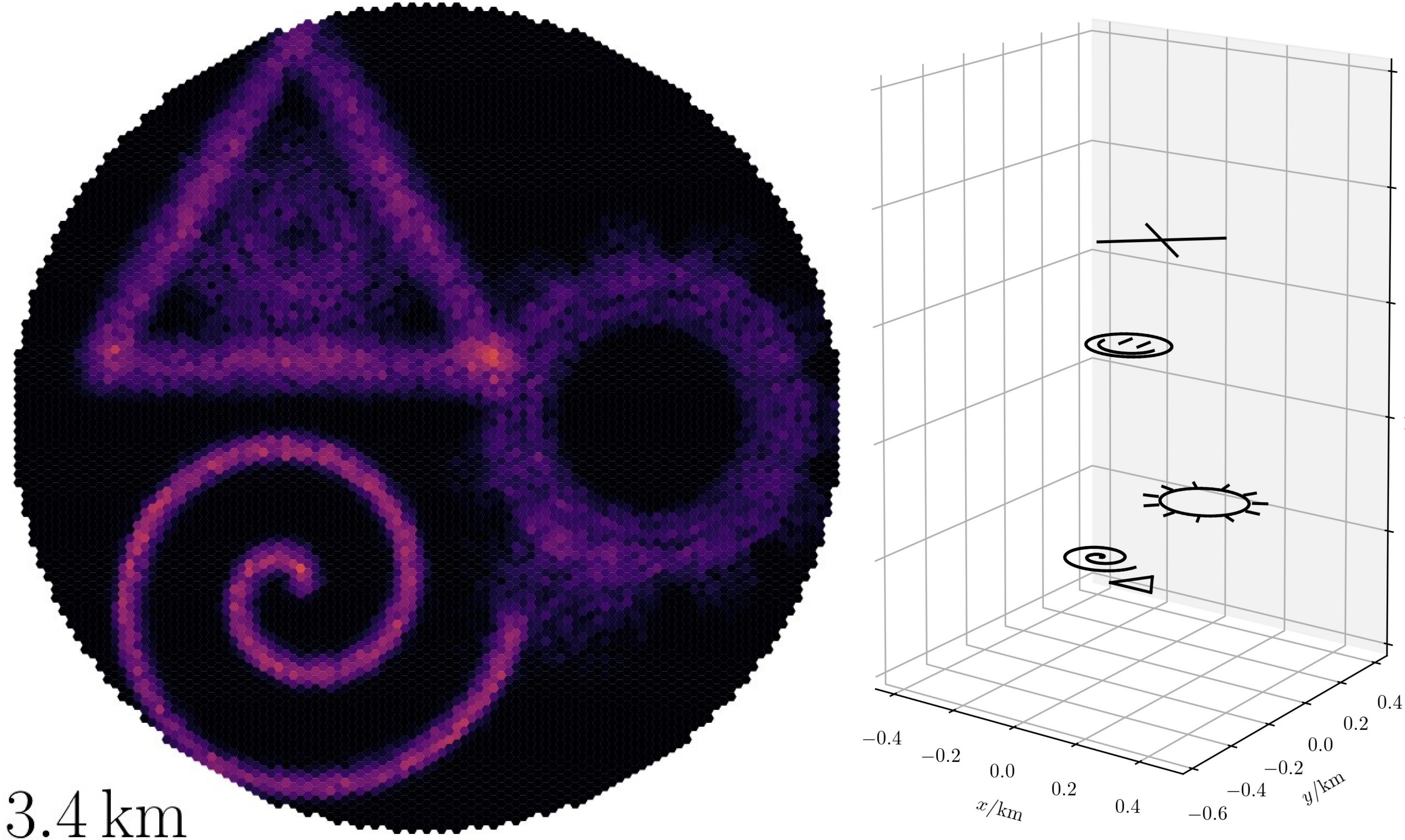

3.4 km
object-distance g/km
0
5
10
15
20
25
x/km
−0.4
−0.2
0.0
0.2
0.4
y/km
−0.6
−0.4
−0.2
0.0
0.2
0.4

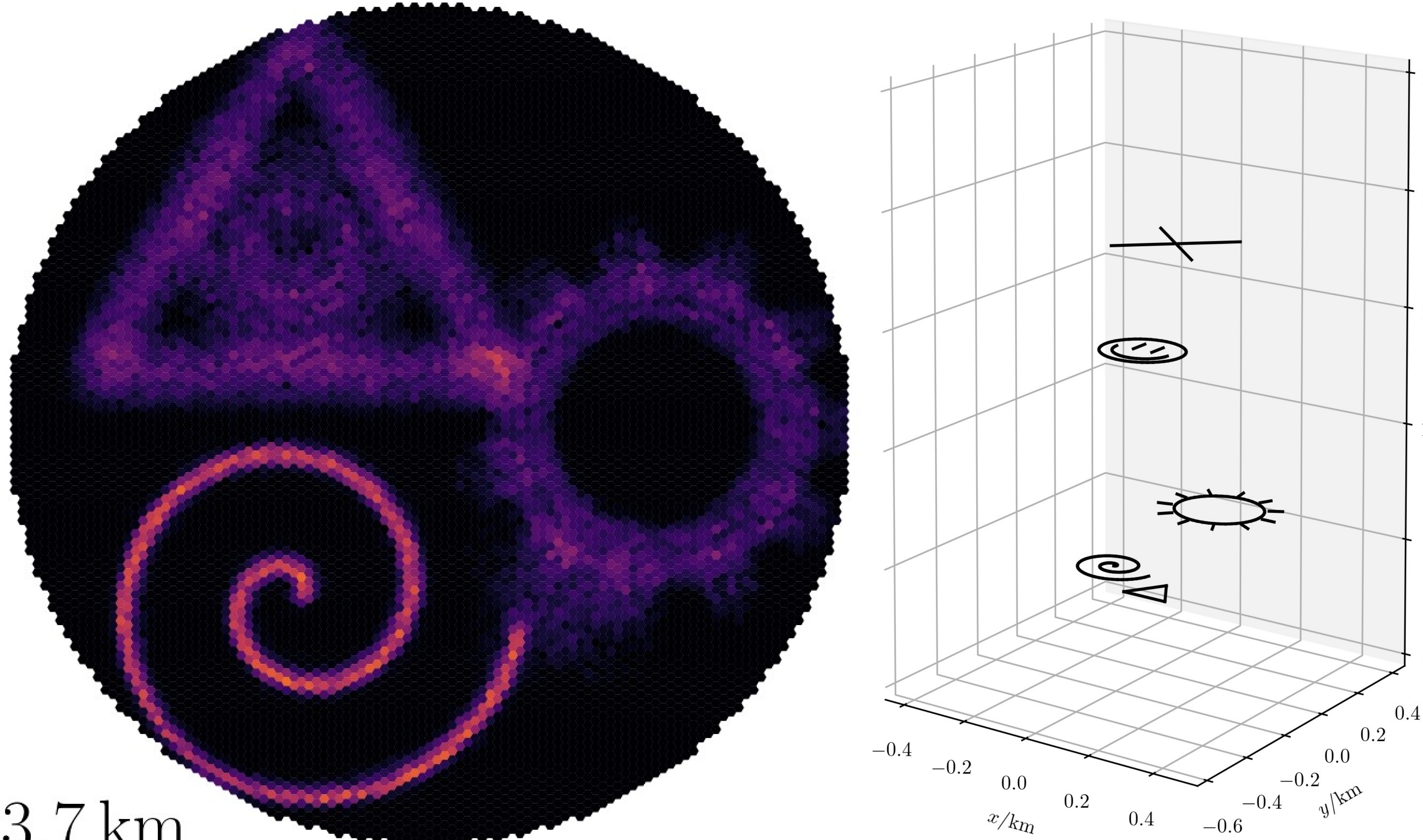
object-distance g/km
0
5
10
15
20
25
x/km
−0.4
−0.2
0.0
0.2
0.4
y/km
−0.6
−0.4
−0.2
0.0
0.2
0.4

3.7 km

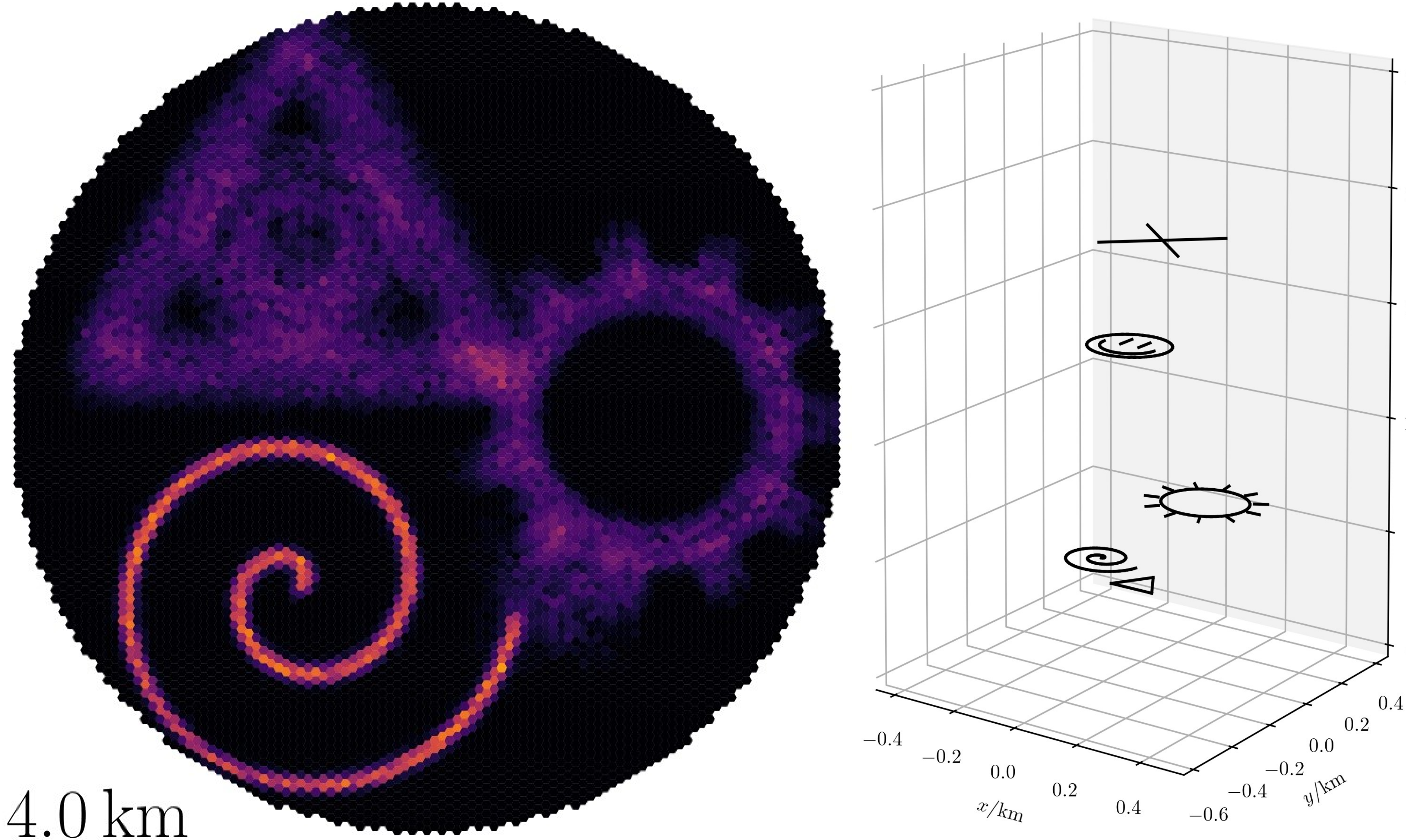
4.0 km
object-distance g/km
25
20
15
10
5
0
−0.4
−0.2
0.0
0.2
0.4
x/km
0.4
0.2
0.0
−0.2
−0.4
−0.6
y/km

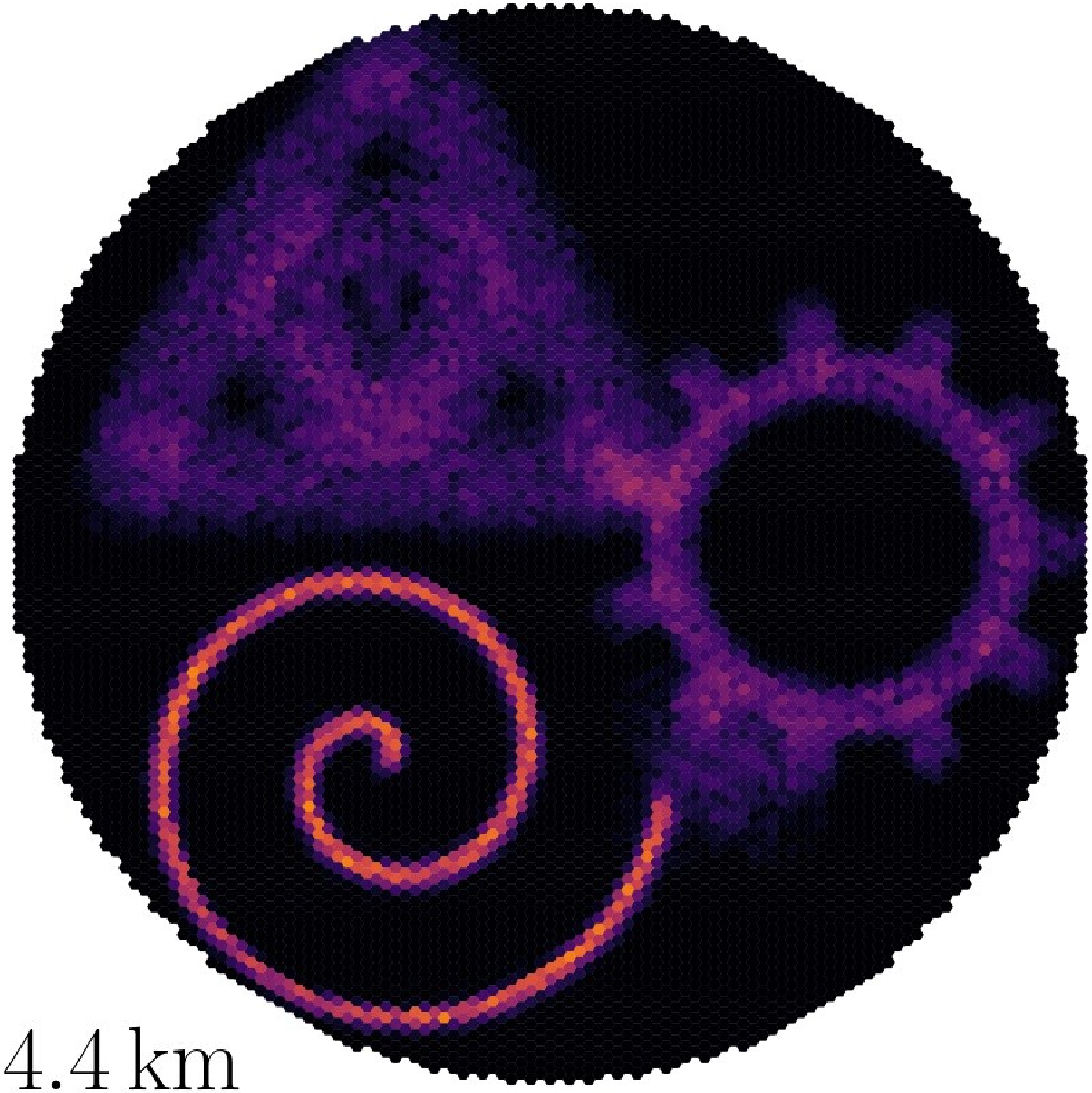
4.4 km

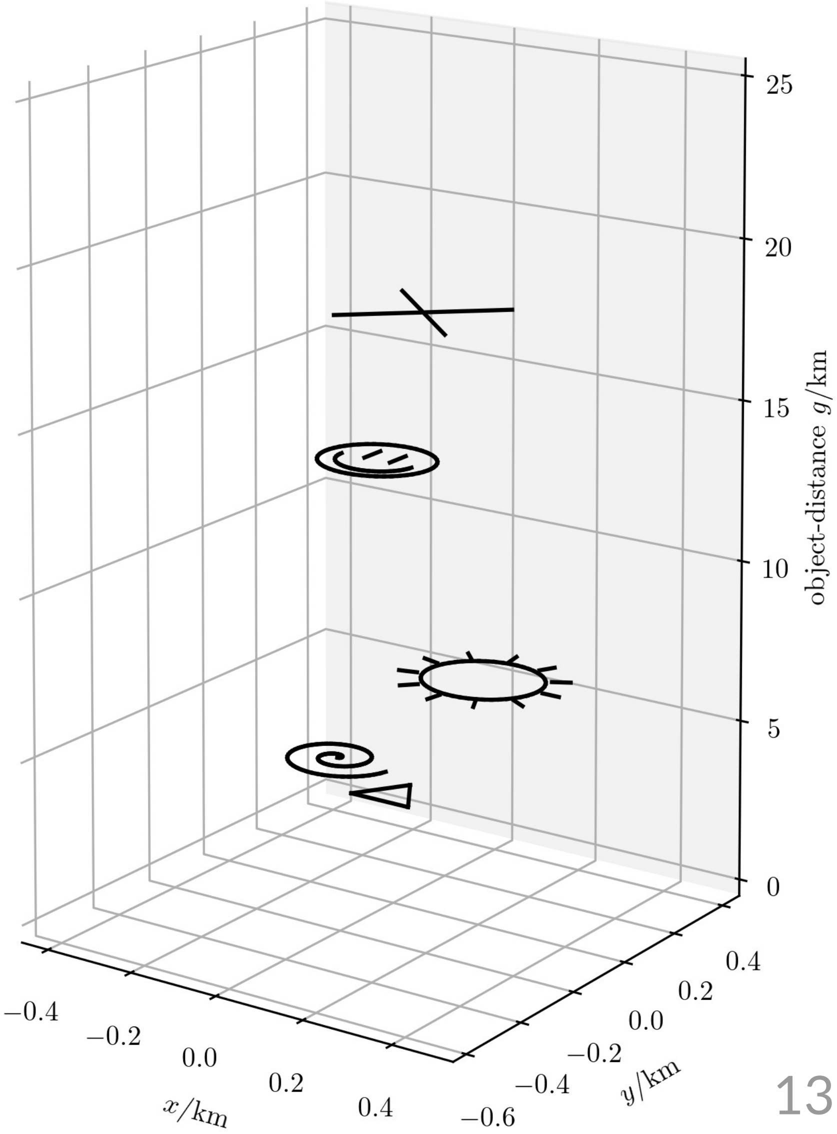
object-distance g/km
0
5
10
15
20
25
x/km
−0.4
−0.2
0.0
0.2
0.4
y/km
−0.6
−0.4
−0.2
0.0
0.2
0.4

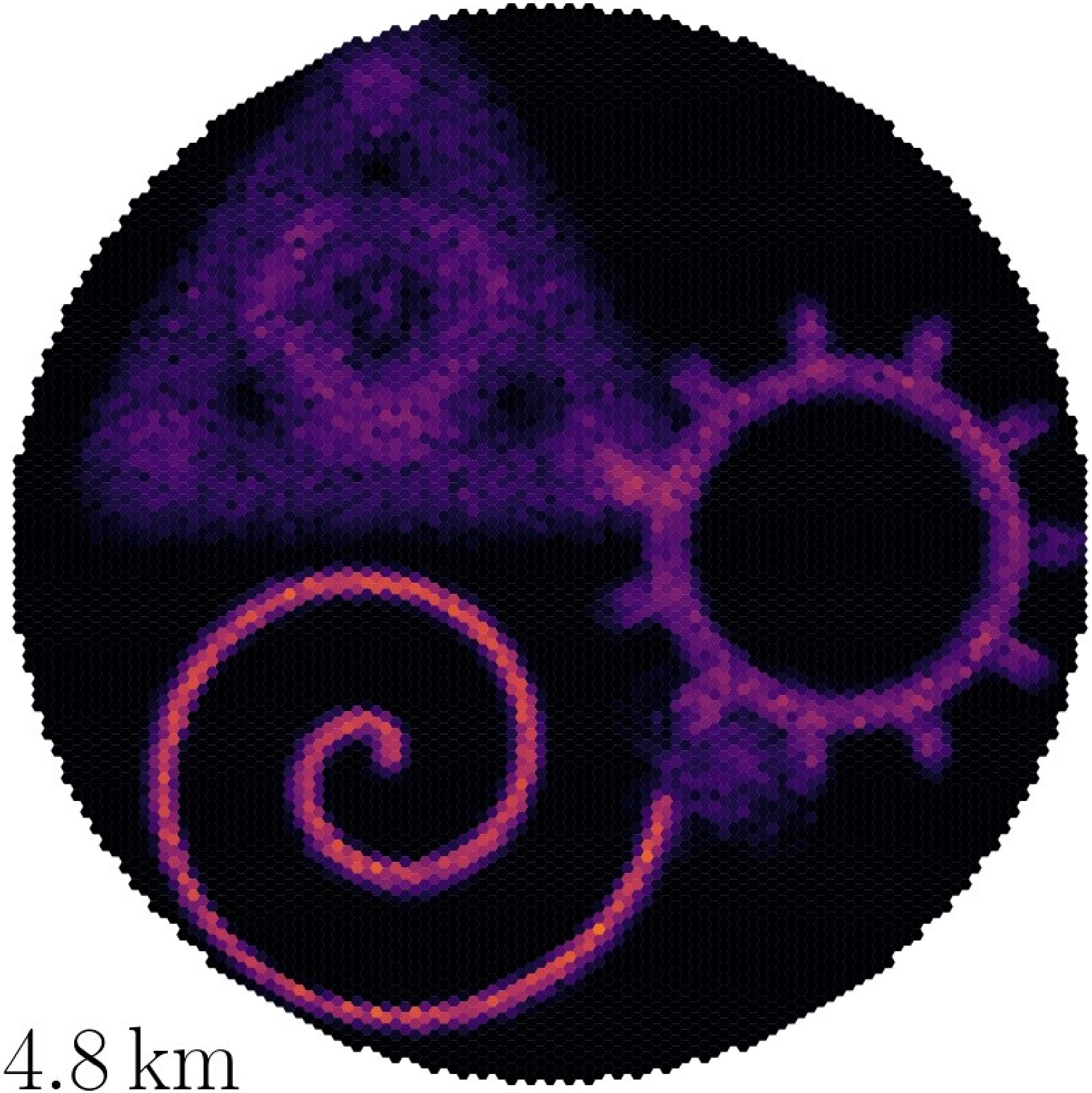

4.8 km

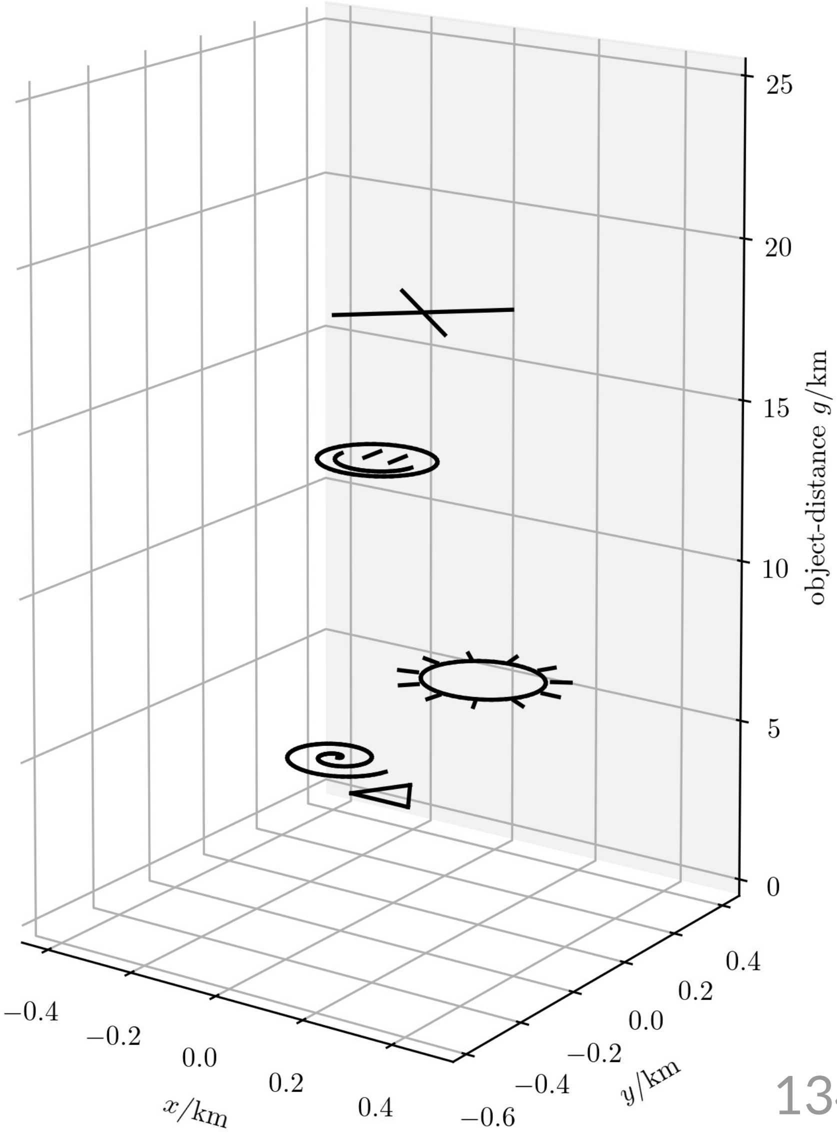

object-distance g/km
25
20
15
10
5
0
x/km
−0.4
−0.2
0.0
0.2
0.4
y/km
−0.6
−0.4
−0.2
0.0
0.2
0.4

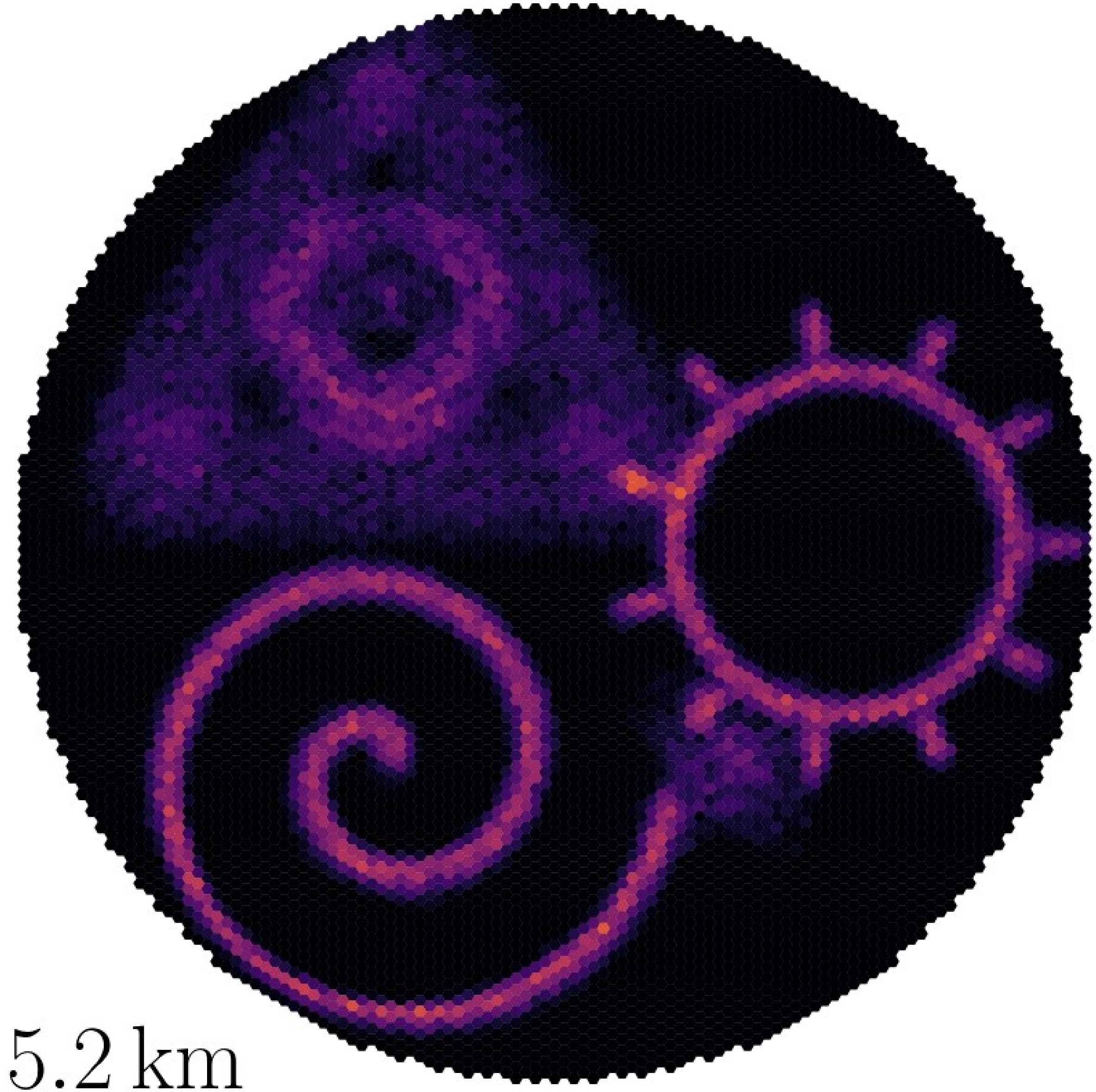
5.2 km

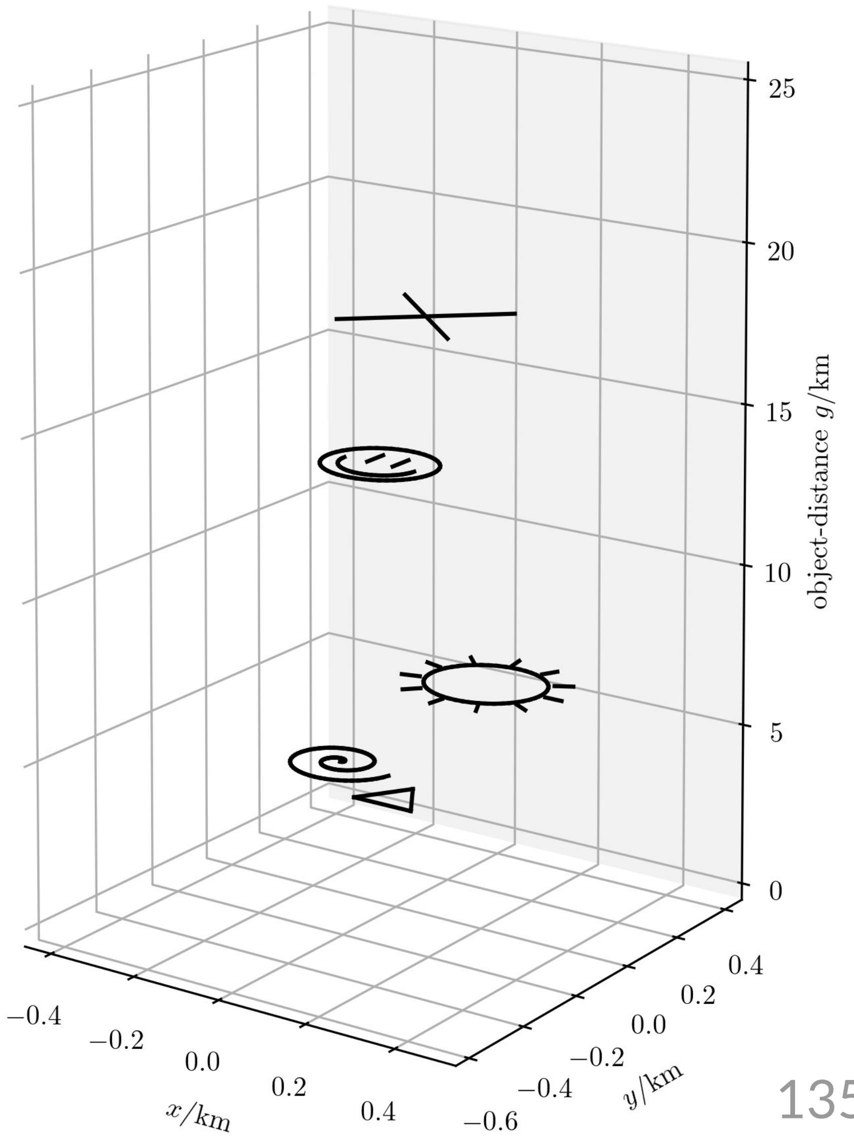
25
20
15
10
5
0
object-distance g/km
−0.4
−0.2
0.0
0.2
0.4
x/km
−0.6
−0.4
−0.2
0.0
0.2
0.4
y/km

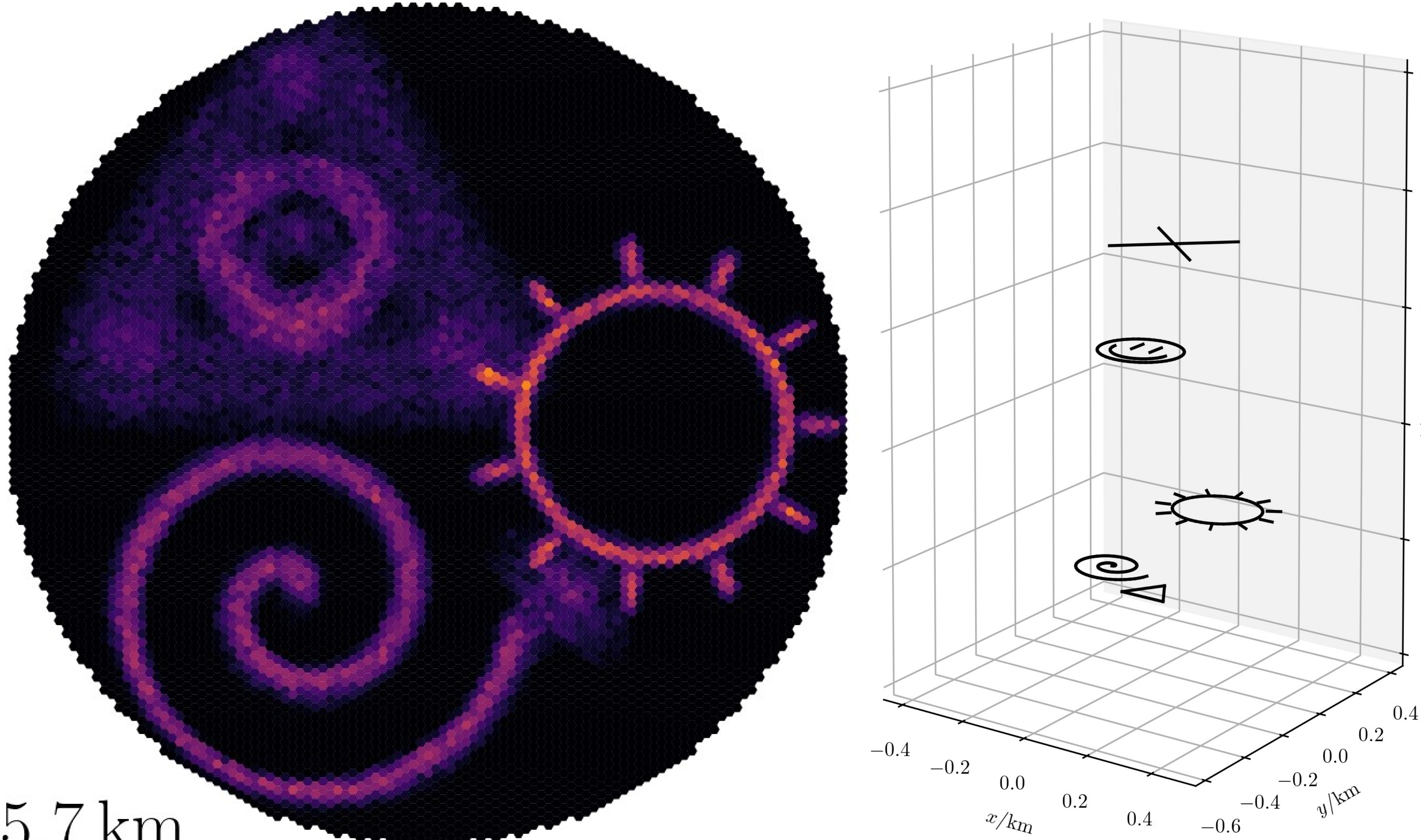
25
20
15
10
5
0
object-distance g/km
−0.4
−0.2
0.0
0.2
0.4
x/km
0.4
0.2
0.0
−0.2
−0.4
−0.6
y/km

5.7 km

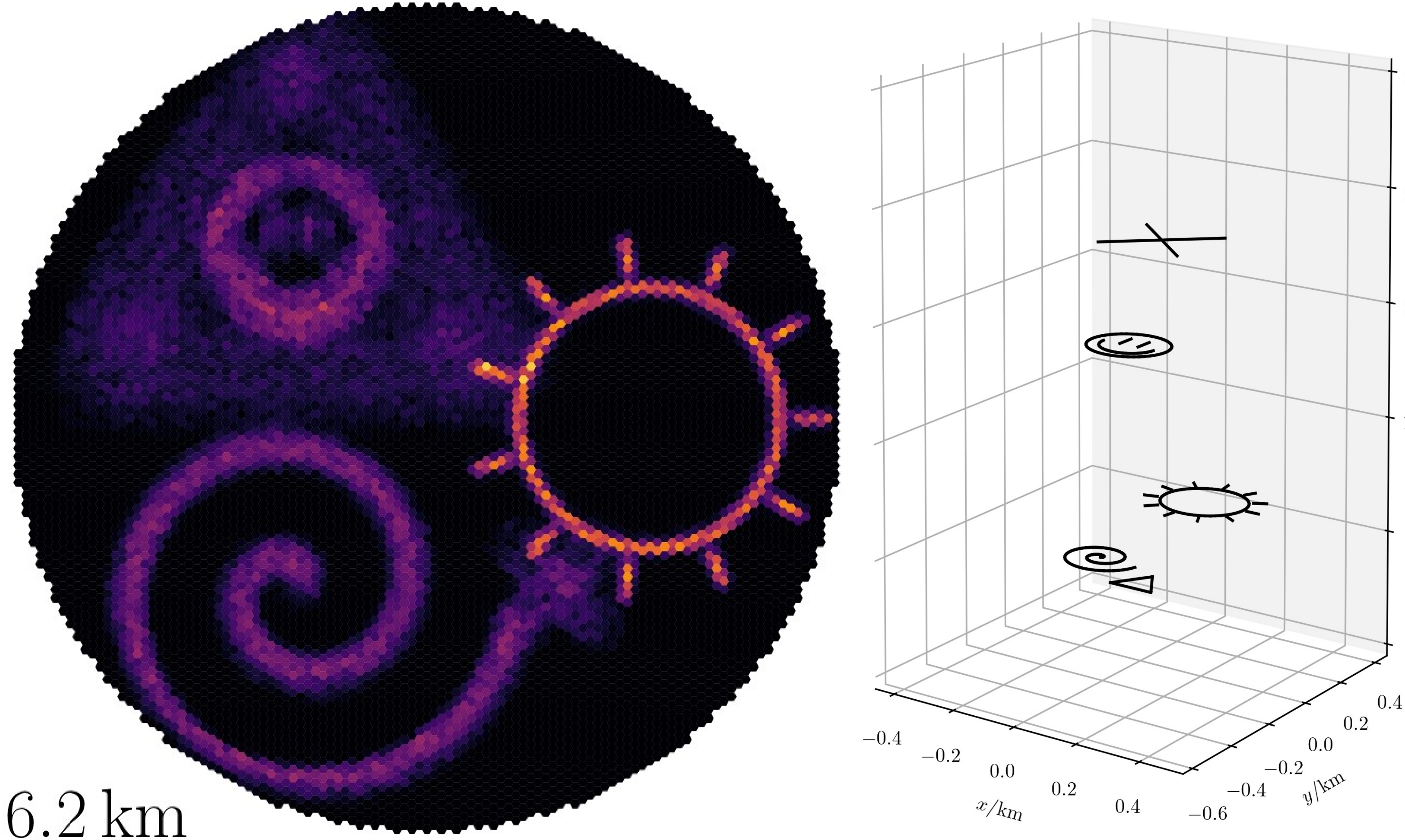

6.2 km
object-distance g/km
25
20
15
10
5
0
−0.4
−0.2
0.0
0.2
0.4
x/km
−0.6
−0.4
−0.2
0.0
0.2
0.4
y/km

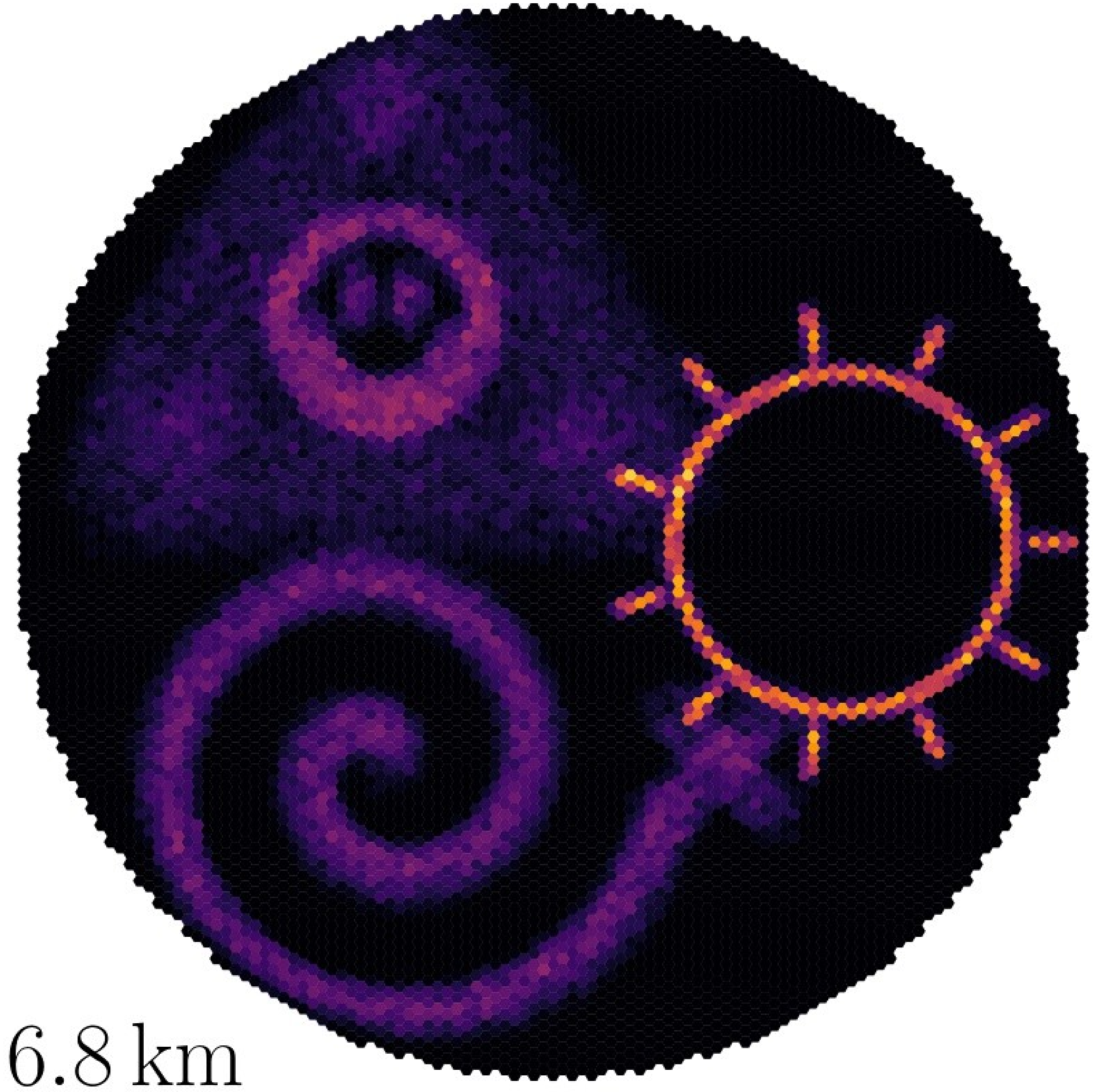
6.8 km

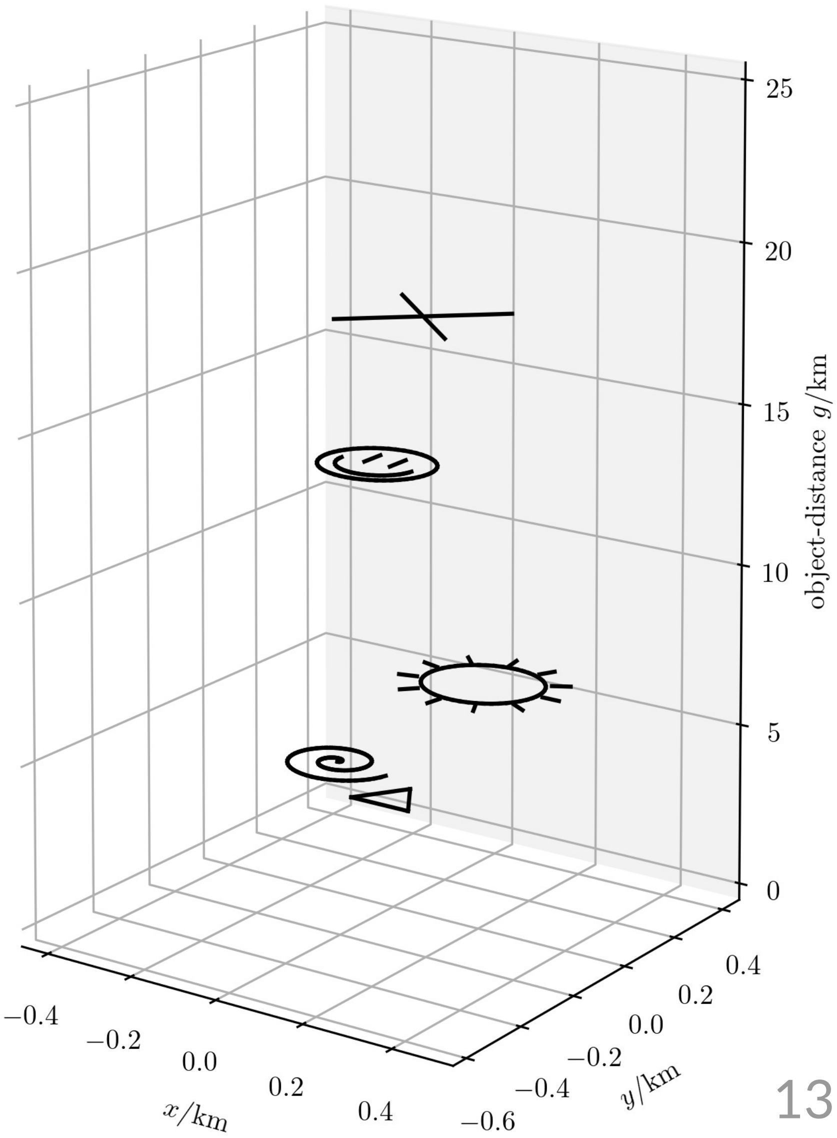
object-distance g/km
25
20
15
10
5
0
−0.4
−0.2
0.0
0.2
0.4
x/km
−0.6
−0.4
−0.2
0.0
0.2
0.4
y/km

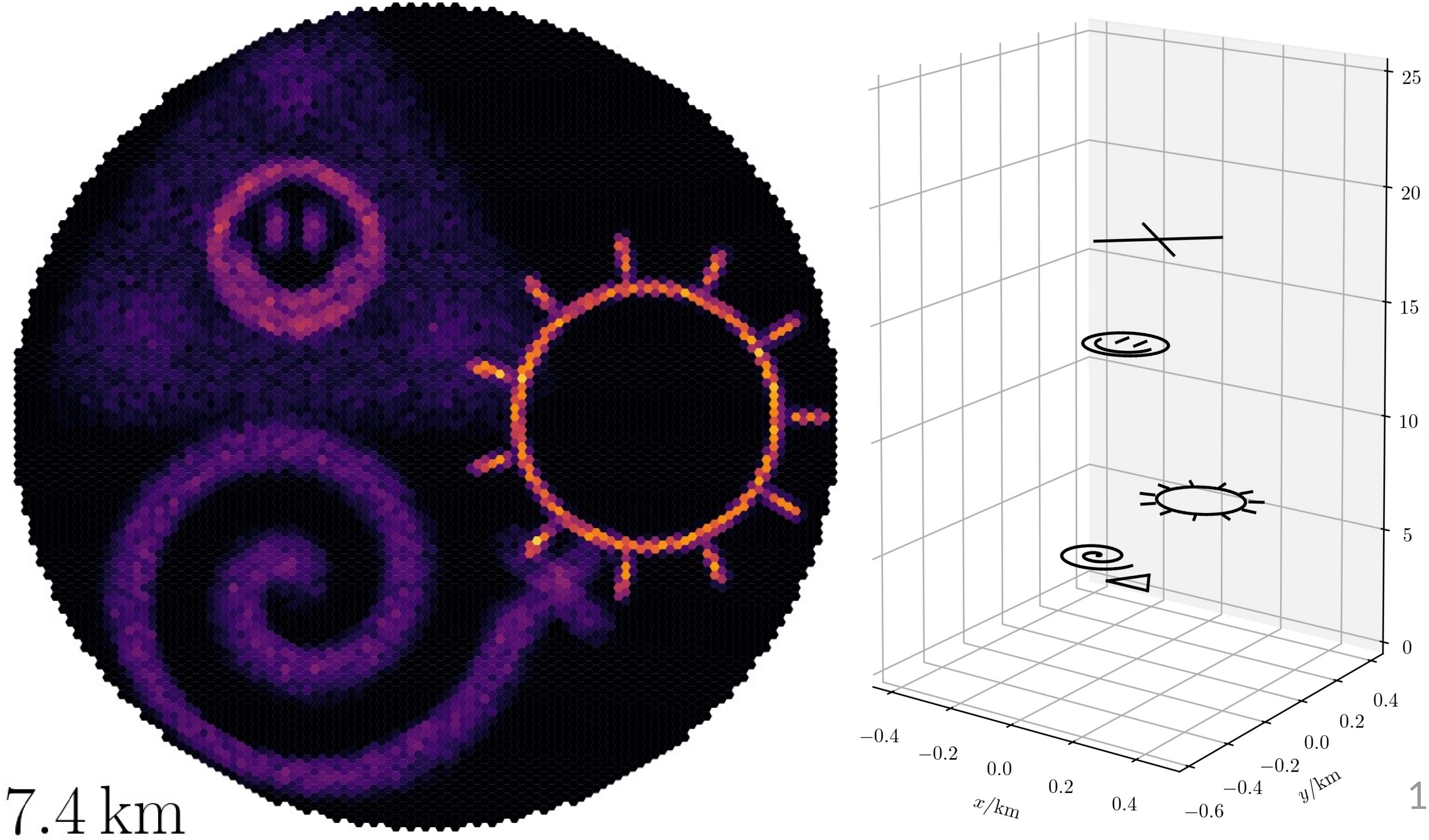

7.4 km
object-distance g/km
x/km
y/km

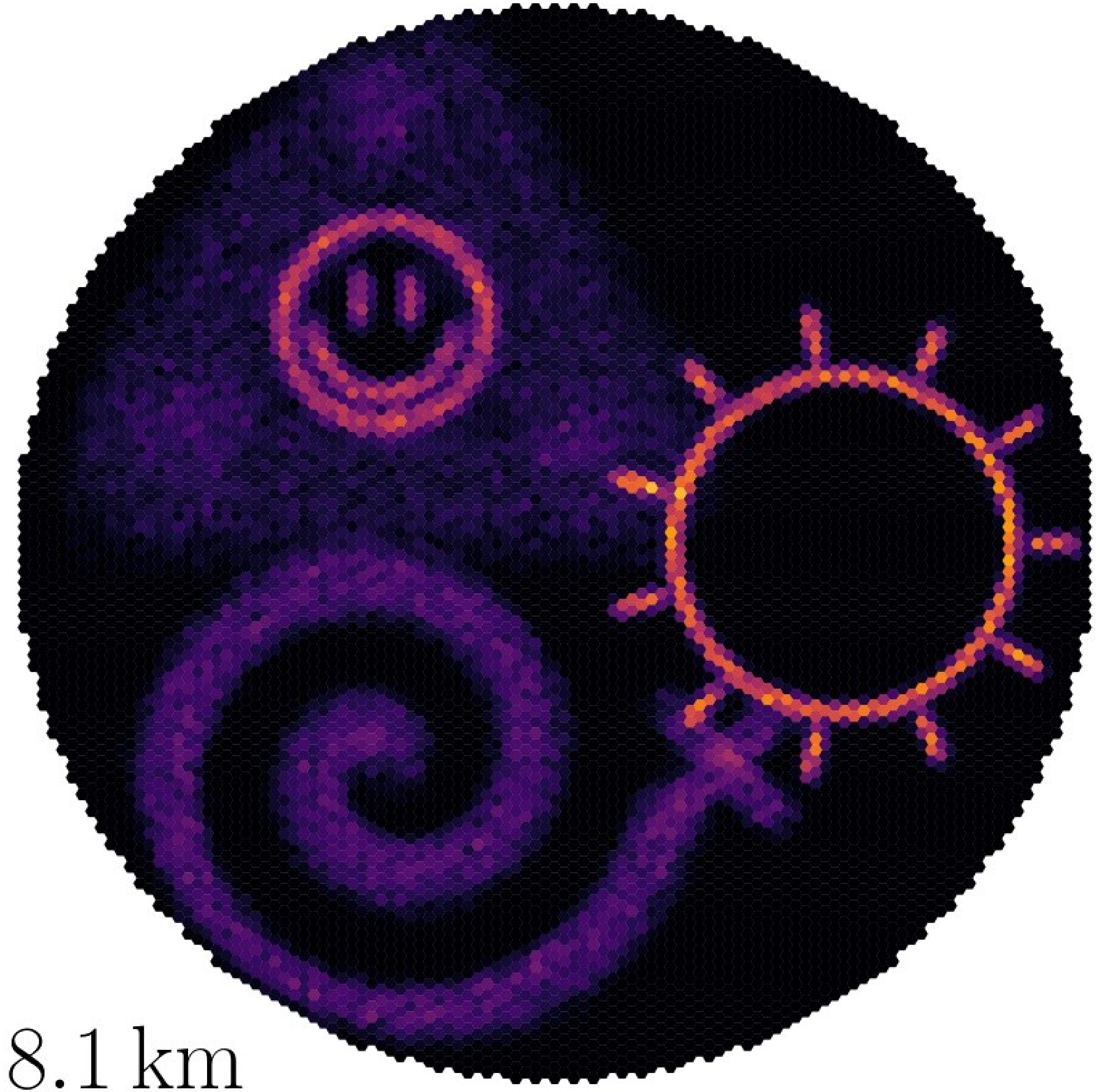
8.1 km

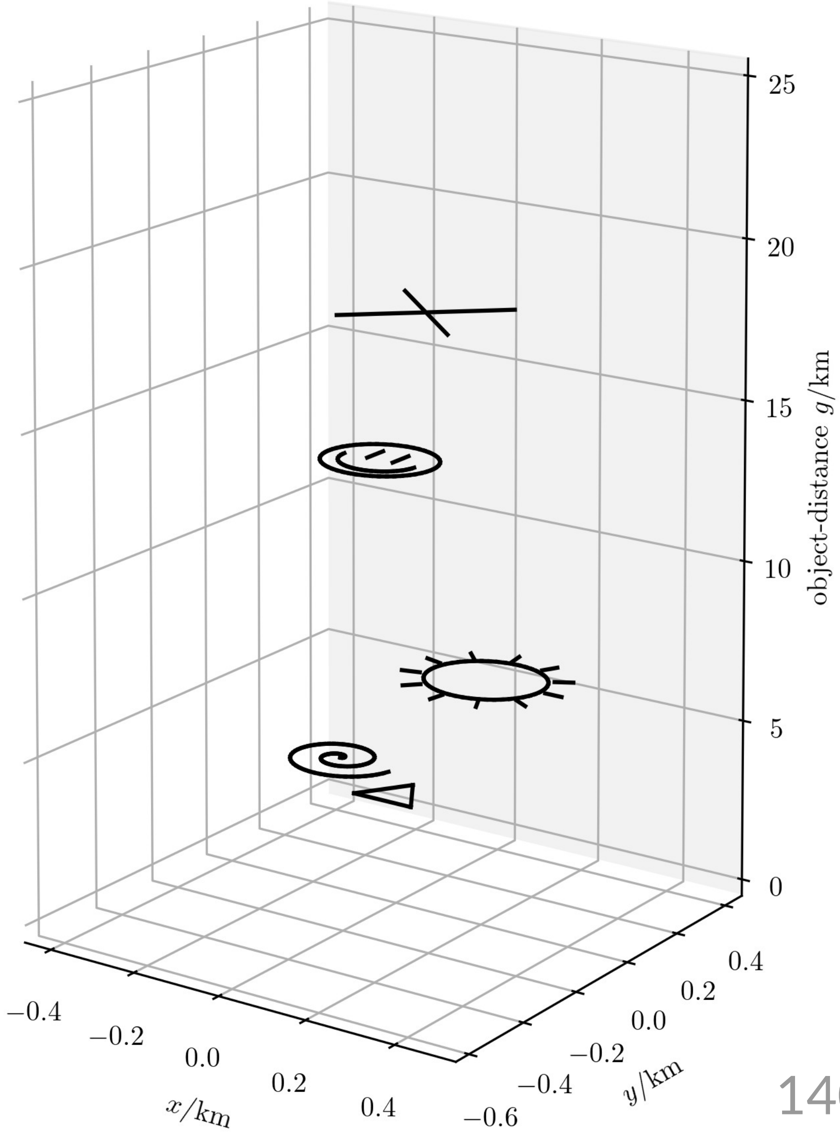
25
20
15
10
5
0
object-distance g/km
−0.4
−0.2
0.0
0.2
0.4
x/km
0.4
0.2
0.0
−0.2
−0.4
−0.6
y/km

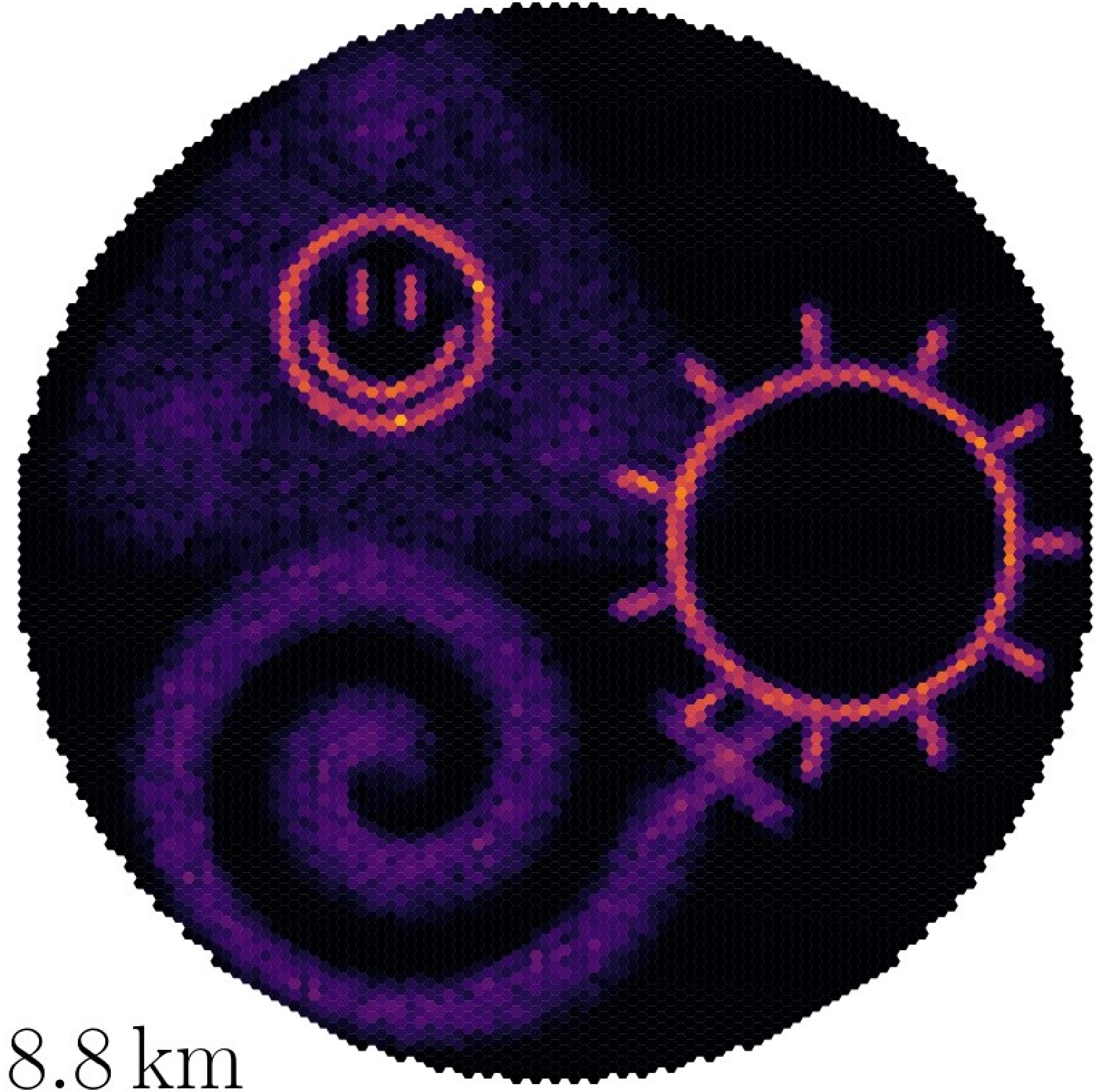
8.8 km

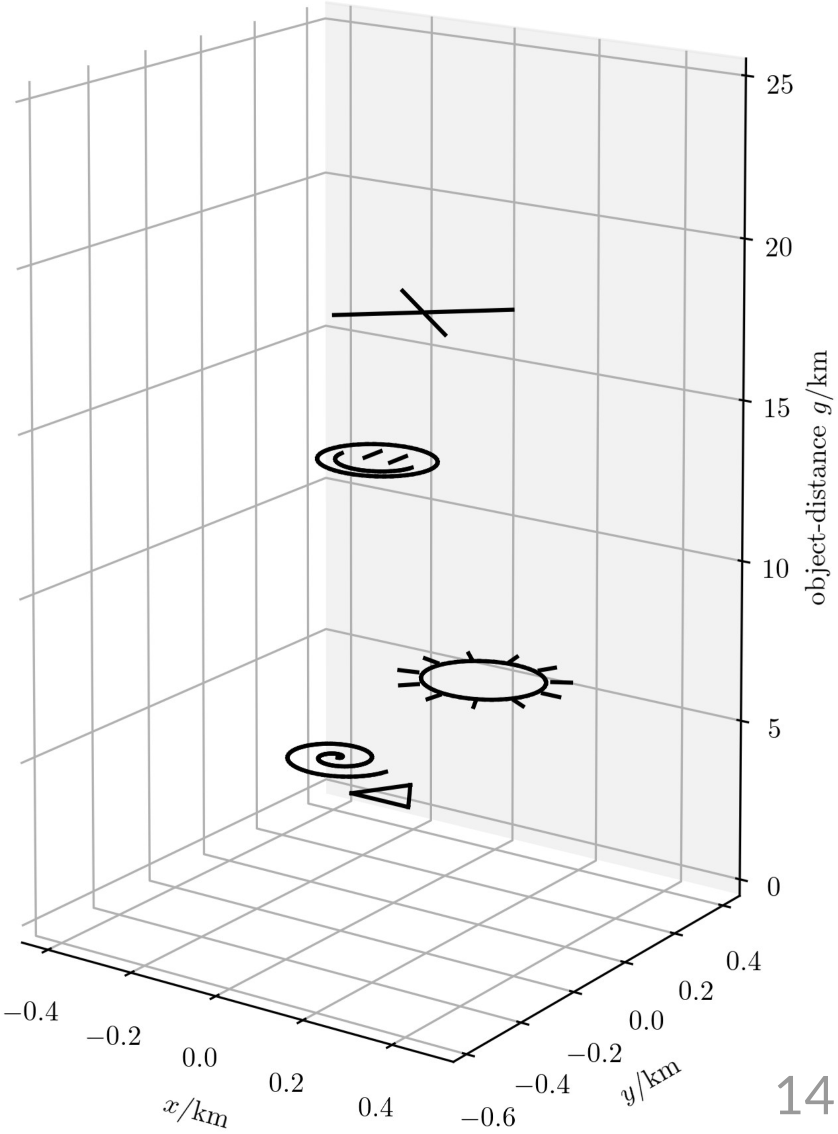
object-distance g/km
0
5
10
15
20
25
x/km
−0.4
−0.2
0.0
0.2
0.4
y/km
−0.6
−0.4
−0.2
0.0
0.2
0.4

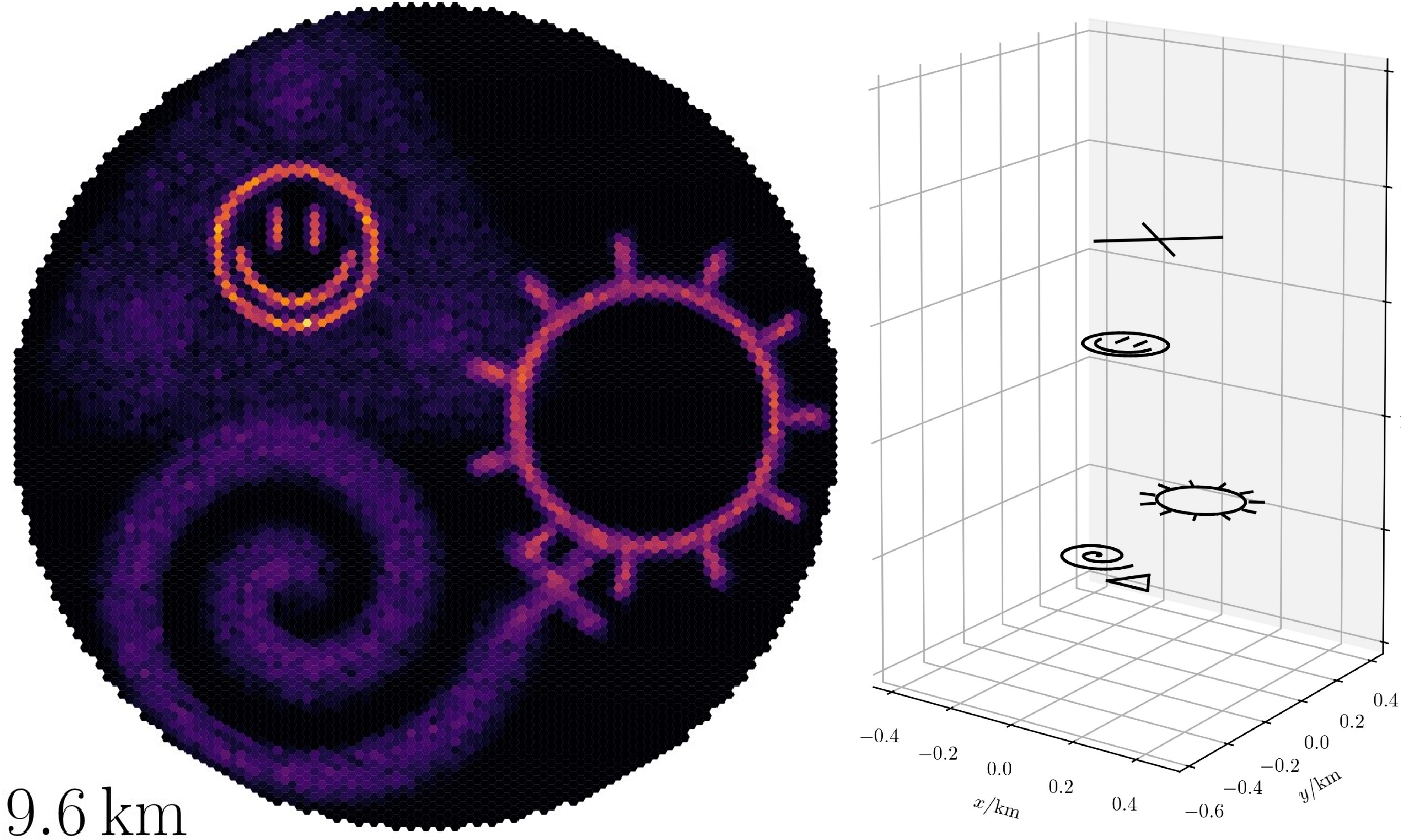
9.6 km
object-distance g/km
0
5
10
15
20
25
x/km
−0.4
−0.2
0.0
0.2
0.4
y/km
−0.6
−0.4
−0.2
0.0
0.2
0.4

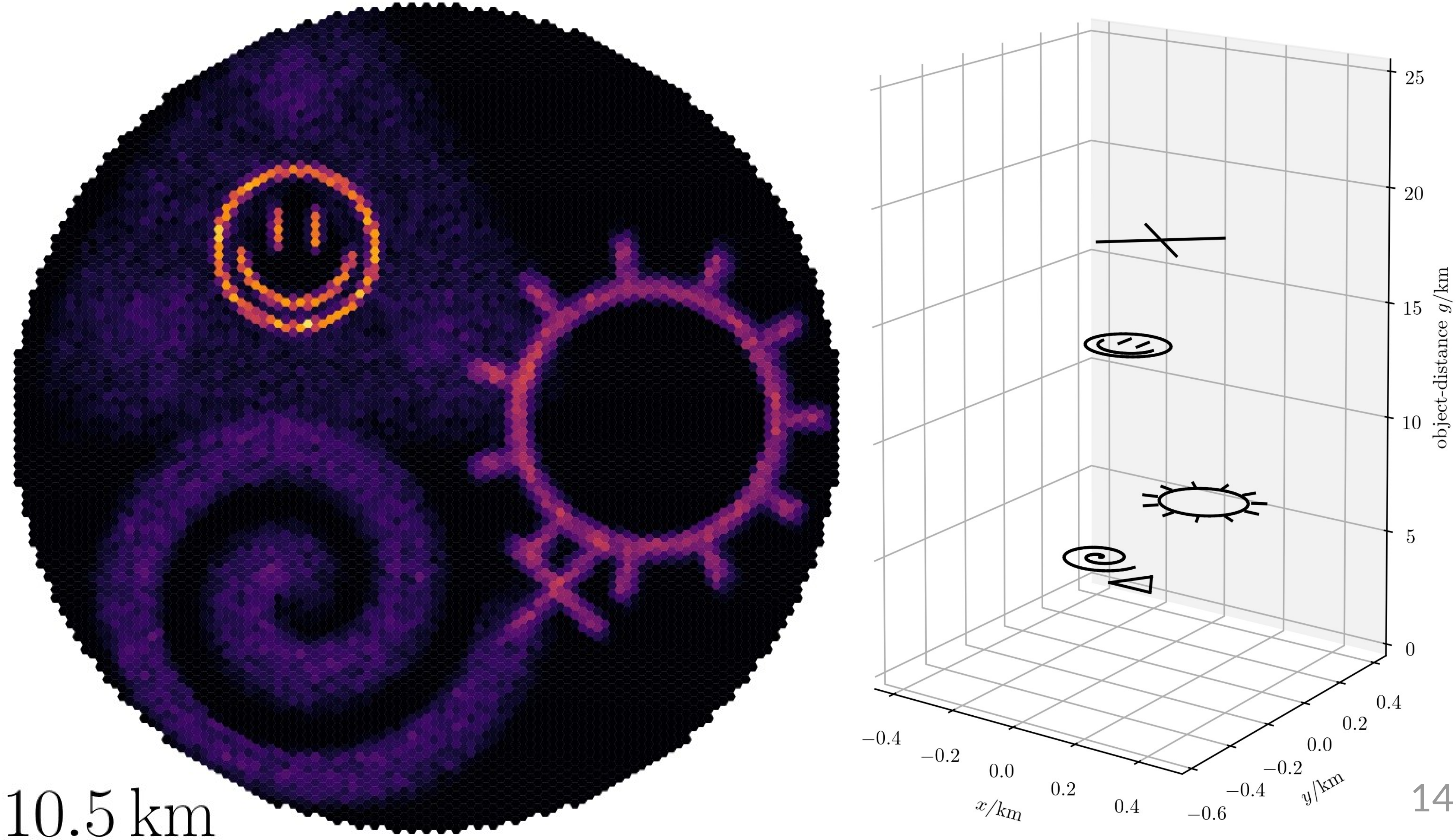
10.5 km
object-distance g/km
0
5
10
15
20
25
x/km
−0.4
−0.2
0.0
0.2
0.4
y/km
−0.6
−0.4
−0.2
0.0
0.2
0.4

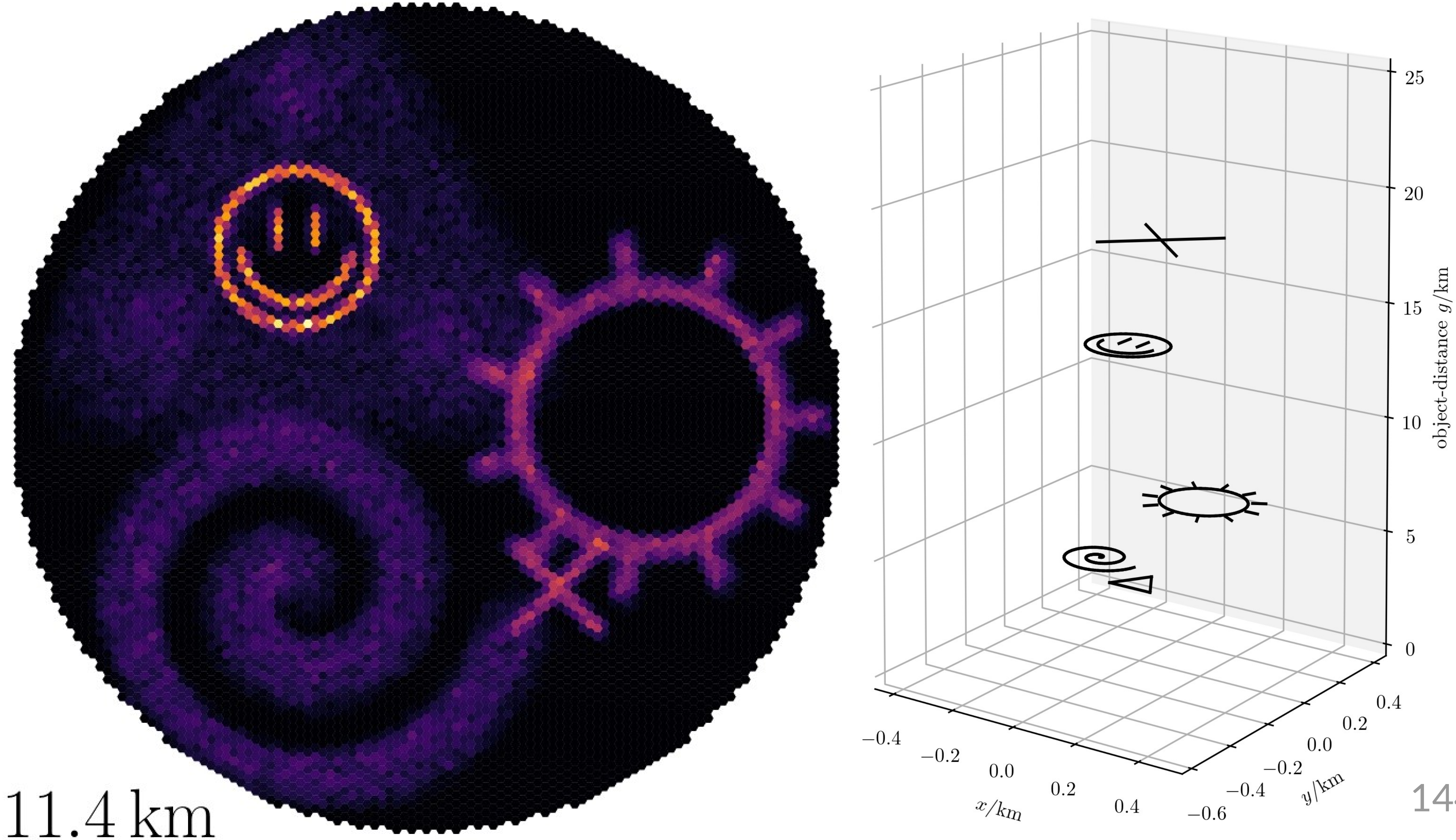
11.4 km
object-distance g/km
0
5
10
15
20
25
x/km
−0.4
−0.2
0.0
0.2
0.4
y/km
−0.6
−0.4
−0.2
0.0
0.2
0.4

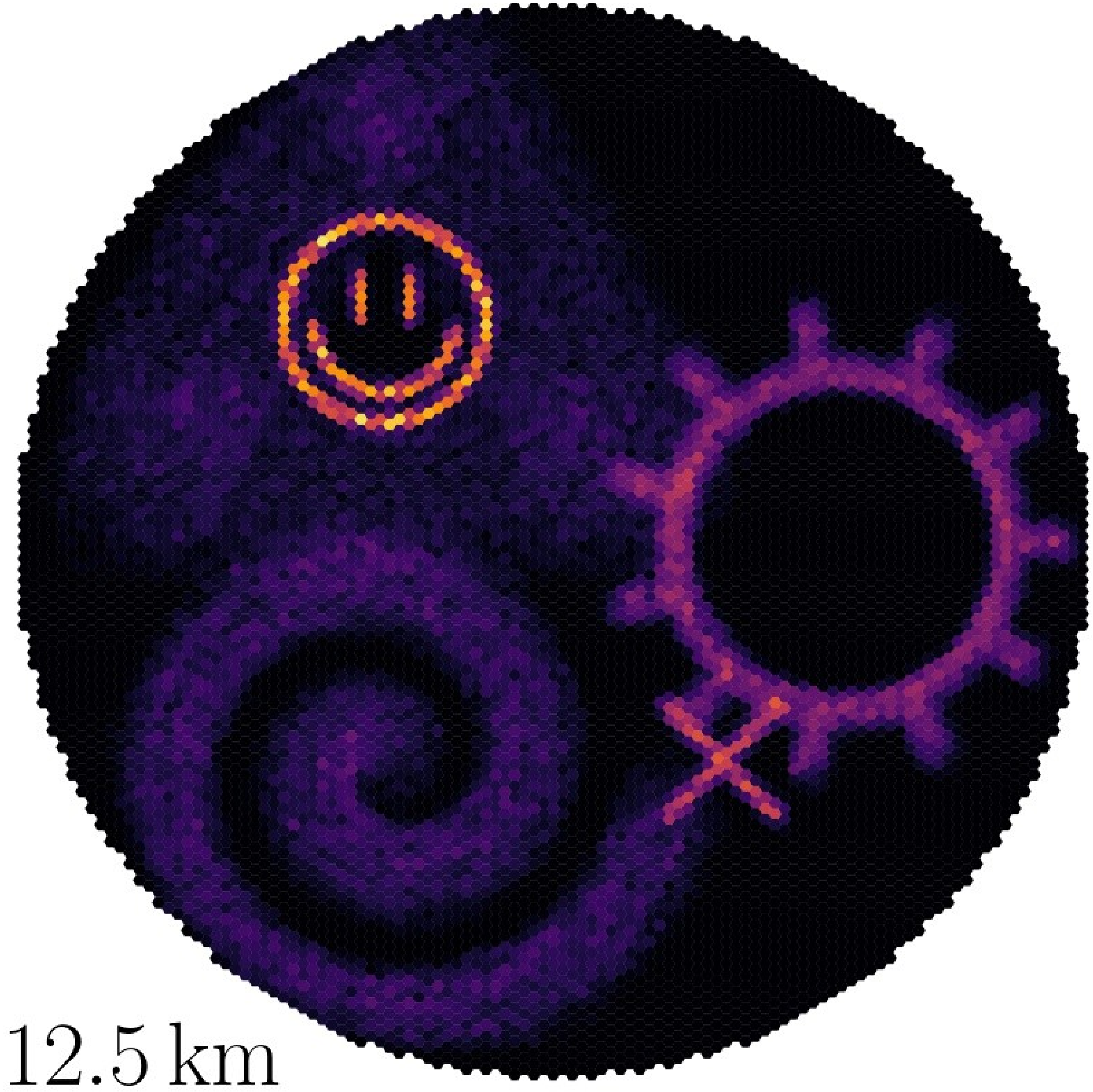
12.5 km

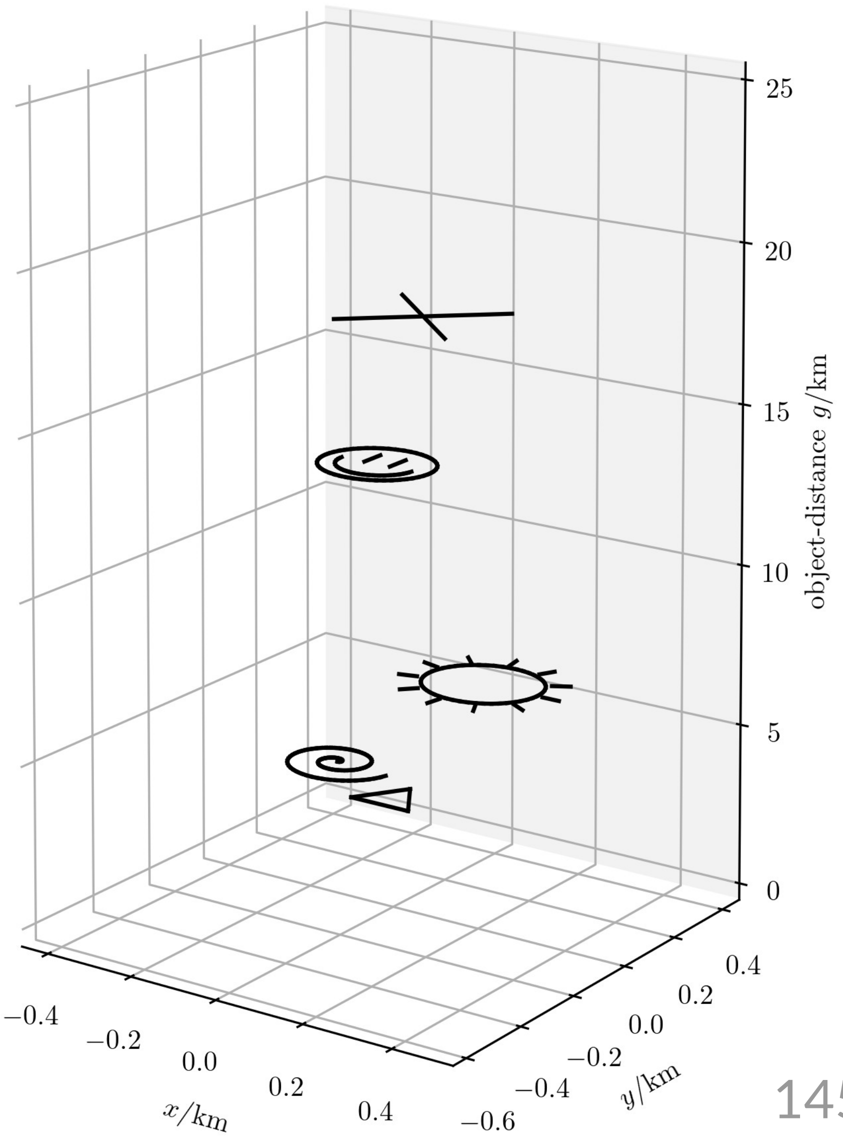
object-distance g/km
0
5
10
15
20
25
x/km
−0.4
−0.2
0.0
0.2
0.4
y/km
−0.6
−0.4
−0.2
0.0
0.2
0.4

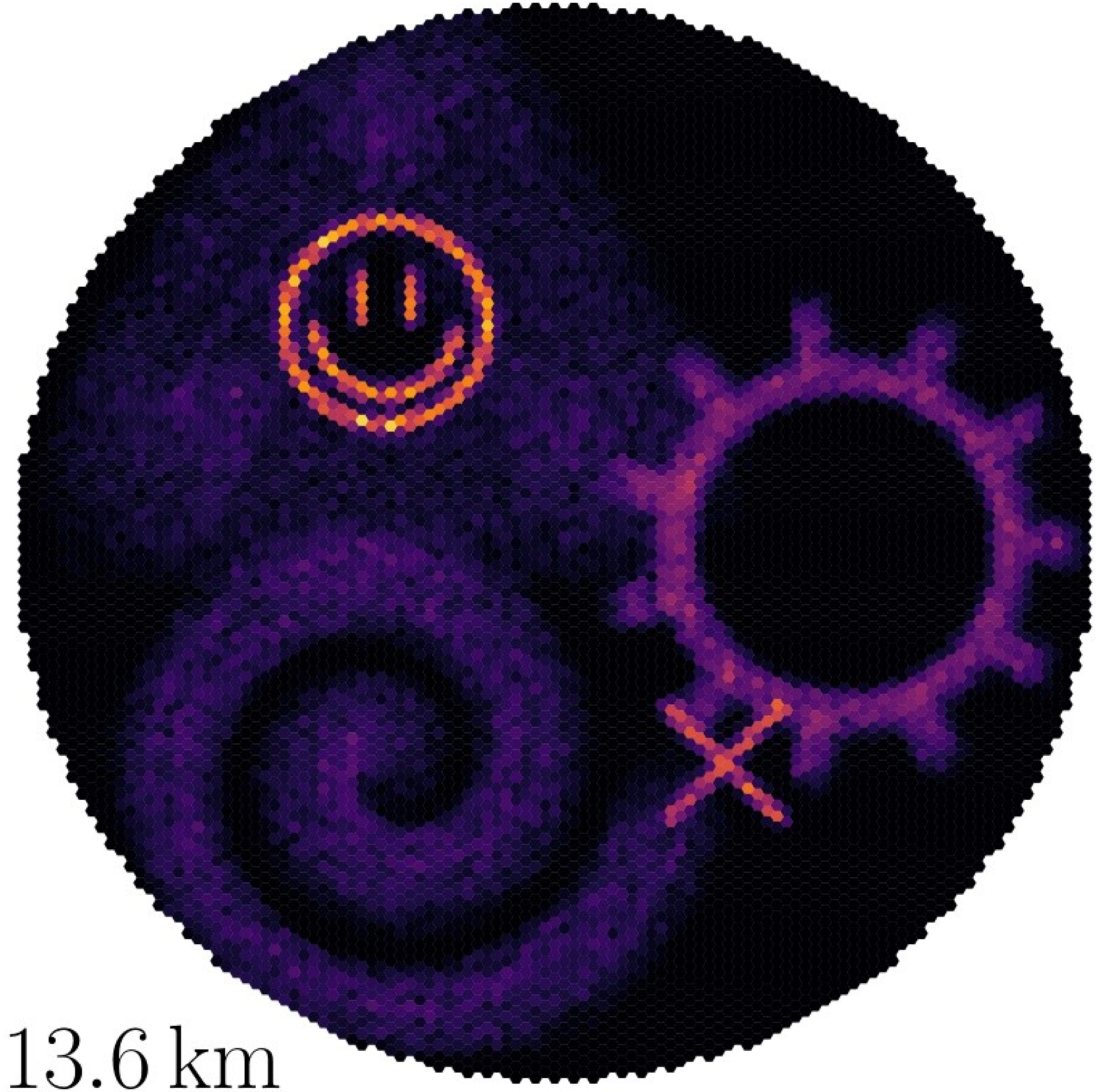
13.6 km

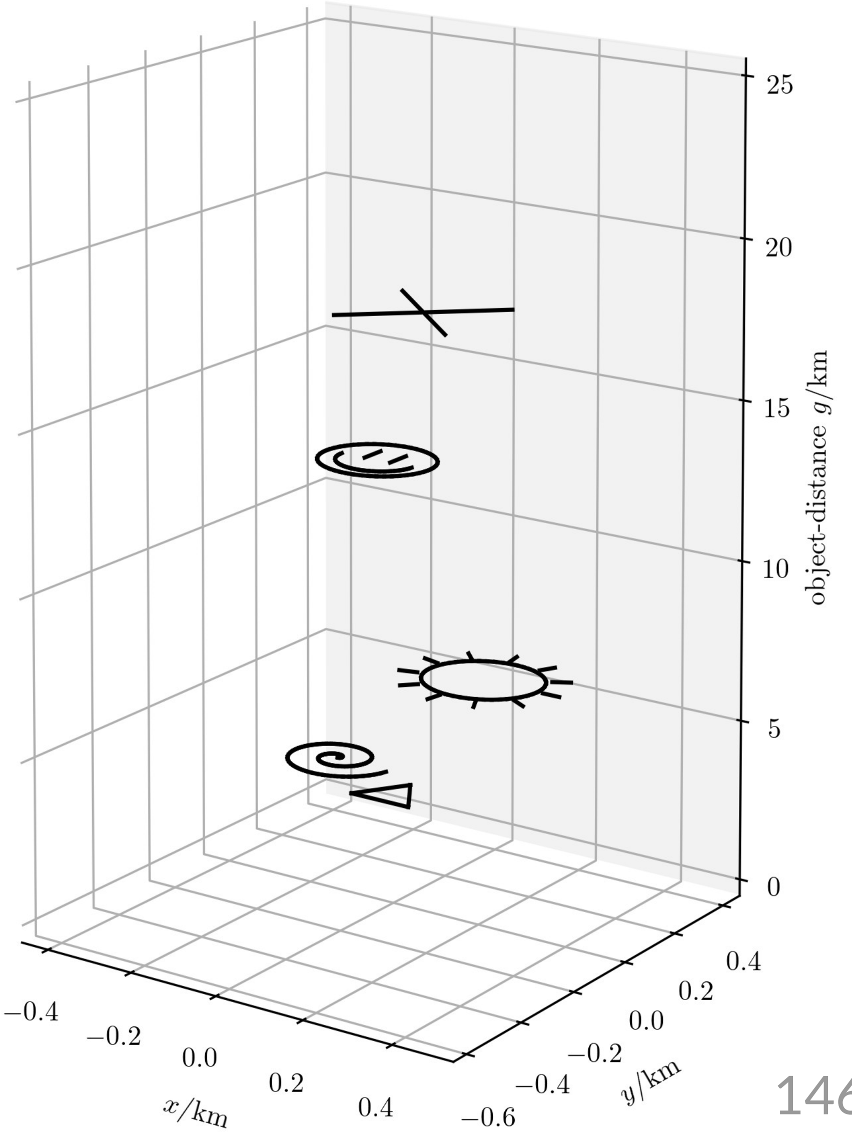
25
20
15
10
5
0
object-distance g/km
−0.4
−0.2
0.0
0.2
0.4
x/km
0.4
0.2
0.0
−0.2
−0.4
−0.6
y/km

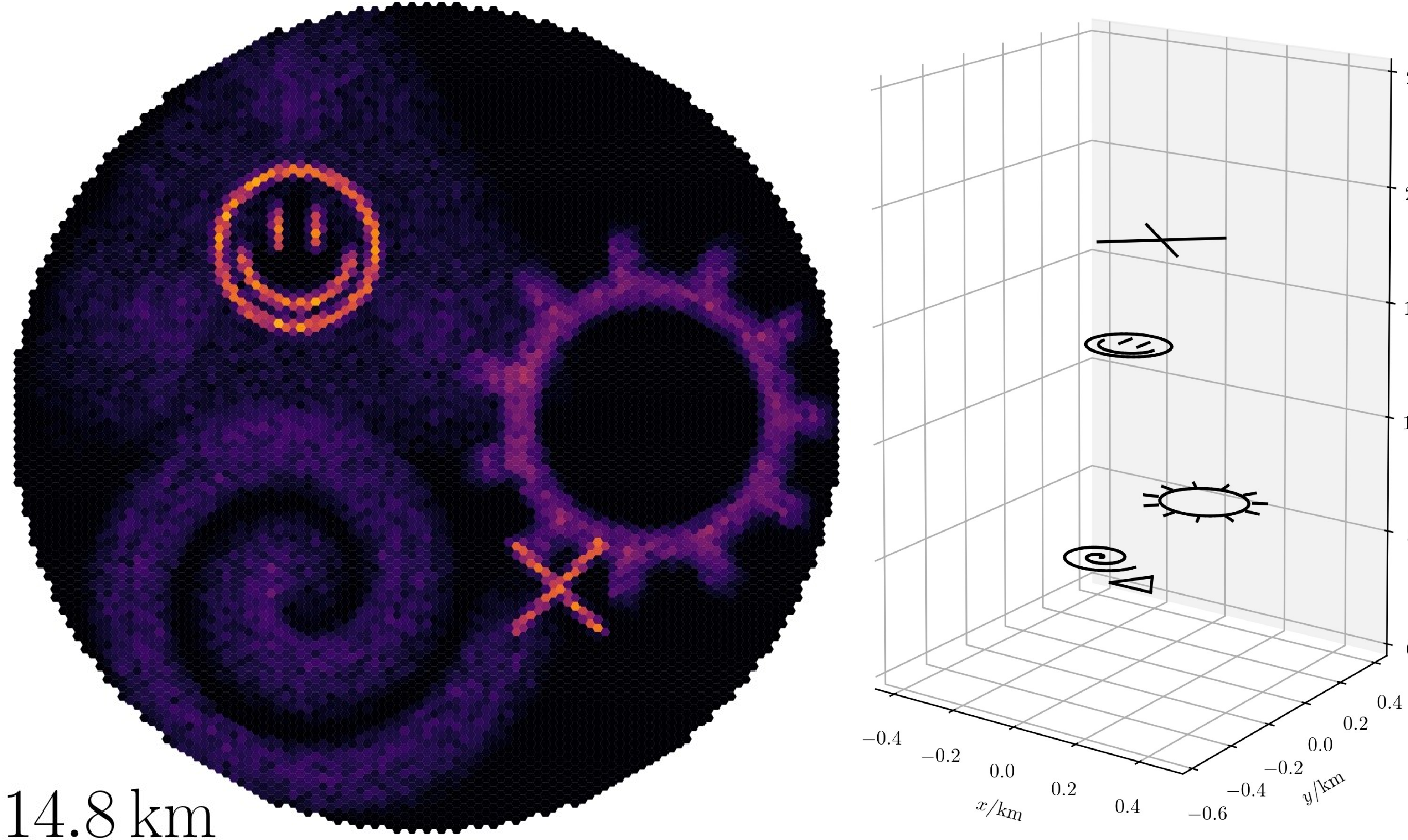
14.8 km
object-distance g/km
25
20
15
10
5
0
−0.4
−0.2
0.0
0.2
0.4
x/km
0.4
0.2
0.0
−0.2
−0.4
−0.6
y/km

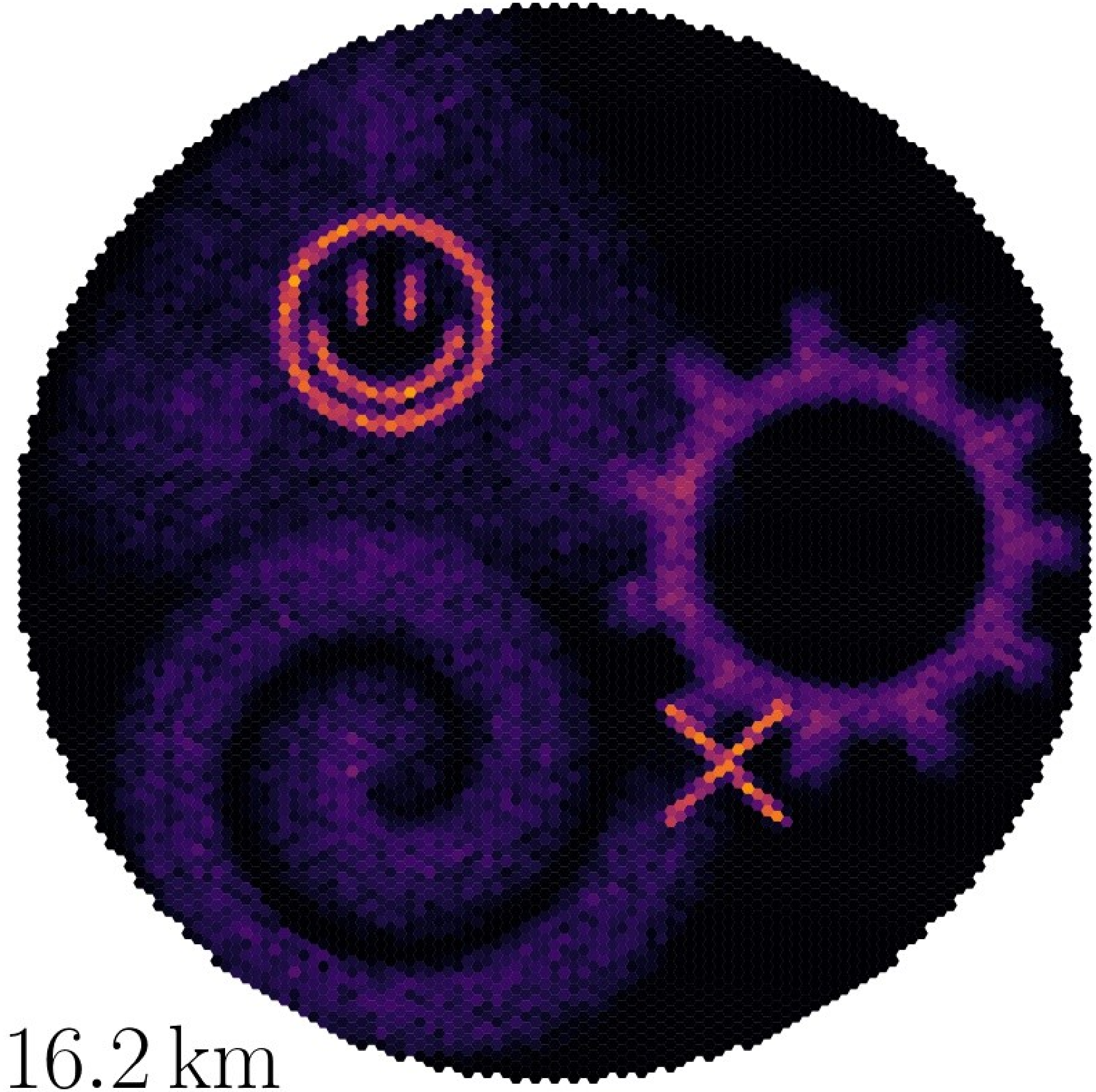
16.2 km

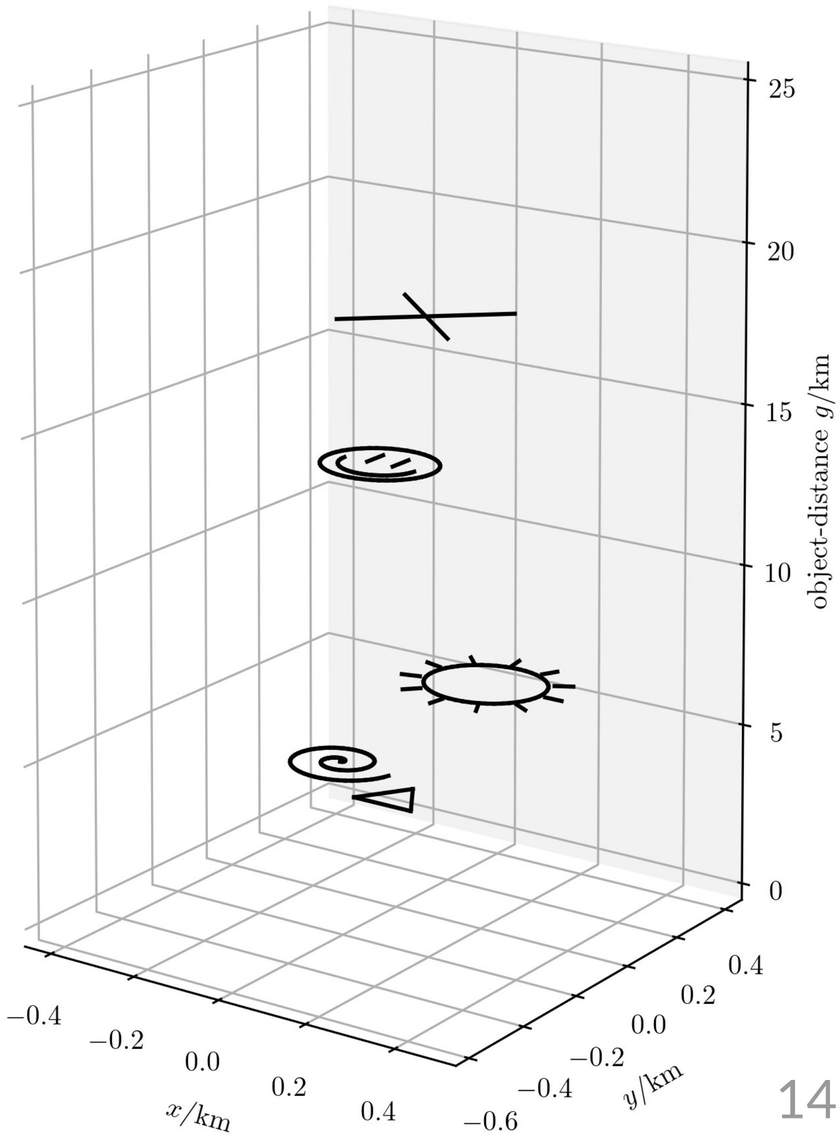
25
20
15
10
5
0
object-distance g/km
−0.4
−0.2
0.0
0.2
0.4
x/km
0.4
0.2
0.0
−0.2
−0.4
−0.6
y/km

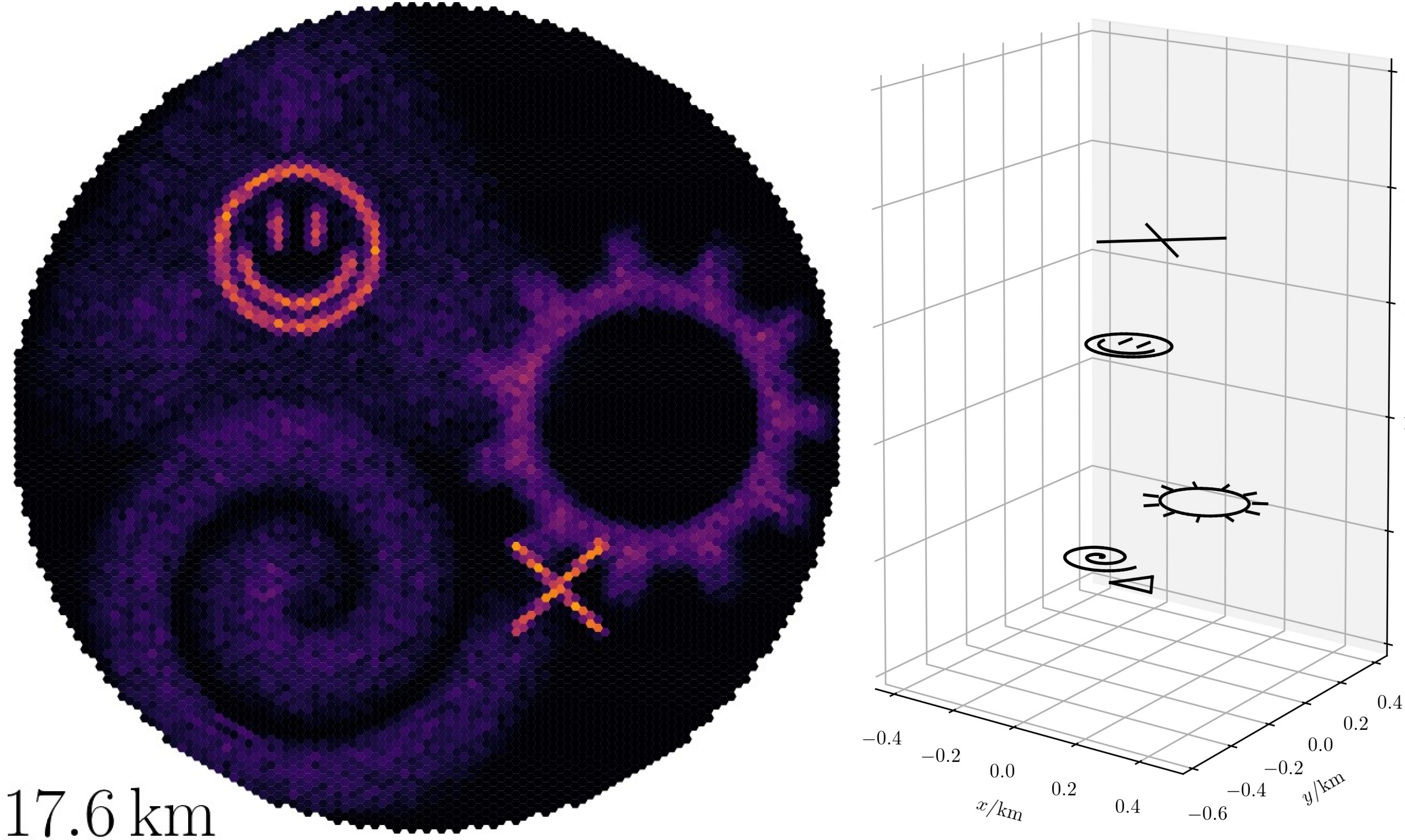
17.6 km
object-distance g/km
25
20
15
10
5
0
−0.4
−0.2
0.0
0.2
0.4
x/km
0.4
0.2
0.0
−0.2
−0.4
−0.6
y/km

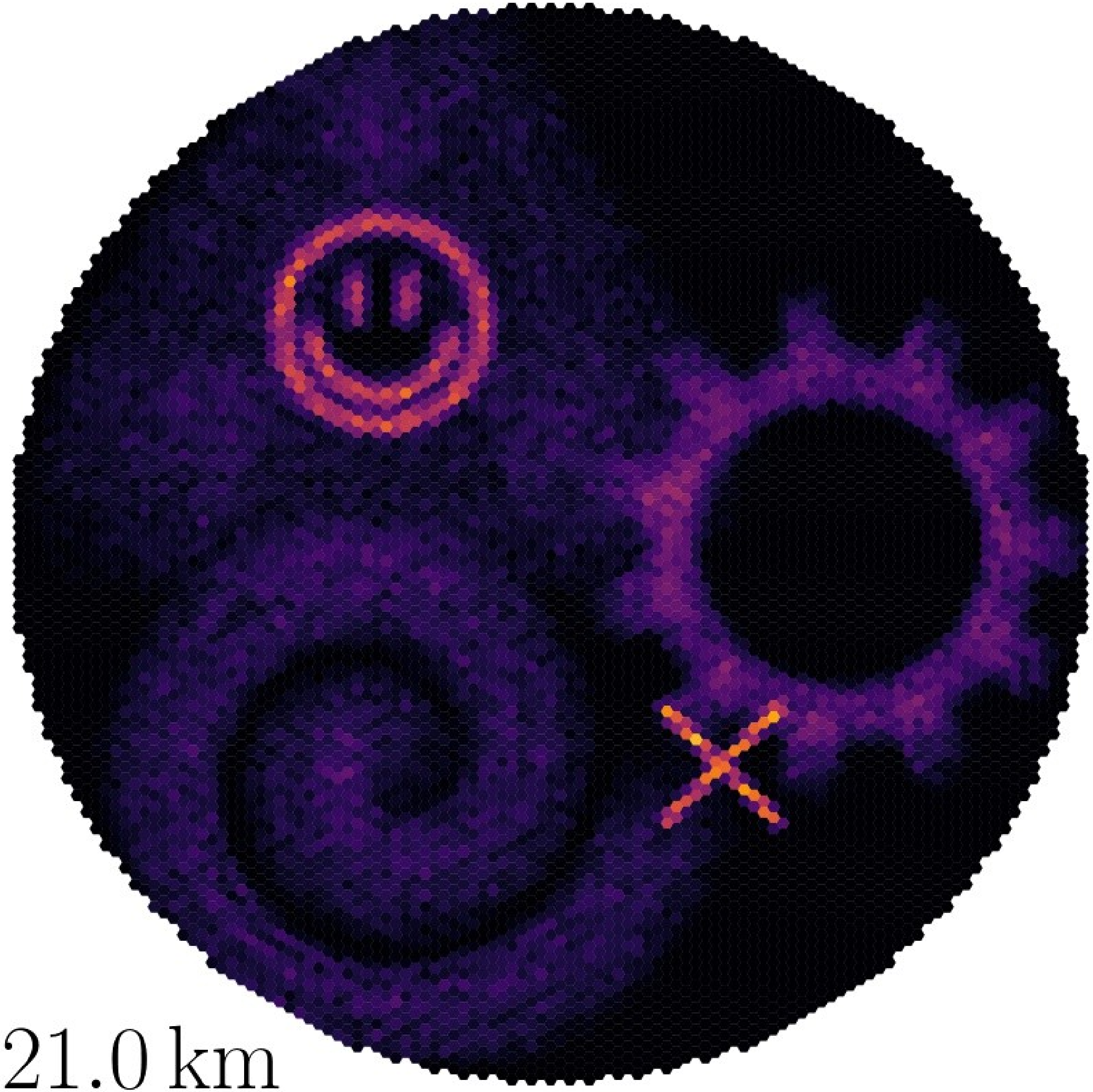

21.0 km

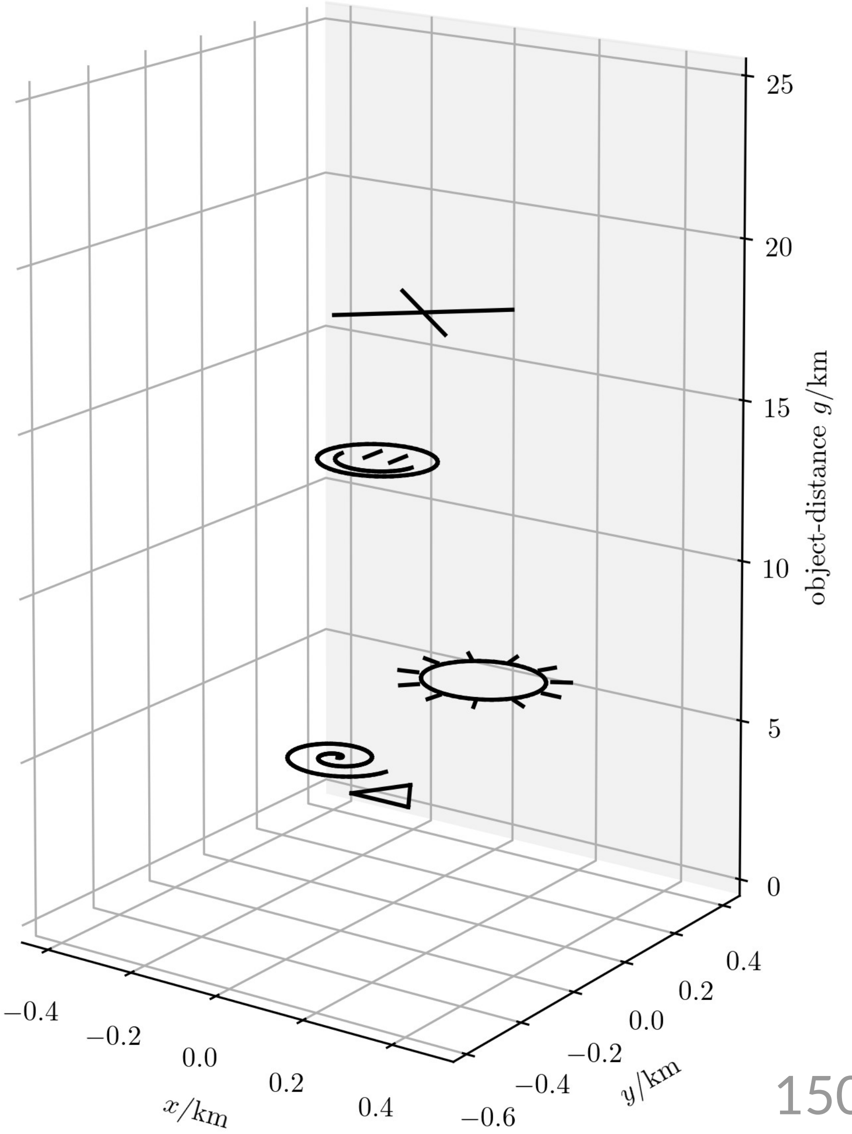

object-distance g/km
0
5
10
15
20
25
x/km
−0.4
−0.2
0.0
0.2
0.4
y/km
−0.6
−0.4
−0.2
0.0
0.2
0.4

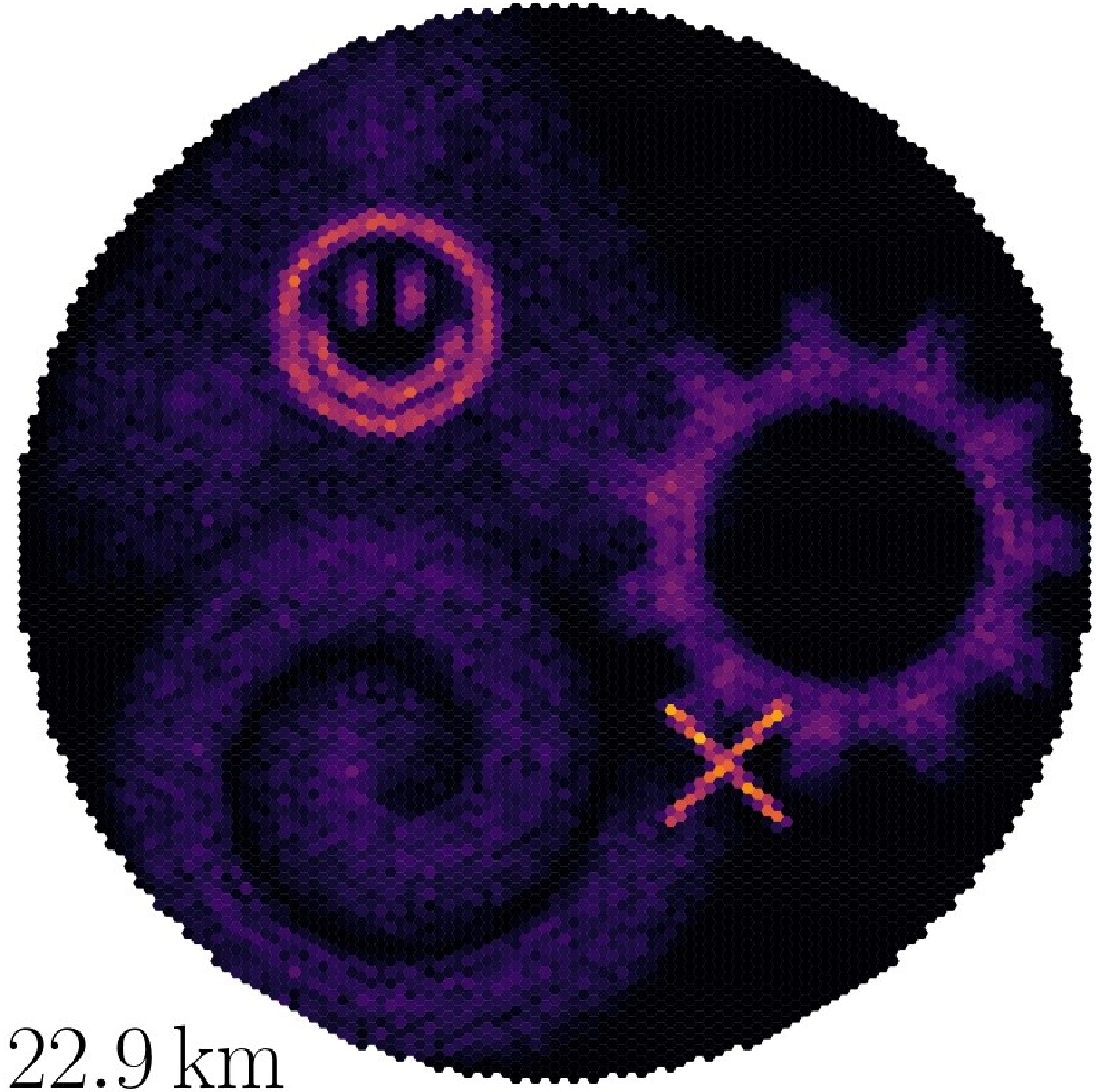
22.9 km

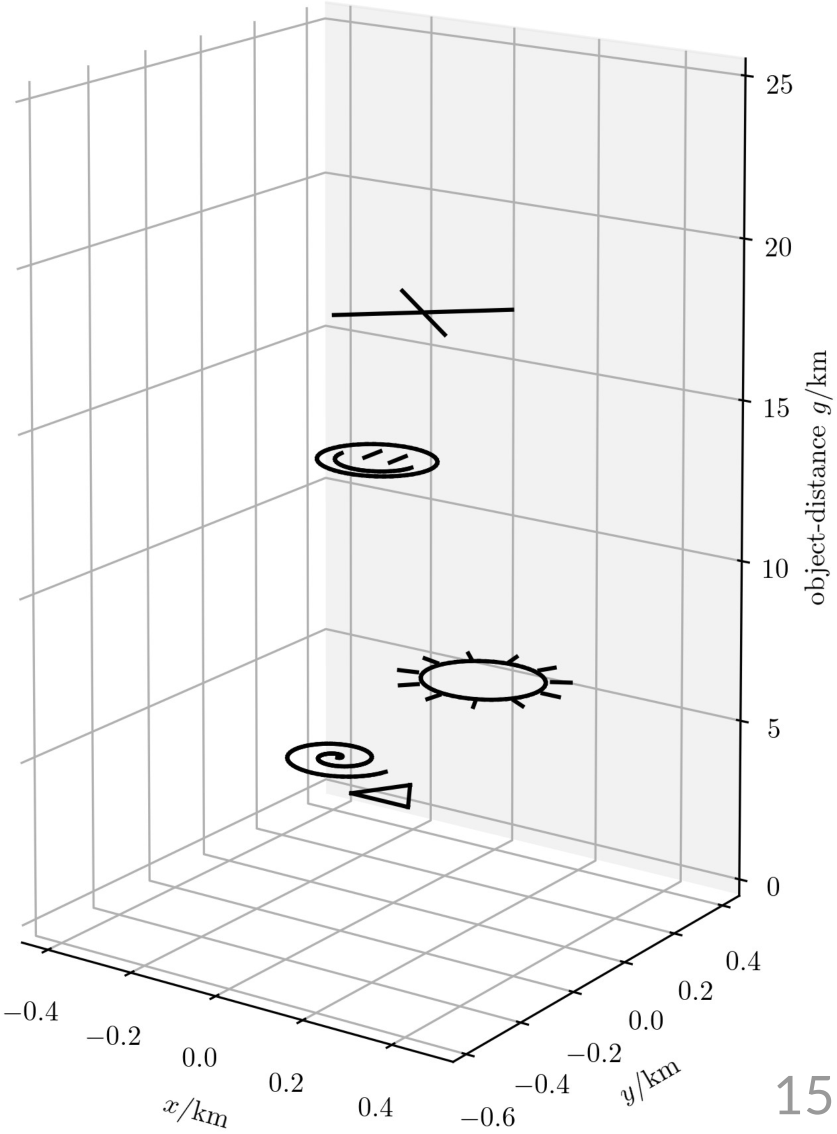
object-distance g/km
25
20
15
10
5
0
−0.4
−0.2
0.0
0.2
0.4
x/km
0.4
0.2
0.0
−0.2
−0.4
−0.6
y/km

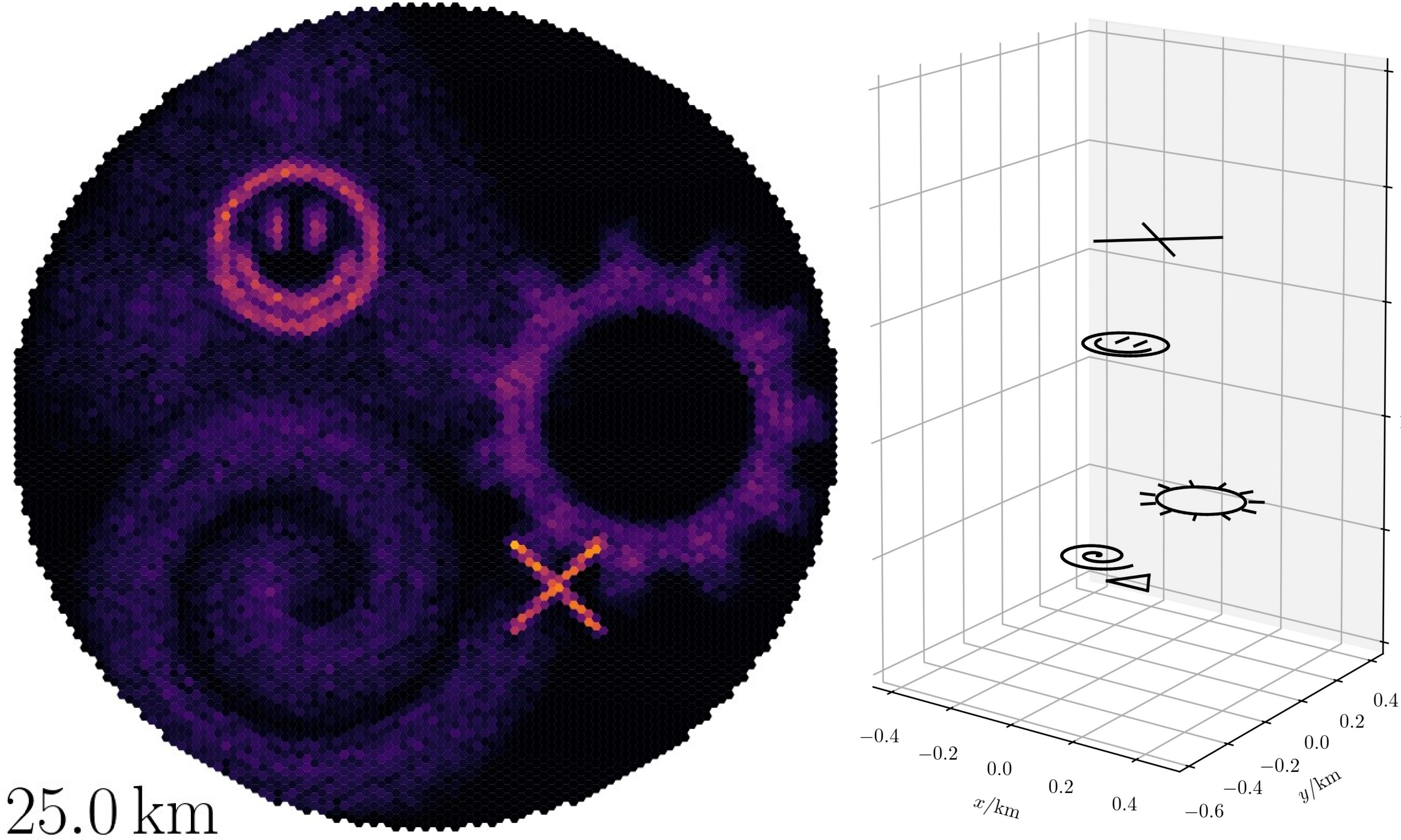
25.0 km
object-distance g/km
25
20
15
10
5
0
−0.4
−0.2
0.0
0.2
0.4
x/km
0.4
0.2
0.0
−0.2
−0.4
−0.6
y/km

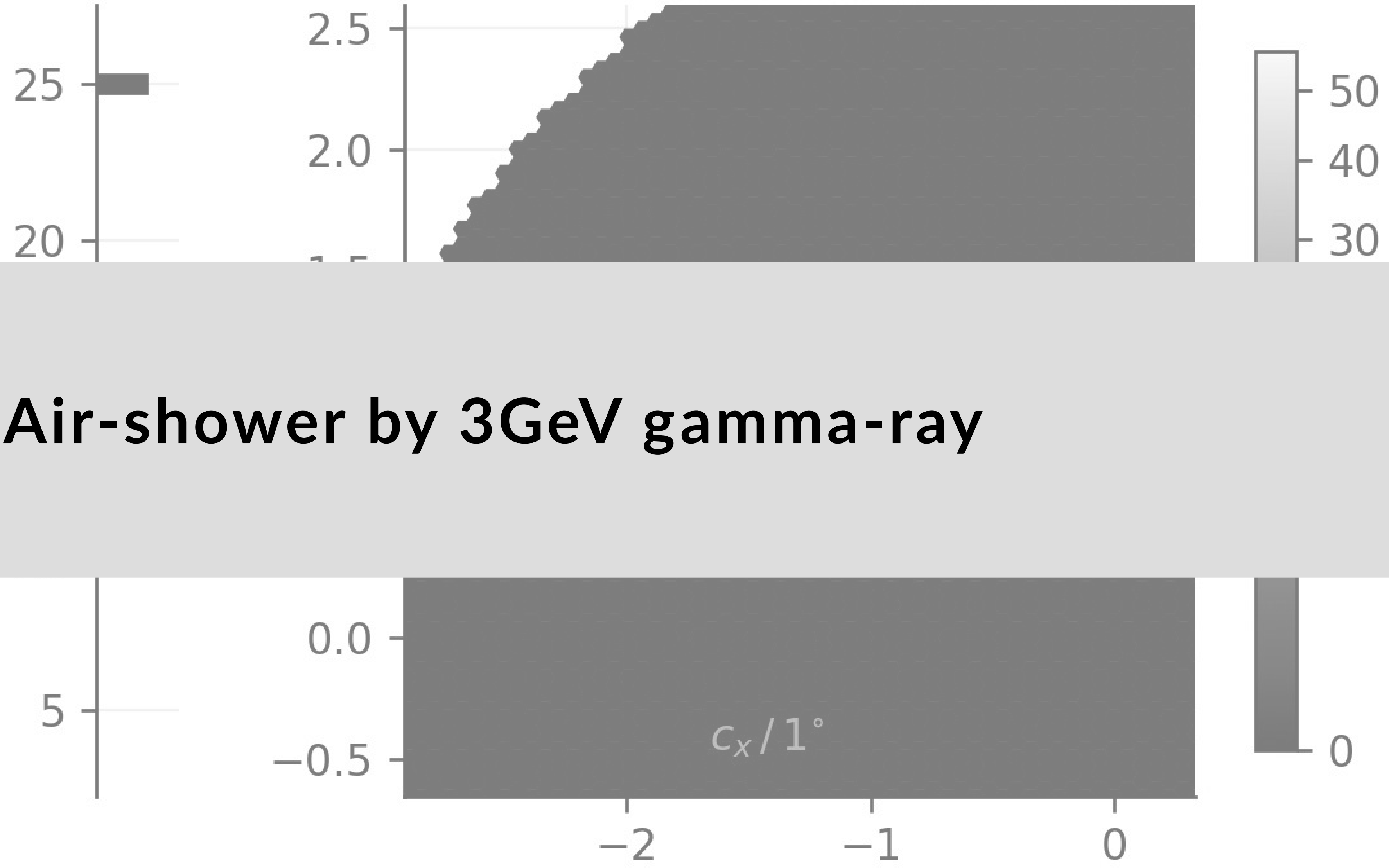

Air-shower by 3GeV gamma-ray

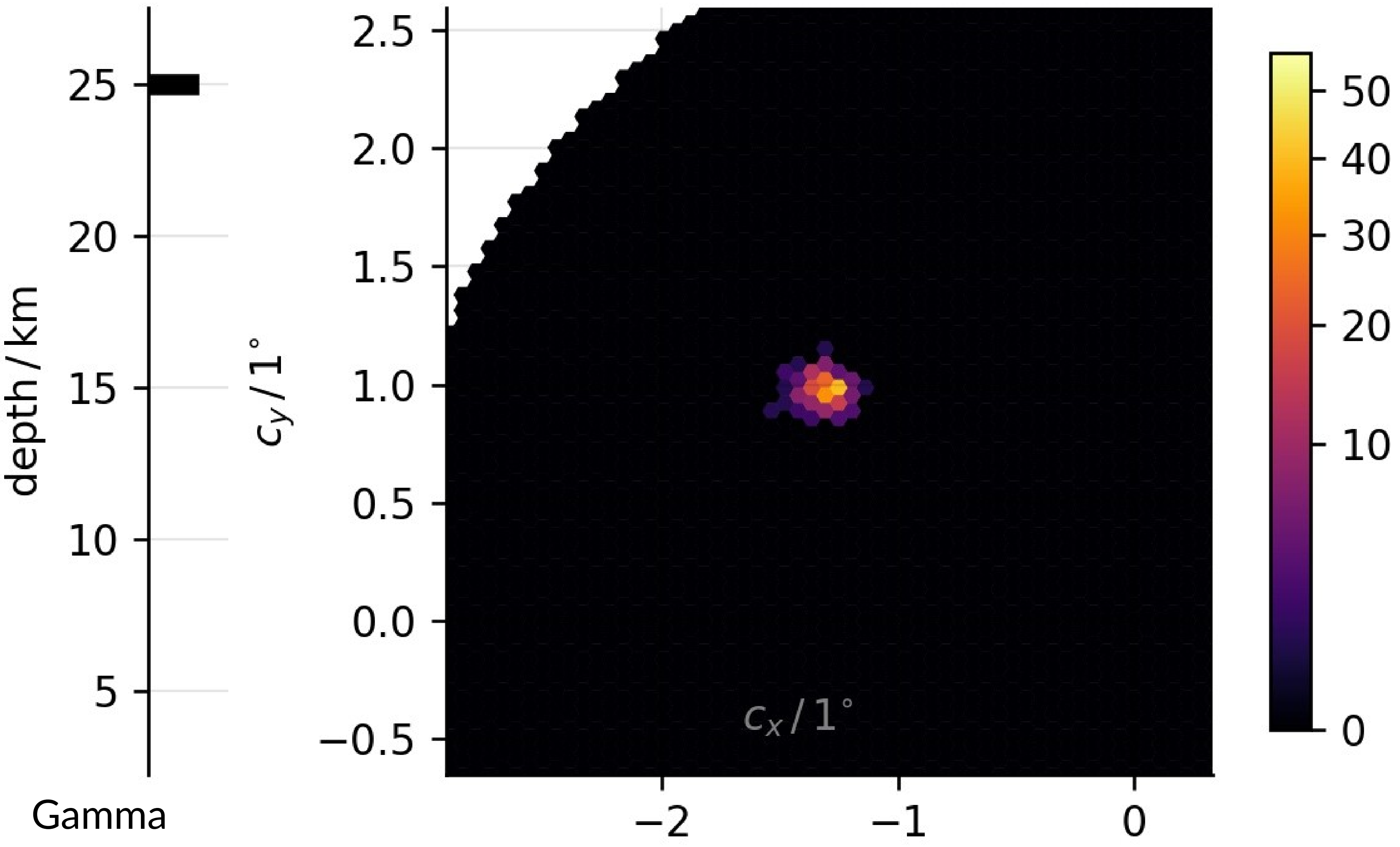

depth / km
25
20
15
10
5
c_y / 1°
2.5
2.0
1.5
1.0
0.5
0.0
−0.5
c_x / 1°
−2
−1
0
50
40
30
20
10
0

Gamma

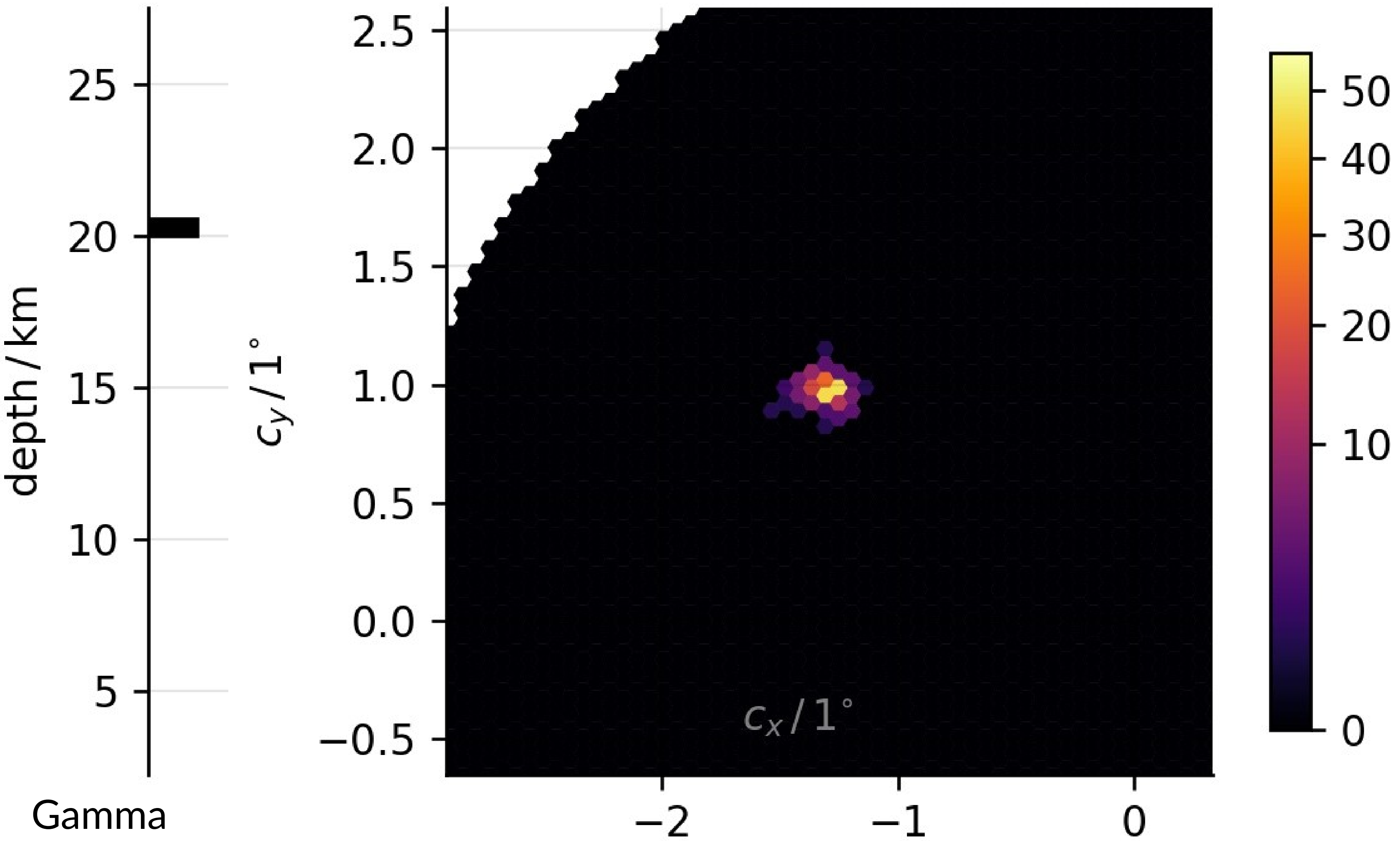

depth / km
25
20
15
10
5
Gamma
c_y / 1°
2.5
2.0
1.5
1.0
0.5
0.0
−0.5
c_x / 1°
−2
−1
0
50
40
30
20
10
0

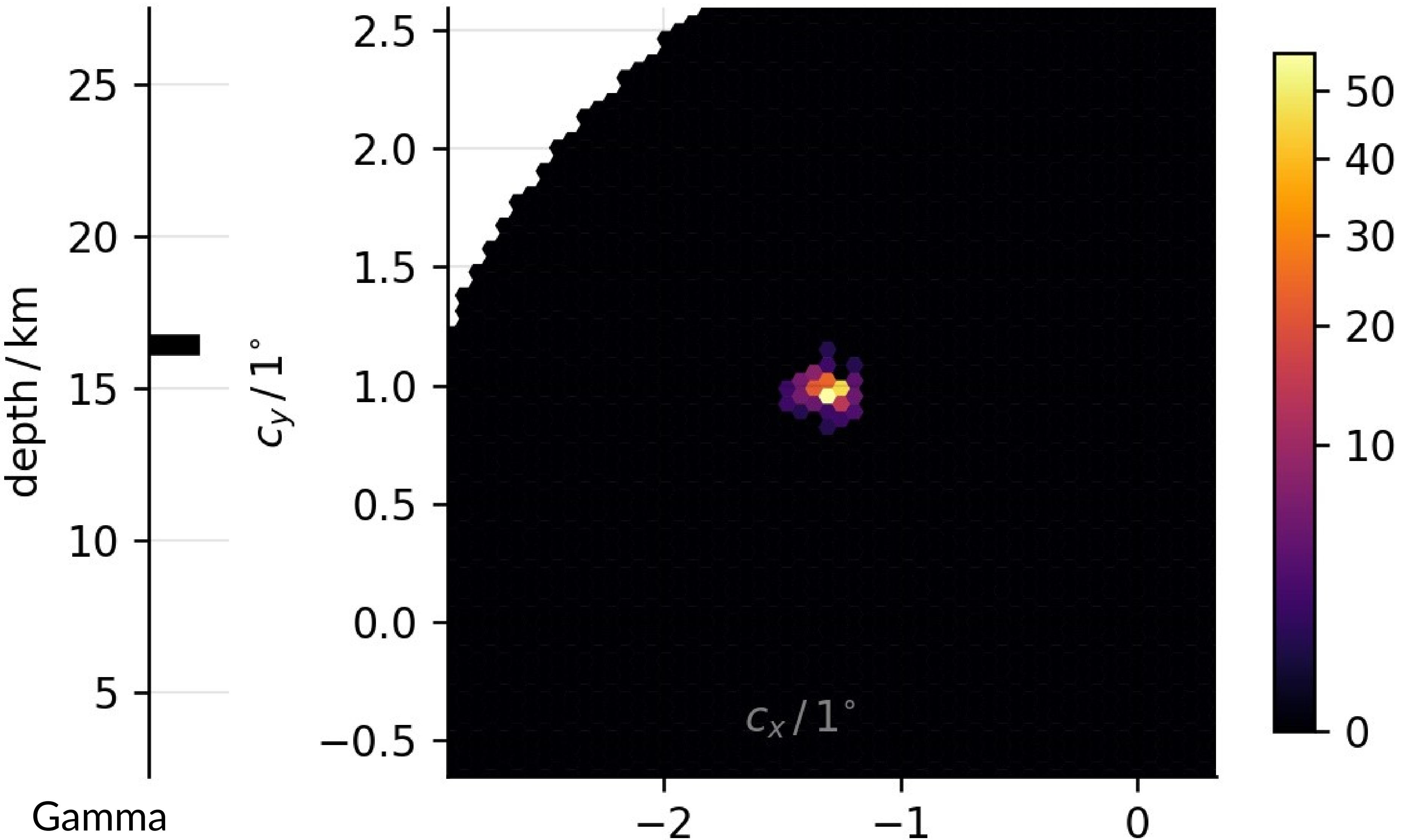
depth / km
25
20
15
10
5
Gamma
c_y / 1°
2.5
2.0
1.5
1.0
0.5
0.0
−0.5
c_x / 1°
−2
−1
0
50
40
30
20
10
0

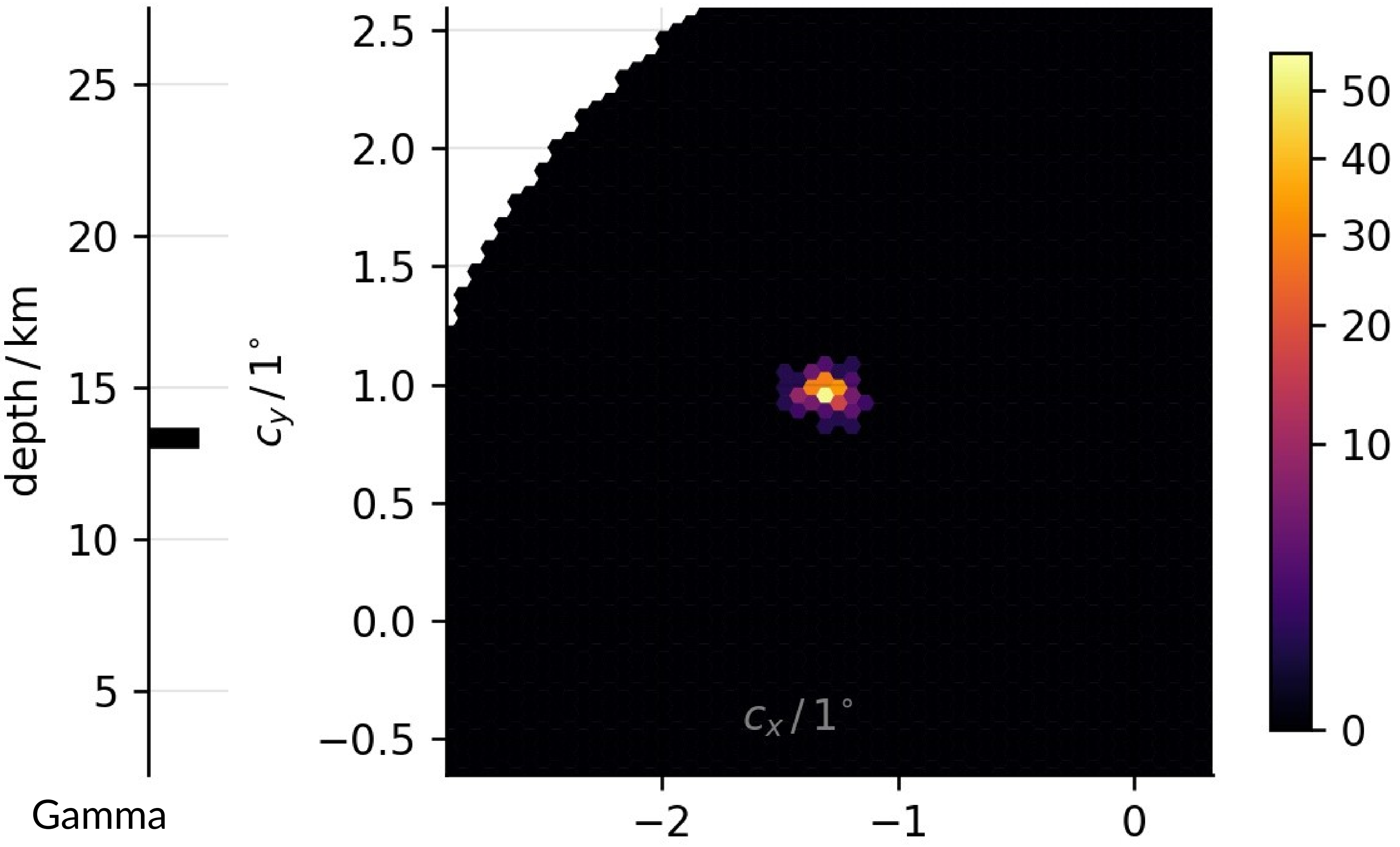

depth / km
25
20
15
10
5
c_y / 1°
2.5
2.0
1.5
1.0
0.5
0.0
−0.5
c_x / 1°
−2
−1
0
50
40
30
20
10
0

Gamma

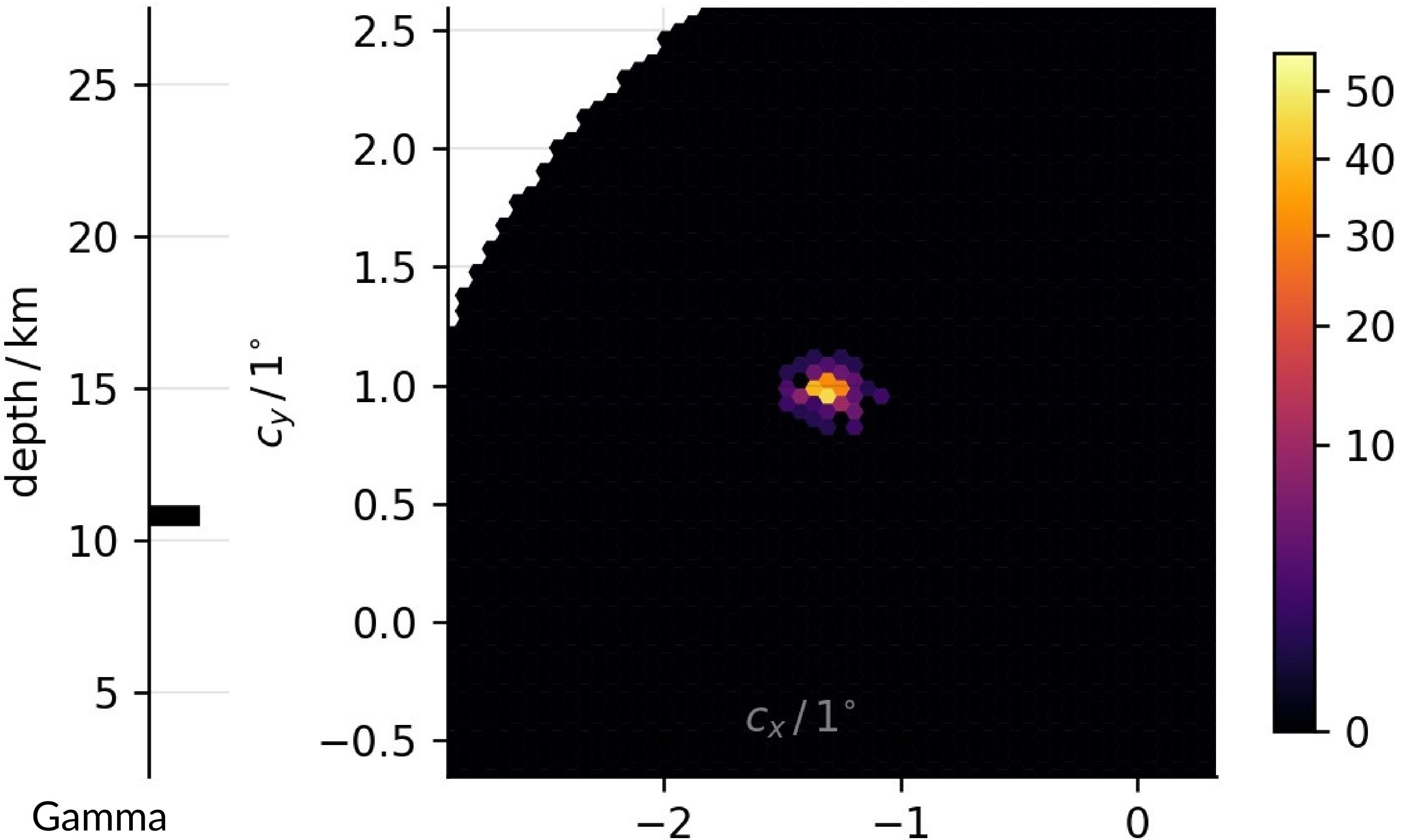
depth / km
25
20
15
10
5
c_y / 1°
2.5
2.0
1.5
1.0
0.5
0.0
−0.5
c_x / 1°
−2
−1
0
50
40
30
20
10
0

Gamma

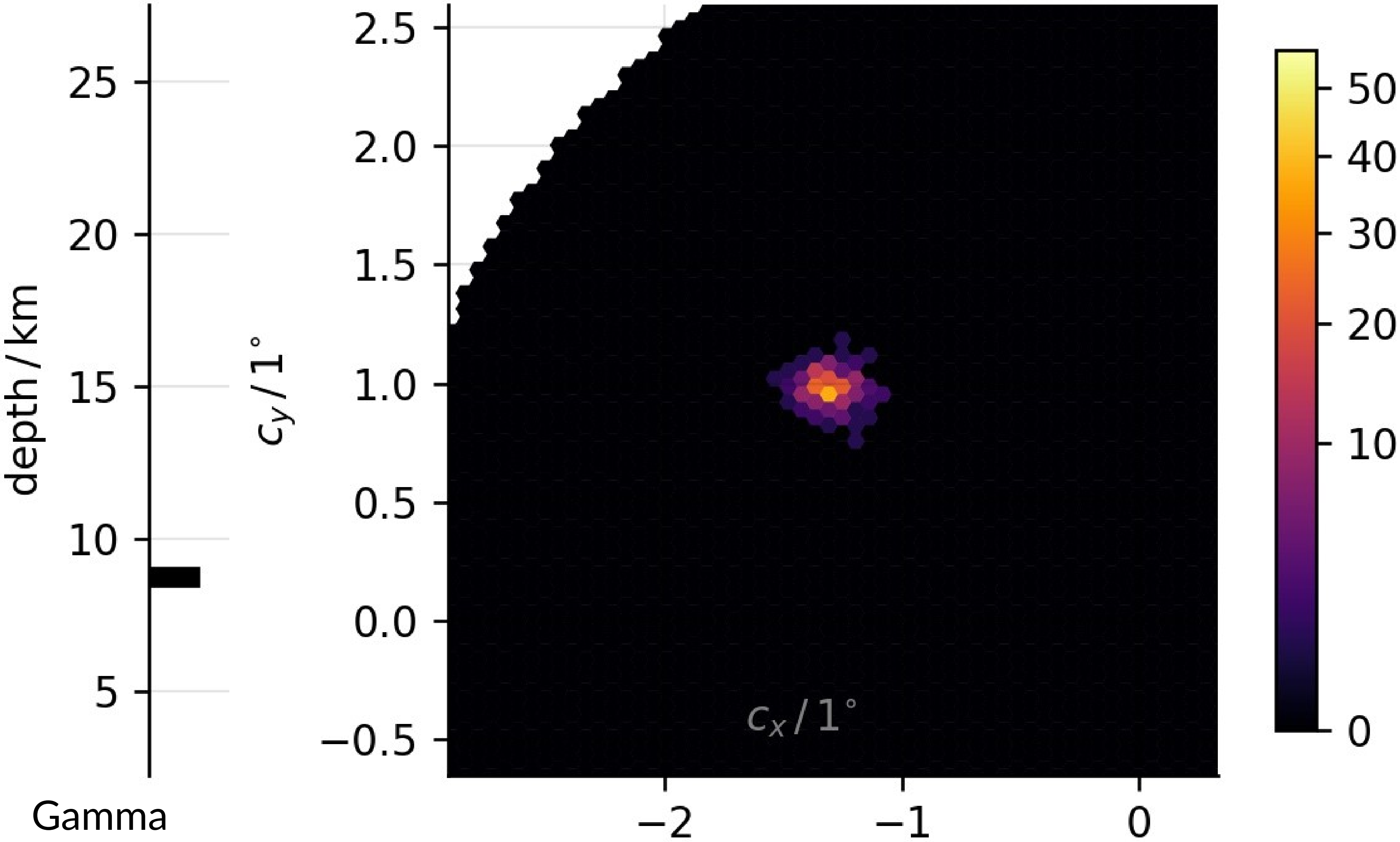

depth / km
25
20
15
10
5
Gamma
c_y / 1°
2.5
2.0
1.5
1.0
0.5
0.0
−0.5
c_x / 1°
−2
−1
0
50
40
30
20
10
0

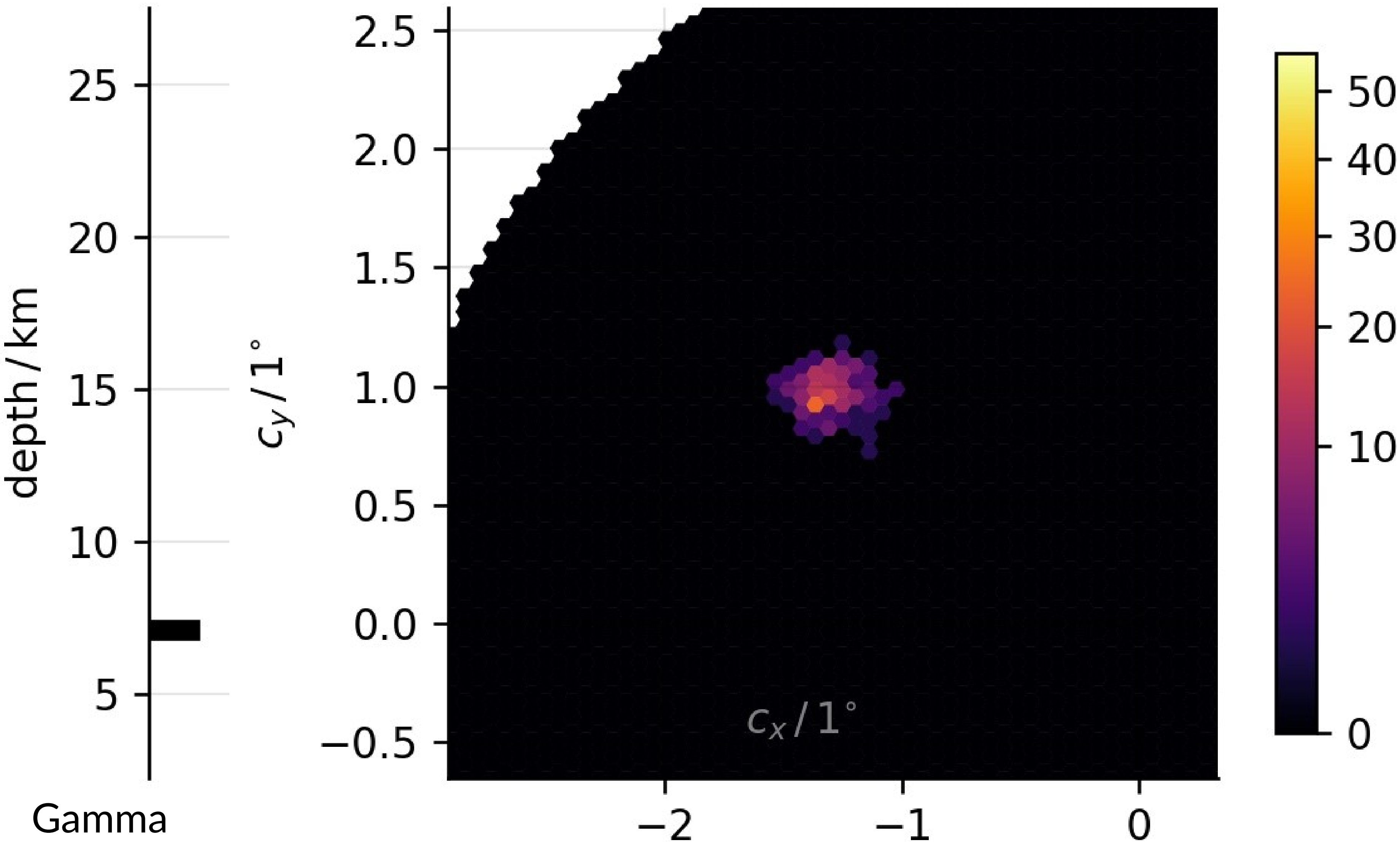
depth / km
25
20
15
10
5
c_y / 1°
2.5
2.0
1.5
1.0
0.5
0.0
−0.5
c_x / 1°
−2
−1
0
50
40
30
20
10
0

Gamma

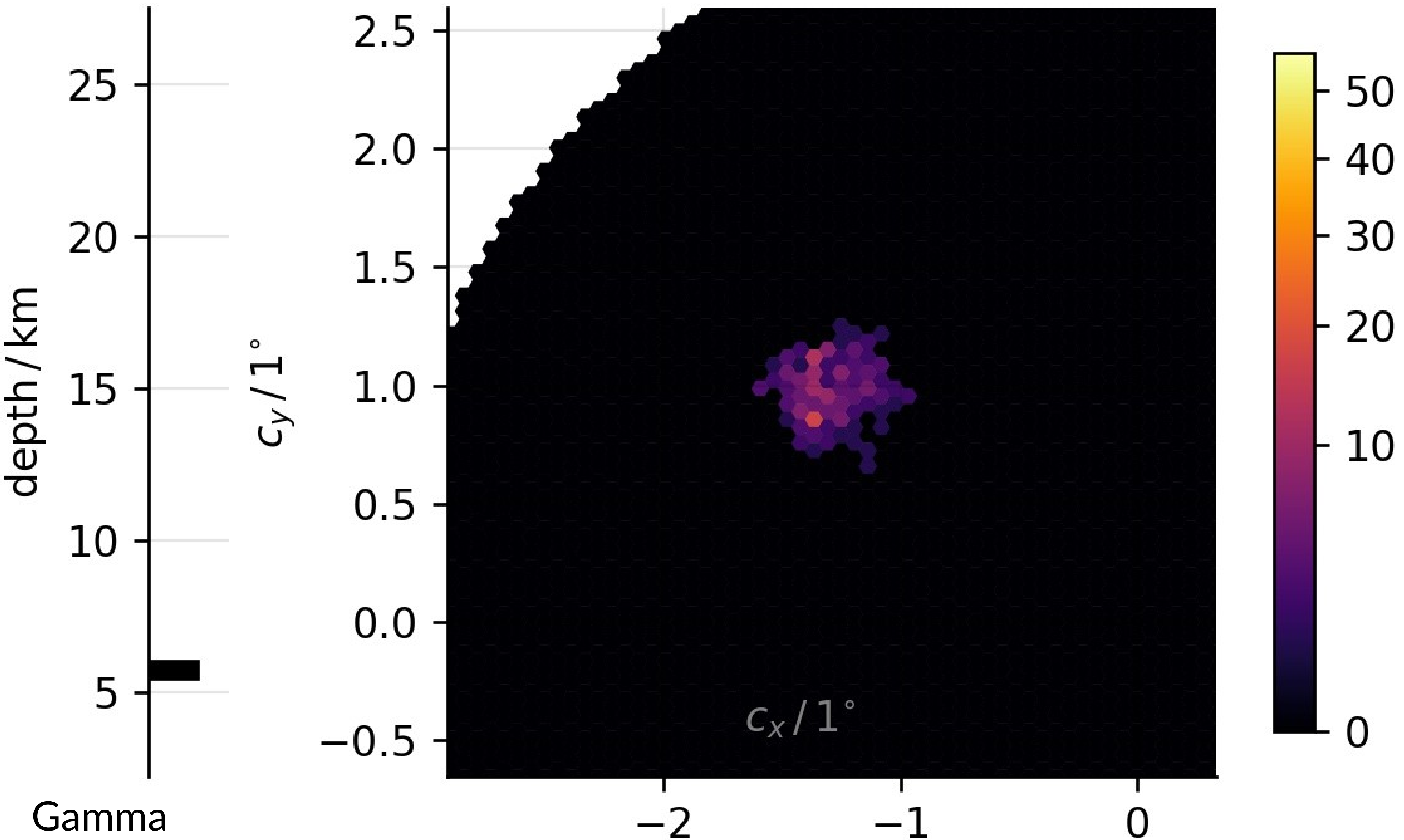

depth / km
25
20
15
10
5
Gamma
c_y / 1°
2.5
2.0
1.5
1.0
0.5
0.0
−0.5
c_x / 1°
−2
−1
0
50
40
30
20
10
0

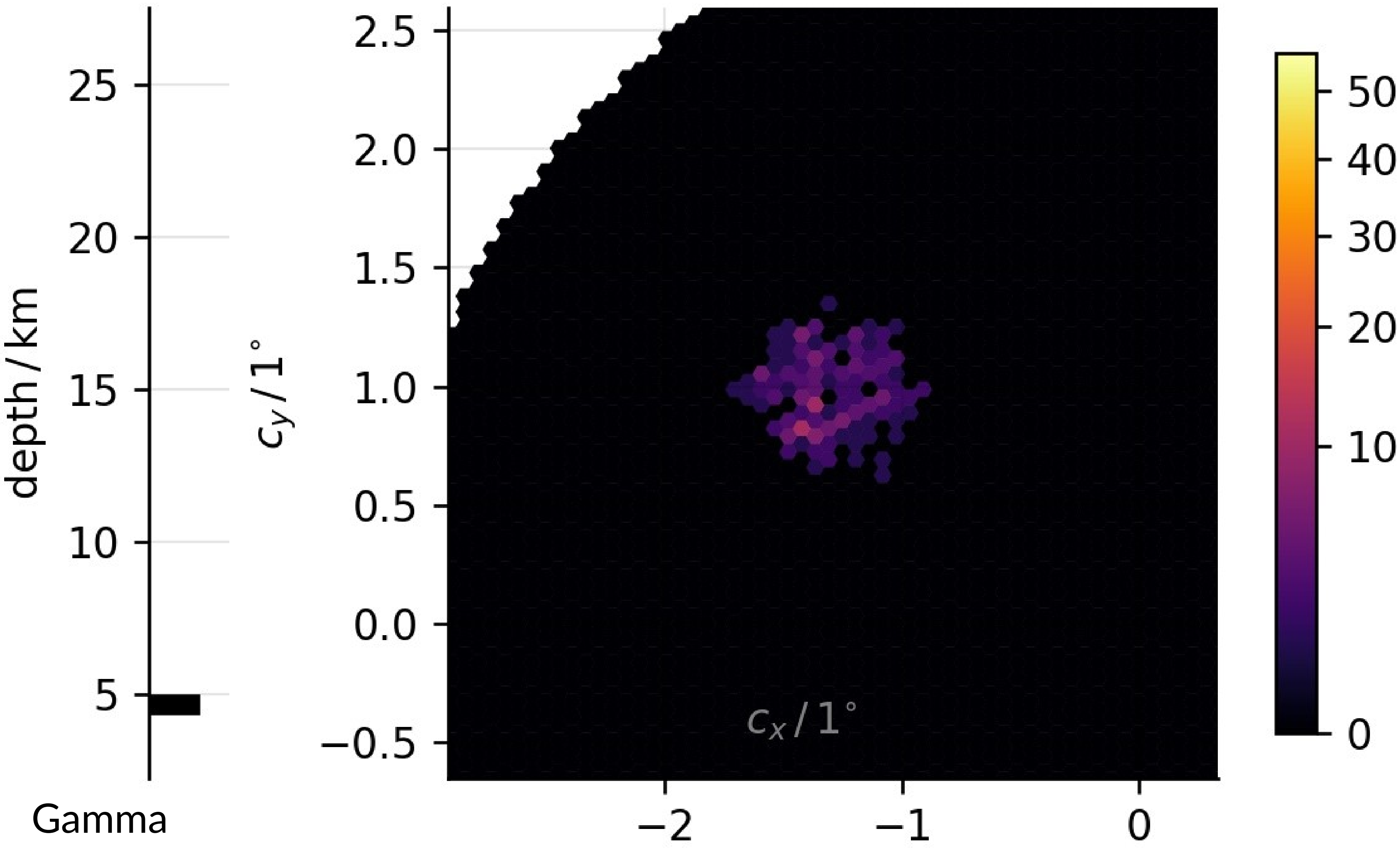

depth / km
25
20
15
10
5
c_y / 1°
2.5
2.0
1.5
1.0
0.5
0.0
−0.5
c_x / 1°
−2
−1
0
50
40
30
20
10
0

Gamma

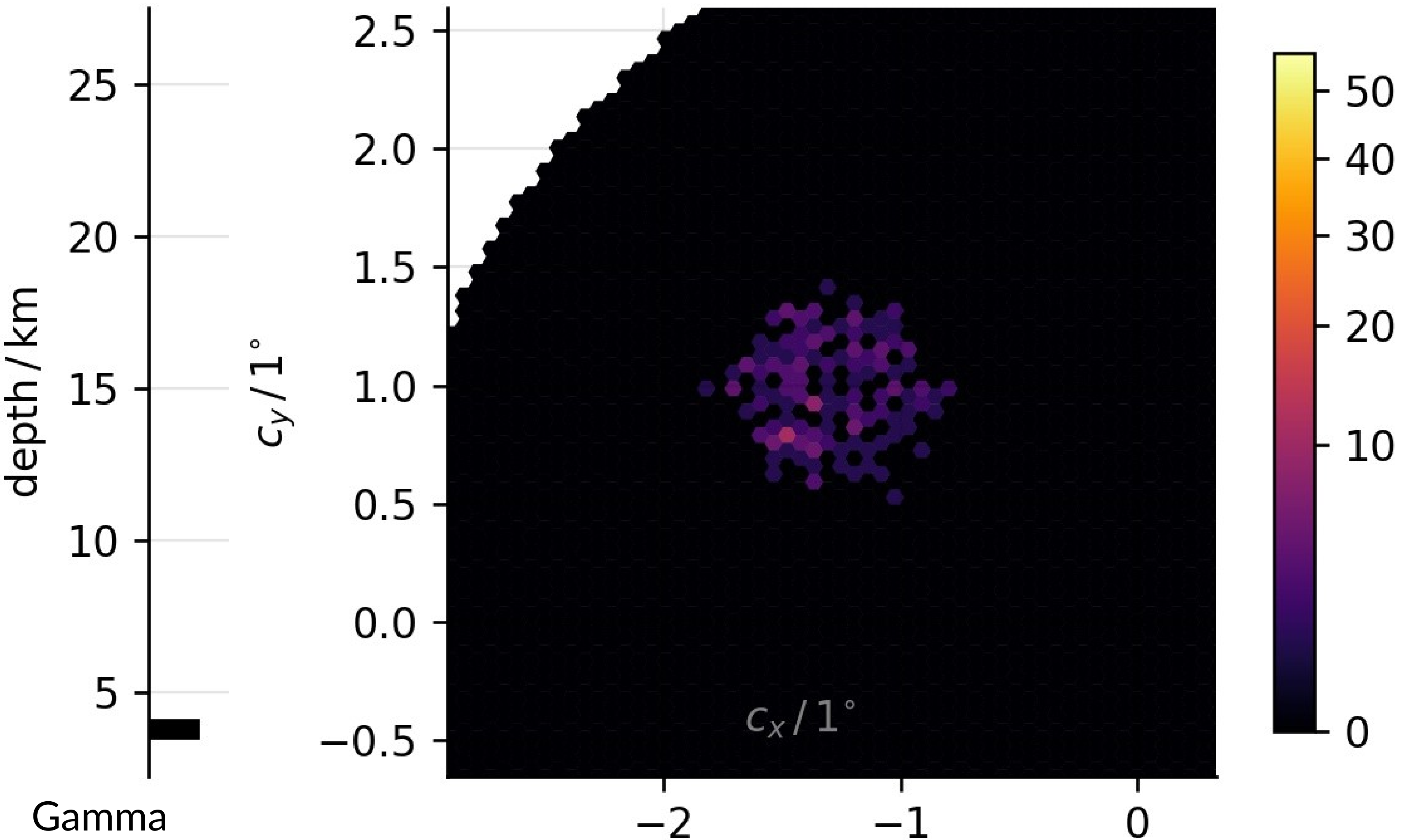
depth / km
25
20
15
10
5
c_y / 1°
2.5
2.0
1.5
1.0
0.5
0.0
−0.5
c_x / 1°
−2
−1
0
50
40
30
20
10
0

Gamma

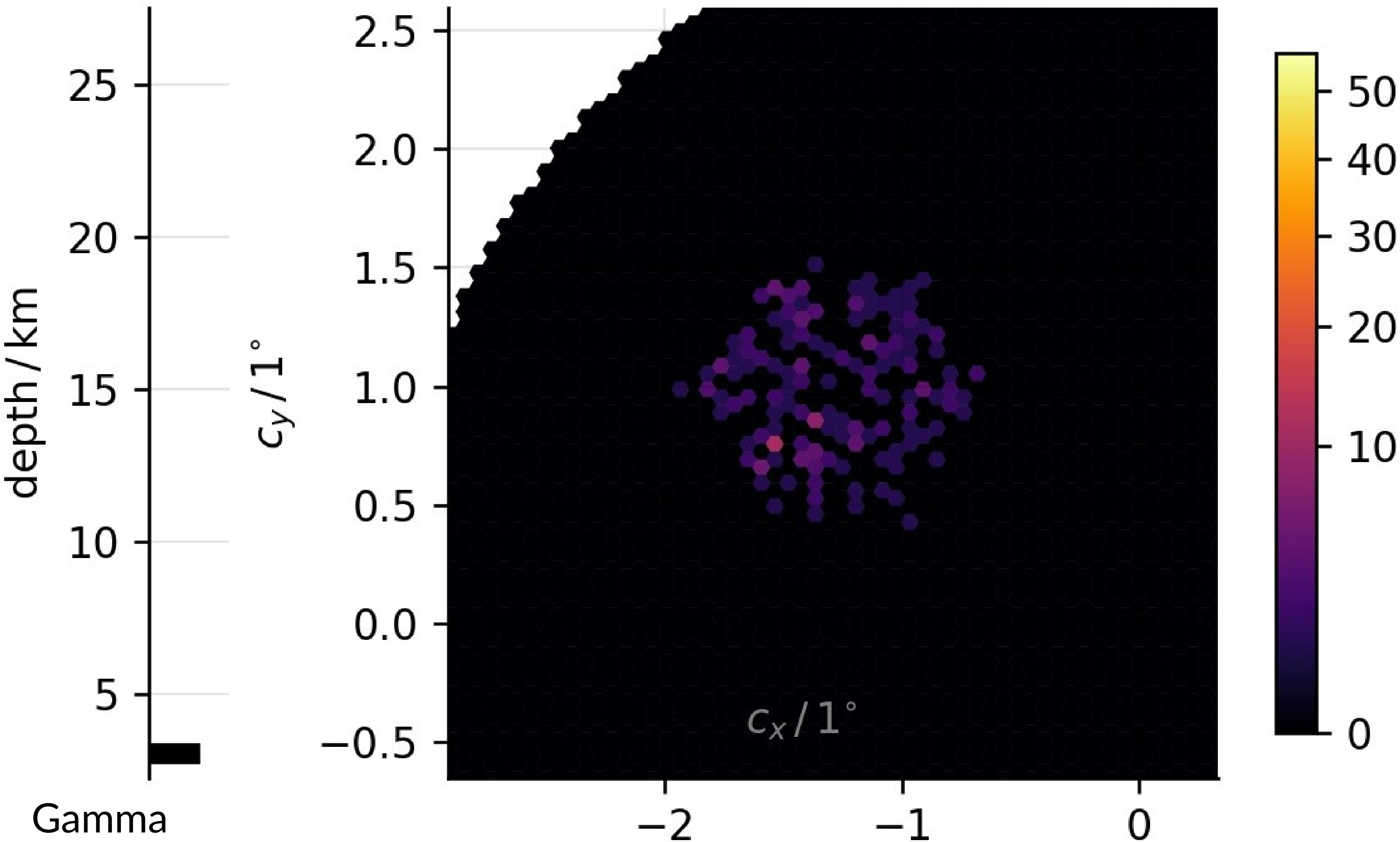
depth / km
25
20
15
10
5
Gamma
c_y / 1°
2.5
2.0
1.5
1.0
0.5
0.0
−0.5
c_x / 1°
−2
−1
0
50
40
30
20
10
0

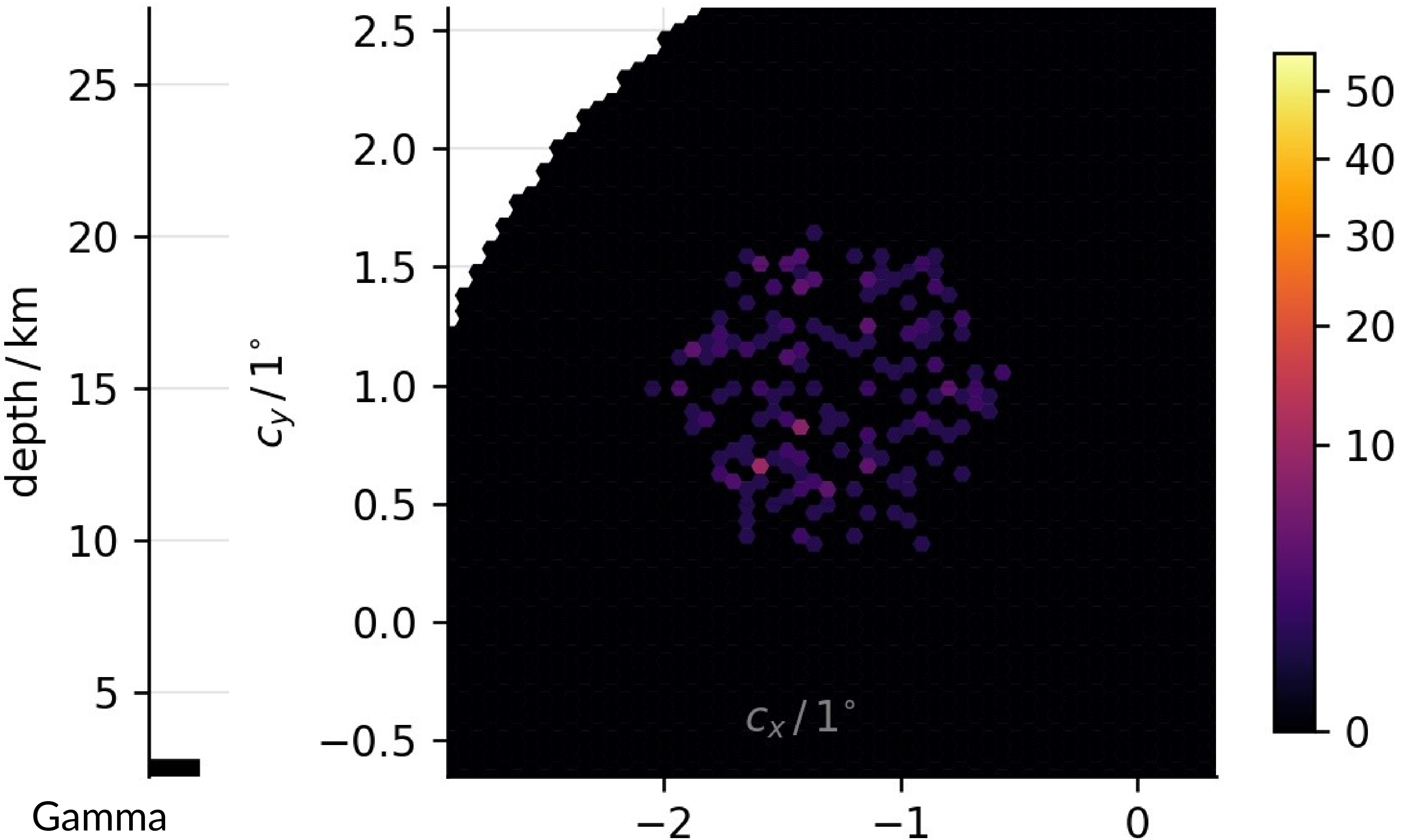

depth / km
25
20
15
10
5
Gamma
c_y / 1°
2.5
2.0
1.5
1.0
0.5
0.0
−0.5
c_x / 1°
−2
−1
0
50
40
30
20
10
0

Air-shower by 8GeV gamma-ray

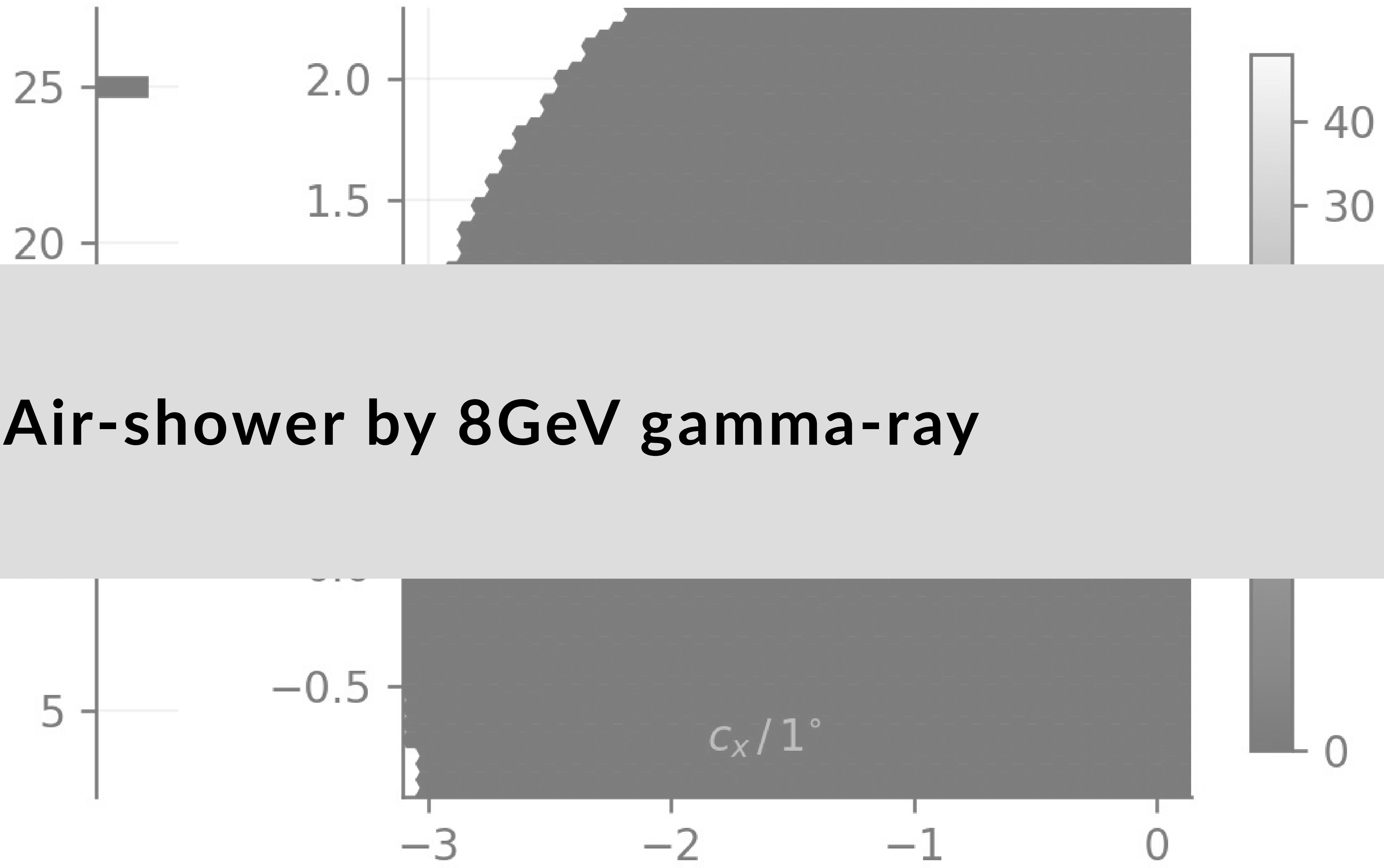

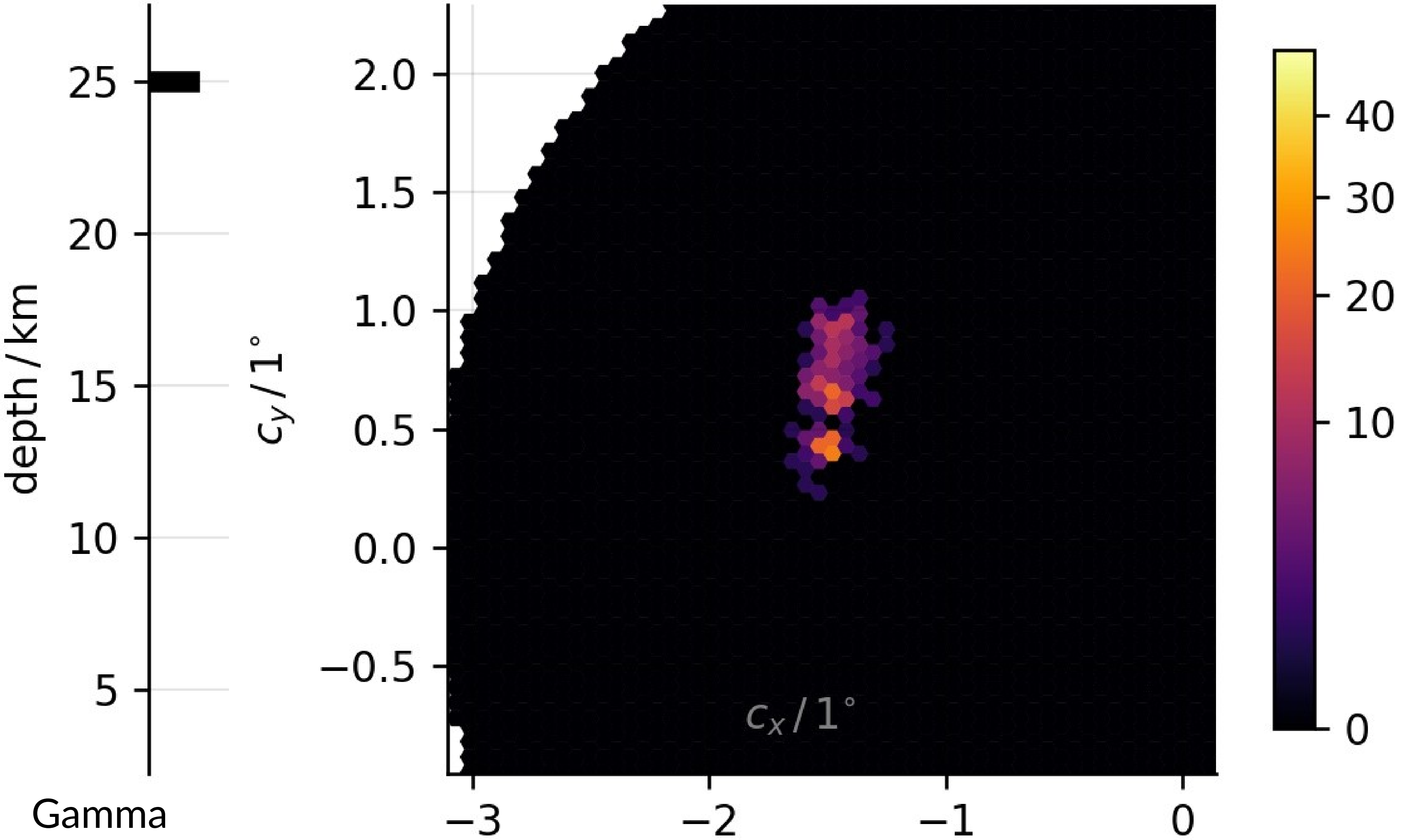

depth / km
25
20
15
10
5
Gamma
c_y / 1°
2.0
1.5
1.0
0.5
0.0
−0.5
c_x / 1°
−3
−2
−1
0
40
30
20
10
0

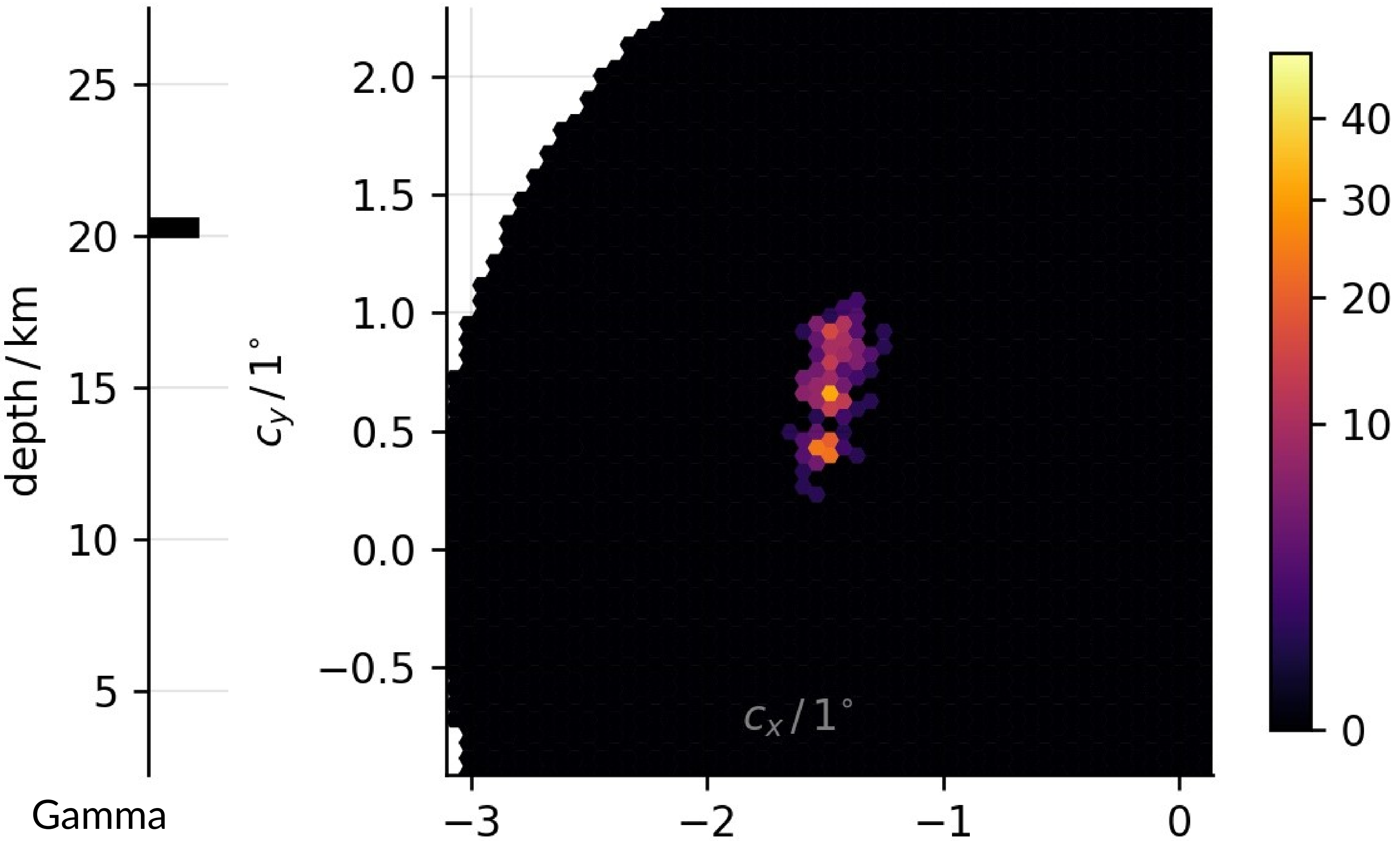

depth / km
25
20
15
10
5
Gamma
c_y / 1°
2.0
1.5
1.0
0.5
0.0
−0.5
c_x / 1°
−3
−2
−1
0
40
30
20
10
0

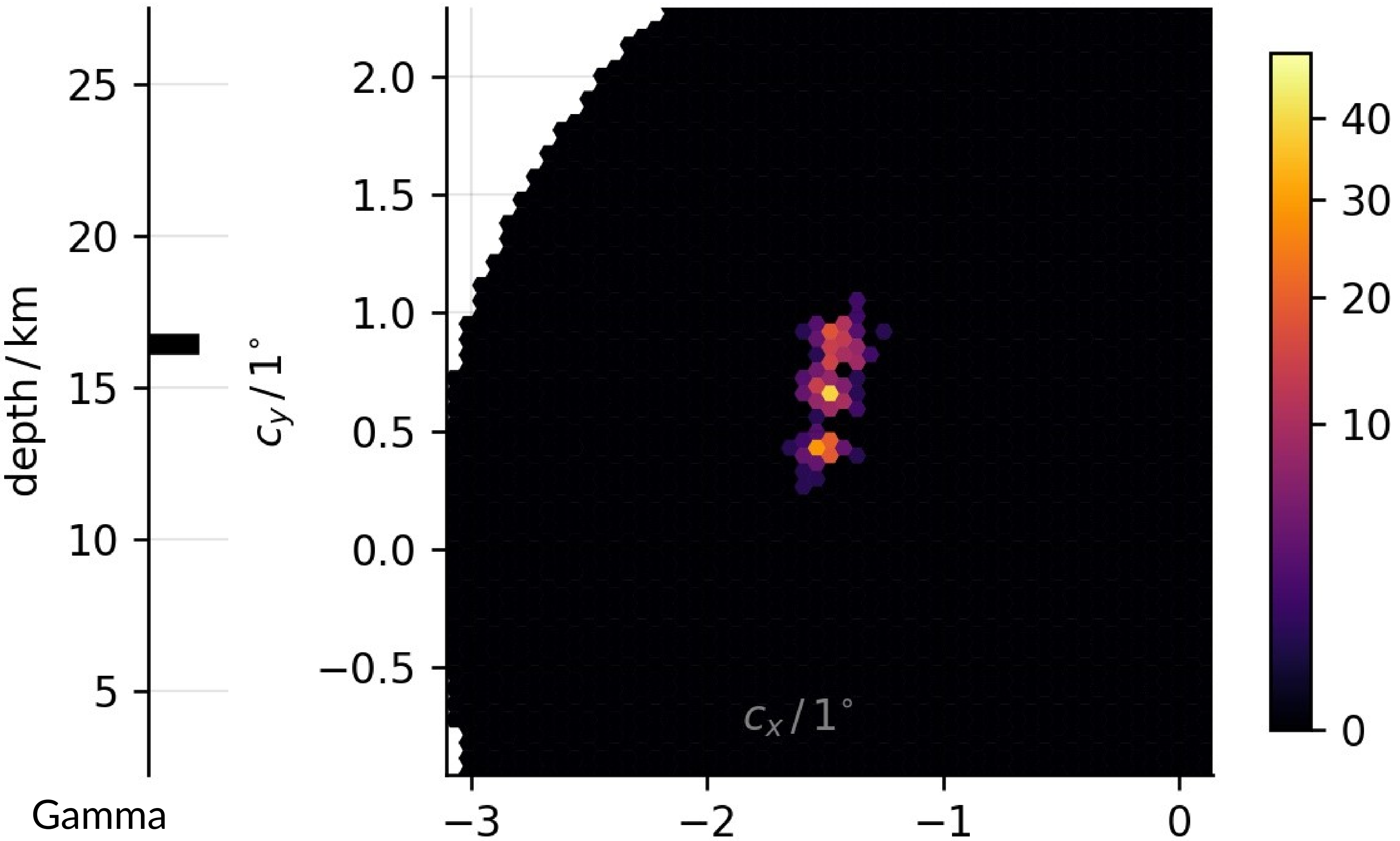

depth / km
25
20
15
10
5
Gamma
c_y / 1°
2.0
1.5
1.0
0.5
0.0
−0.5
c_x / 1°
−3
−2
−1
0
40
30
20
10
0

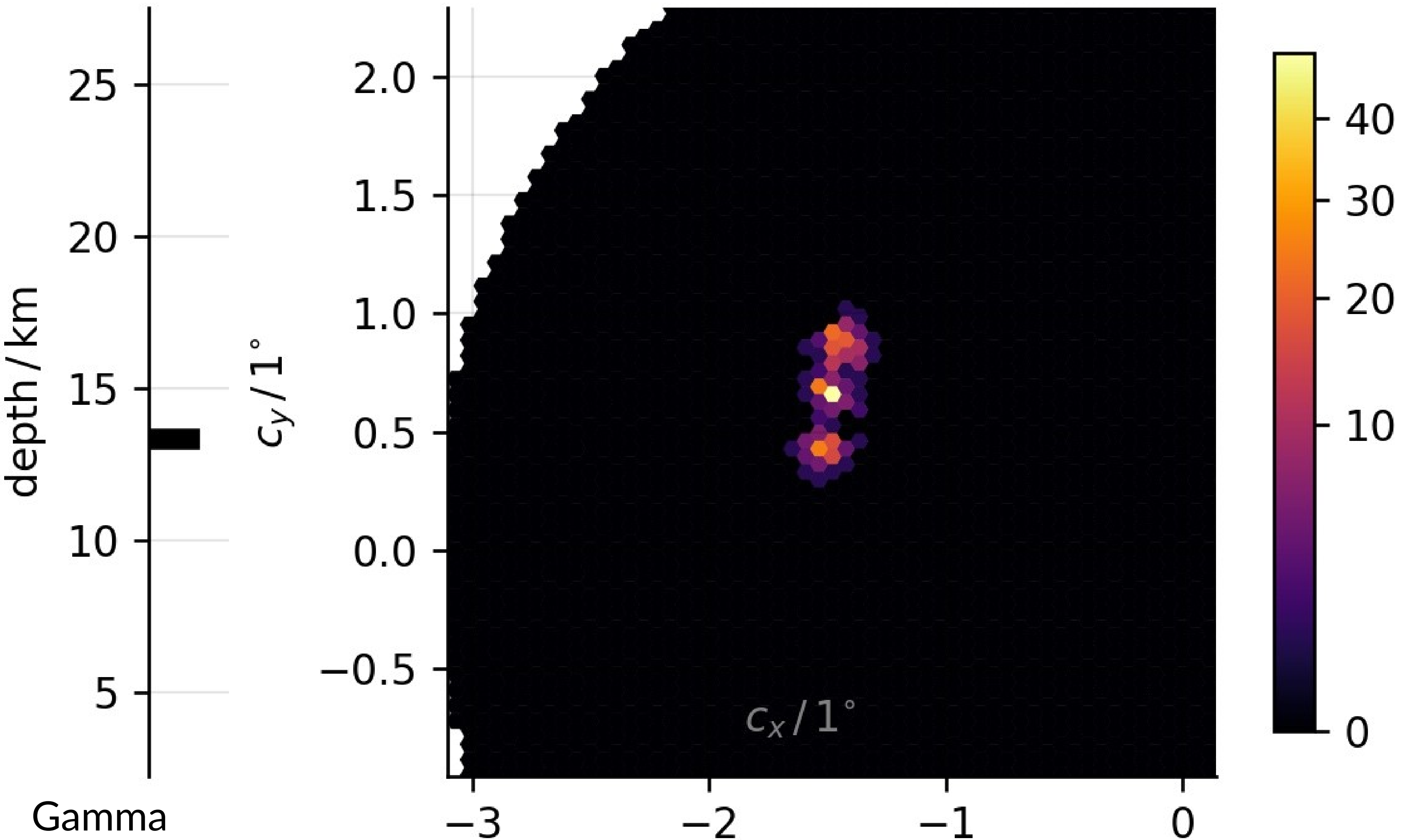

Gamma

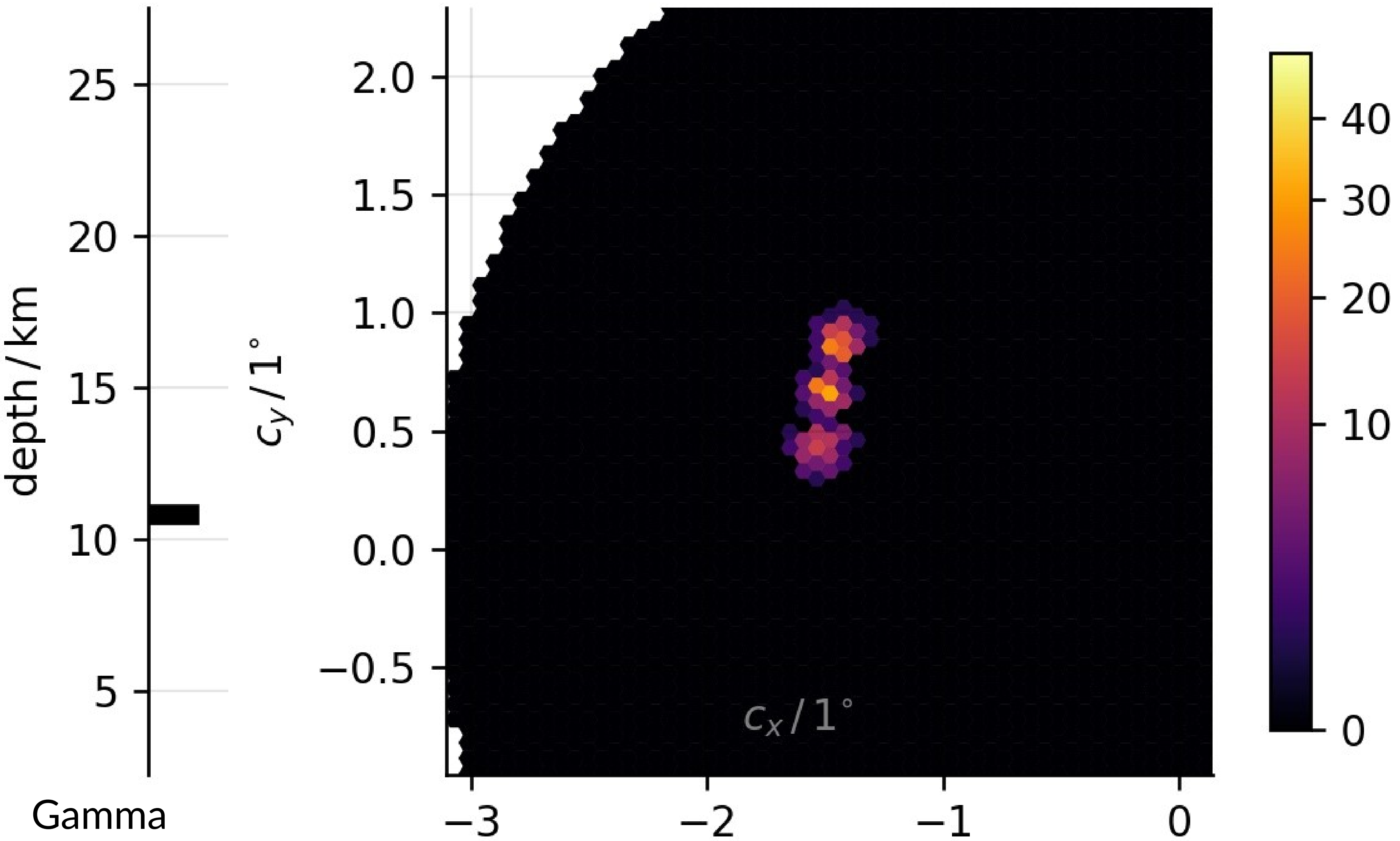

depth / km
25
20
15
10
5
Gamma
c_y / 1°
2.0
1.5
1.0
0.5
0.0
−0.5
c_x / 1°
−3
−2
−1
0
40
30
20
10
0

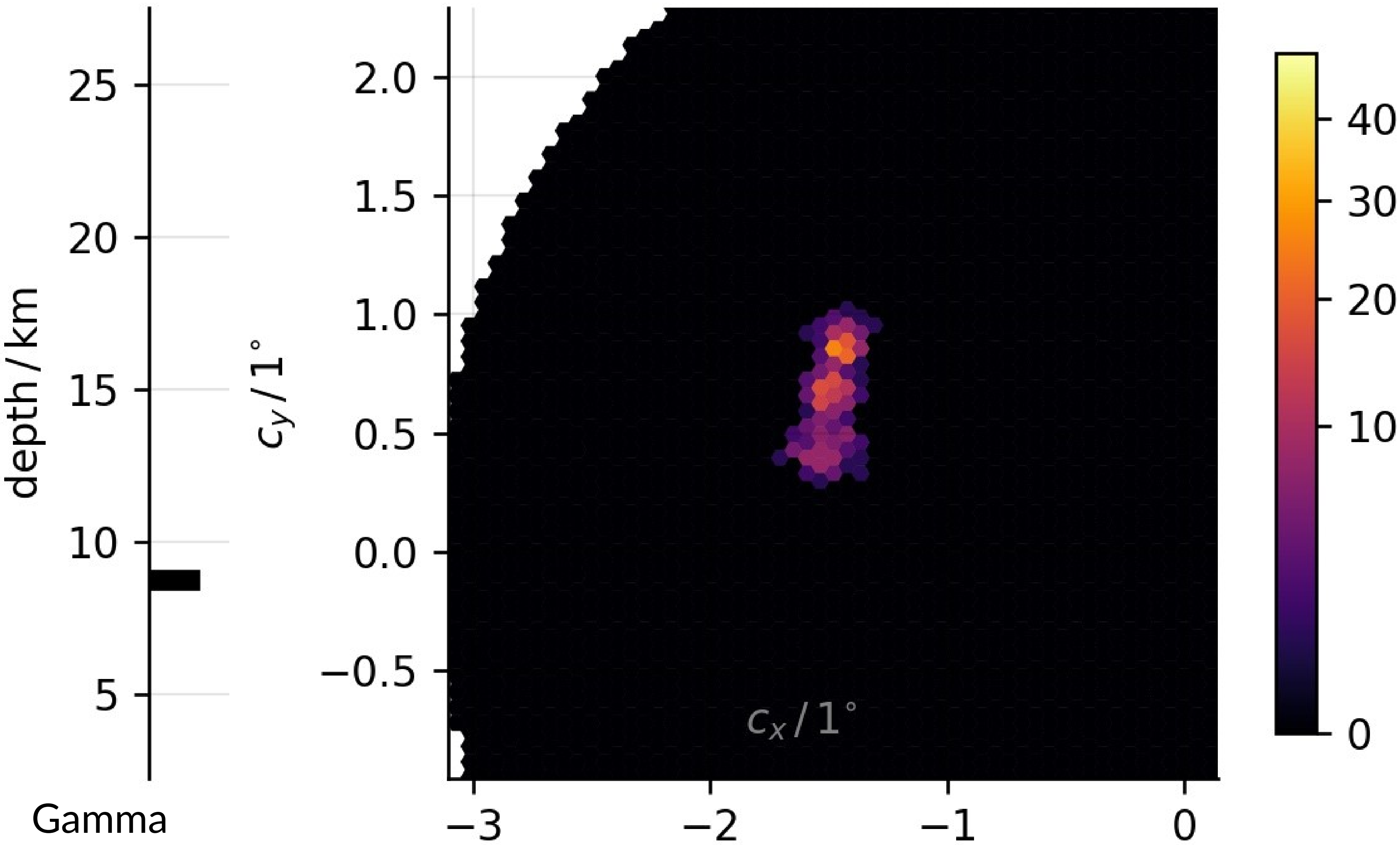

depth / km
25
20
15
10
5
Gamma
c_y / 1°
2.0
1.5
1.0
0.5
0.0
−0.5
c_x / 1°
−3
−2
−1
0
40
30
20
10
0

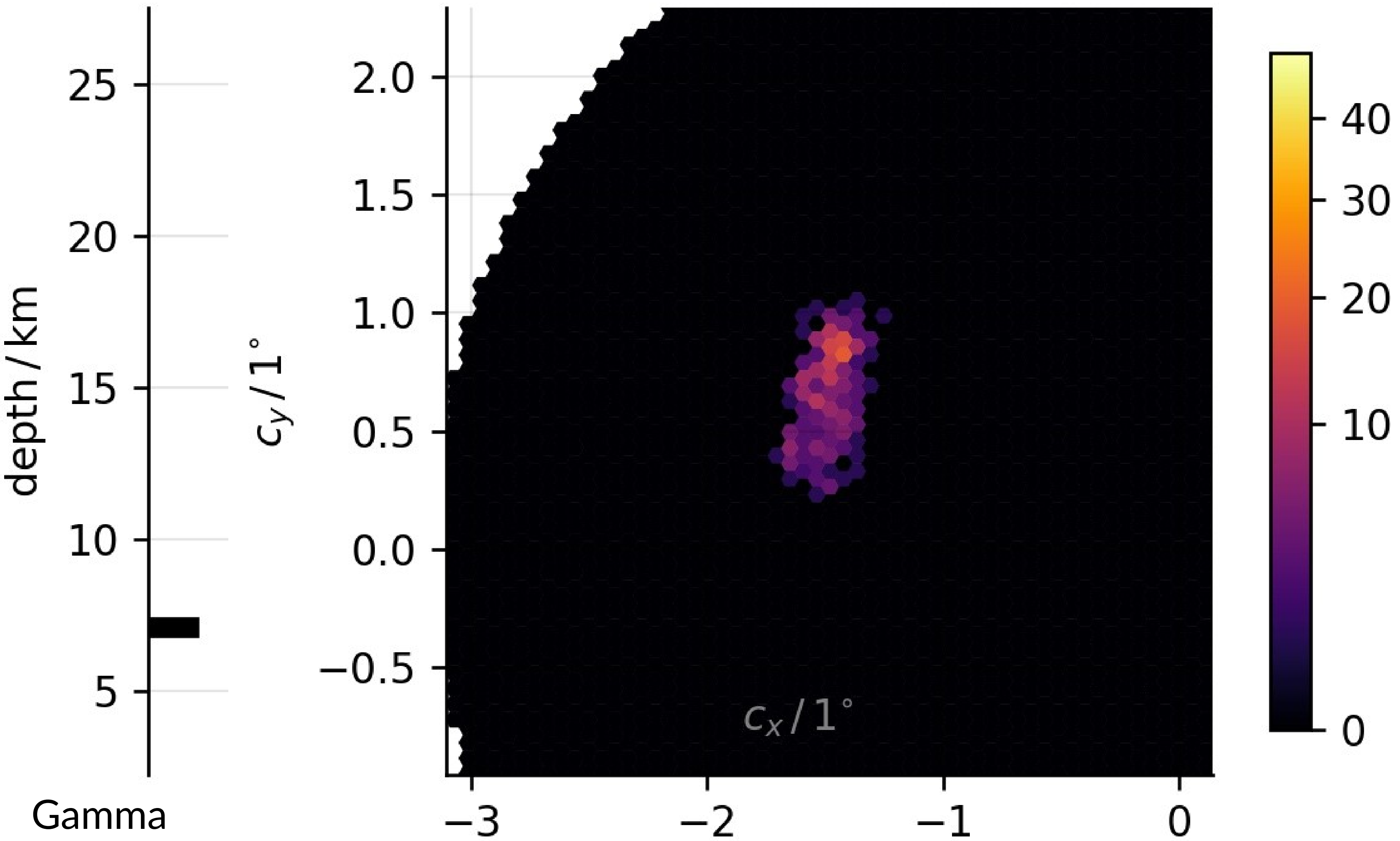

depth / km
25
20
15
10
5
Gamma
c_y / 1°
2.0
1.5
1.0
0.5
0.0
−0.5
c_x / 1°
−3
−2
−1
0
40
30
20
10
0

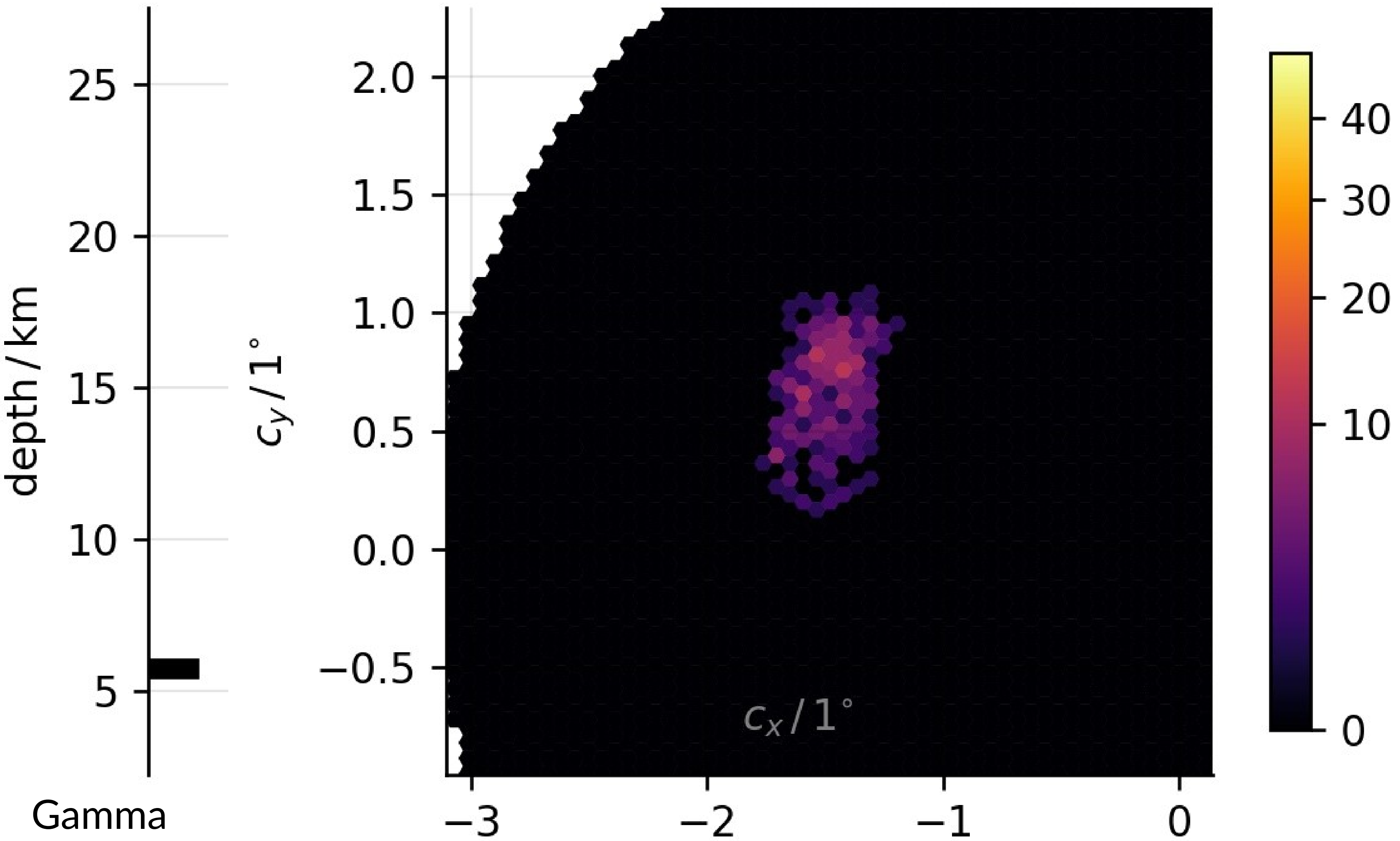

depth / km
25
20
15
10
5
Gamma
c_y / 1°
2.0
1.5
1.0
0.5
0.0
−0.5
c_x / 1°
−3
−2
−1
0
40
30
20
10
0

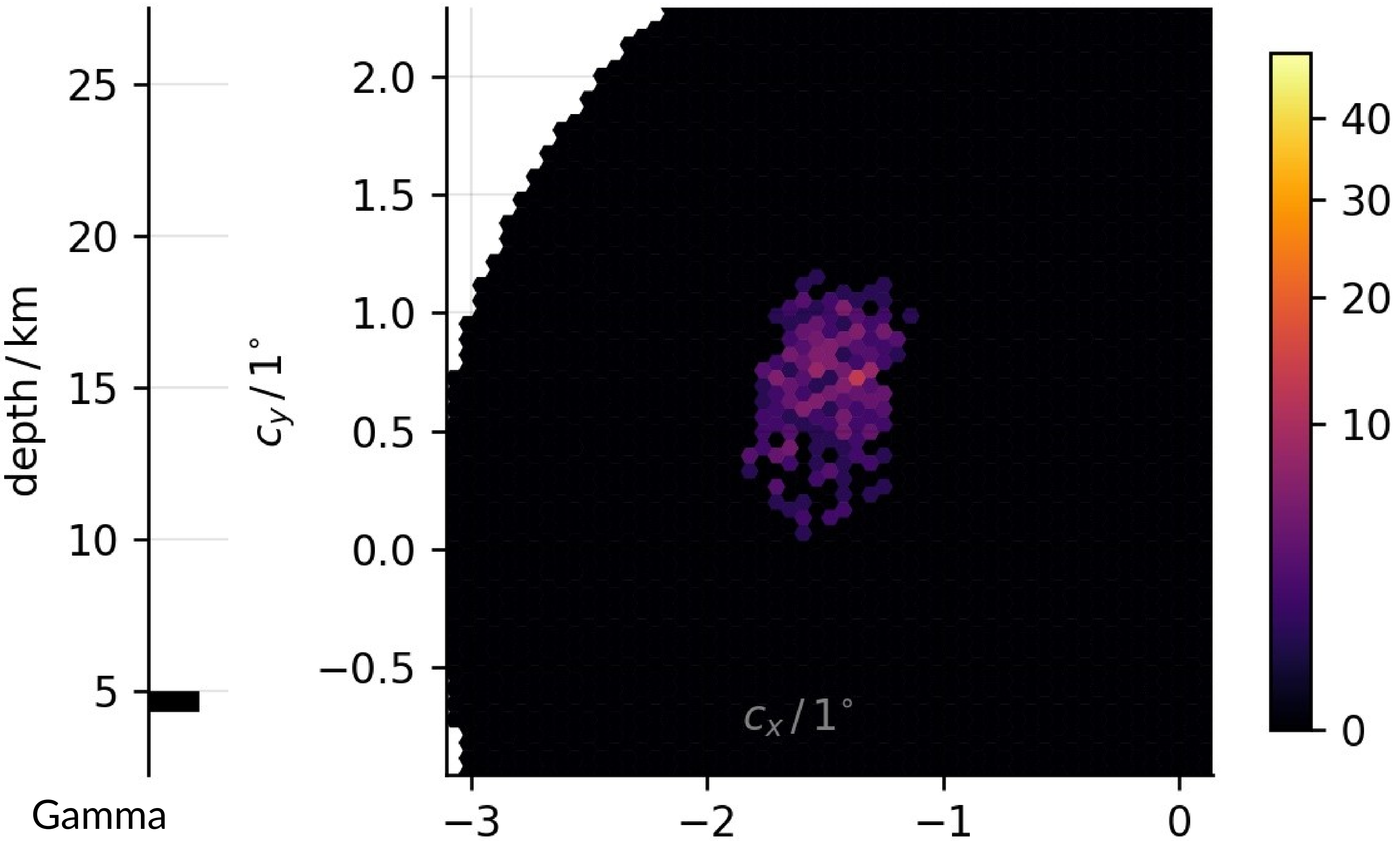

depth / km
25
20
15
10
5
Gamma
c_y / 1°
2.0
1.5
1.0
0.5
0.0
−0.5
c_x / 1°
−3
−2
−1
0
40
30
20
10
0

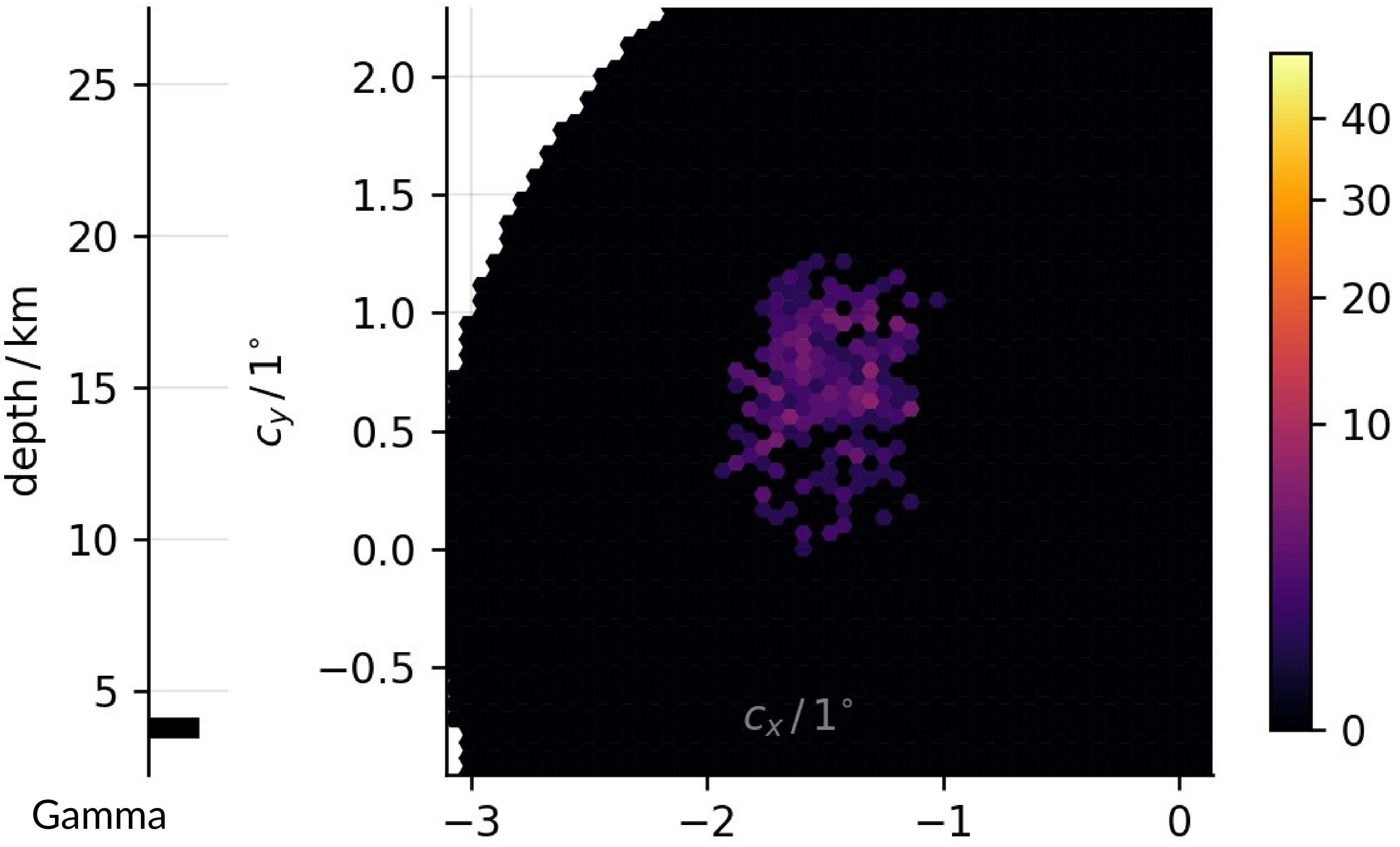

depth / km
25
20
15
10
5
Gamma
$c_y / 1^\circ$
2.0
1.5
1.0
0.5
0.0
−0.5
$c_x / 1^\circ$
−3
−2
−1
0
40
30
20
10
0

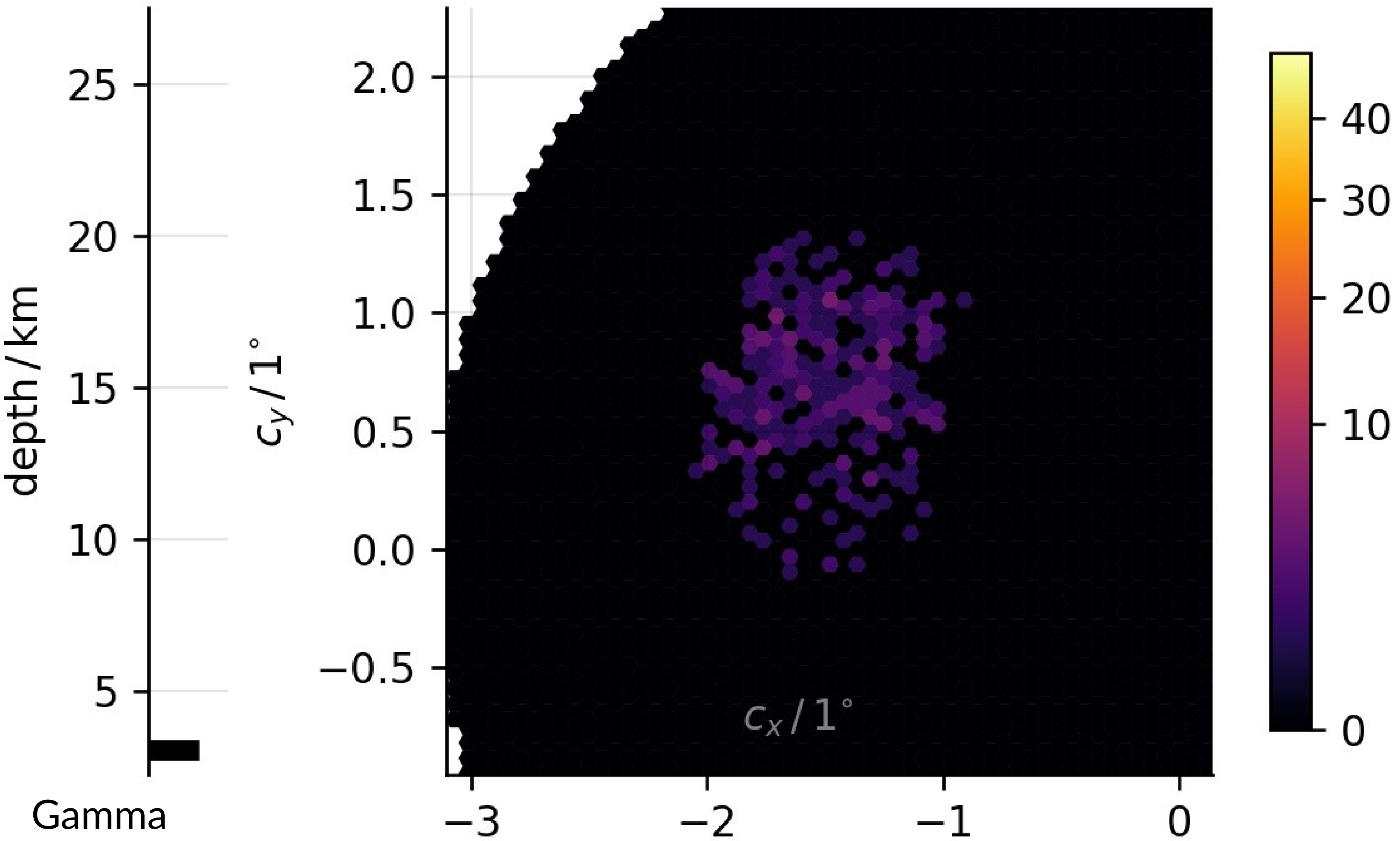

depth / km
25
20
15
10
5
Gamma
c_y / 1°
2.0
1.5
1.0
0.5
0.0
−0.5
c_x / 1°
−3
−2
−1
0
40
30
20
10
0

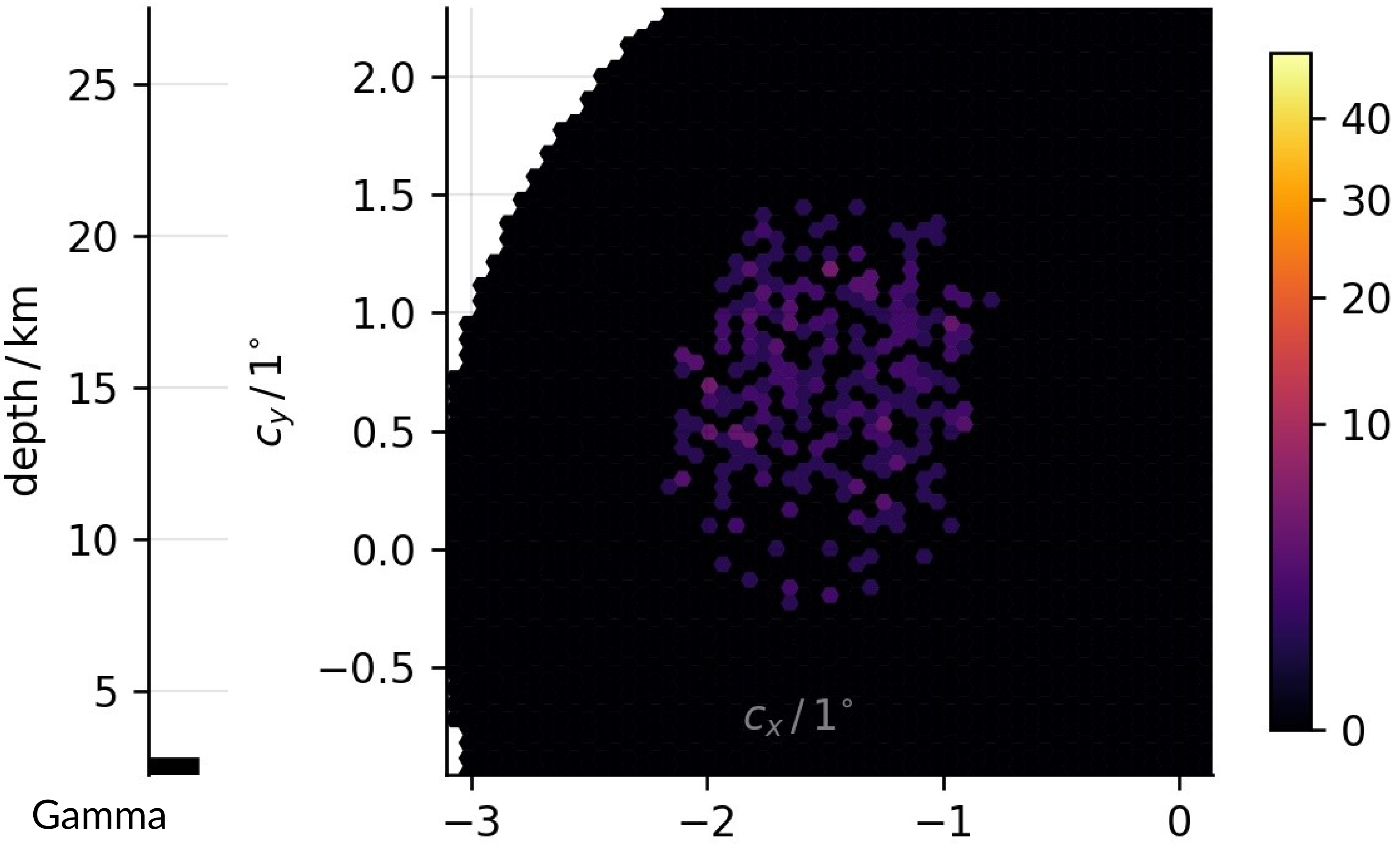

Gamma

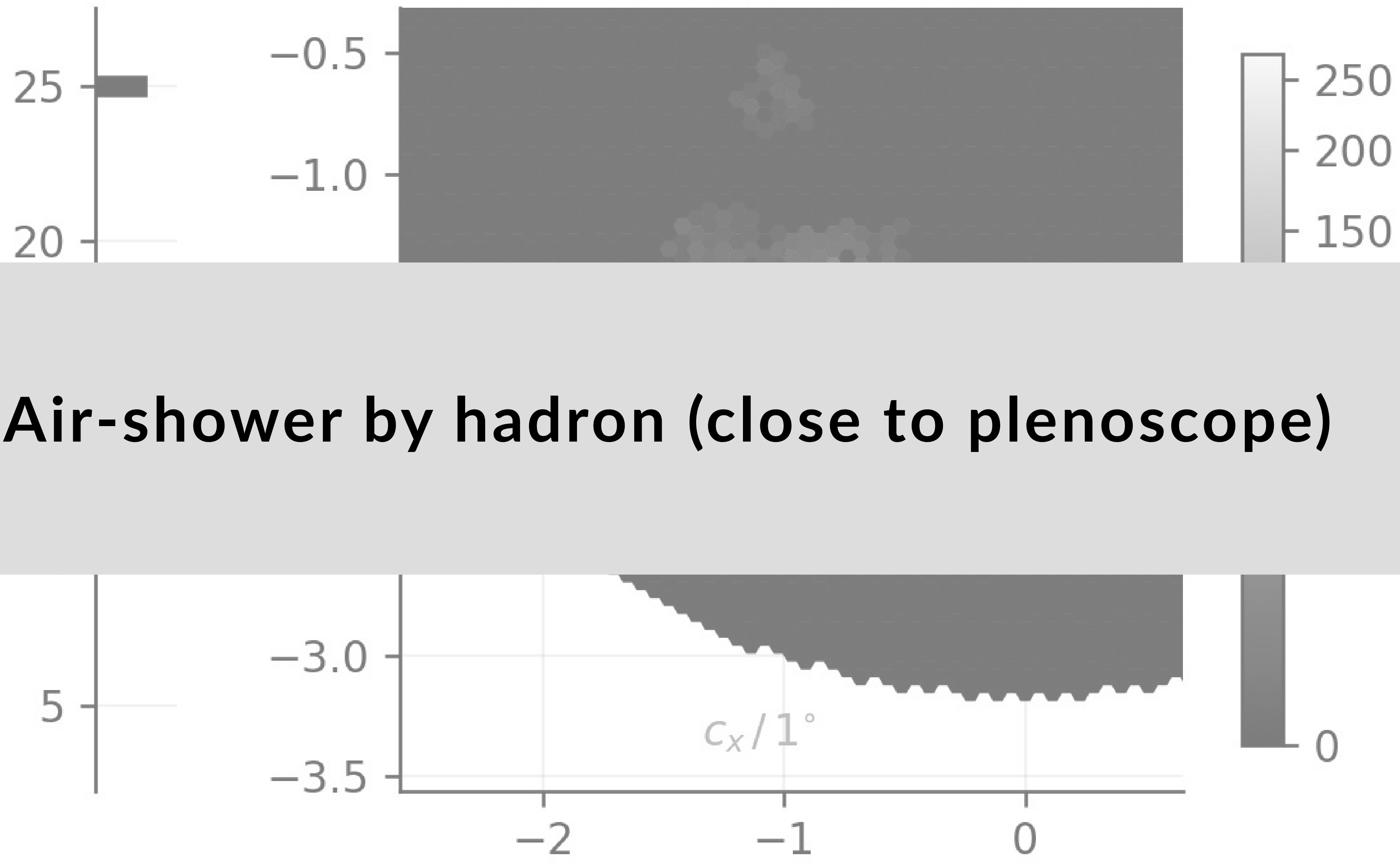

Air-shower by hadron (close to plenoscope)

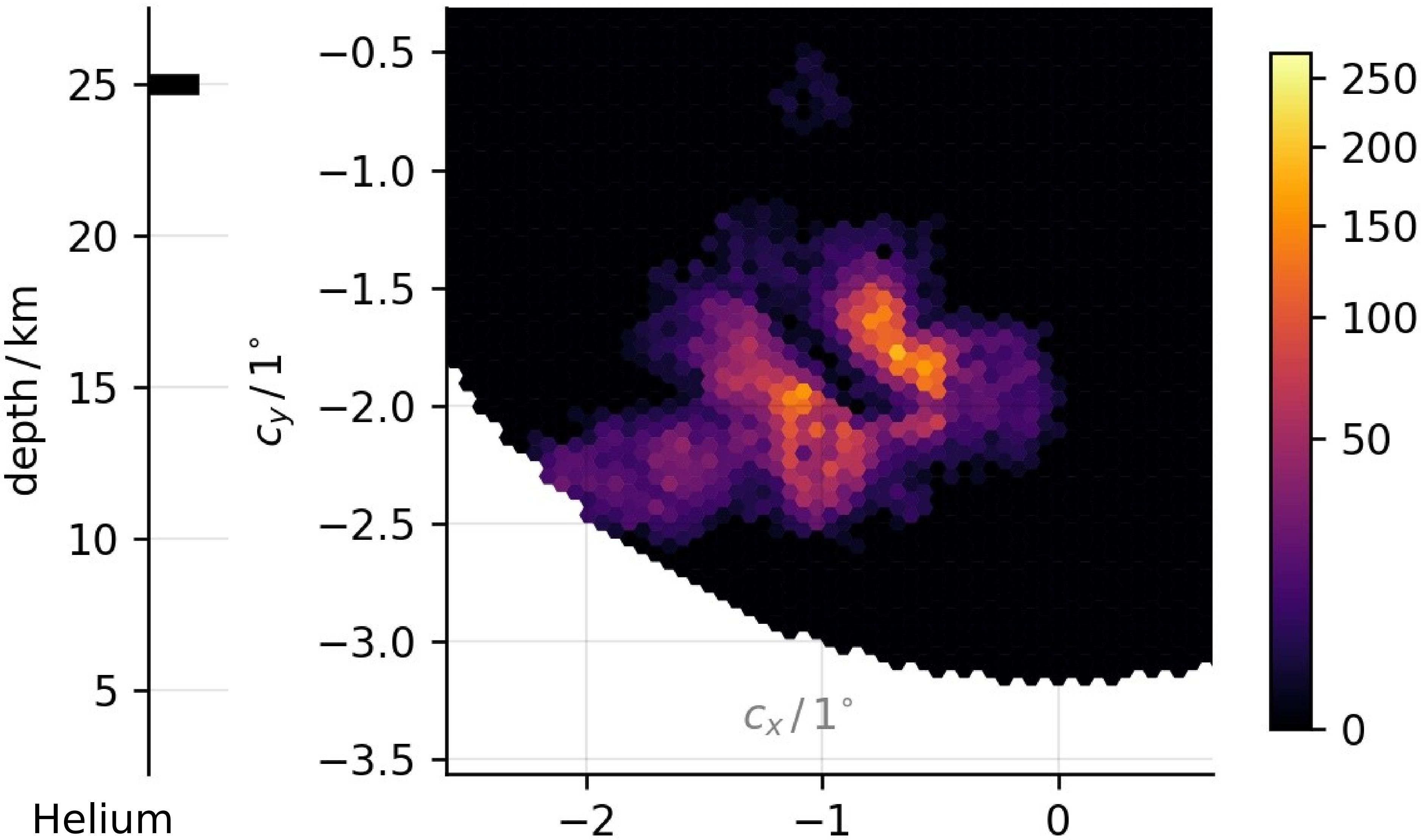

depth / km
25
20
15
10
5
Helium
c_y / 1°
−0.5
−1.0
−1.5
−2.0
−2.5
−3.0
−3.5
c_x / 1°
−2
−1
0
250
200
150
100
50
0

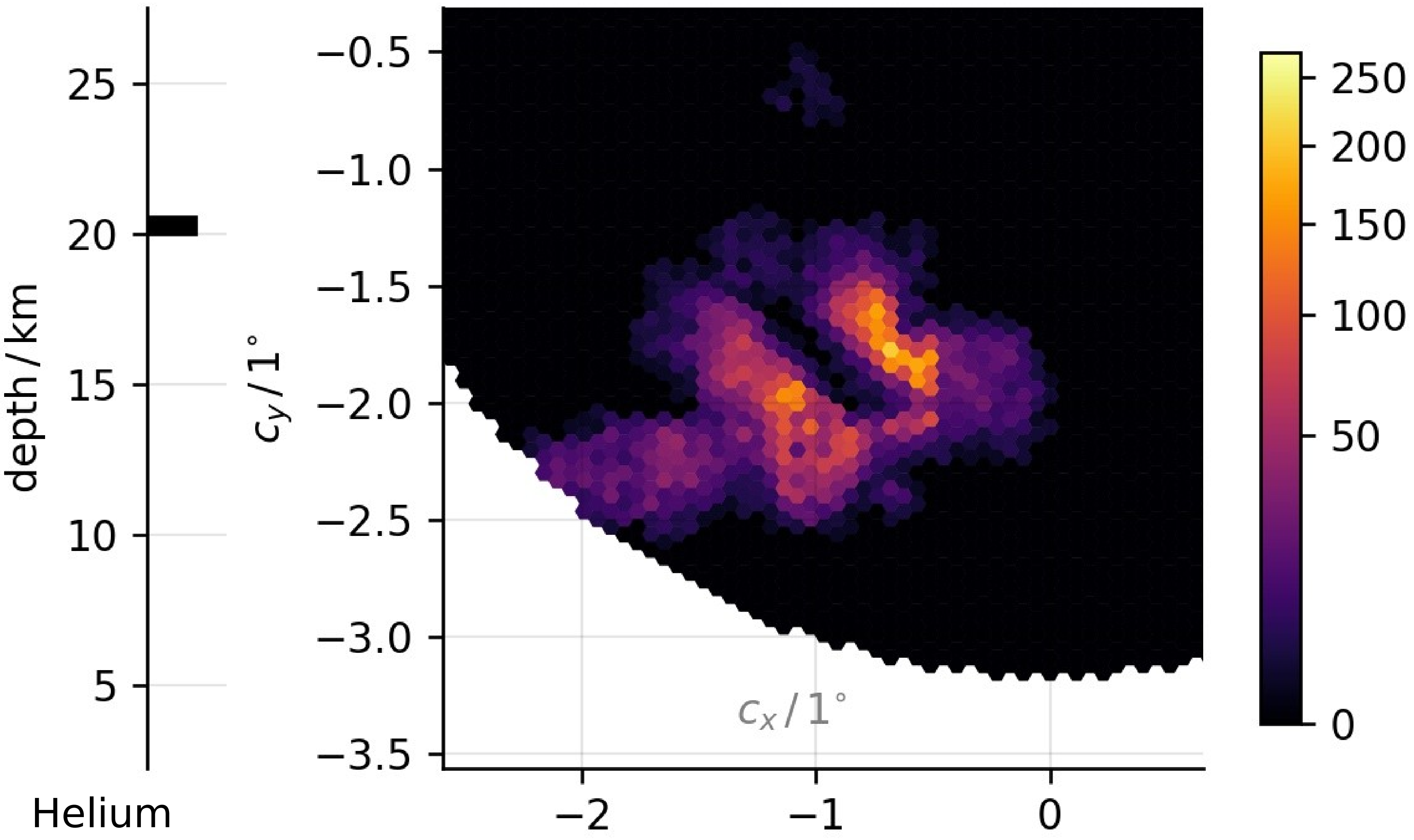

25
20
15
10
5
depth / km
Helium
−0.5
−1.0
−1.5
−2.0
−2.5
−3.0
−3.5
c_y / 1°
c_x / 1°
−2
−1
0
250
200
150
100
50
0

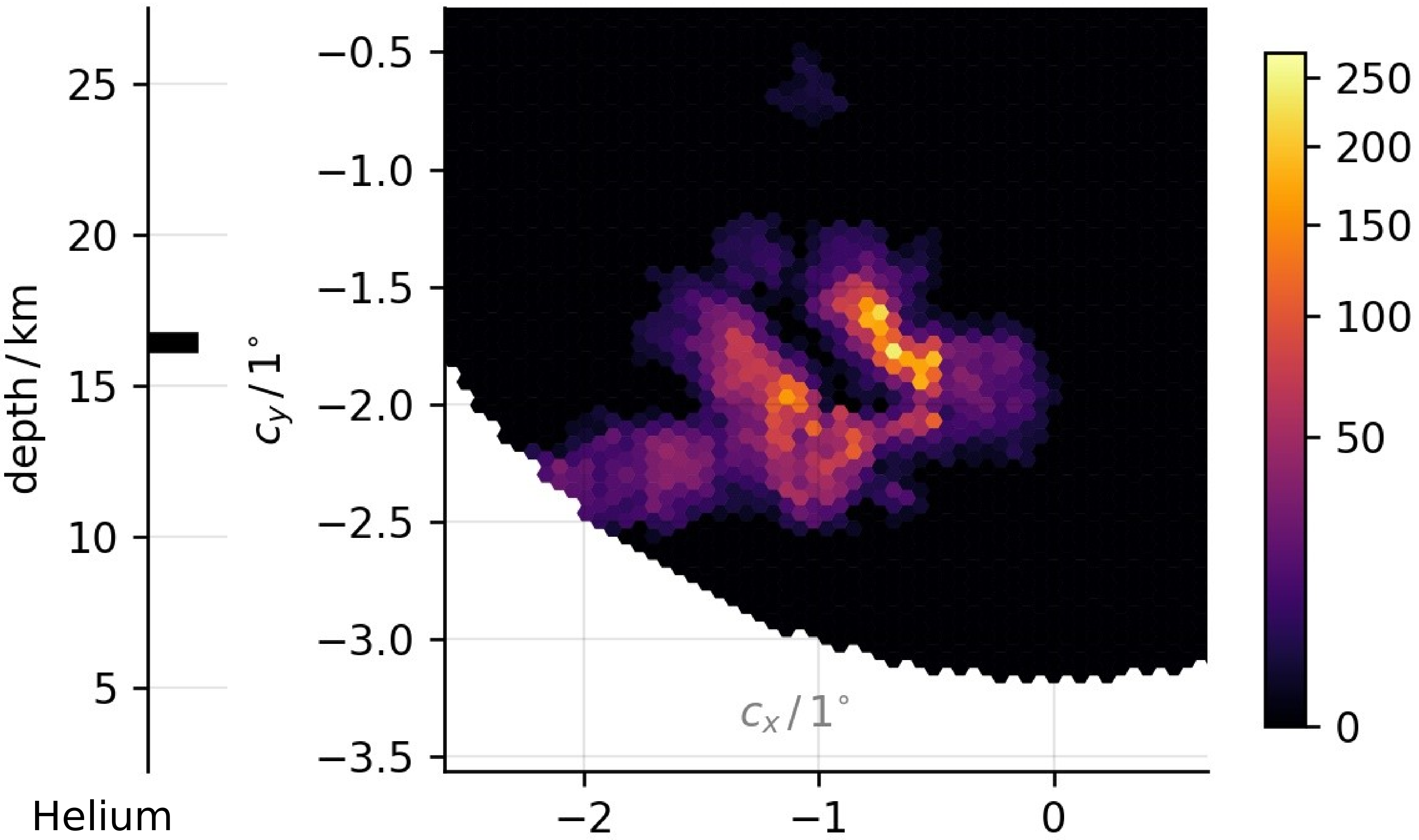

depth / km
25
20
15
10
5
Helium
c_y / 1°
−0.5
−1.0
−1.5
−2.0
−2.5
−3.0
−3.5
c_x / 1°
−2
−1
0
250
200
150
100
50
0

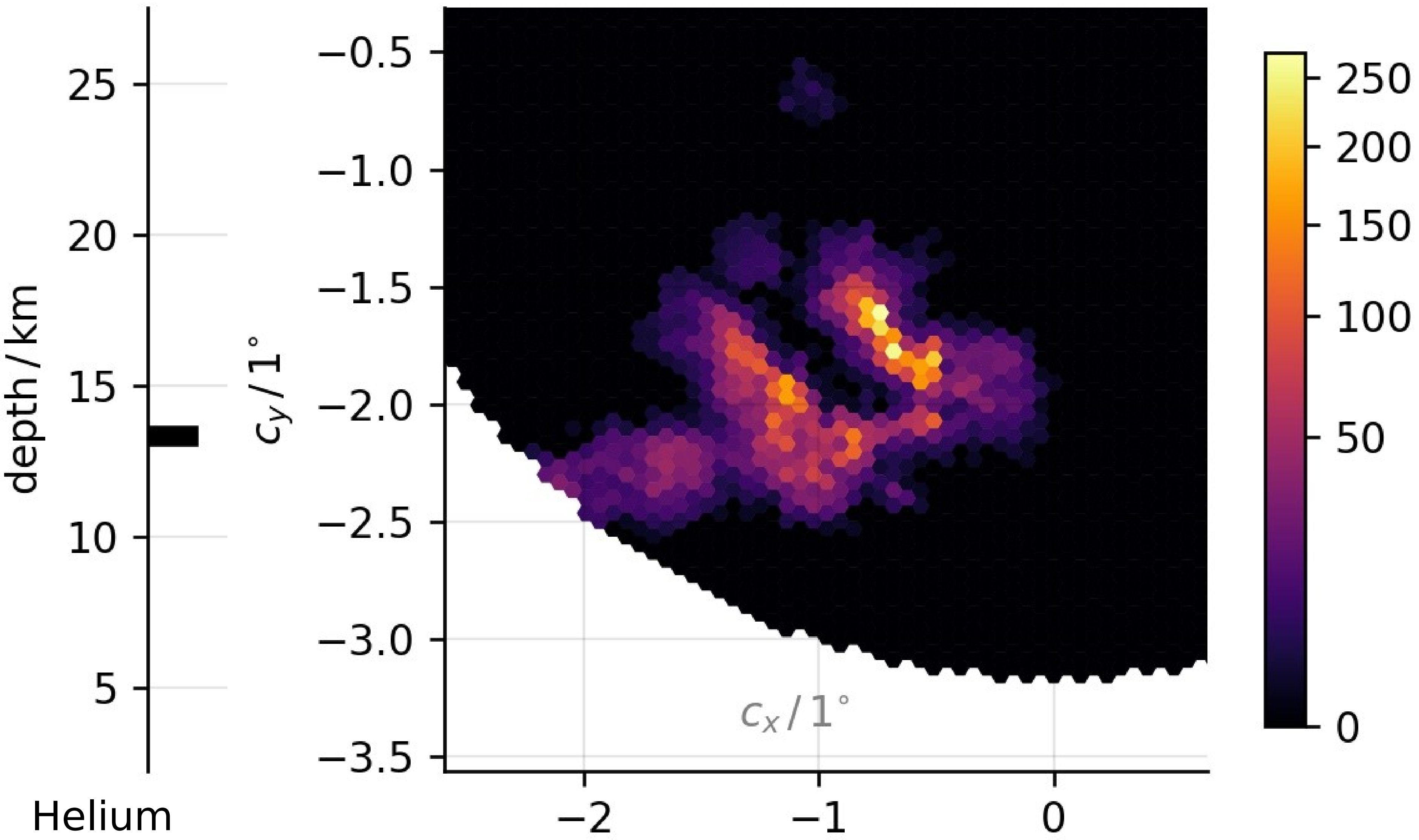

depth / km
25
20
15
10
5
Helium
$c_y / 1^\circ$
−0.5
−1.0
−1.5
−2.0
−2.5
−3.0
−3.5
$c_x / 1^\circ$
−2
−1
0
250
200
150
100
50
0

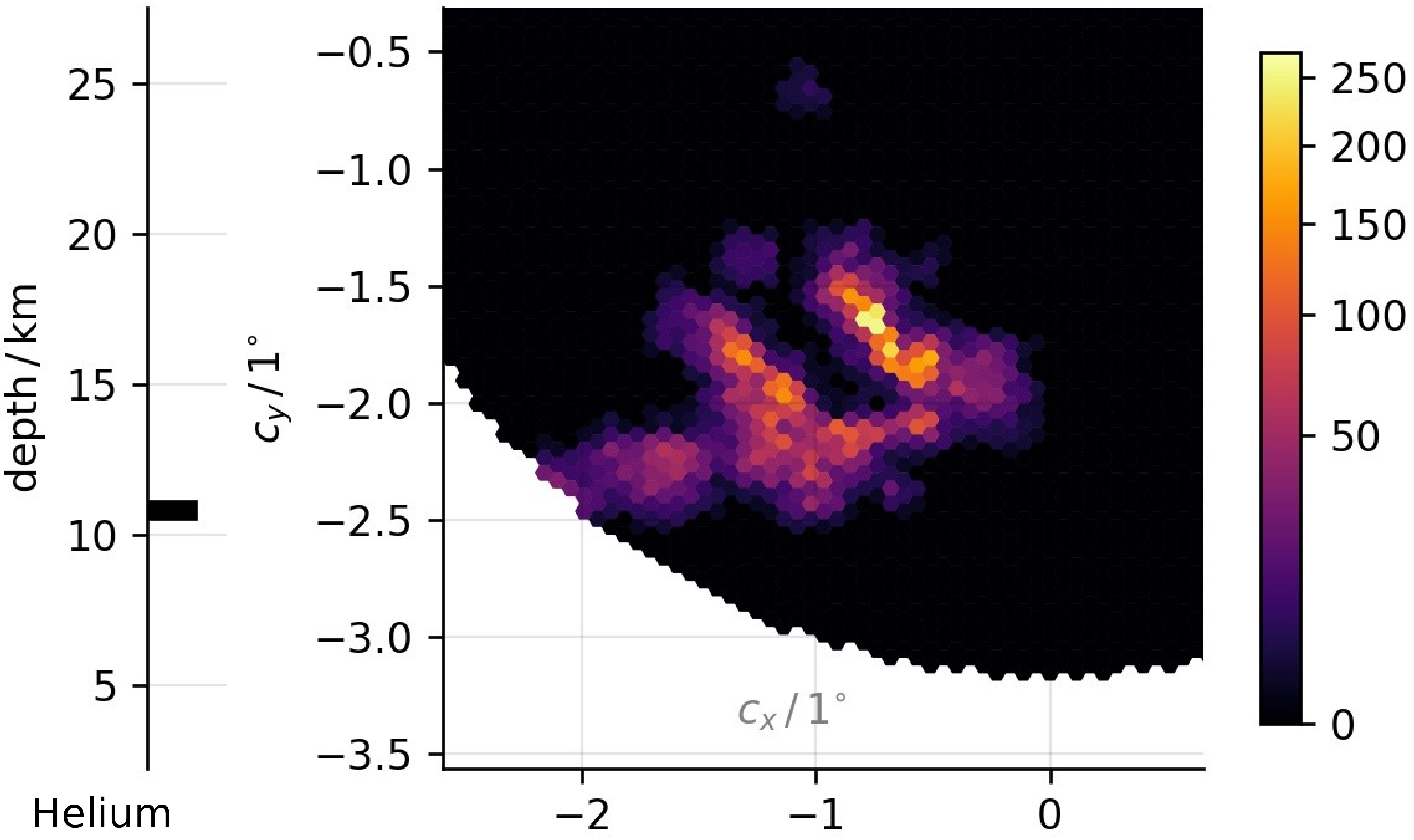
depth / km
25
20
15
10
5
Helium
c_y / 1°
−0.5
−1.0
−1.5
−2.0
−2.5
−3.0
−3.5
c_x / 1°
−2
−1
0
250
200
150
100
50
0

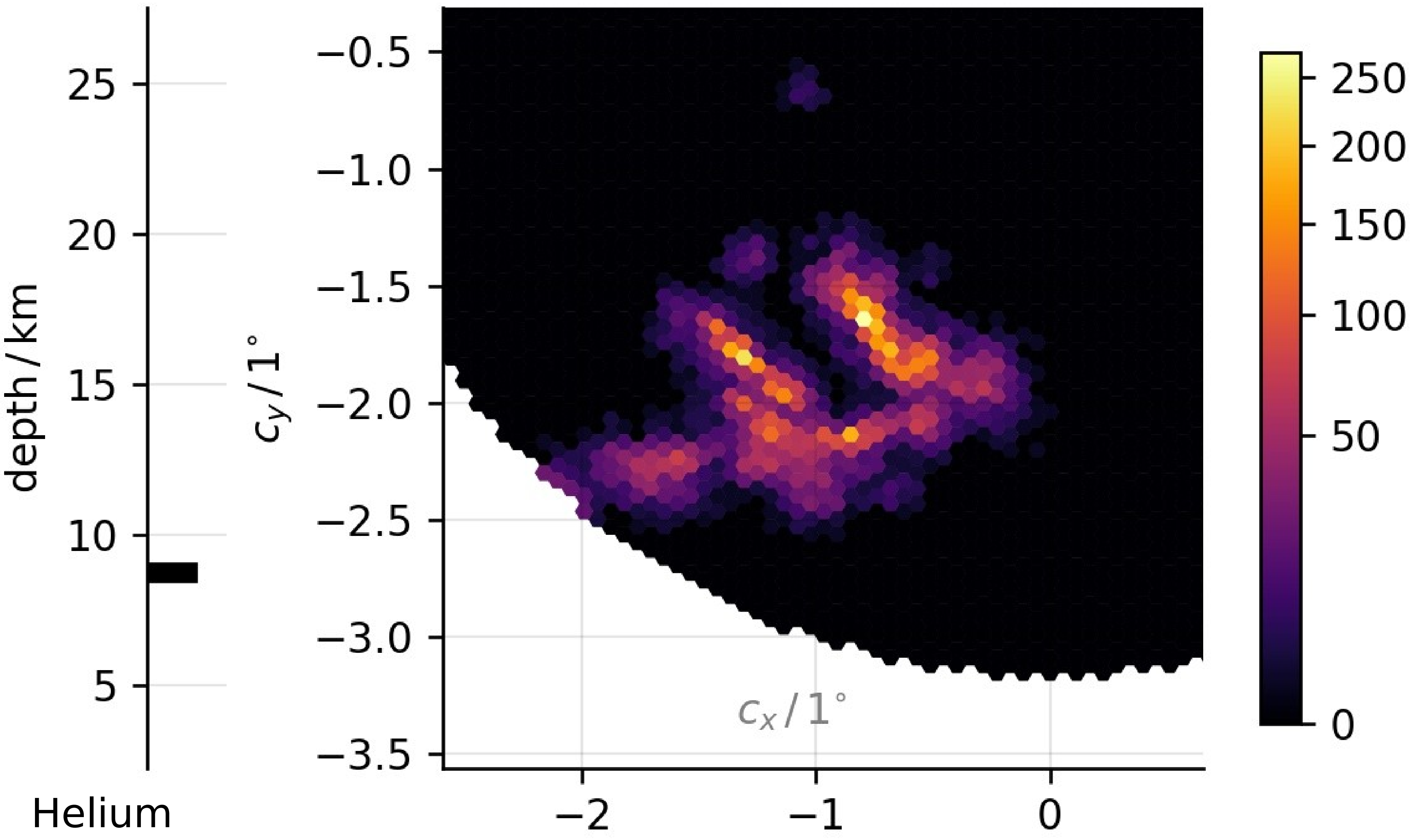
depth / km
25
20
15
10
5
Helium
c_y / 1°
−0.5
−1.0
−1.5
−2.0
−2.5
−3.0
−3.5
c_x / 1°
−2
−1
0
250
200
150
100
50
0

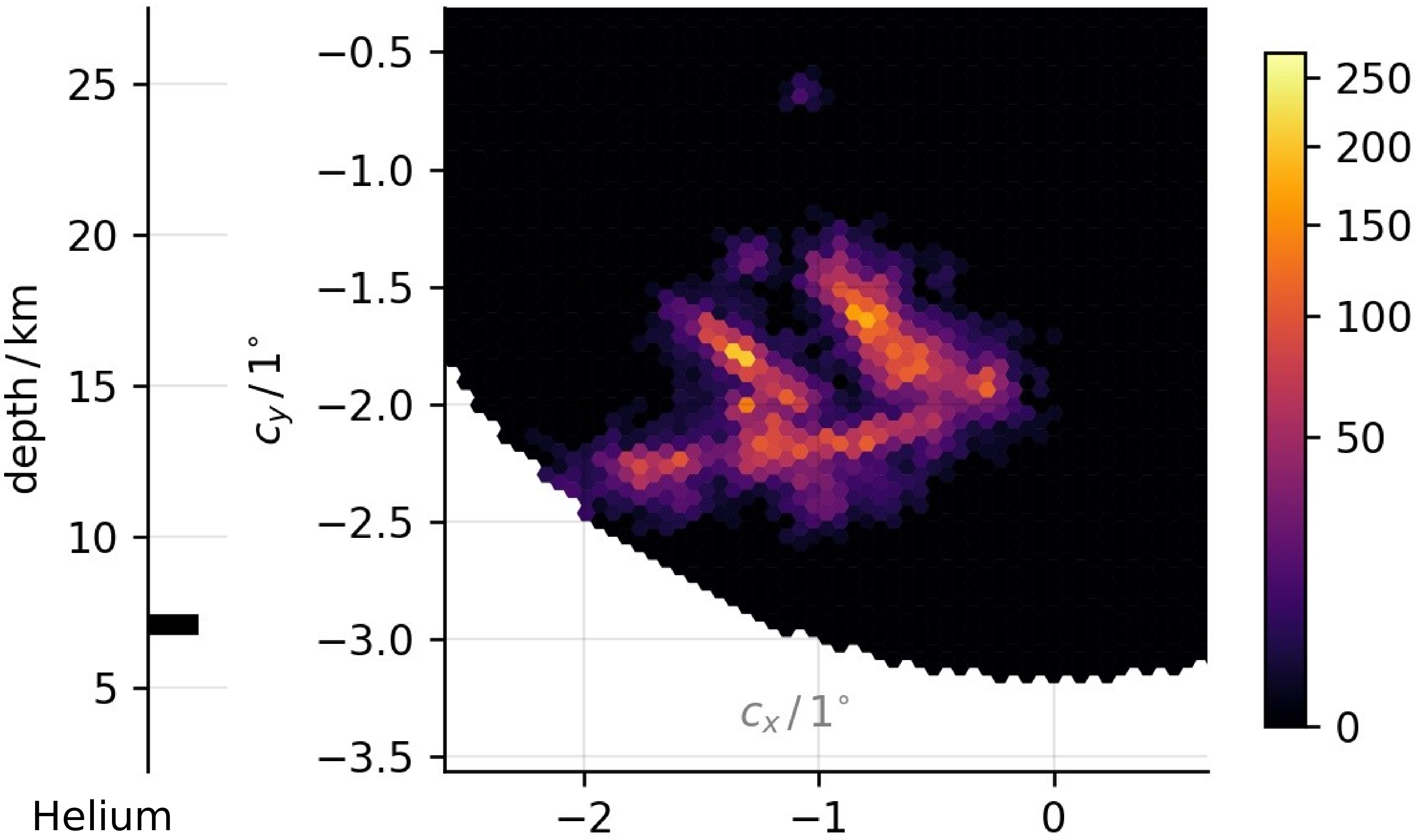
depth / km
25
20
15
10
5
Helium
c_y / 1°
−0.5
−1.0
−1.5
−2.0
−2.5
−3.0
−3.5
c_x / 1°
−2
−1
0
250
200
150
100
50
0

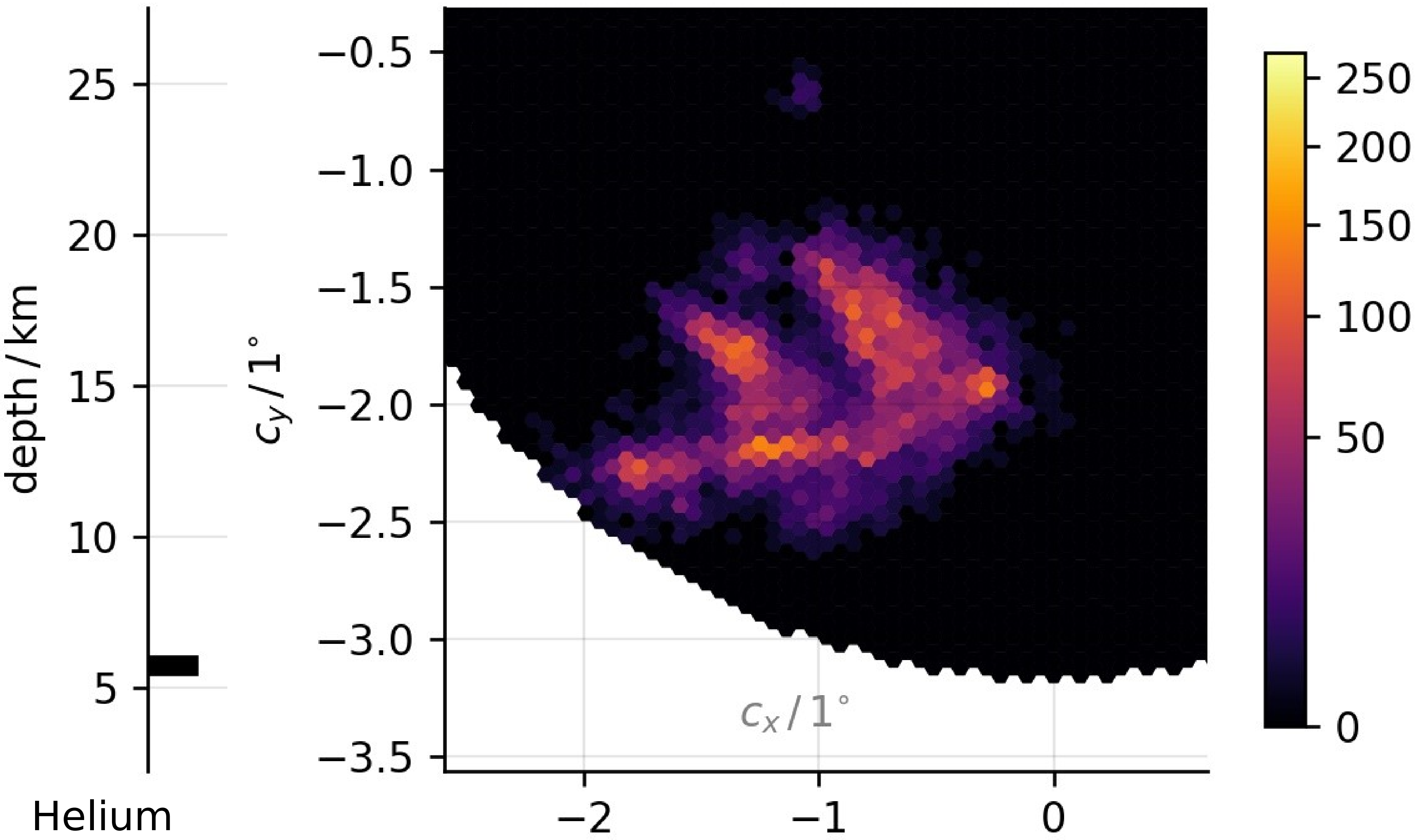

depth / km
25
20
15
10
5
Helium
c_y / 1°
−0.5
−1.0
−1.5
−2.0
−2.5
−3.0
−3.5
c_x / 1°
−2
−1
0
250
200
150
100
50
0

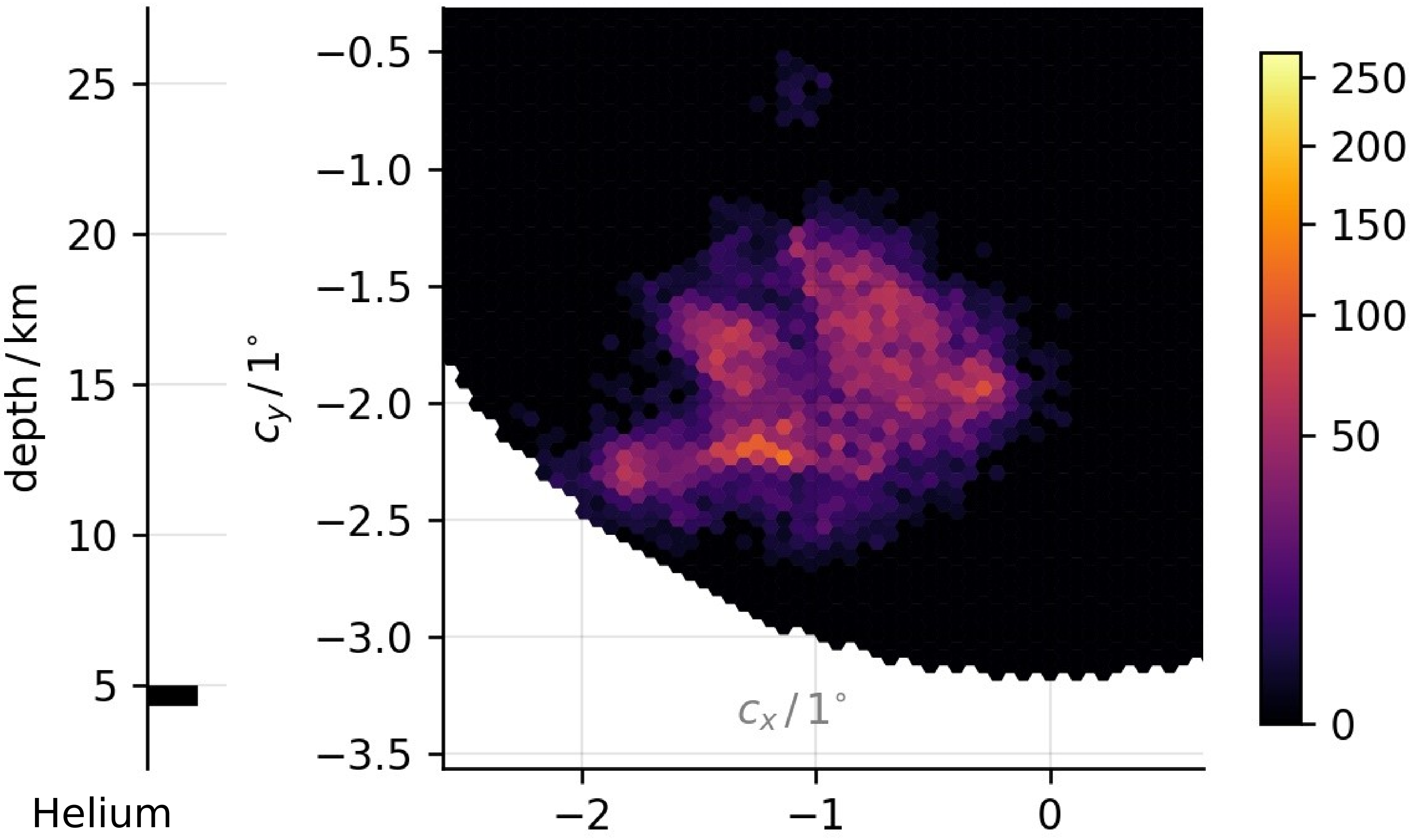
depth / km
25
20
15
10
5
Helium
c_y / 1°
−0.5
−1.0
−1.5
−2.0
−2.5
−3.0
−3.5
c_x / 1°
−2
−1
0
250
200
150
100
50
0

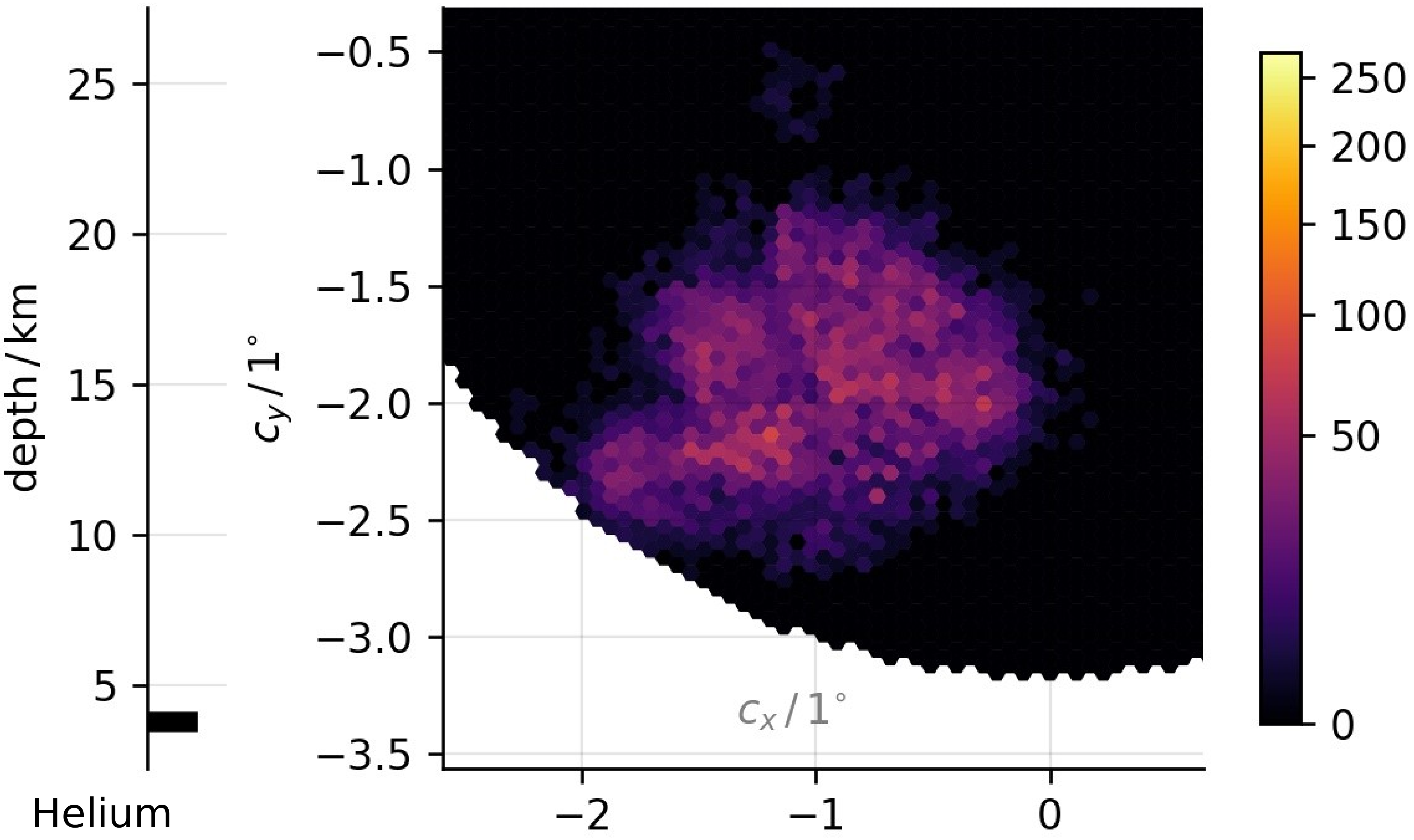
depth / km
25
20
15
10
5
Helium
c_y / 1°
−0.5
−1.0
−1.5
−2.0
−2.5
−3.0
−3.5
c_x / 1°
−2
−1
0
250
200
150
100
50
0

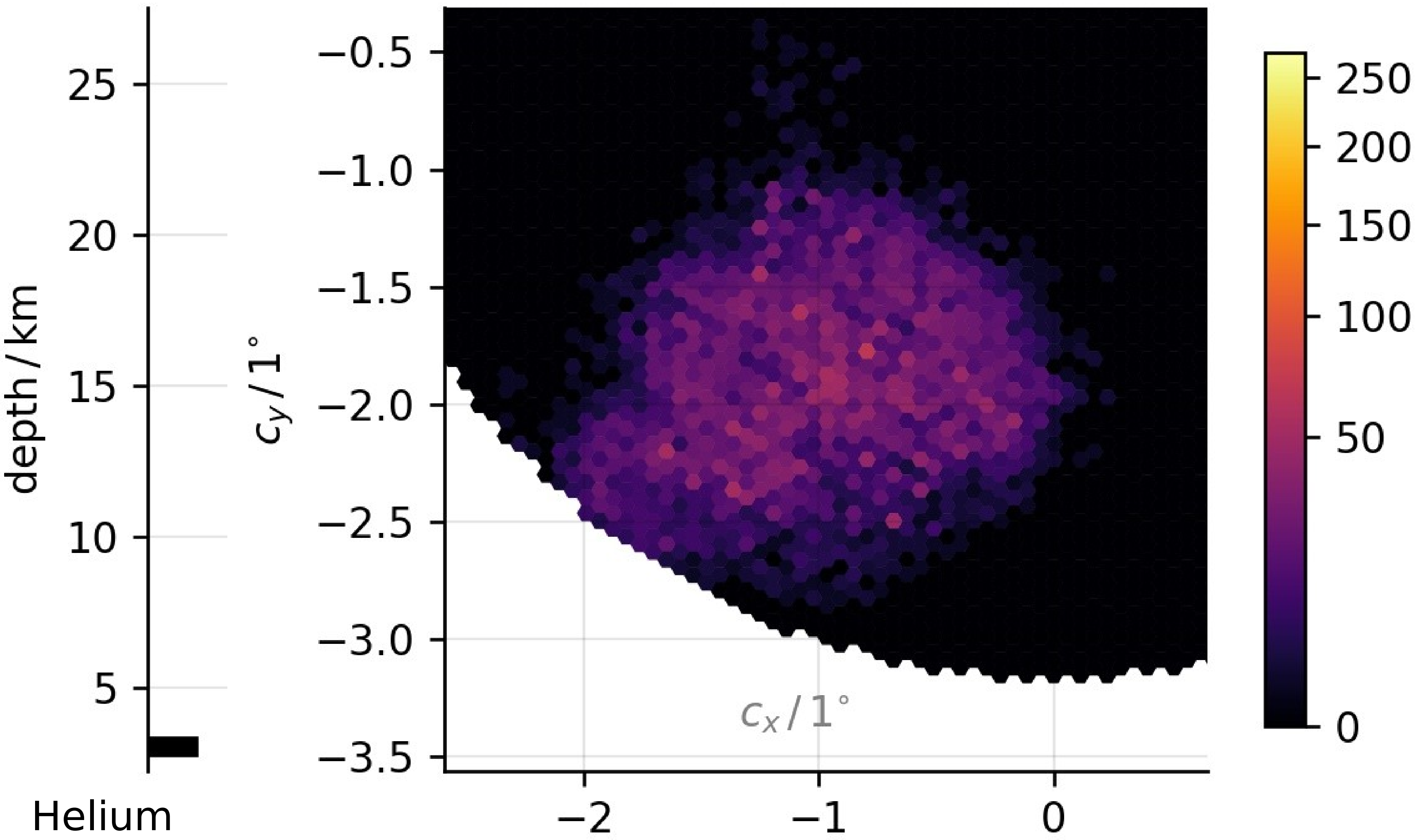

depth / km
25
20
15
10
5
Helium
c_y / 1°
−0.5
−1.0
−1.5
−2.0
−2.5
−3.0
−3.5
c_x / 1°
−2
−1
0
250
200
150
100
50
0

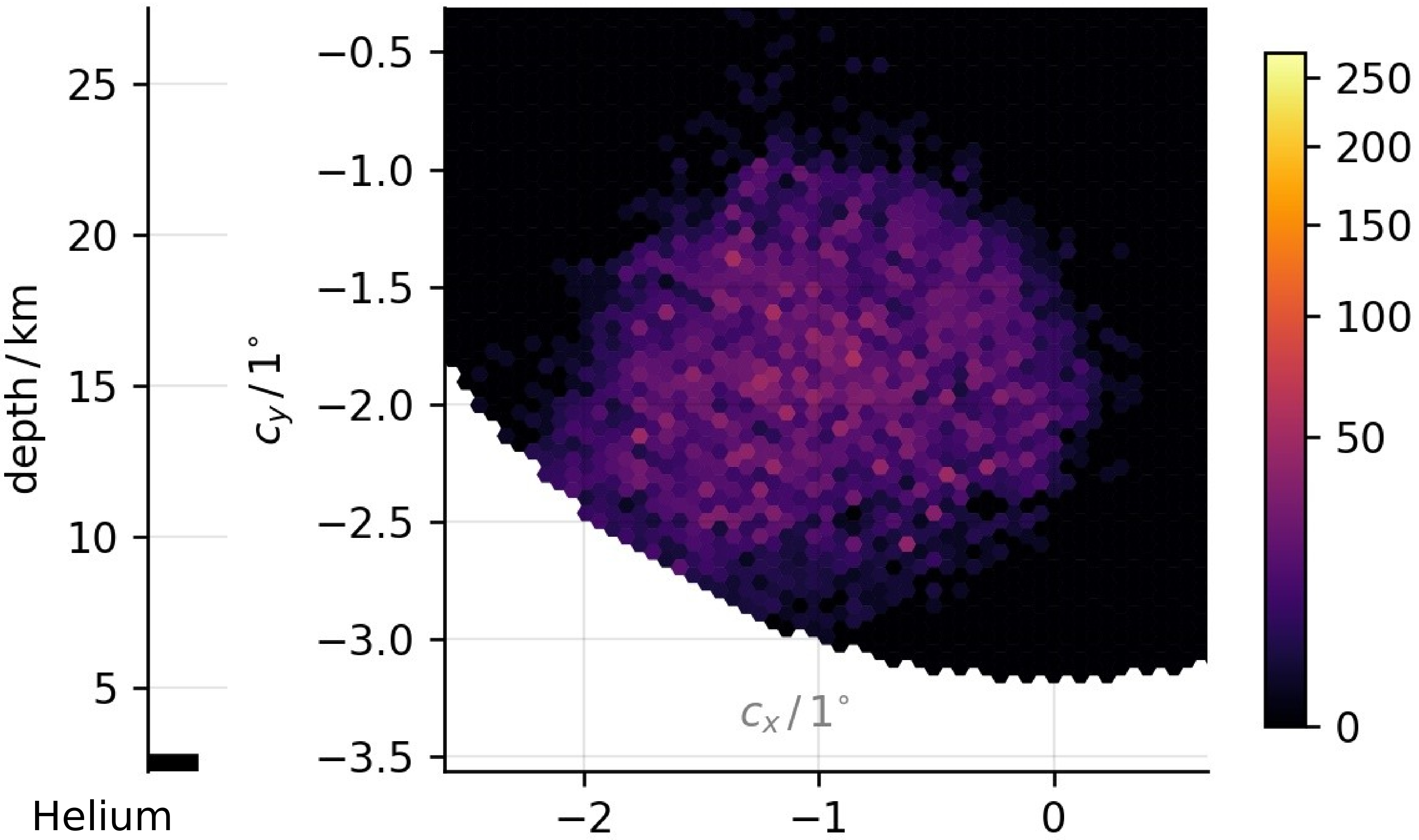
depth / km
25
20
15
10
5
Helium
c_y / 1°
−0.5
−1.0
−1.5
−2.0
−2.5
−3.0
−3.5
c_x / 1°
−2
−1
0
250
200
150
100
50
0

Estimating background from cosmic-rays

Deflection of shower

Deflection of shower

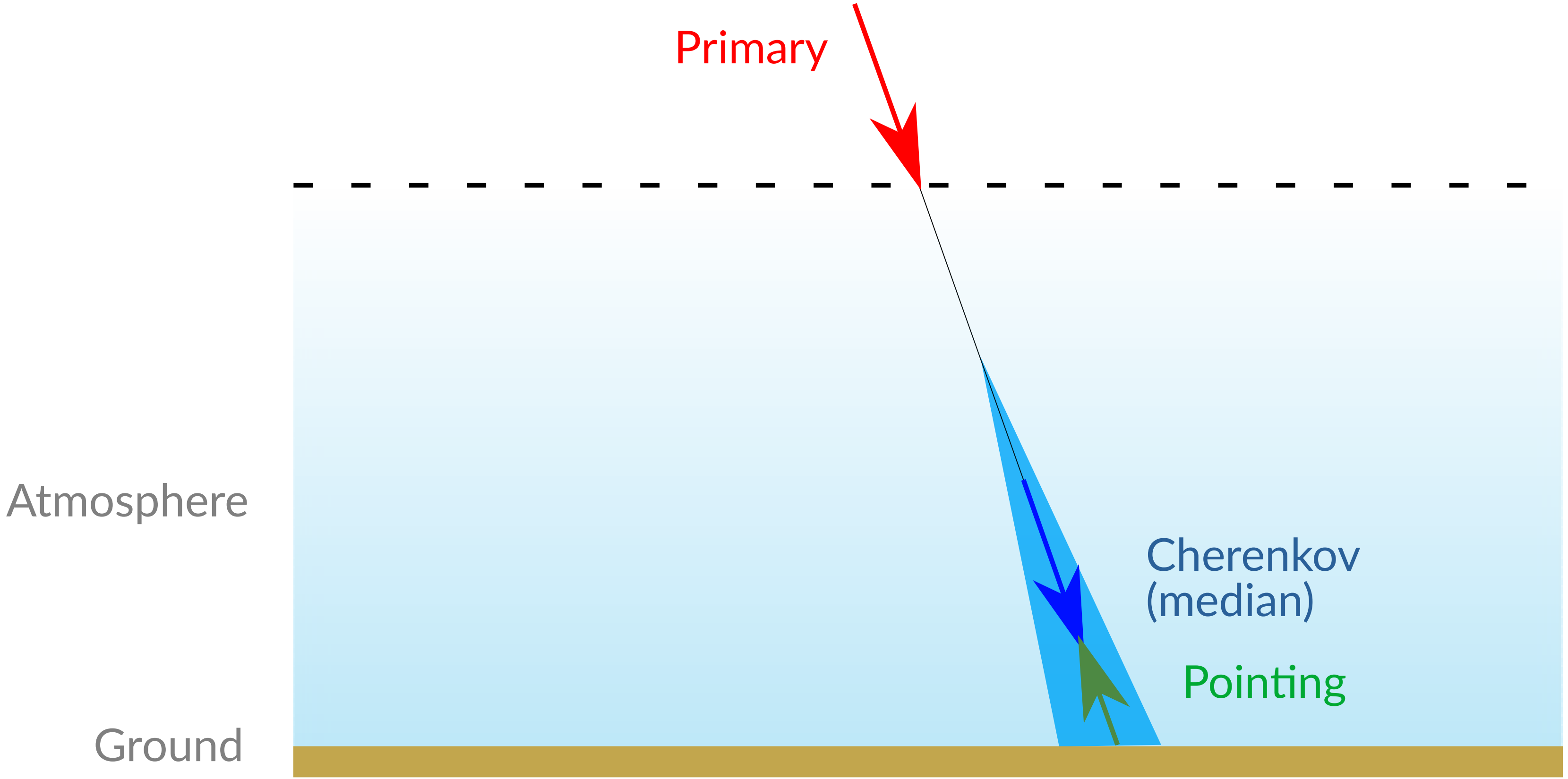

Deflection of shower

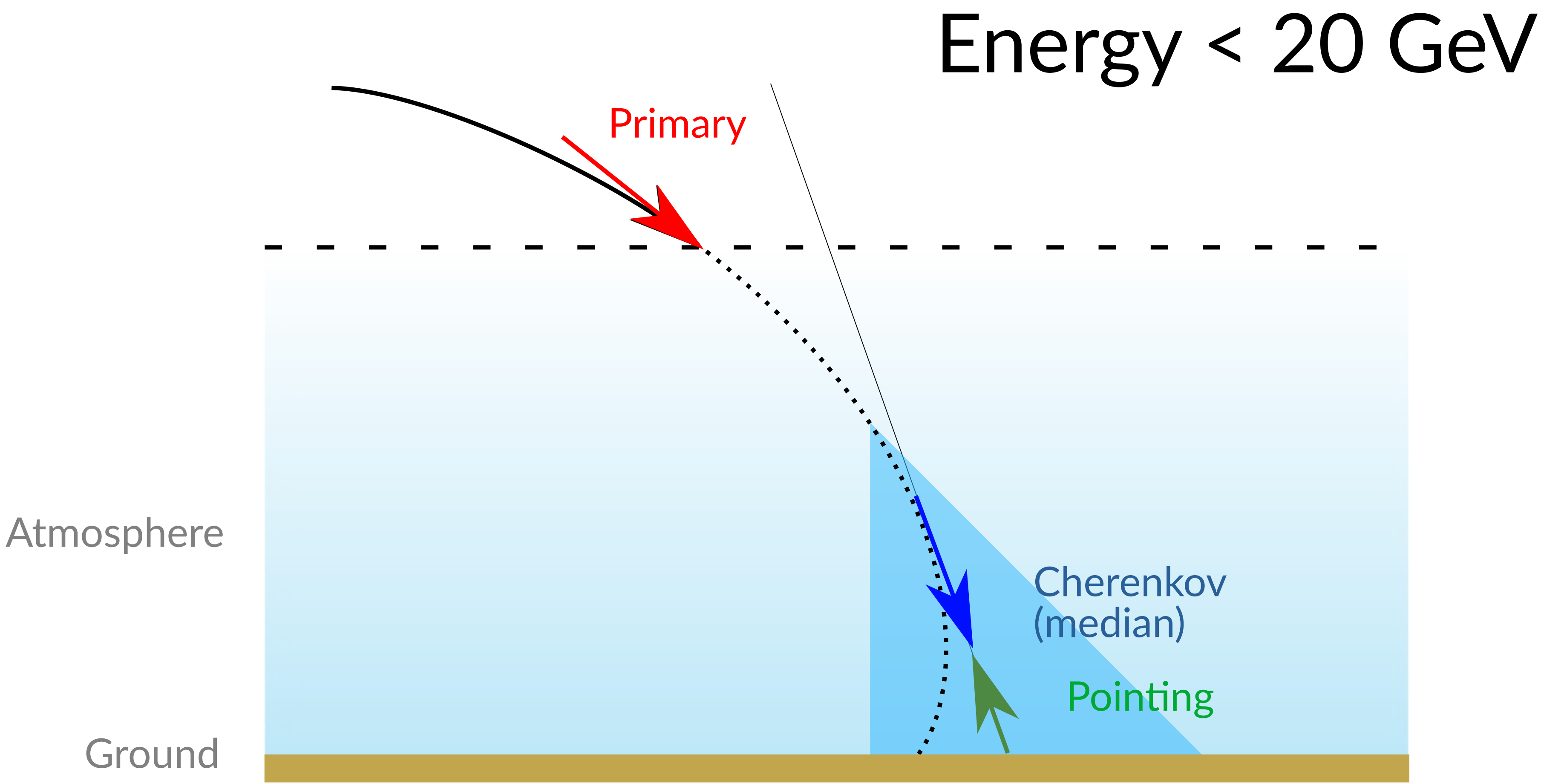

Deflection of shower

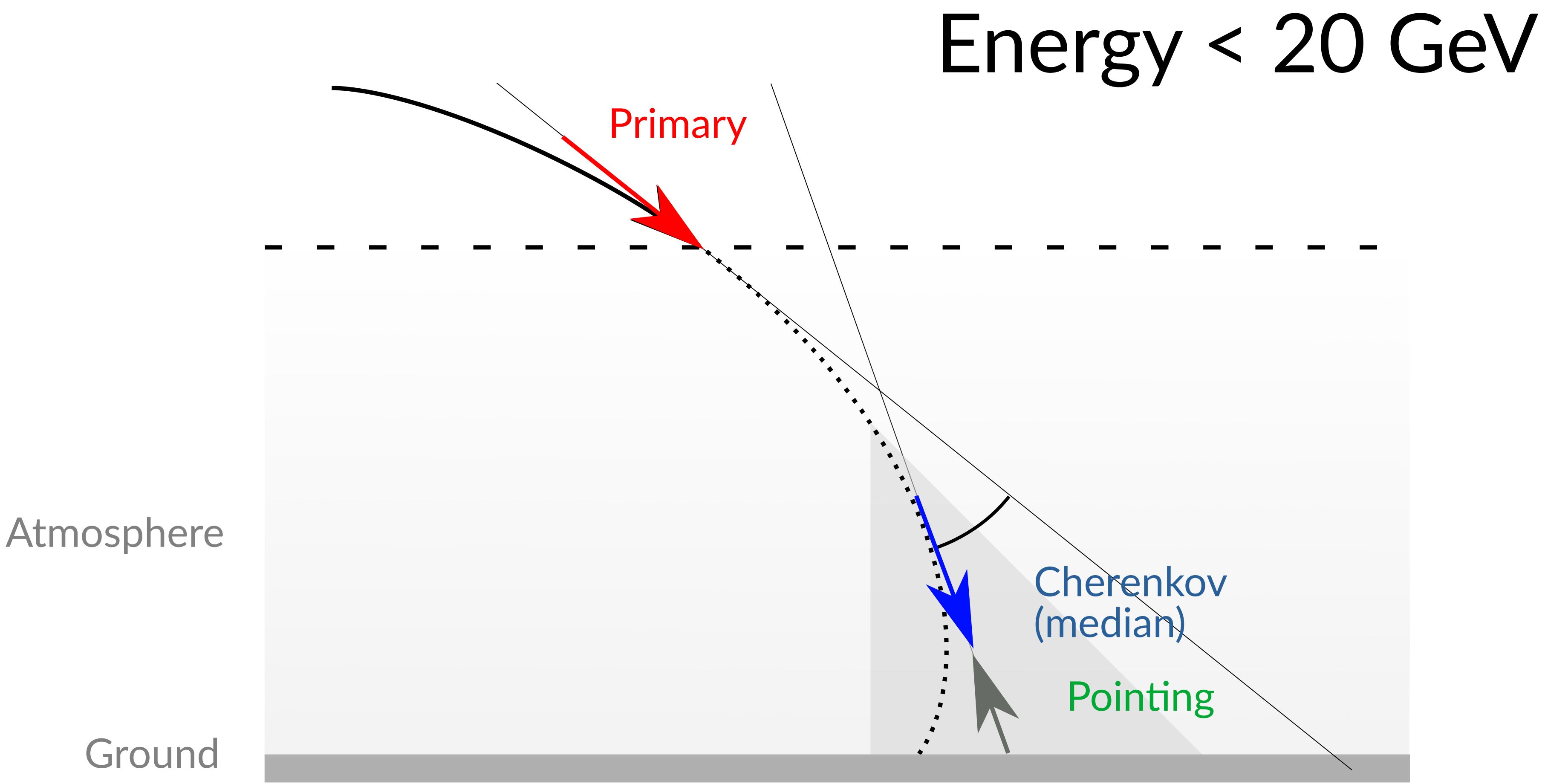

Deflection of shower

Helium

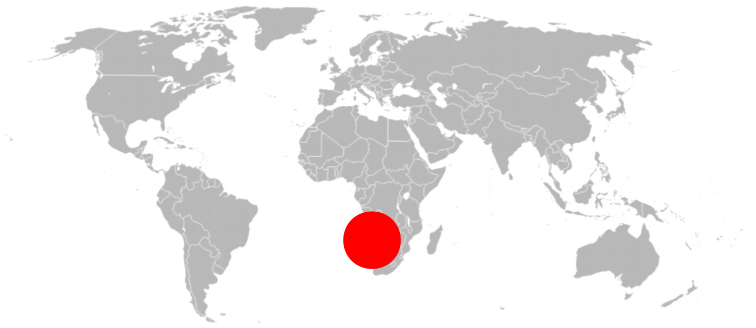

Gamsberg, Namibia

horizontal: 12.5uT
vertical: -25.9uT
2300m a.s.l.

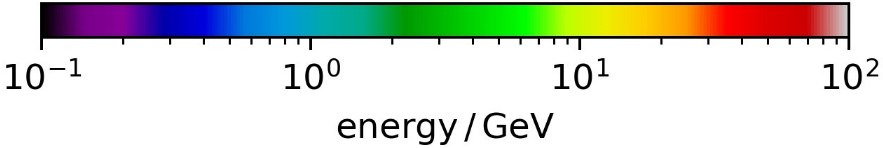

Direction of primary to get
Cherenkov-light from zenith.

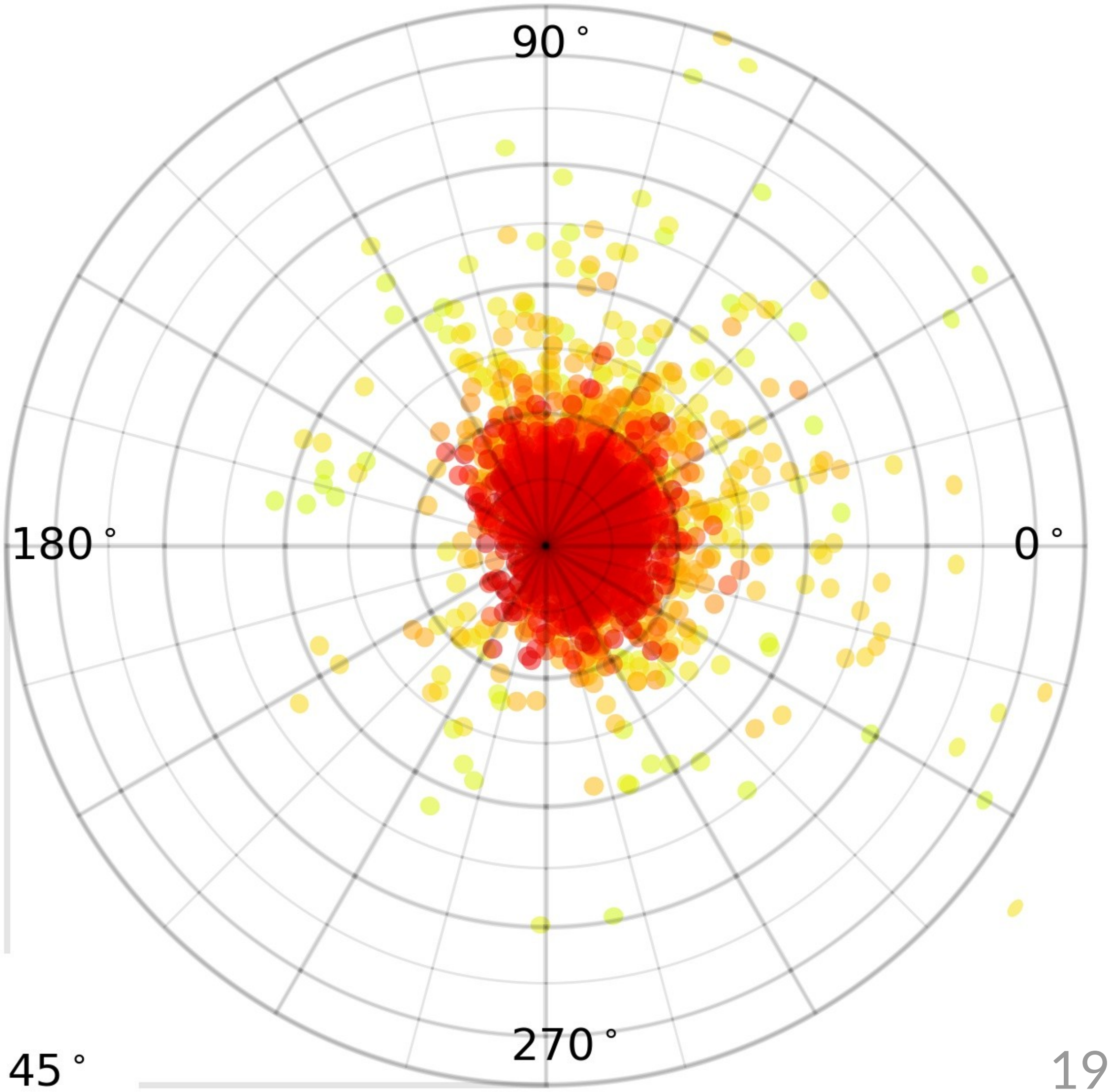

Deflection of shower

Proton

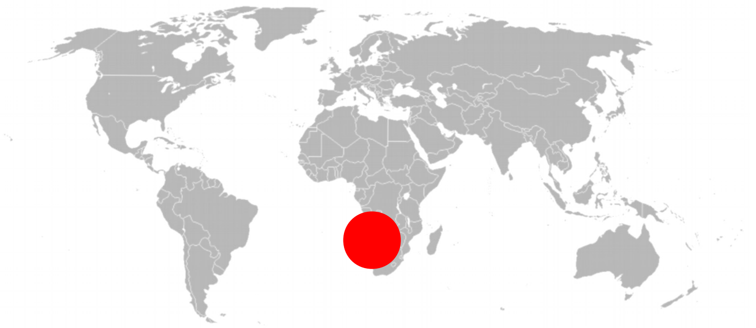

Gamsberg, Namibia

horizontal: 12.5uT
vertical: -25.9uT
2300m a.s.l.

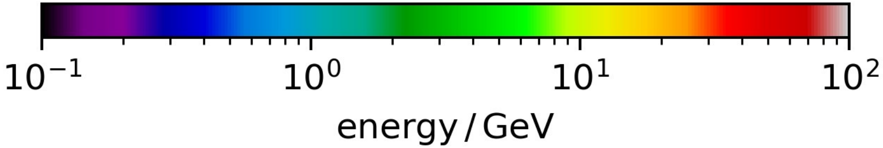

Direction of primary to get Cherenkov-light from zenith.

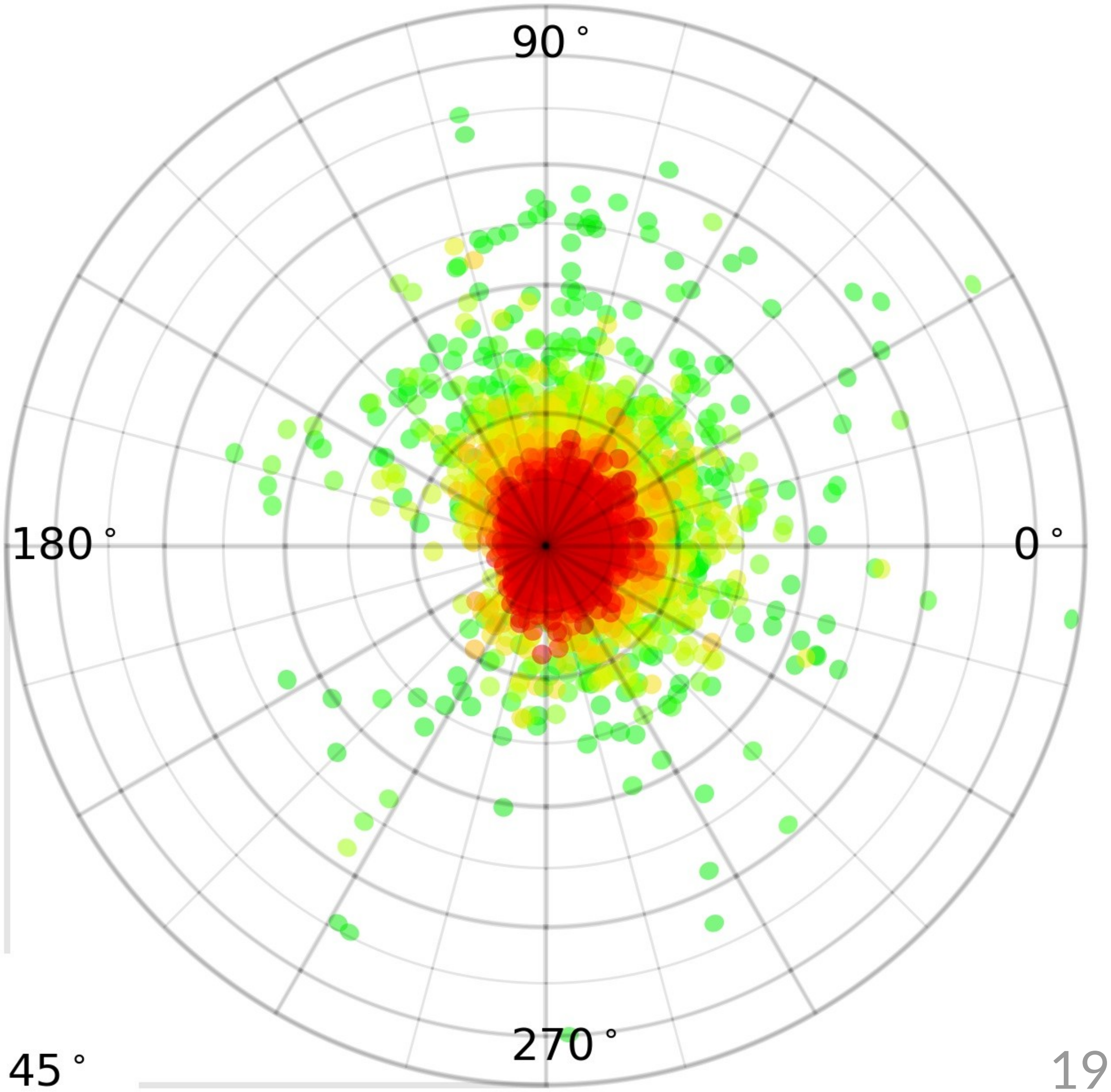

Deflection of shower

Electron

Gamsberg, Namibia

horizontal: 12.5uT
vertical: -25.9uT
2300m a.s.l.

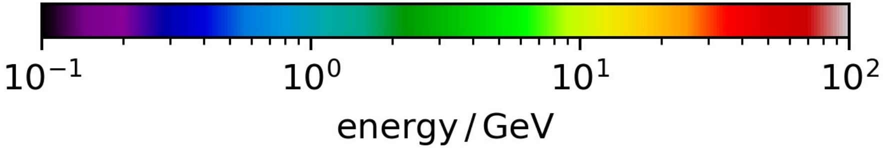

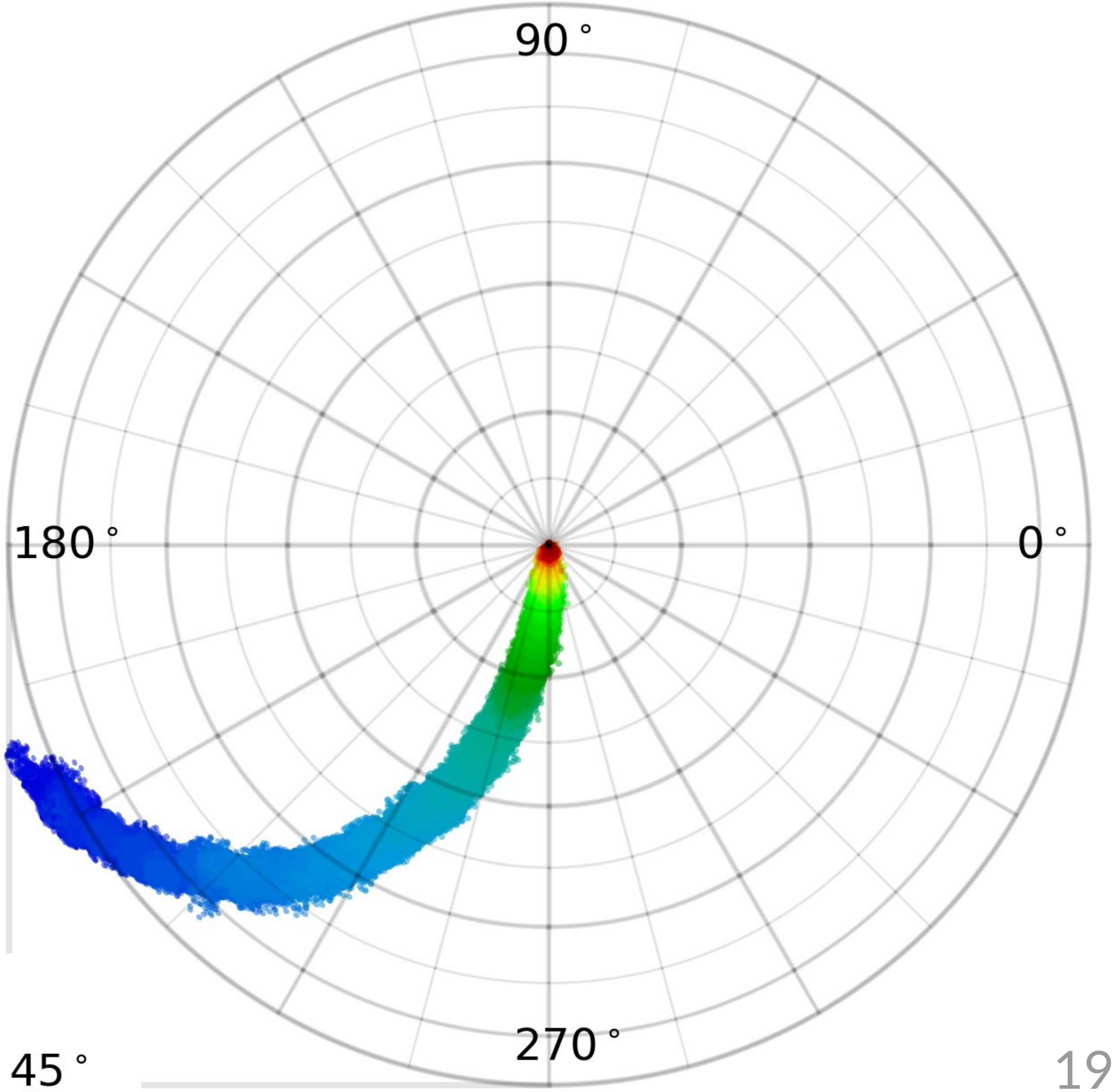

Direction of primary to get
Cherenkov-light from zenith.

Deflection of shower

Gamma-ray

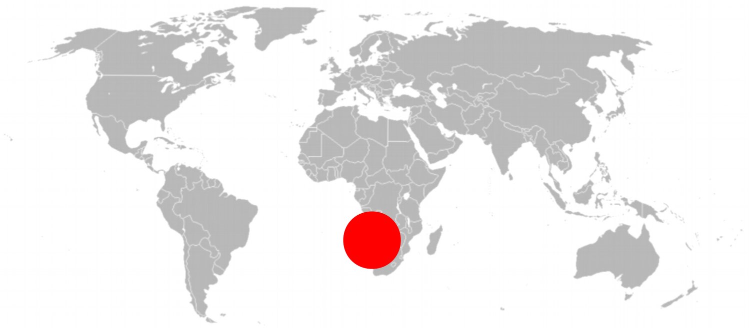

Gamsberg, Namibia

horizontal: 12.5uT
vertical: -25.9uT
2300m a.s.l.

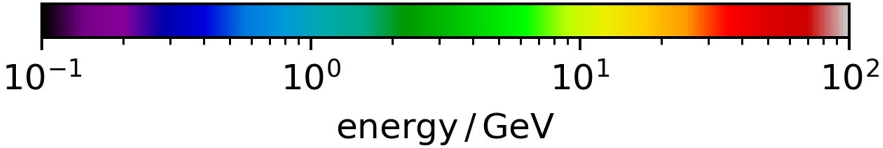

Direction of primary to get Cherenkov-light from zenith.

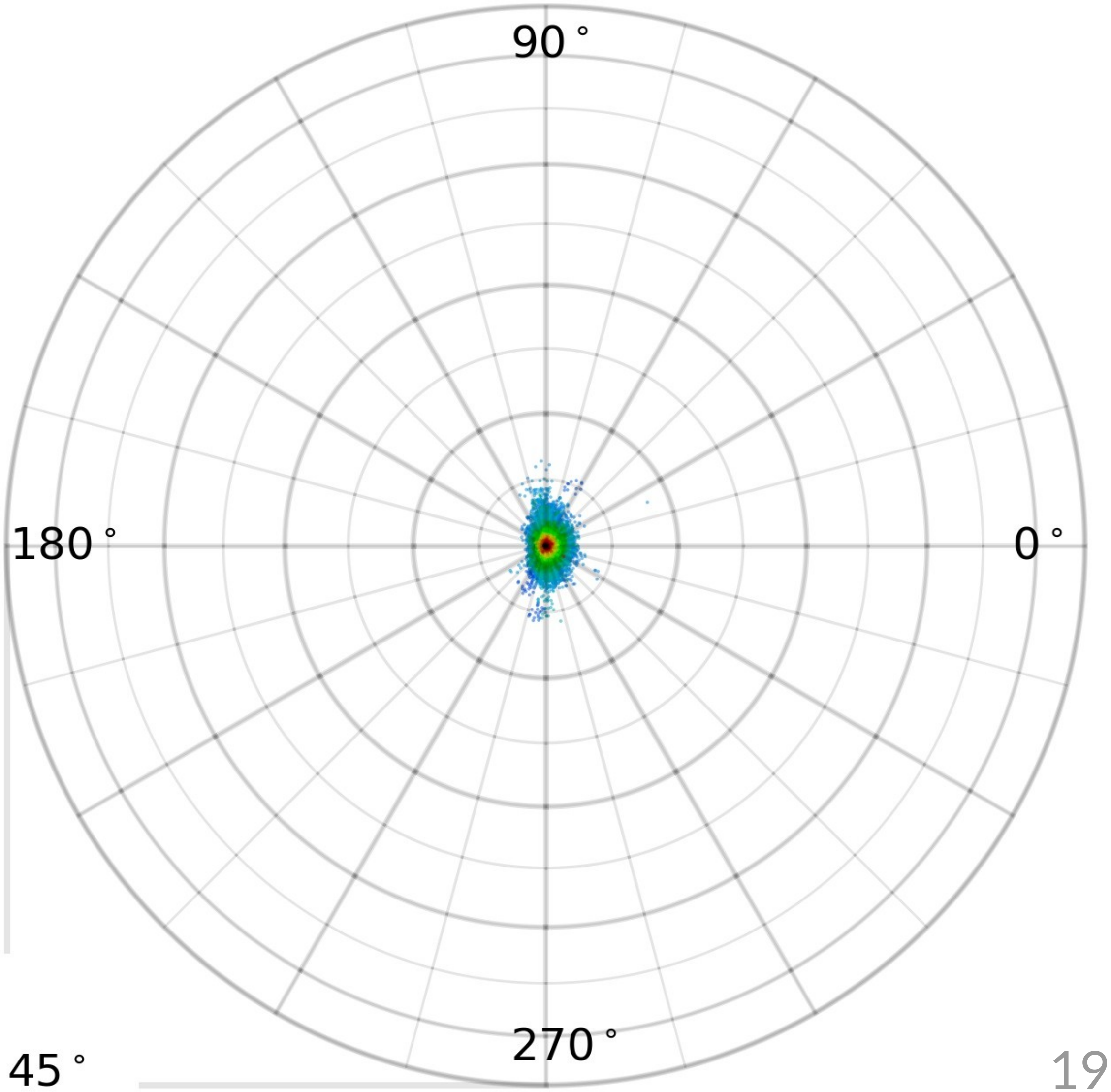

Deflection of shower

Gamma-ray

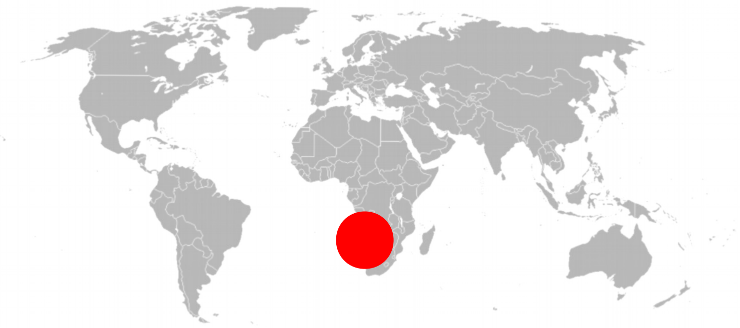

Gamsberg, Namibia

horizontal: 12.5uT
vertical: -25.9uT
2300m a.s.l.

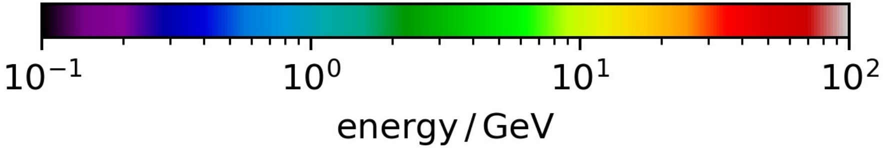

Direction of primary to get Cherenkov-light from zenith.

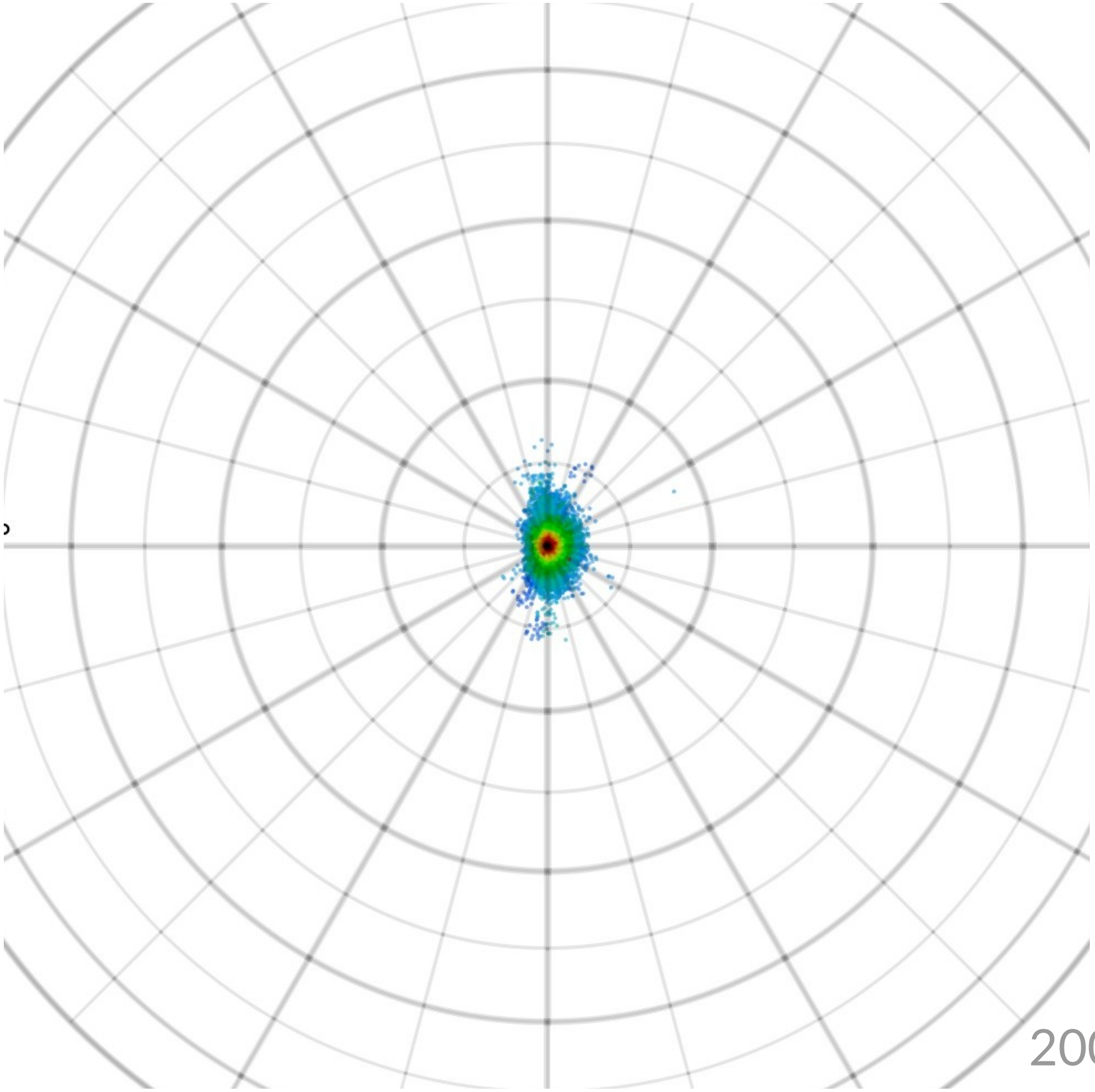

Deflection of shower

Gamma-ray

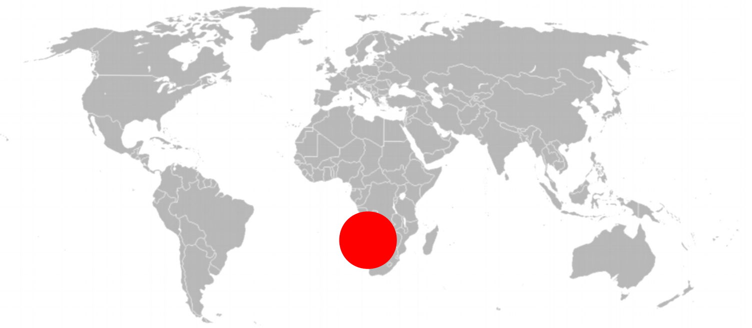

Gamsberg, Namibia

horizontal: 12.5uT
vertical: -25.9uT
2300m a.s.l.

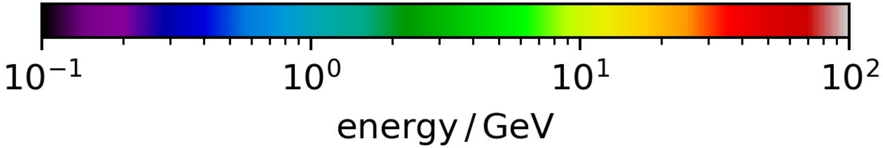

Direction of primary to get Cherenkov-light from zenith.

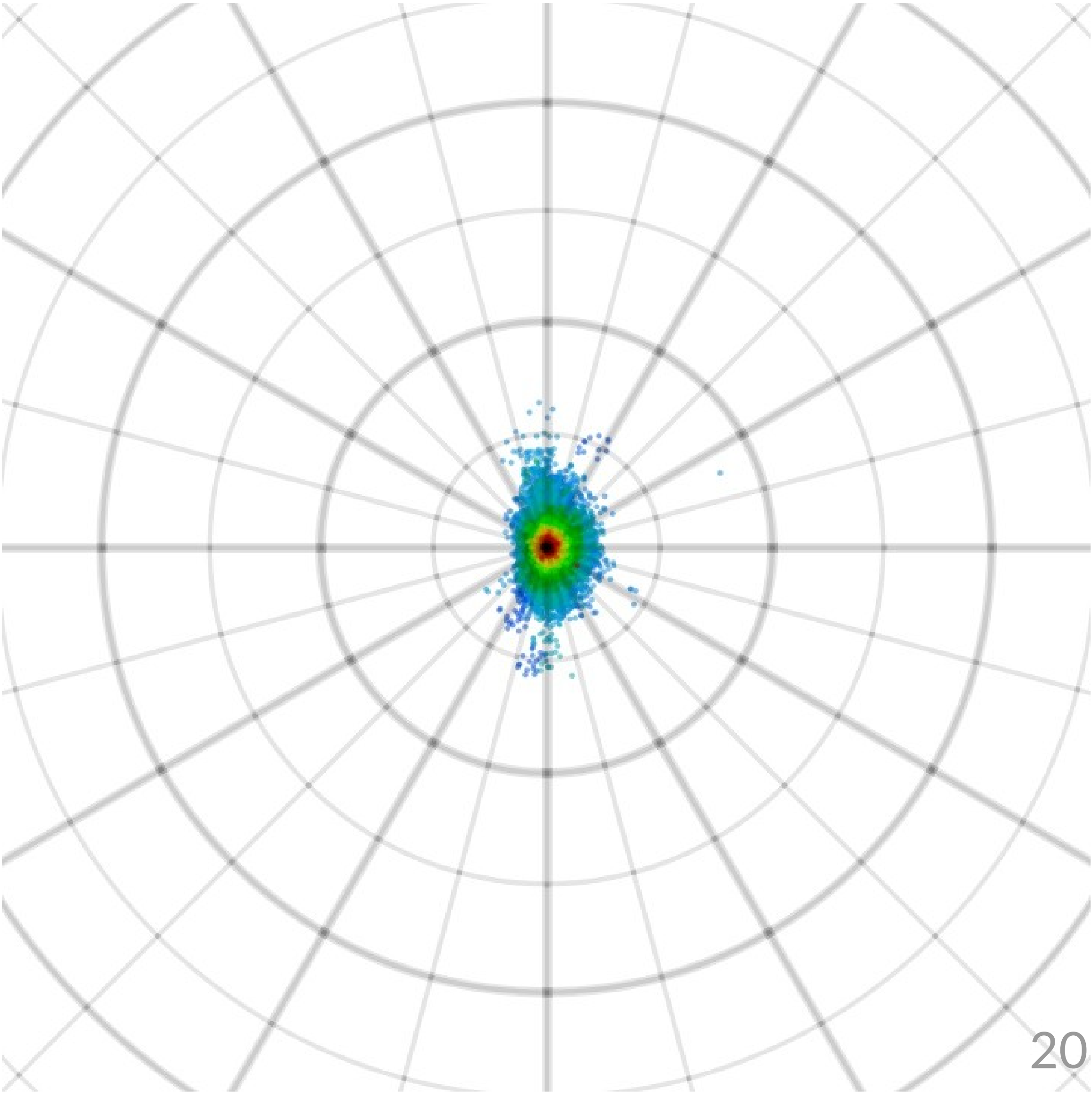

Deflection of shower

Gamma-ray

Gamsberg, Namibia

horizontal: 12.5uT
vertical: -25.9uT
2300m a.s.l.

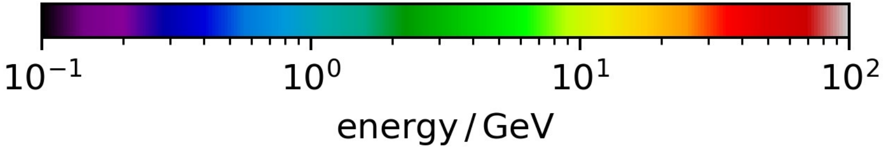

Direction of primary to get Cherenkov-light from zenith.

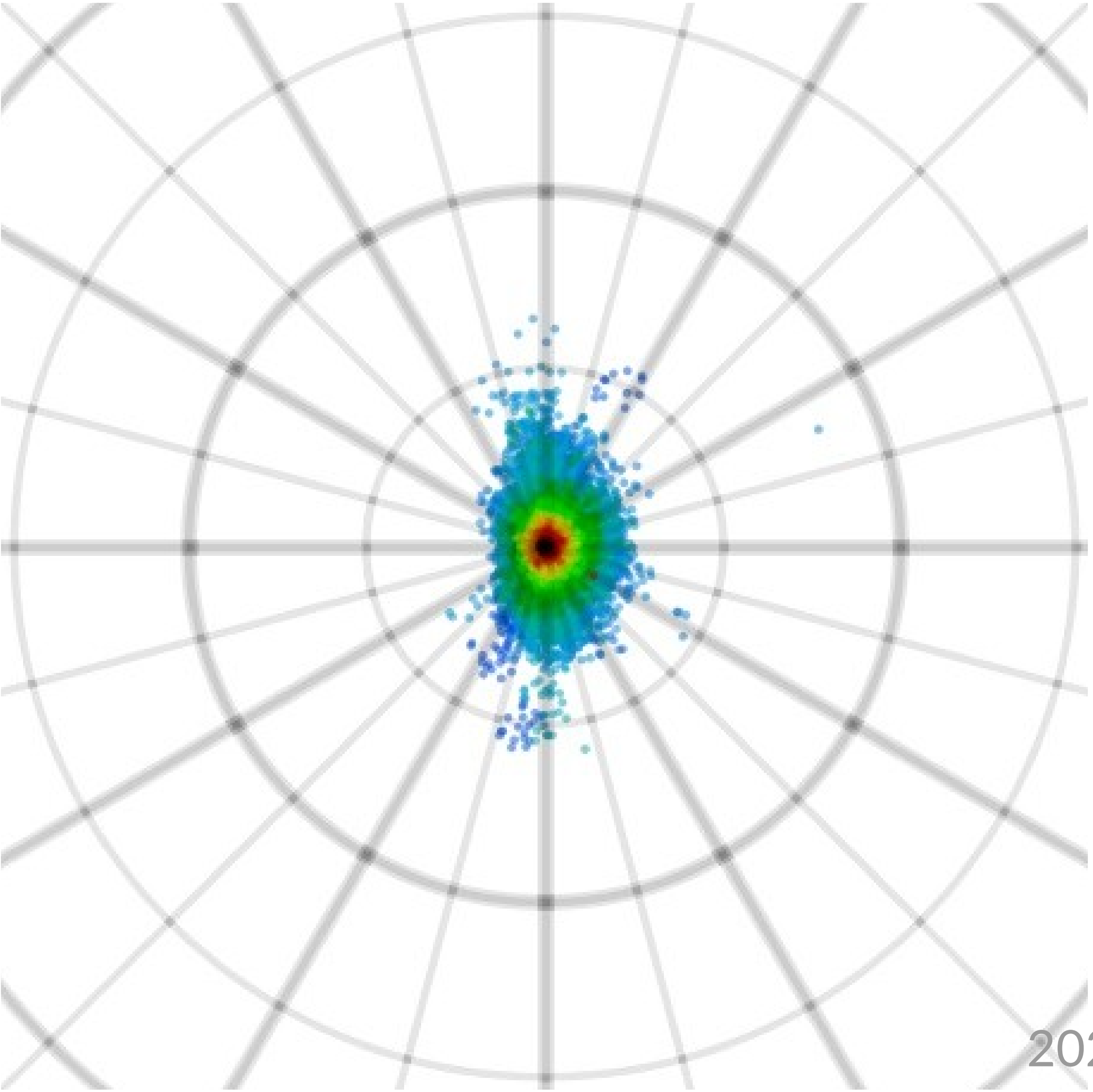

Deflection of shower

Gamma-ray

Gamsberg, Namibia

horizontal: 12.5uT
vertical: -25.9uT
2300m a.s.l.

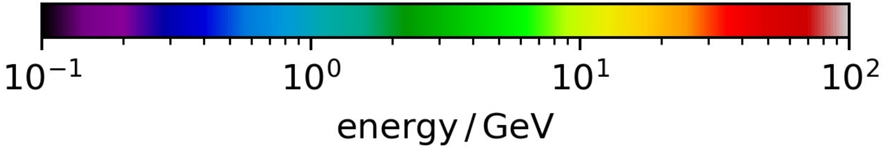

Direction of primary to get Cherenkov-light from zenith.

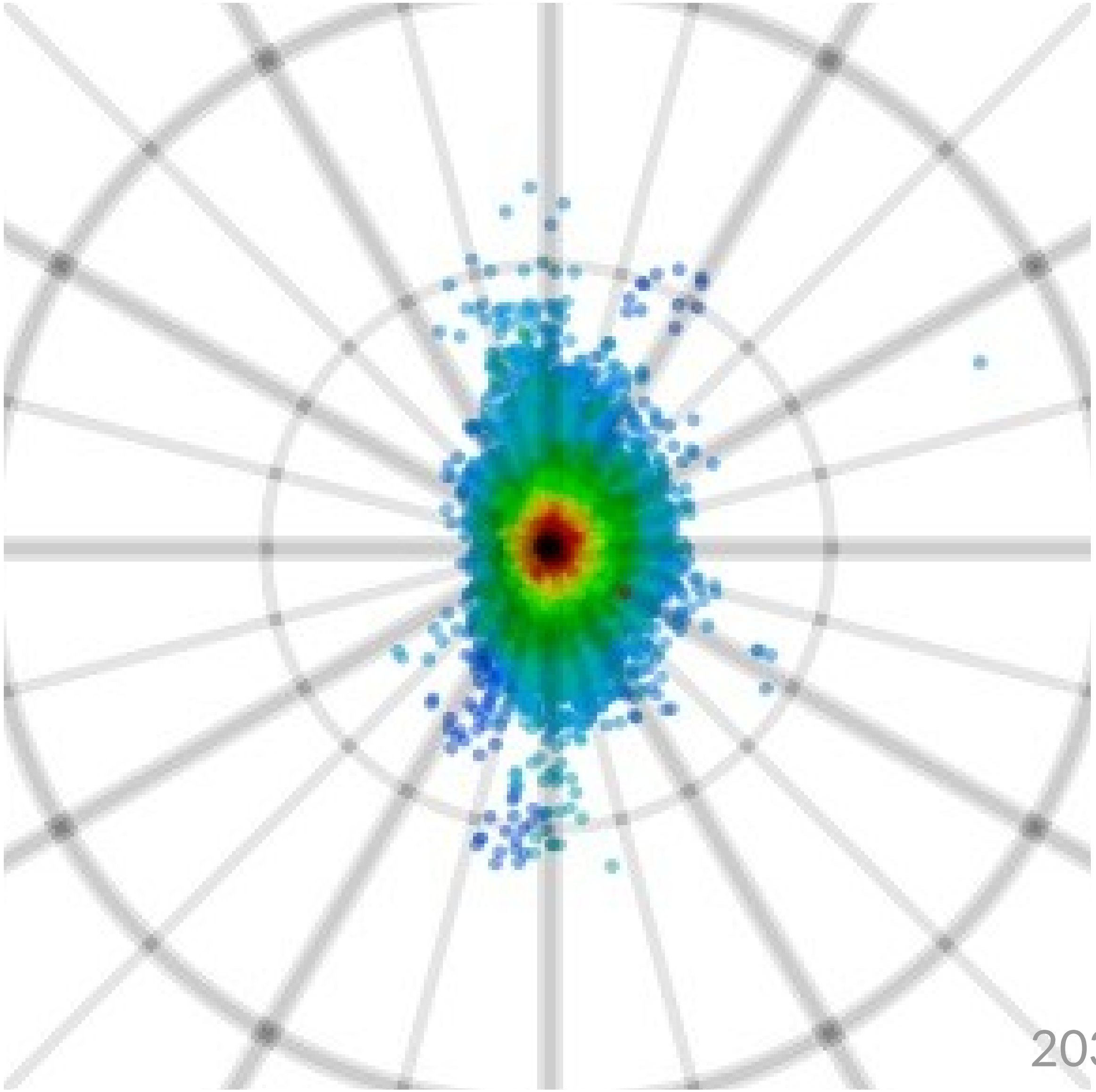

Deflection of shower

Gamma-ray

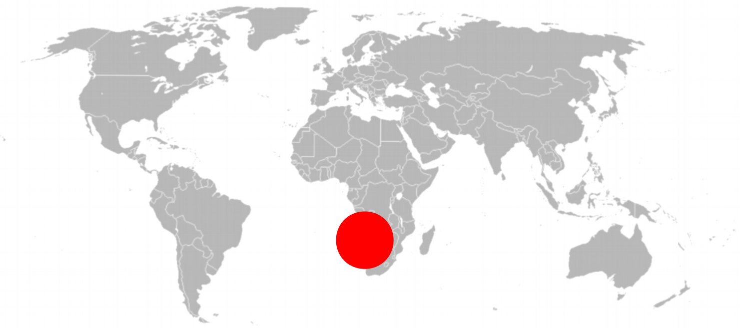

Gamsberg, Namibia

horizontal: 12.5uT
vertical: -25.9uT
2300m a.s.l.

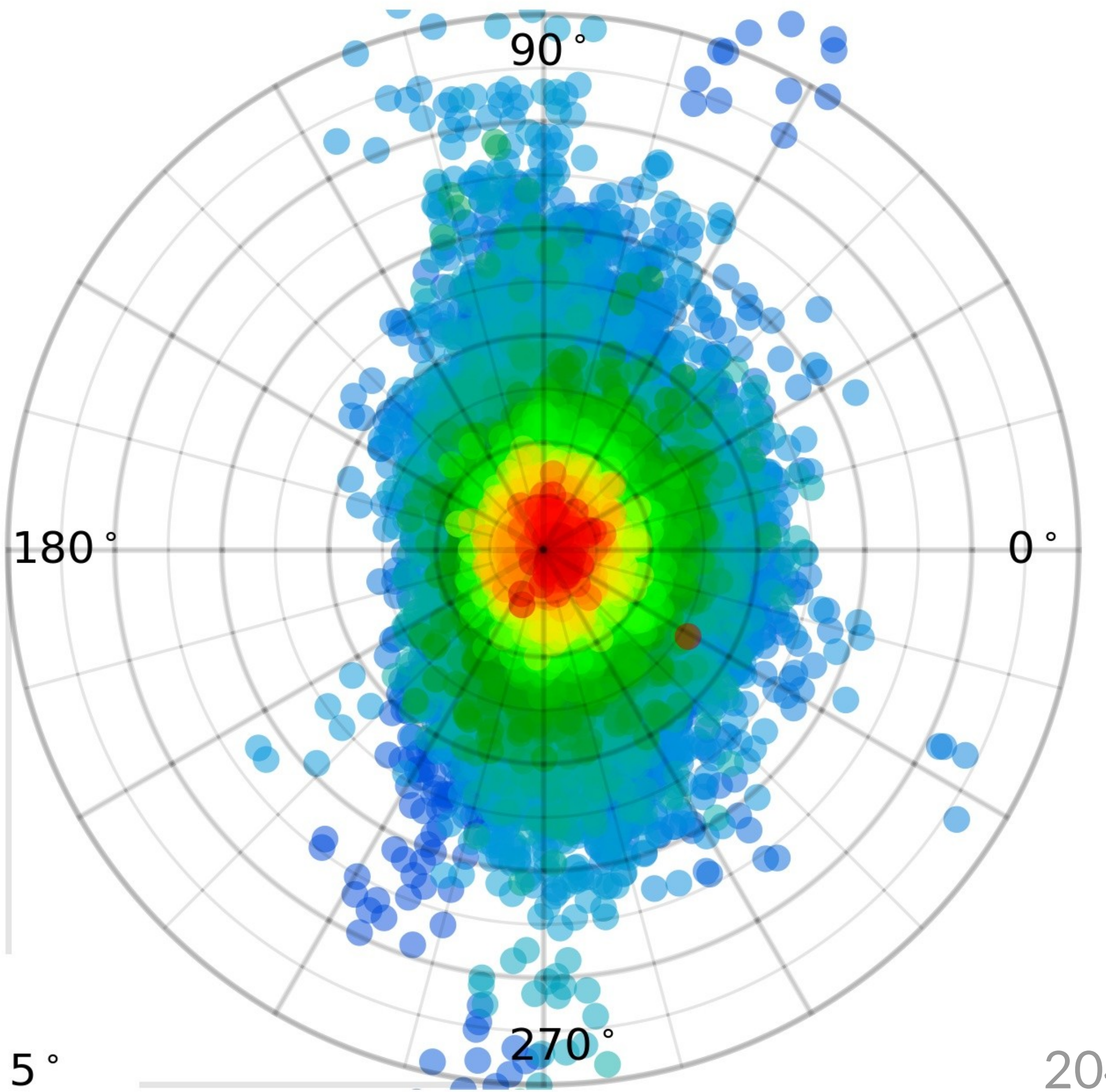

Direction of primary to get Cherenkov-light from zenith.

Deflection of shower

Gamma-ray

Chajnantor, Chile

horizontal: 20.8uT
vertical: -11.4uT
5000m a.s.l.

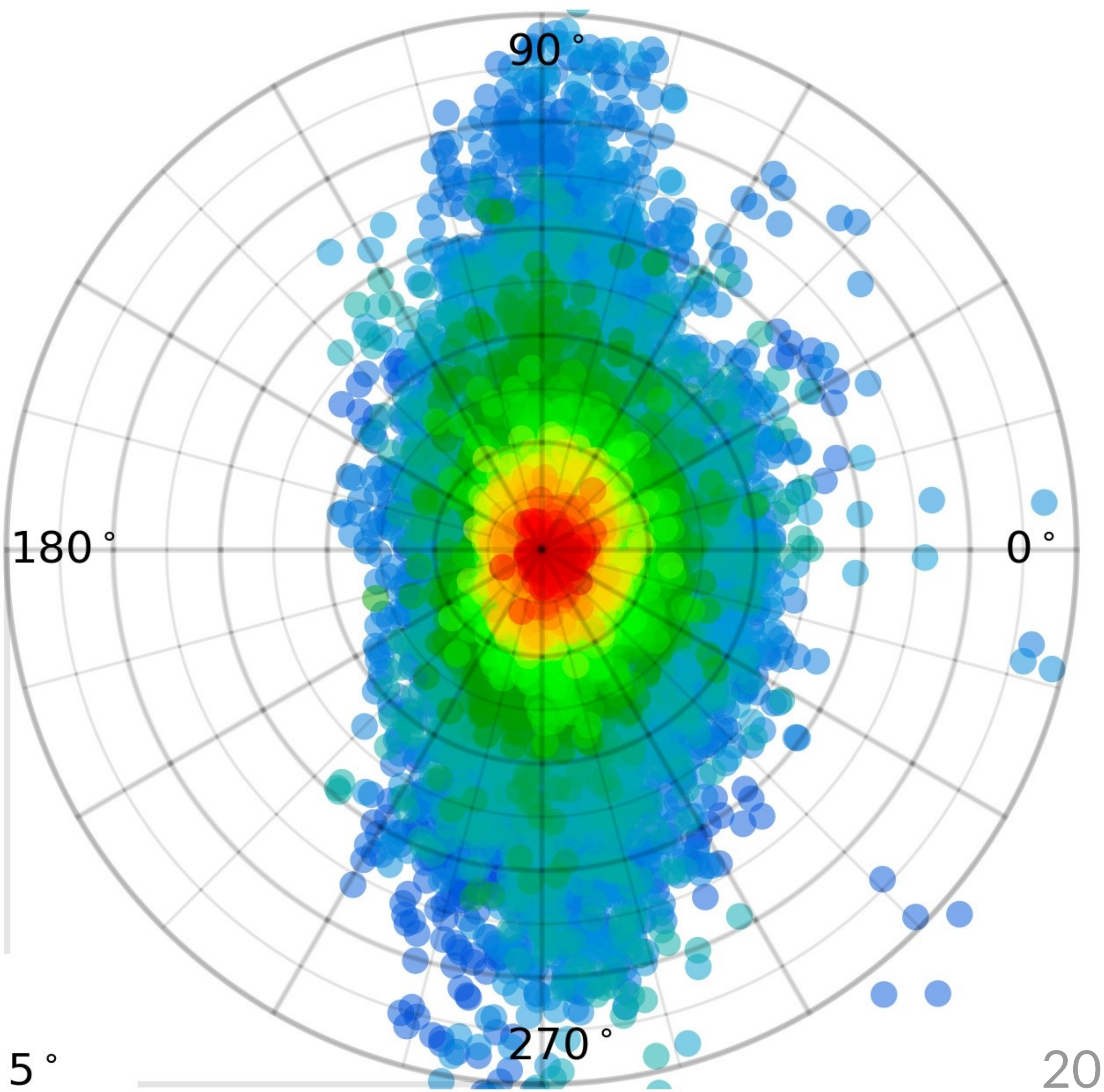

Direction of primary to get Cherenkov-light from zenith.

Deflection of shower

Gamma-ray

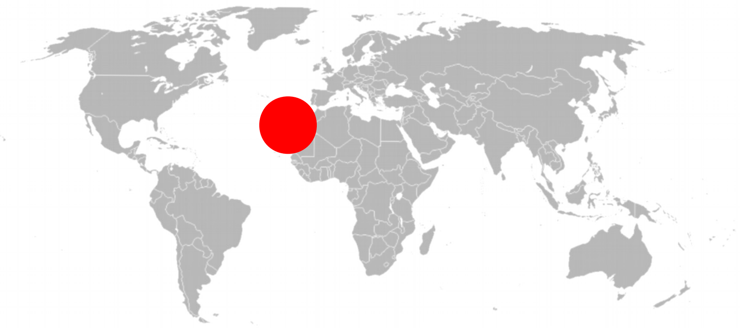

Roque, La Palma
horizontal: 30.4uT
vertical: -23.8uT
2200m a.s.l.

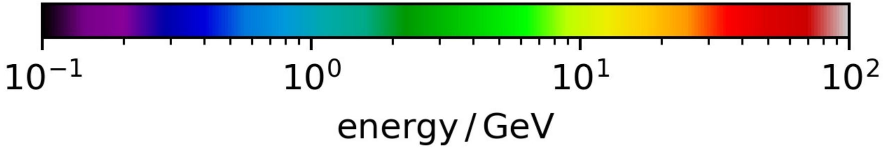

Direction of primary to get
Cherenkov-light from zenith.

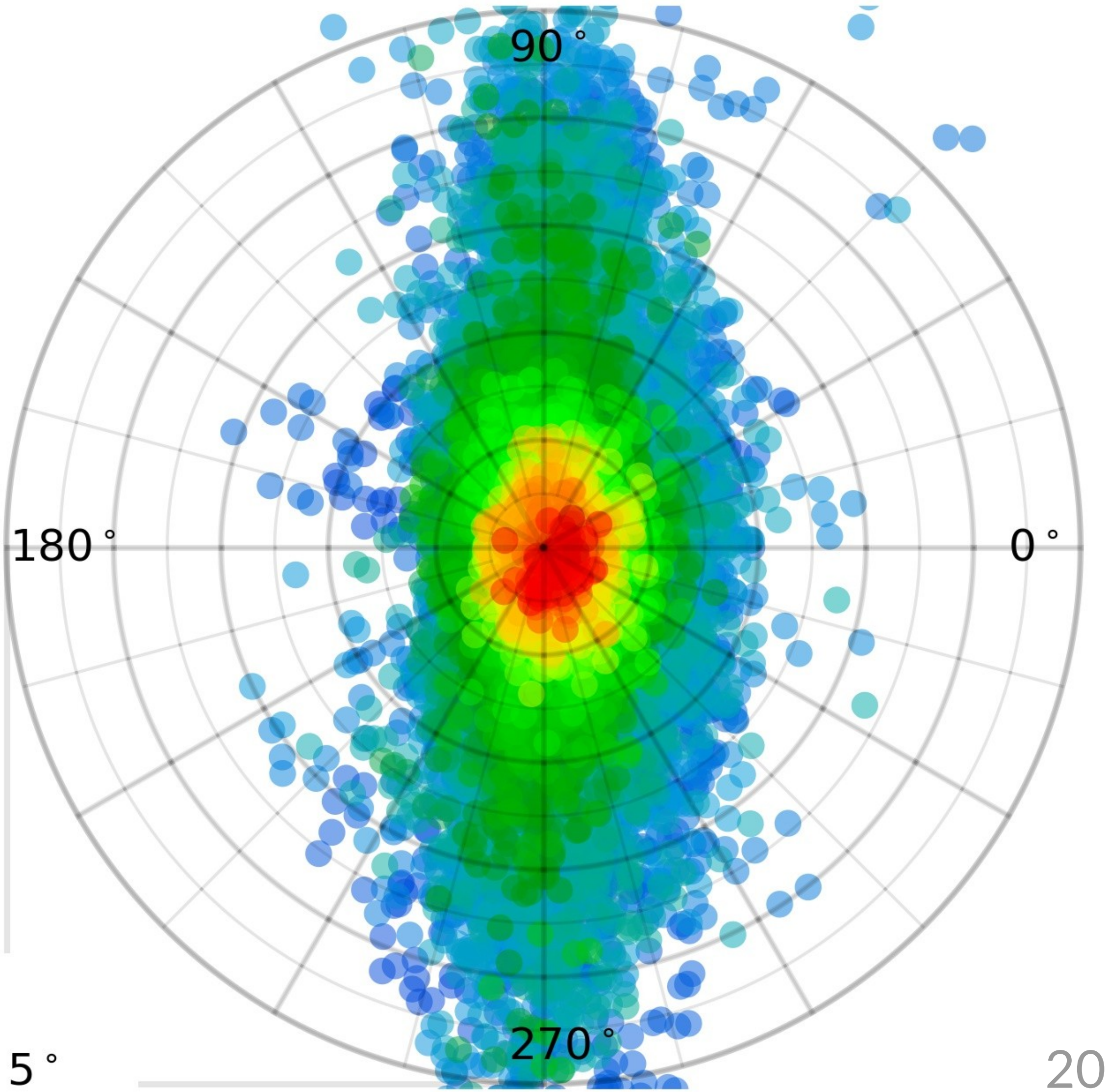

Estimating background from cosmic-rays

Geomagnetic Cutoff

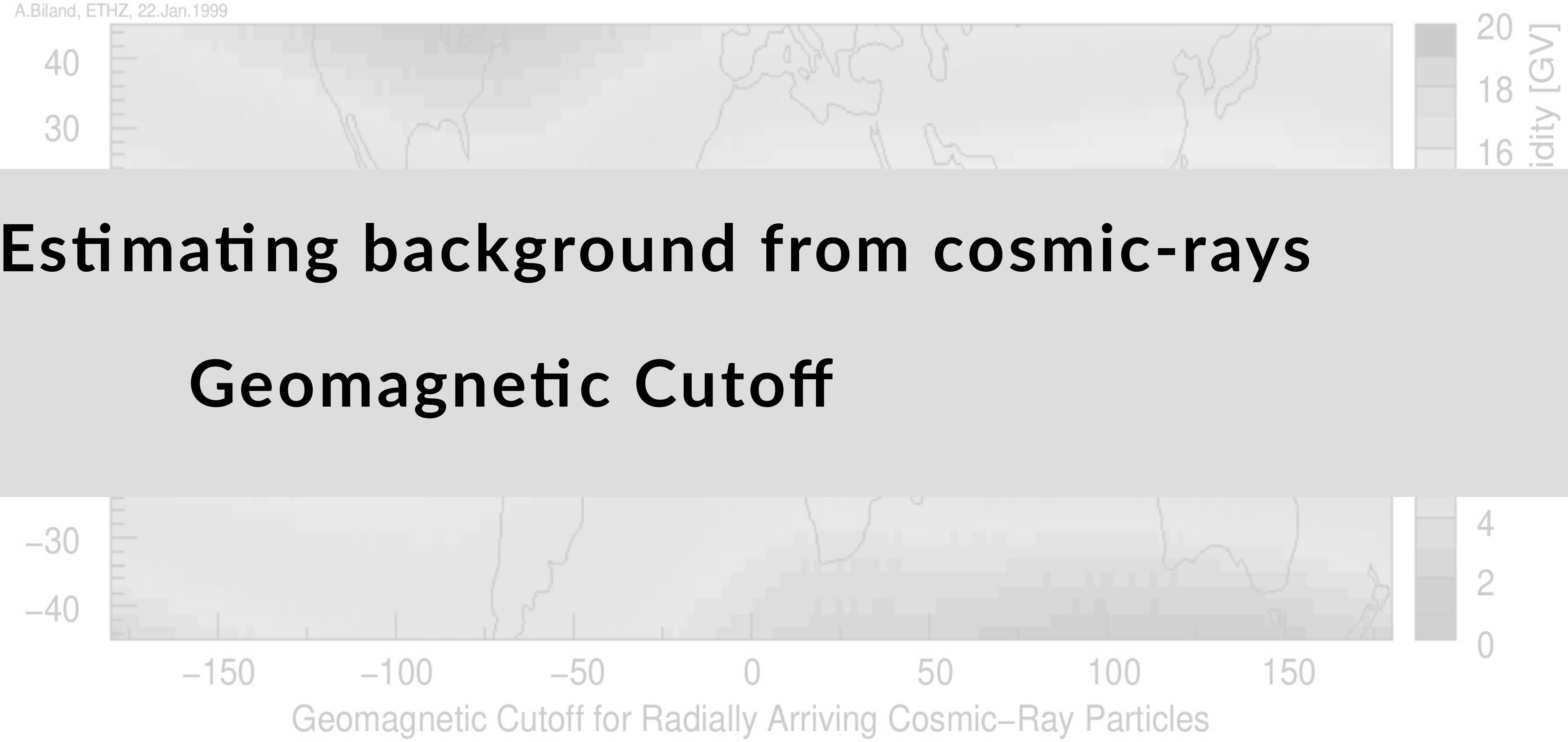

Geomagnetic Cutoff

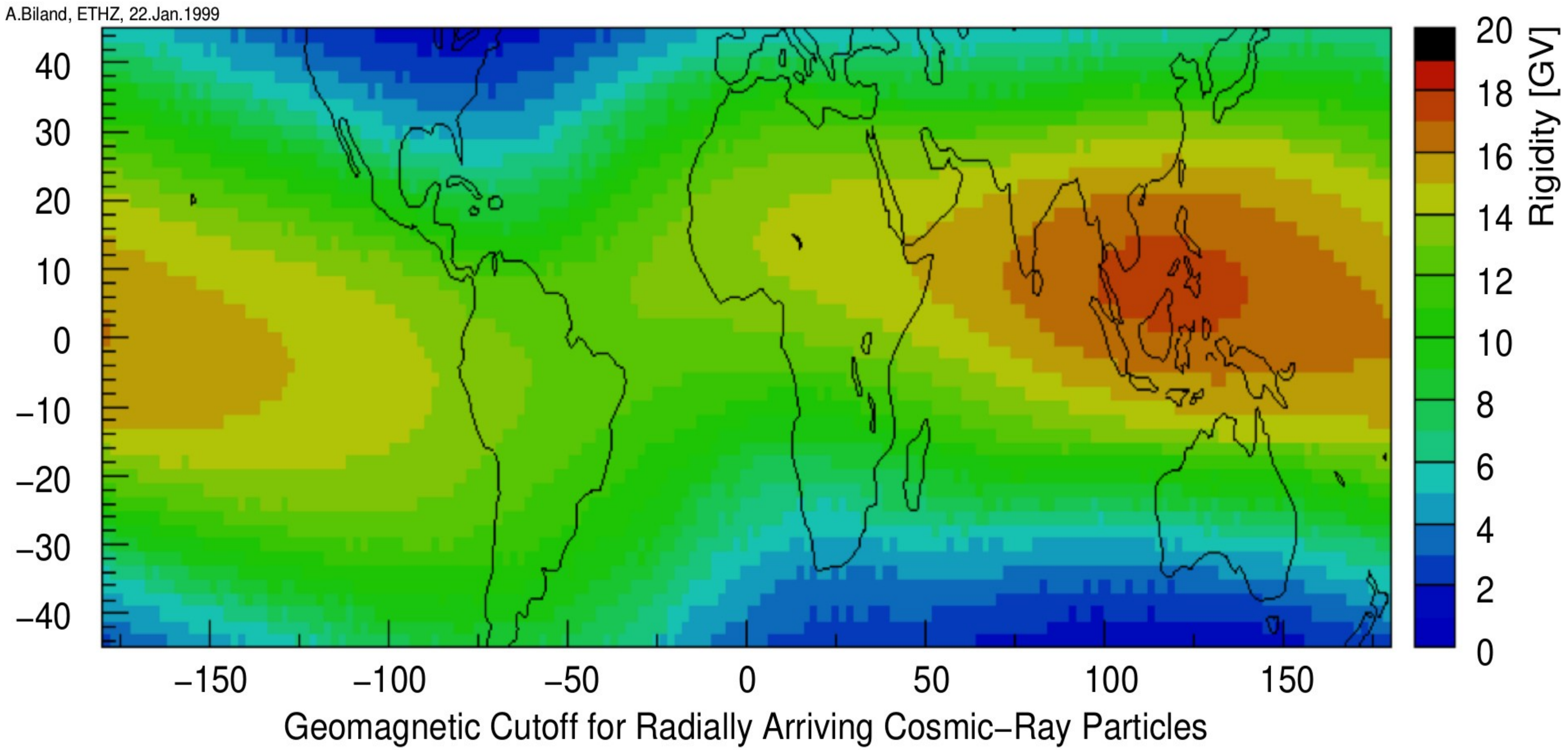

Adrian Biland, ETH Zurich, 1999

Geomagnetic Cutoff

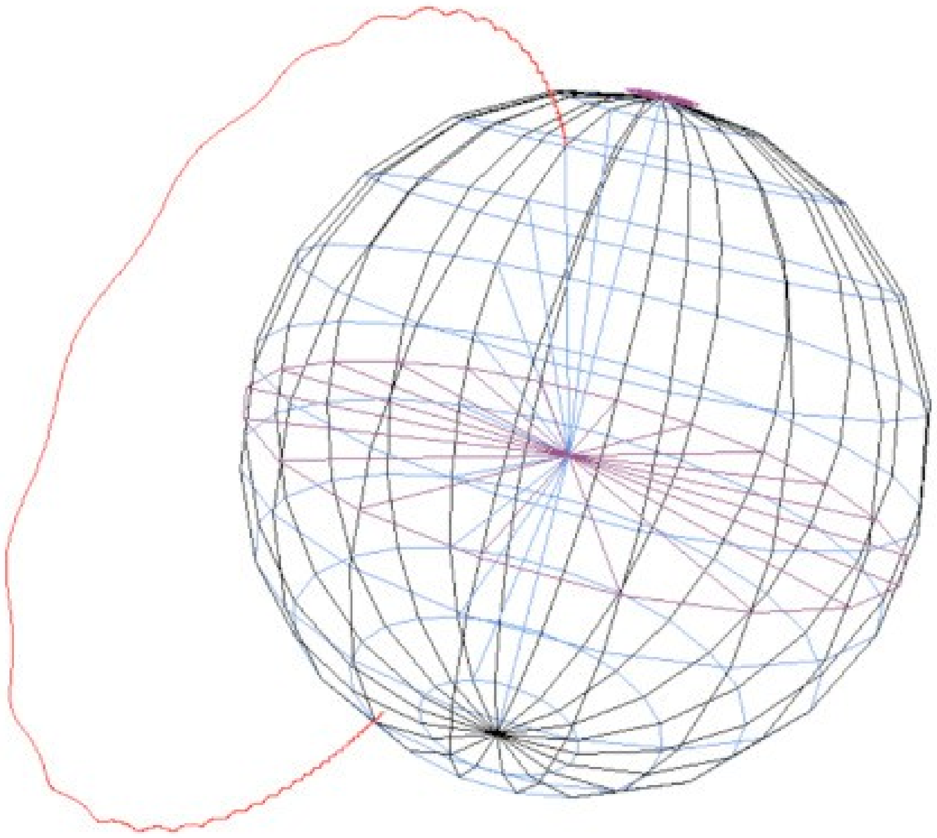

no-bounce

Geomagnetic Cutoff

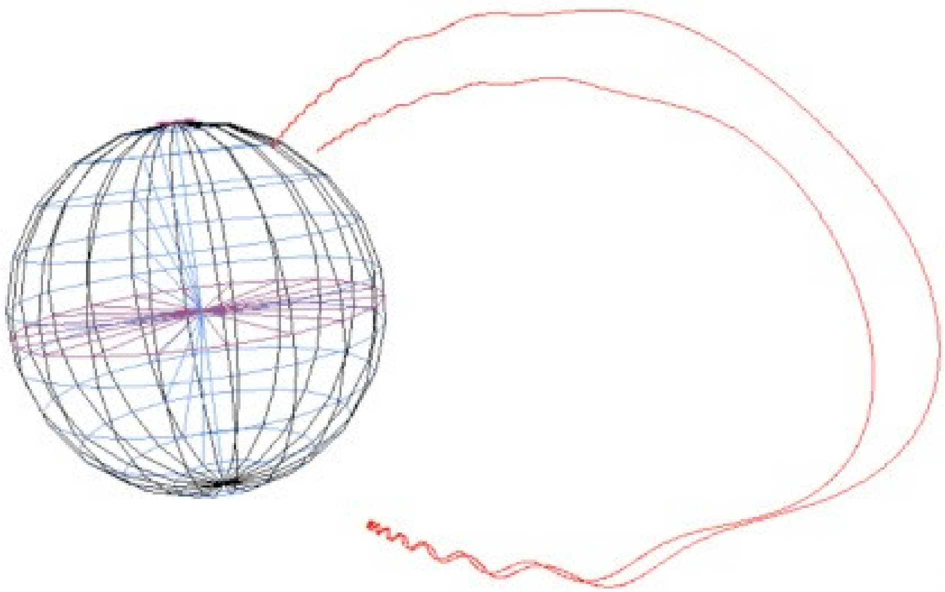

one-bounce

Geomagnetic Cutoff

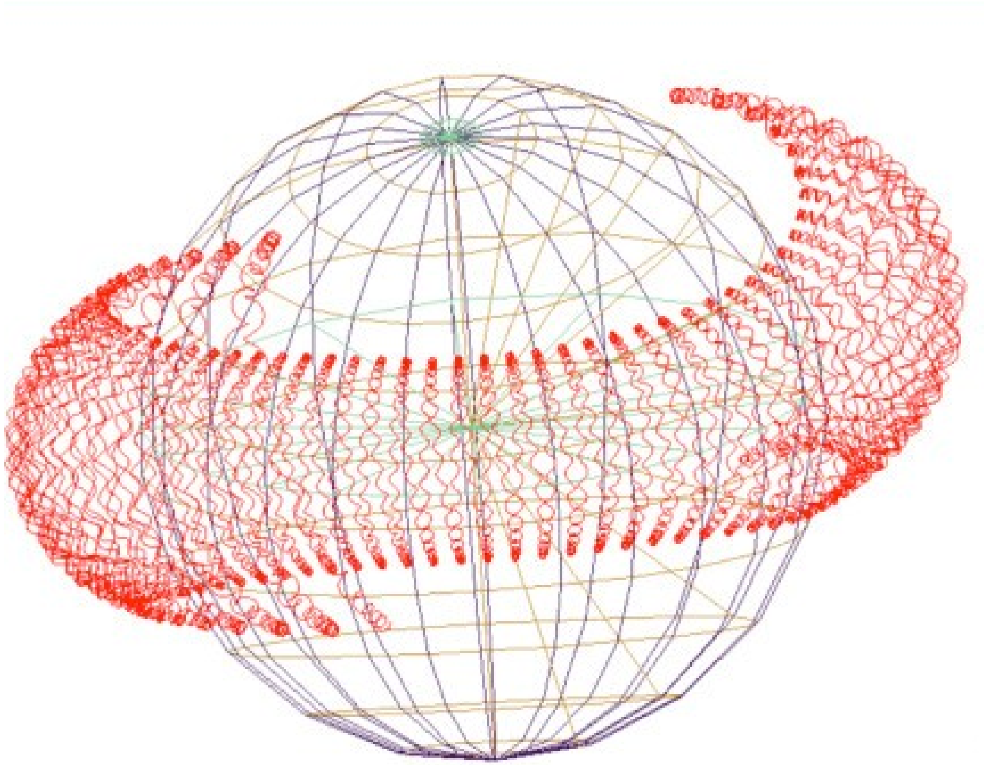

multi-bounce

Background from Airshowers

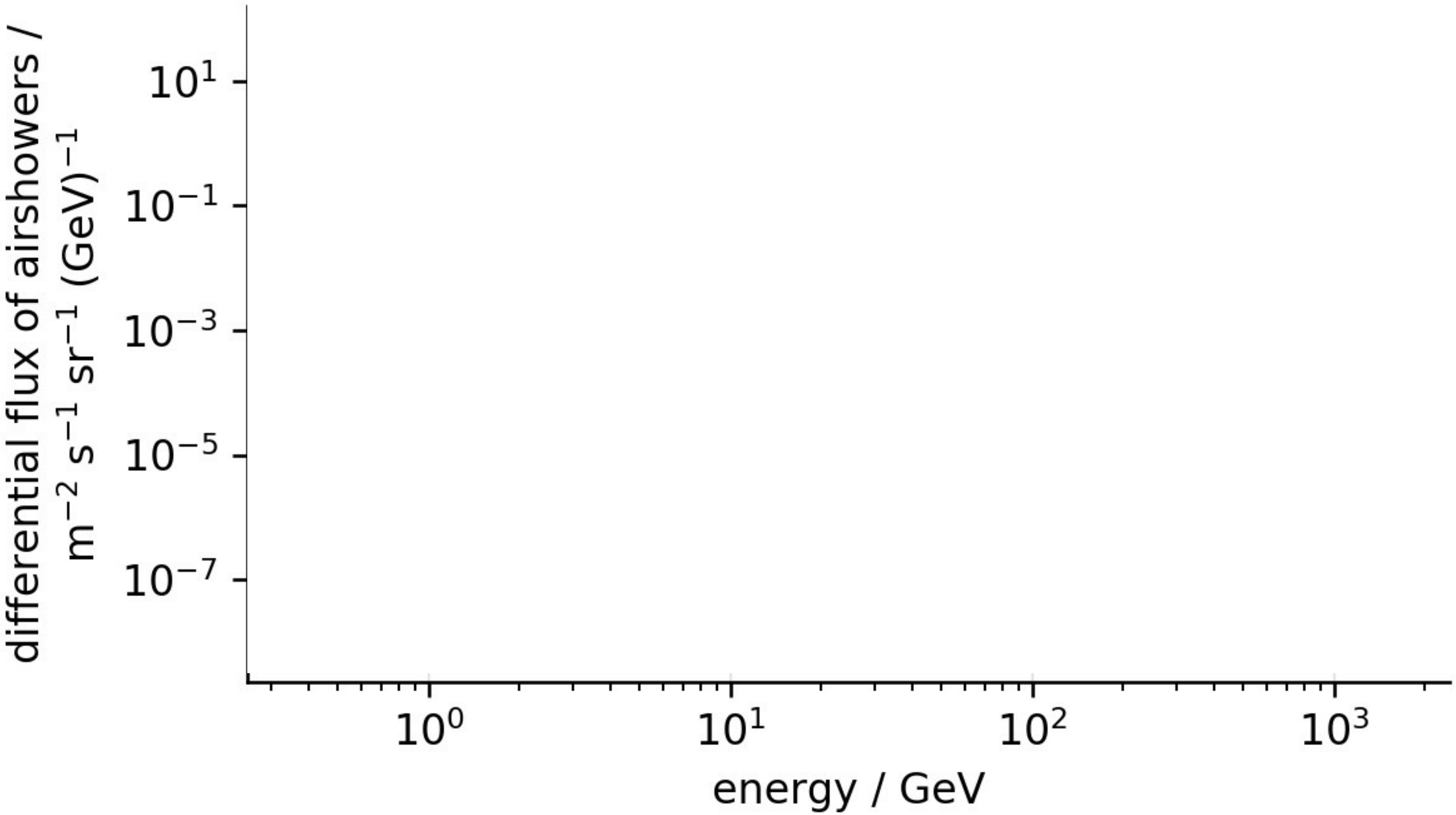

Background from Airshowers

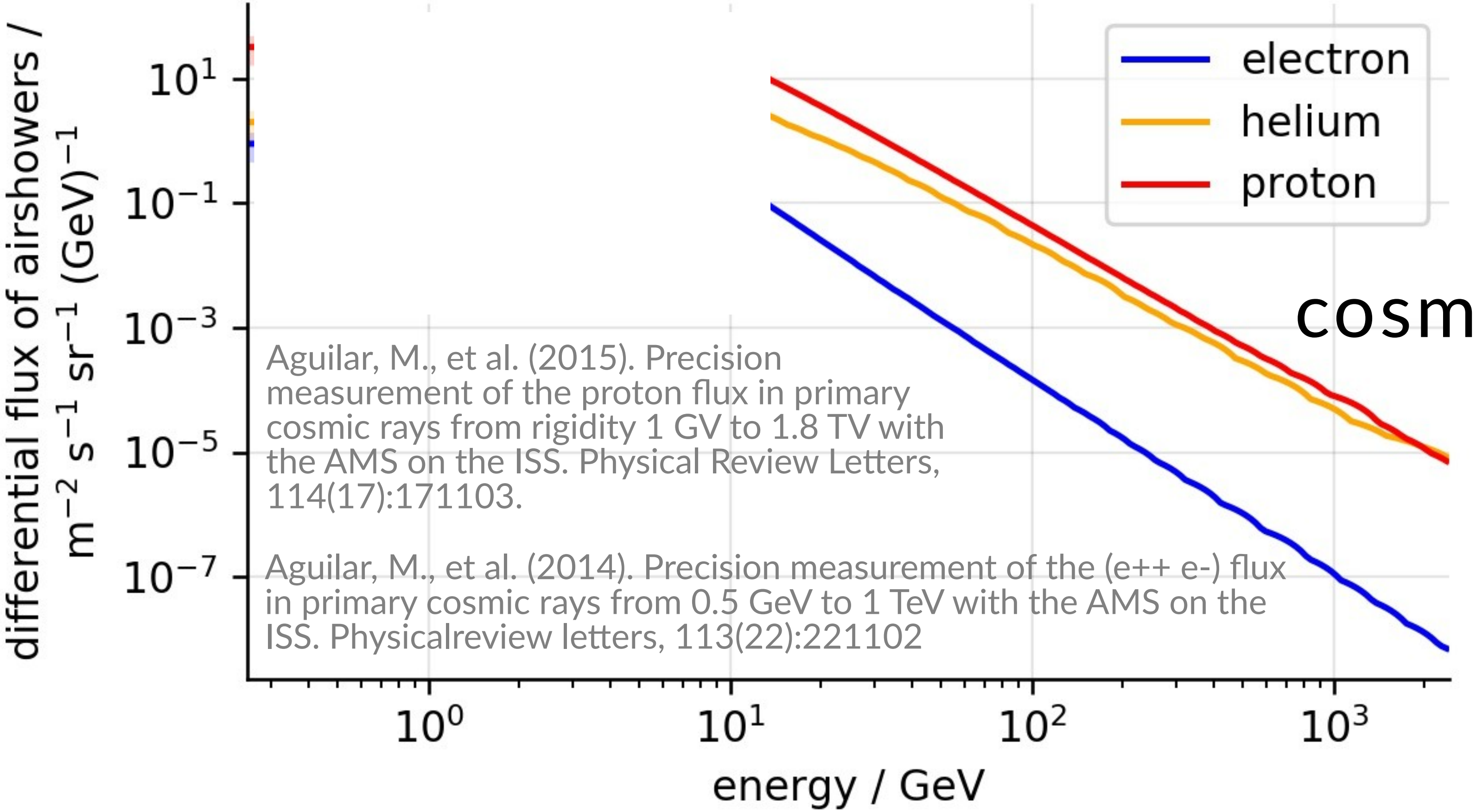

cosmic

Aguilar, M., et al. (2015). Precision measurement of the proton flux in primary cosmic rays from rigidity 1 GV to 1.8 TV with the AMS on the ISS. Physical Review Letters, 114(17):171103.

Aguilar, M., et al. (2014). Precision measurement of the (e++ e-) flux in primary cosmic rays from 0.5 GeV to 1 TeV with the AMS on the ISS. Physicalreview letters, 113(22):221102

Background from Airshowers

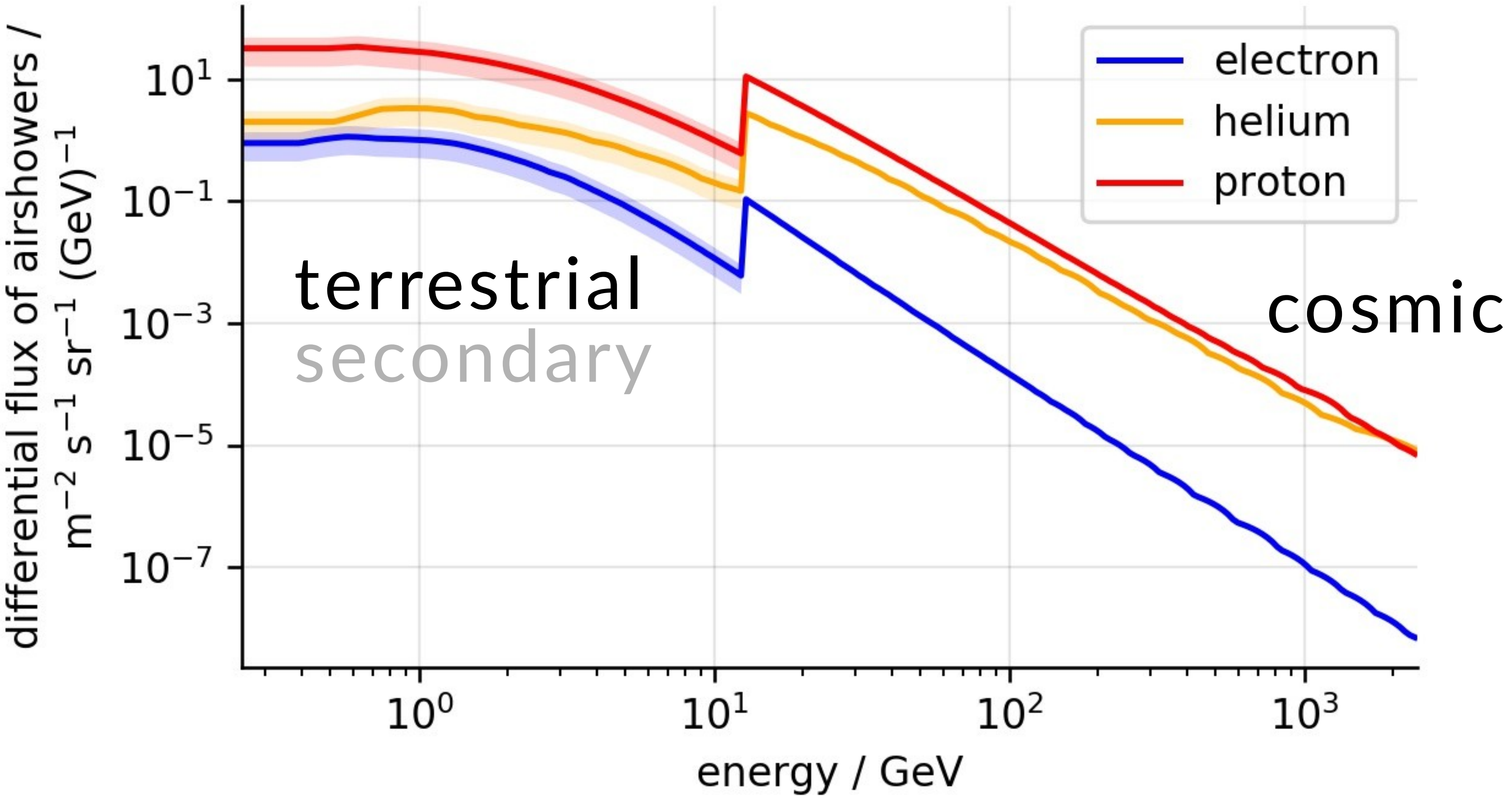

Background from Airshowers

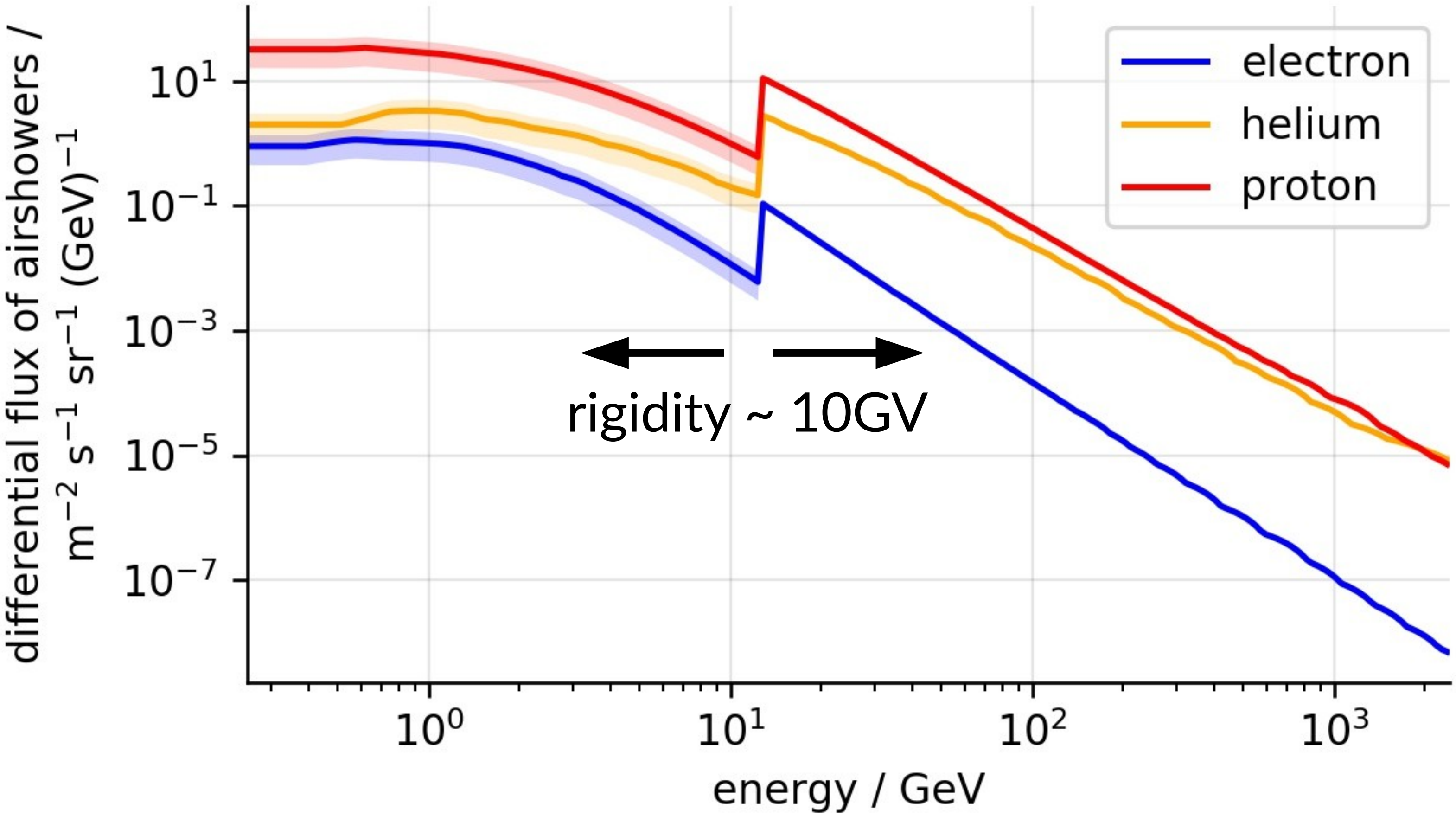

Background from Airshowers

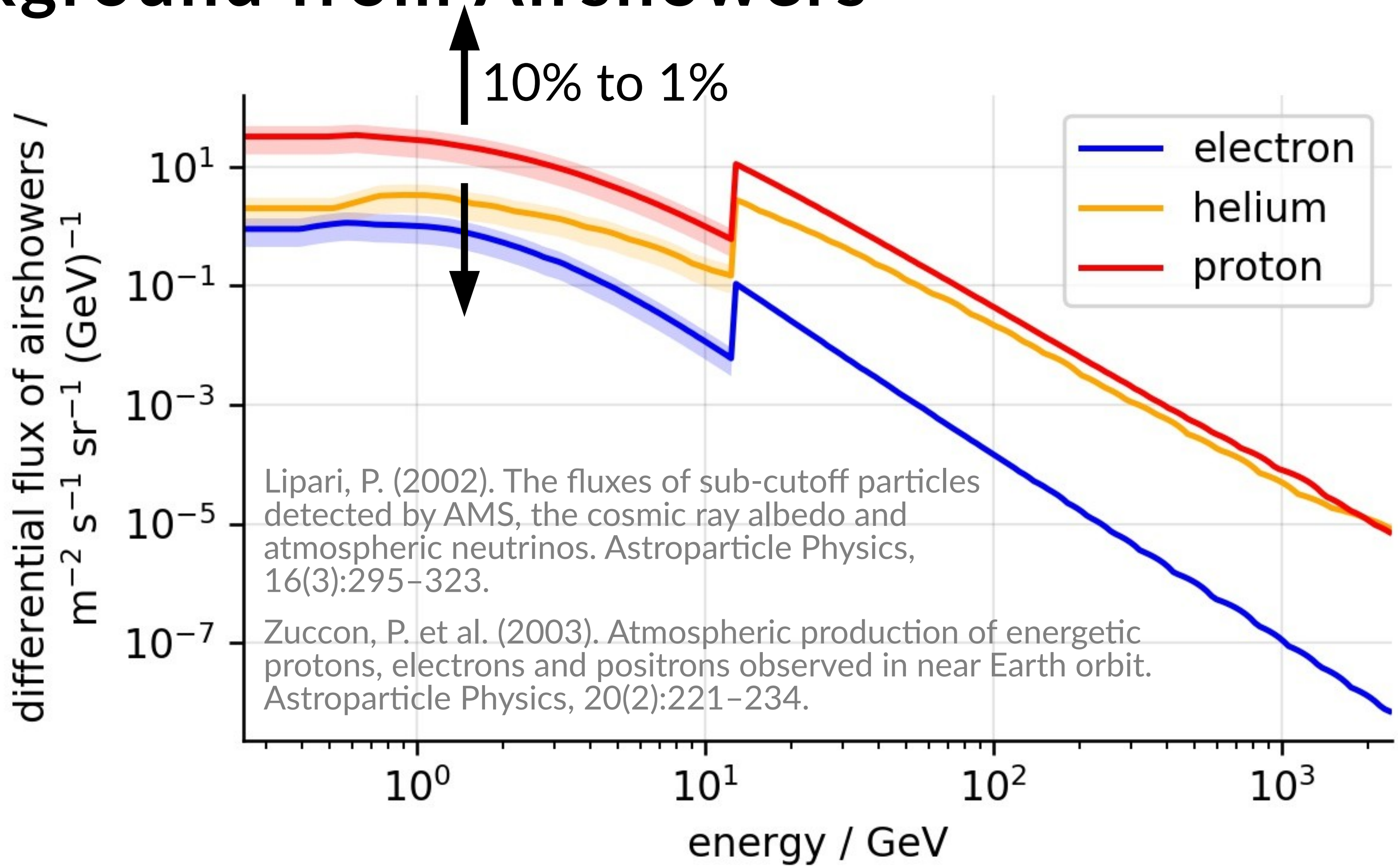

Lipari, P. (2002). The fluxes of sub-cutoff particles detected by AMS, the cosmic ray albedo and atmospheric neutrinos. Astroparticle Physics, 16(3):295–323.

Zuccon, P. et al. (2003). Atmospheric production of energetic protons, electrons and positrons observed in near Earth orbit. Astroparticle Physics, 20(2):221–234.

Performance (so far)

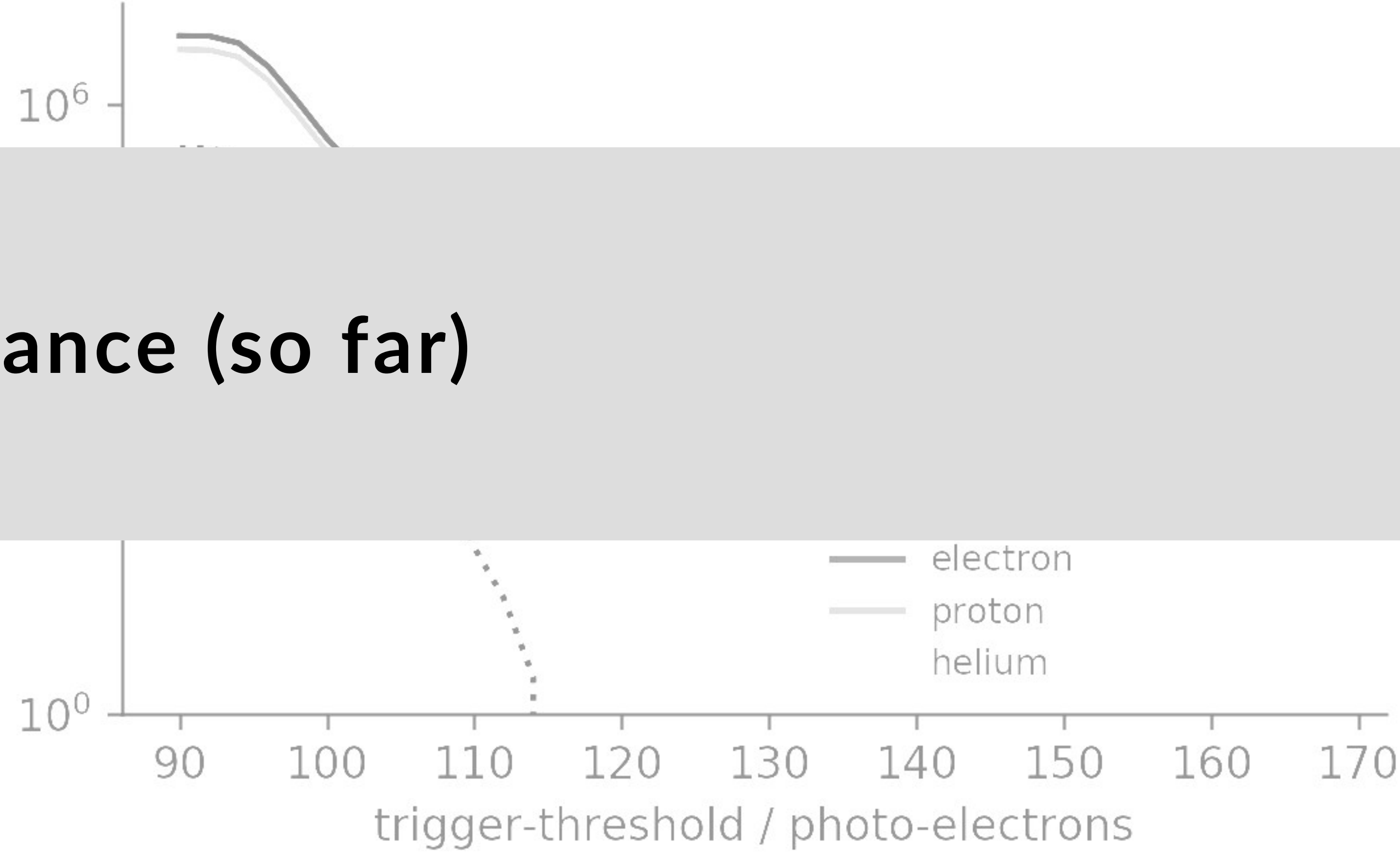

Performance, Rate-Scan

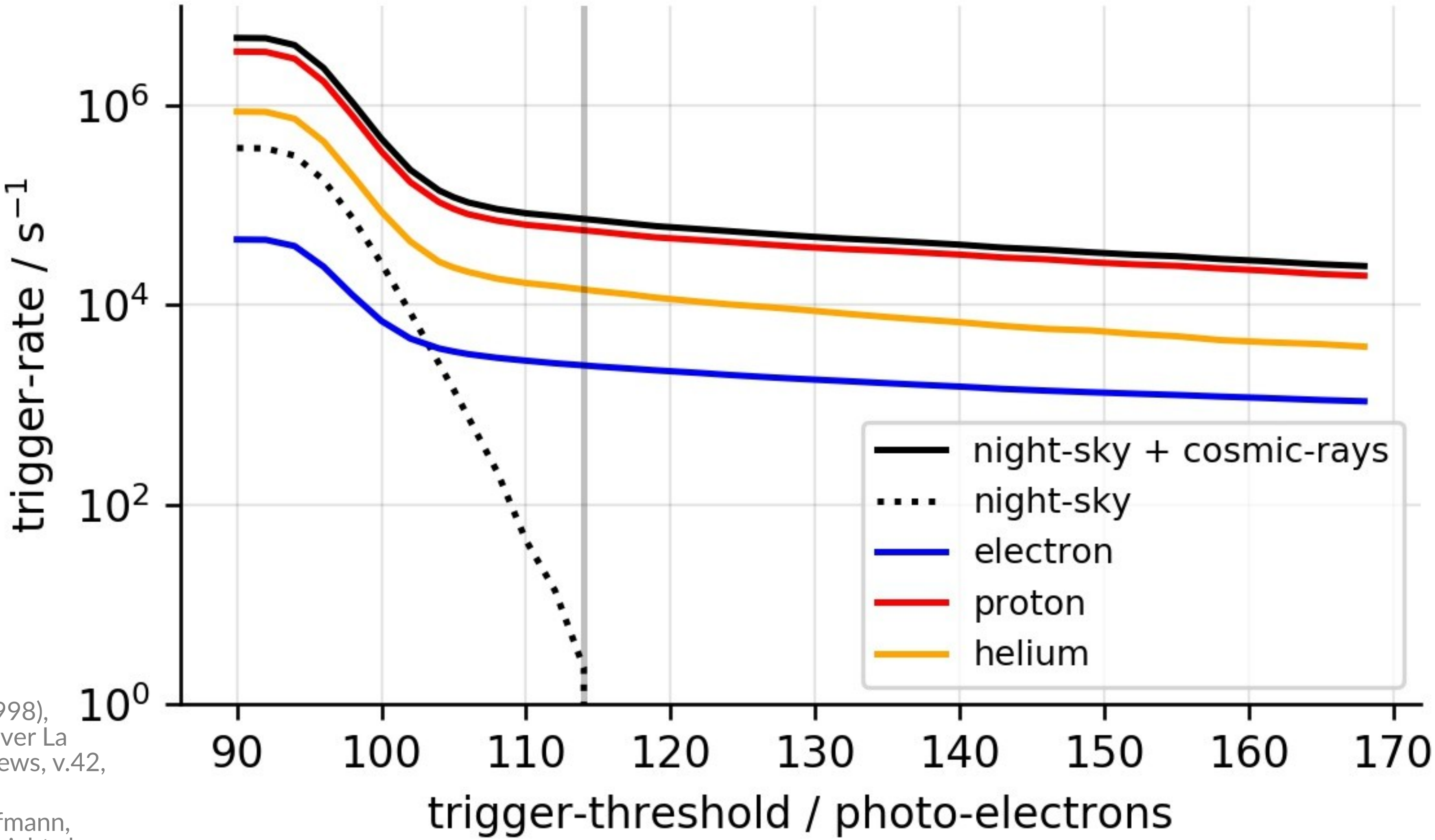

C.R. Benn and S.L .Ellison (1998), Brightness of the night sky over La Palma, New Astronomy Reviews, v.42, n.6-8, p.503-507

S.Preuss, G.Hermann, W.Hofmann, A.Kohnle (2002) Study of ... night sky at La Palma and Namibia..., NIM-A, v.481, p.229-240

Performance, Rates on 3FGL J0534.5+2201

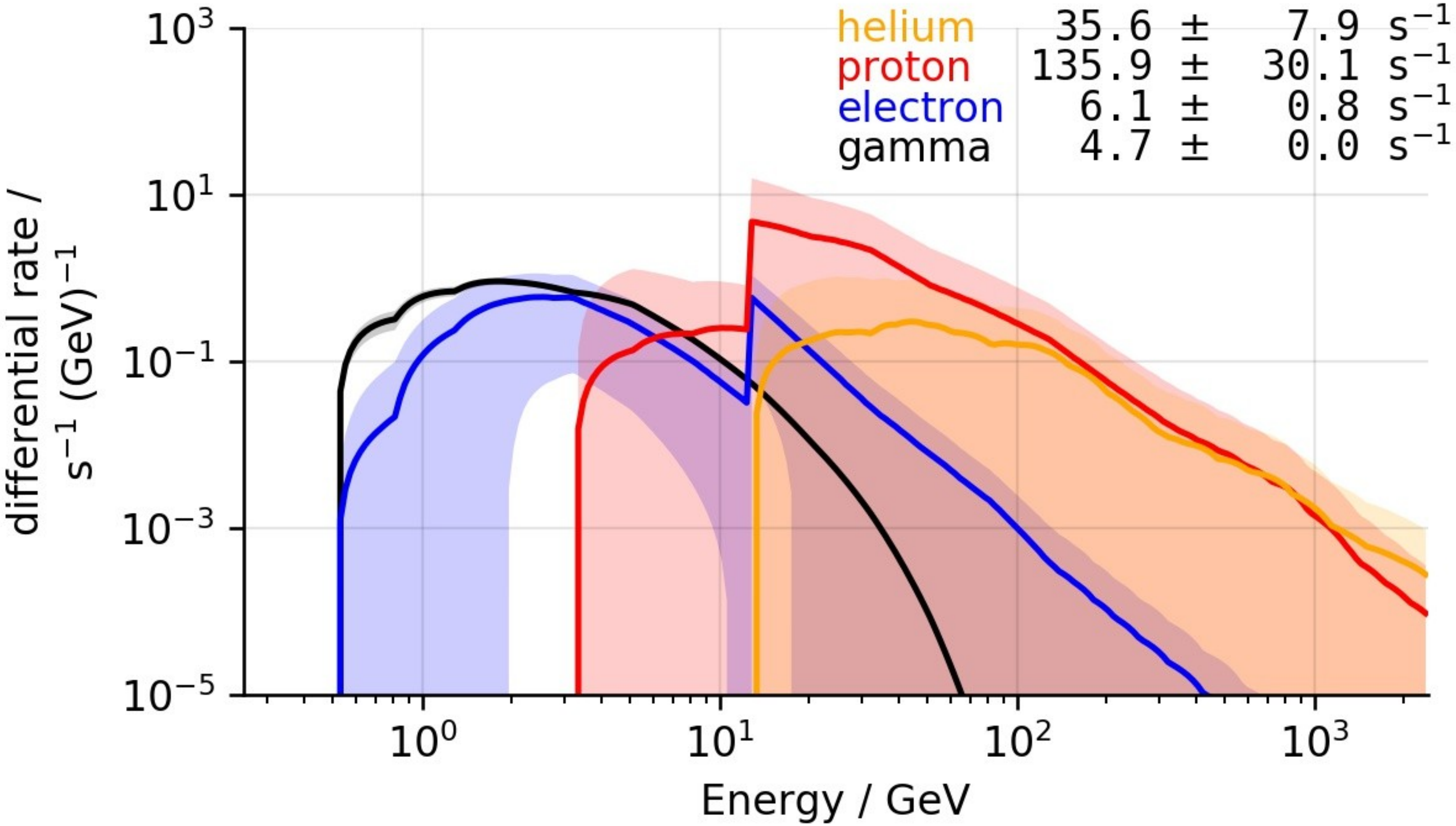

Performance, Gamma-Hadron-Seperation

Not yet.

Performance, Direction

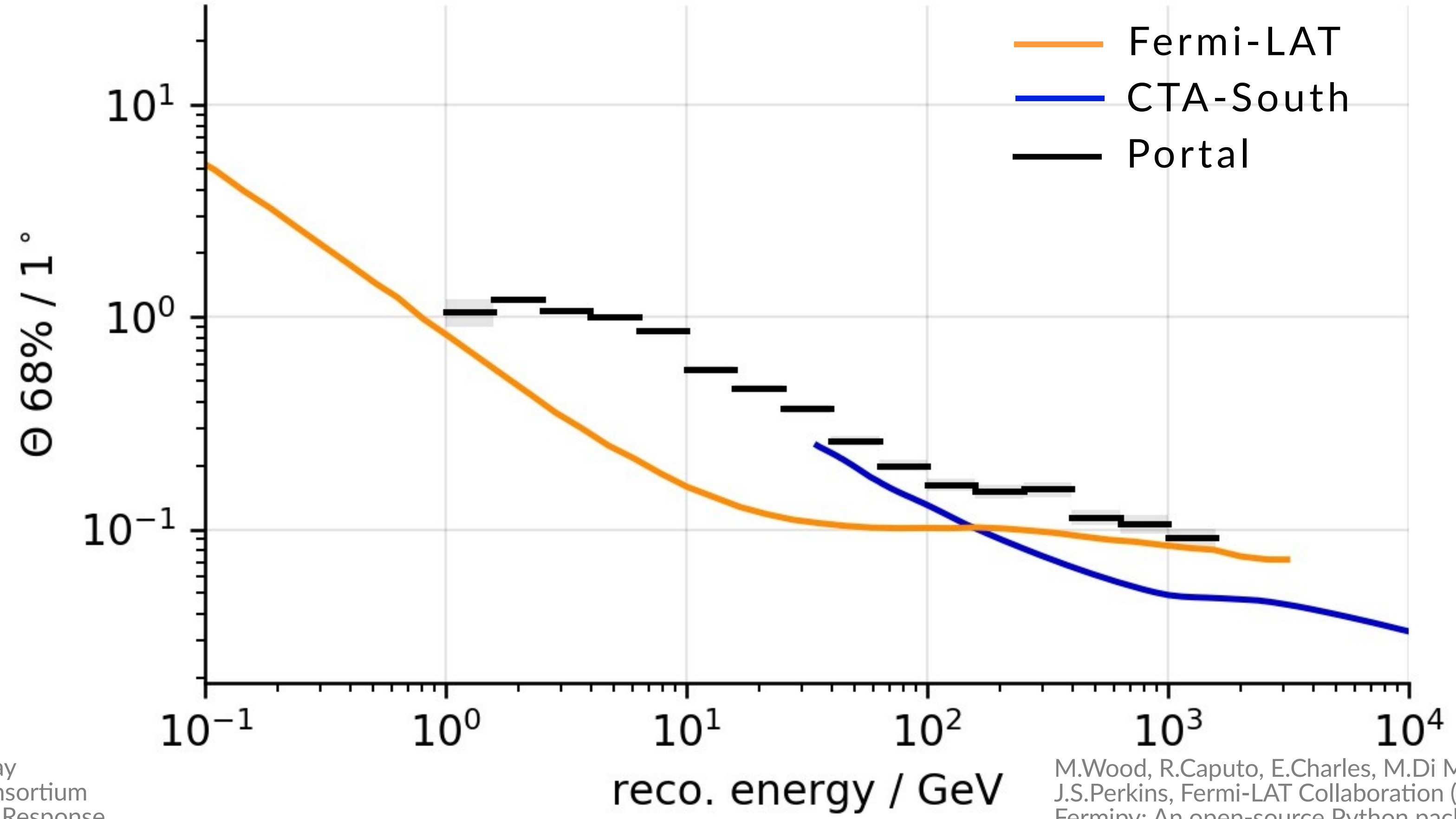

Cherenkov Telescope Array Observatory and CTA Consortium (2021). CTAO Instrument Response Functions - prod5 version v0.1, doi:10.5281/zenodo.5499840

M.Wood, R.Caputo, E.Charles, M.Di Mauro, J.Magill, J.S.Perkins, Fermi-LAT Collaboration (2017), Fermipy: An open-source Python package for analysis of Fermi-LAT Data, Proc. 35th ICRC, PoS(ICRC2017)824, IRF: P8R2_SOURCE_V6

Performance, Energy

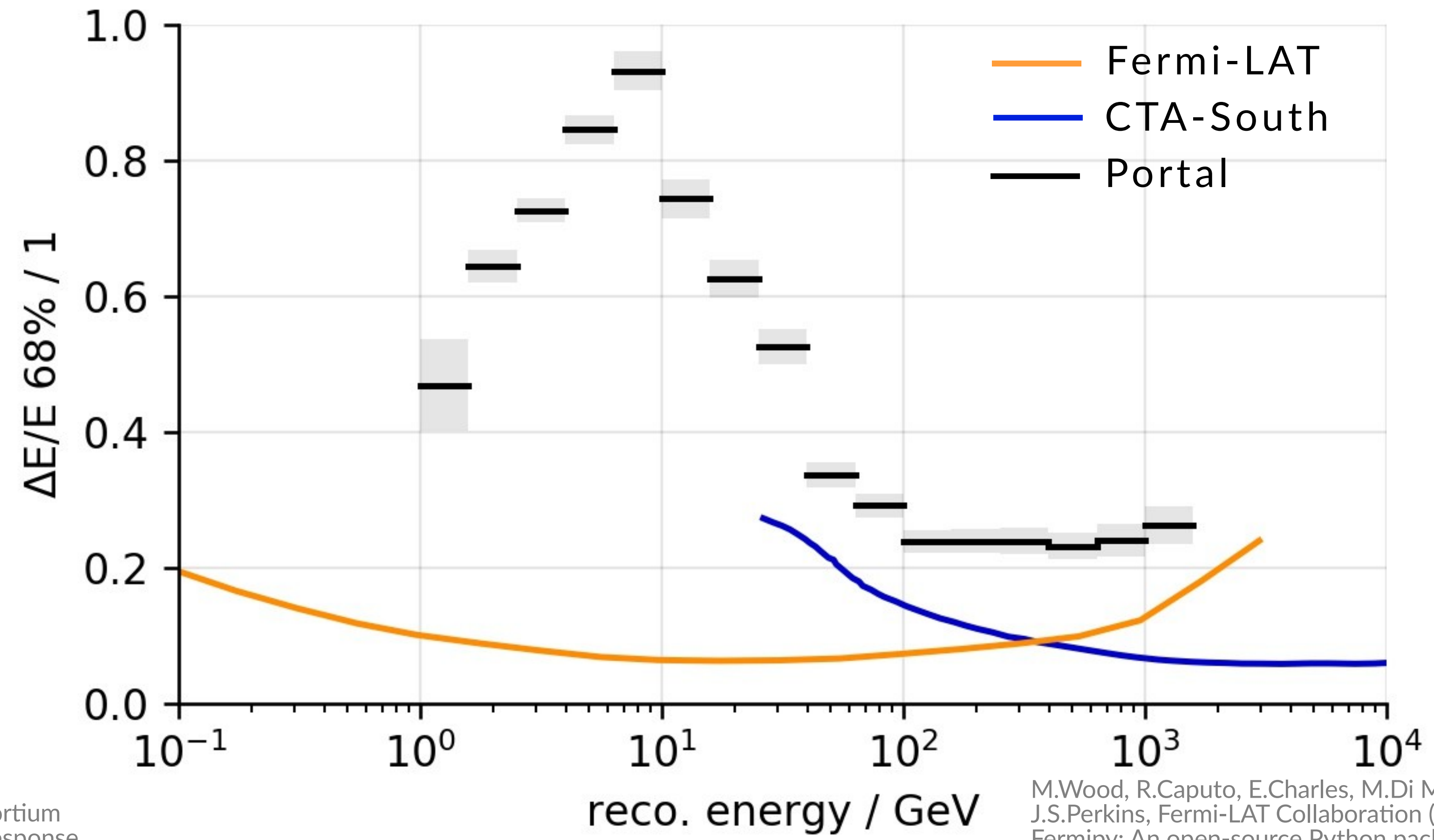

Cherenkov Telescope Array Observatory and CTA Consortium (2021). CTAO Instrument Response Functions - prod5 version v0.1, doi:10.5281/zenodo.5499840

M.Wood, R.Caputo, E.Charles, M.Di Mauro, J.Magill, J.S.Perkins, Fermi-LAT Collaboration (2017), Fermipy: An open-source Python package for analysis of Fermi-LAT Data, Proc. 35th ICRC, PoS(ICRC2017)824, IRF: P8R2_SOURCE_V6

Performance, Sensitivity vs. Energy at 3min

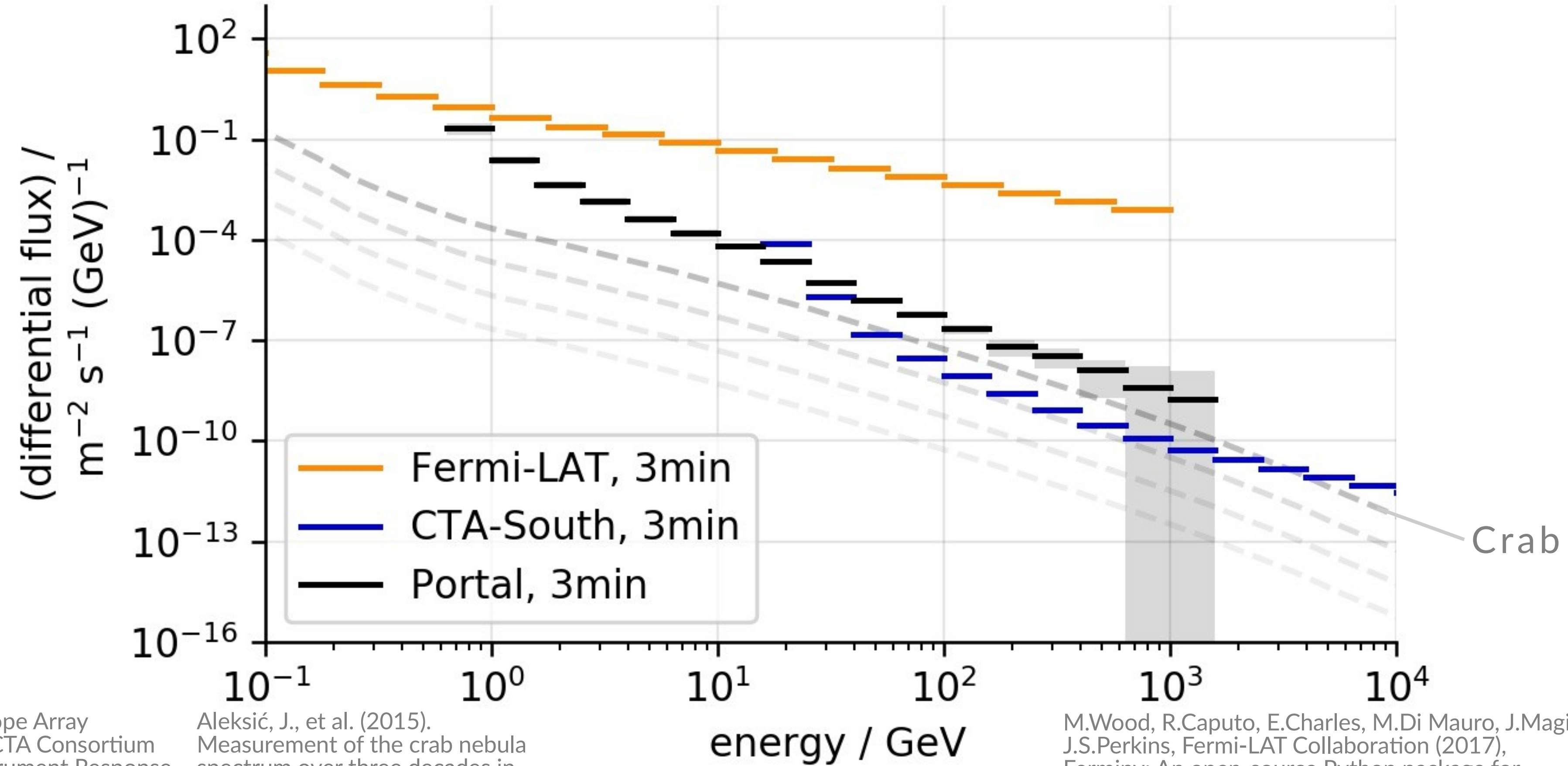

Cherenkov Telescope Array Observatory and CTA Consortium (2021). CTAO Instrument Response Functions - prod5 version v0.1, doi:10.5281/zenodo.5499840

Aleksić, J., et al. (2015). Measurement of the crab nebula spectrum over three decades in energy with the magic telescopes. High Energy Astrophysics, 5:30–38.

M.Wood, R.Caputo, E.Charles, M.Di Mauro, J.Magill, J.S.Perkins, Fermi-LAT Collaboration (2017), Fermipy: An open-source Python package for analysis of Fermi-LAT Data, Proc. 35th ICRC, PoS(ICRC2017)824, IRF: P8R2_SOURCE_V6

Performance, Sensitivity vs. Time at 2.5GeV

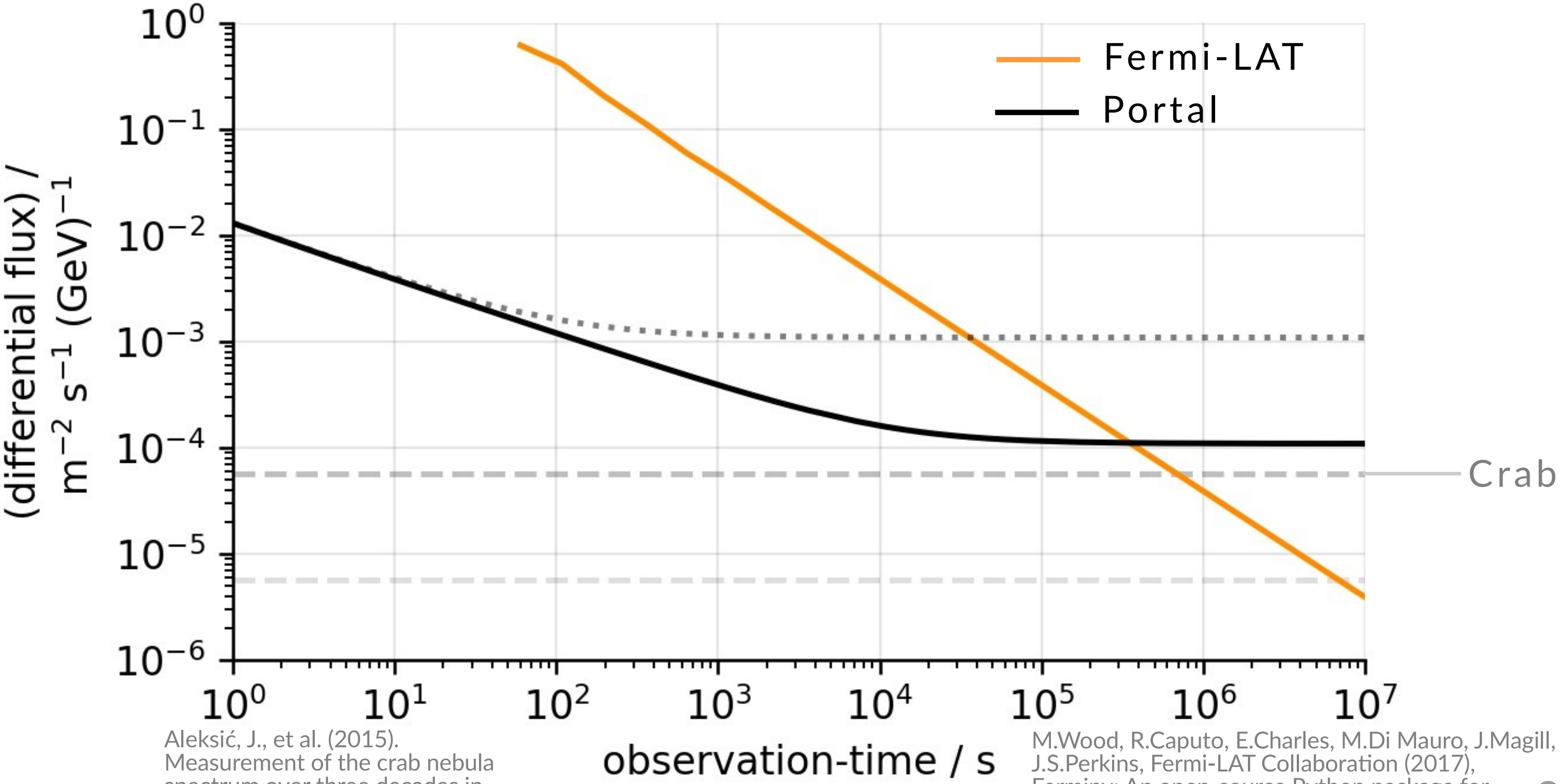

Aleksić, J., et al. (2015). Measurement of the crab nebula spectrum over three decades in energy with the magic telescopes. High Energy Astrophysics, 5:30–38.

M.Wood, R.Caputo, E.Charles, M.Di Mauro, J.Magill, J.S.Perkins, Fermi-LAT Collaboration (2017), Fermipy: An open-source Python package for analysis of Fermi-LAT Data, Proc. 35th ICRC, PoS(ICRC2017)824, IRF: P8R2_SOURCE_V6

Gamma-Ray-Timing-Explorer

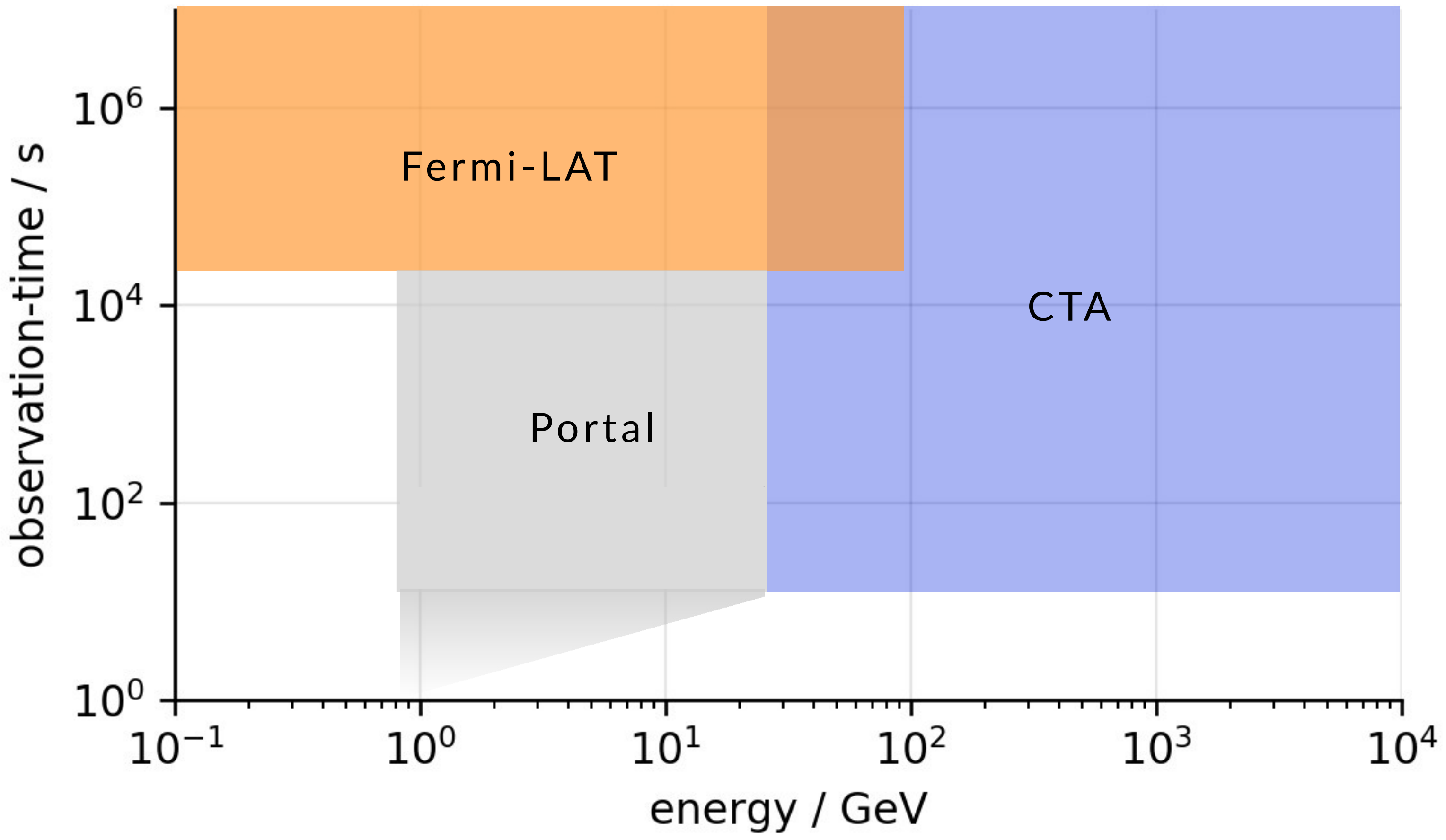

Acknowledgment

MAX-PLANCK-INSTITUT
FÜR KERNPHYSIK

Werner Hofmann,
Jim Hinton

ETH zürich

Adrian Biland, Felicitas Pauss,
Max L. Ahnen, Dominik Neise,
Spyridon Daglas, Axel A. Engels,
Eleni Chatzi, Adrian Egger

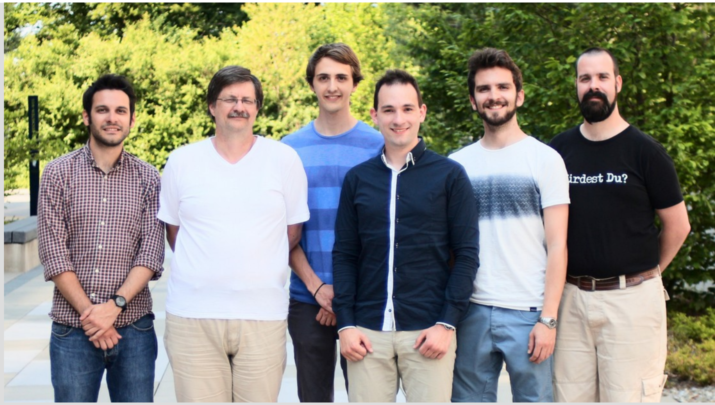

Questions

SALE! ONLY 224,000,000

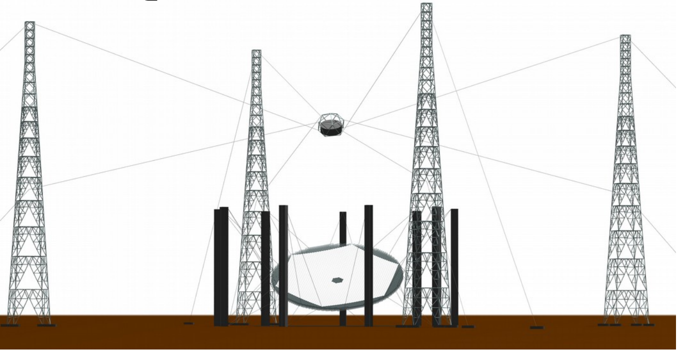

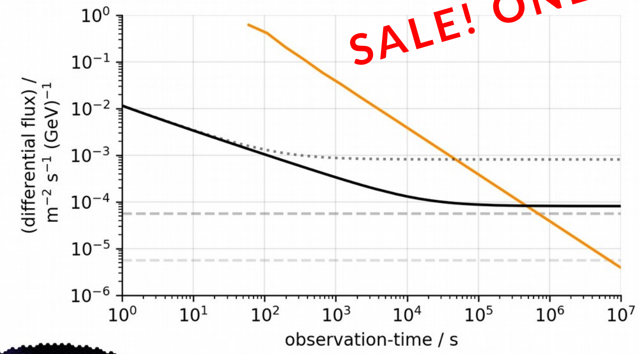

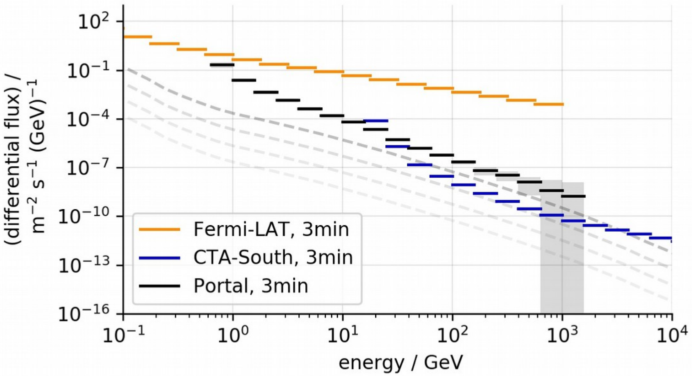

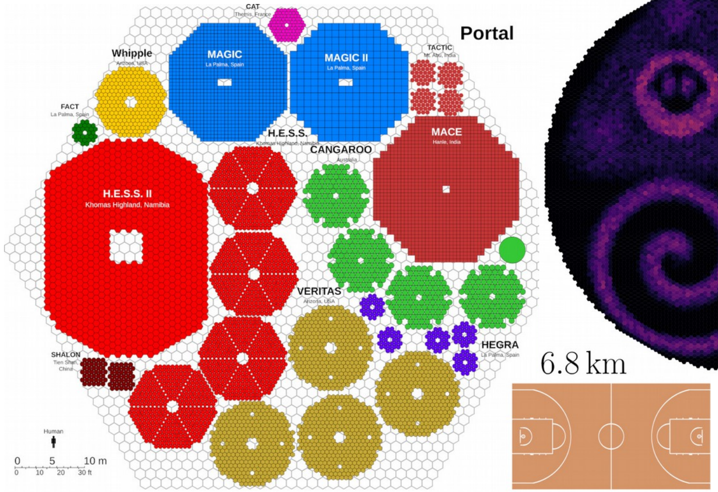

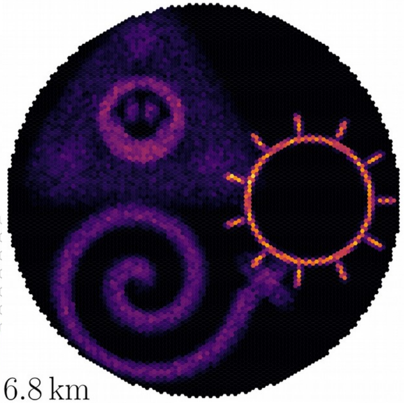

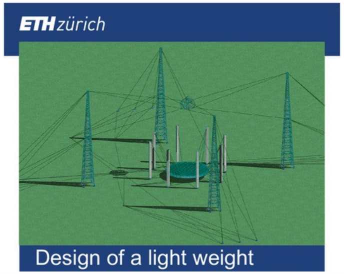

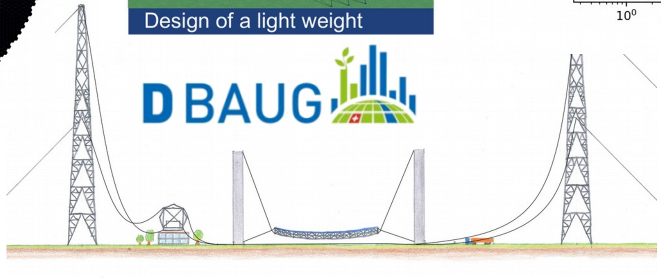

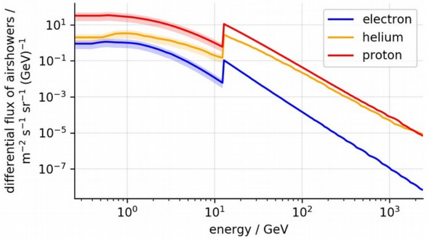

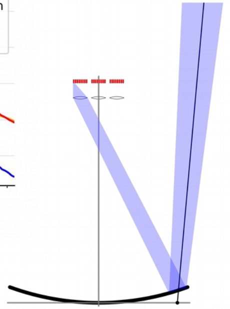

arXiv:1904.13368
(astro-ph)

https://github.com/cherenkov-plenoscope

Size

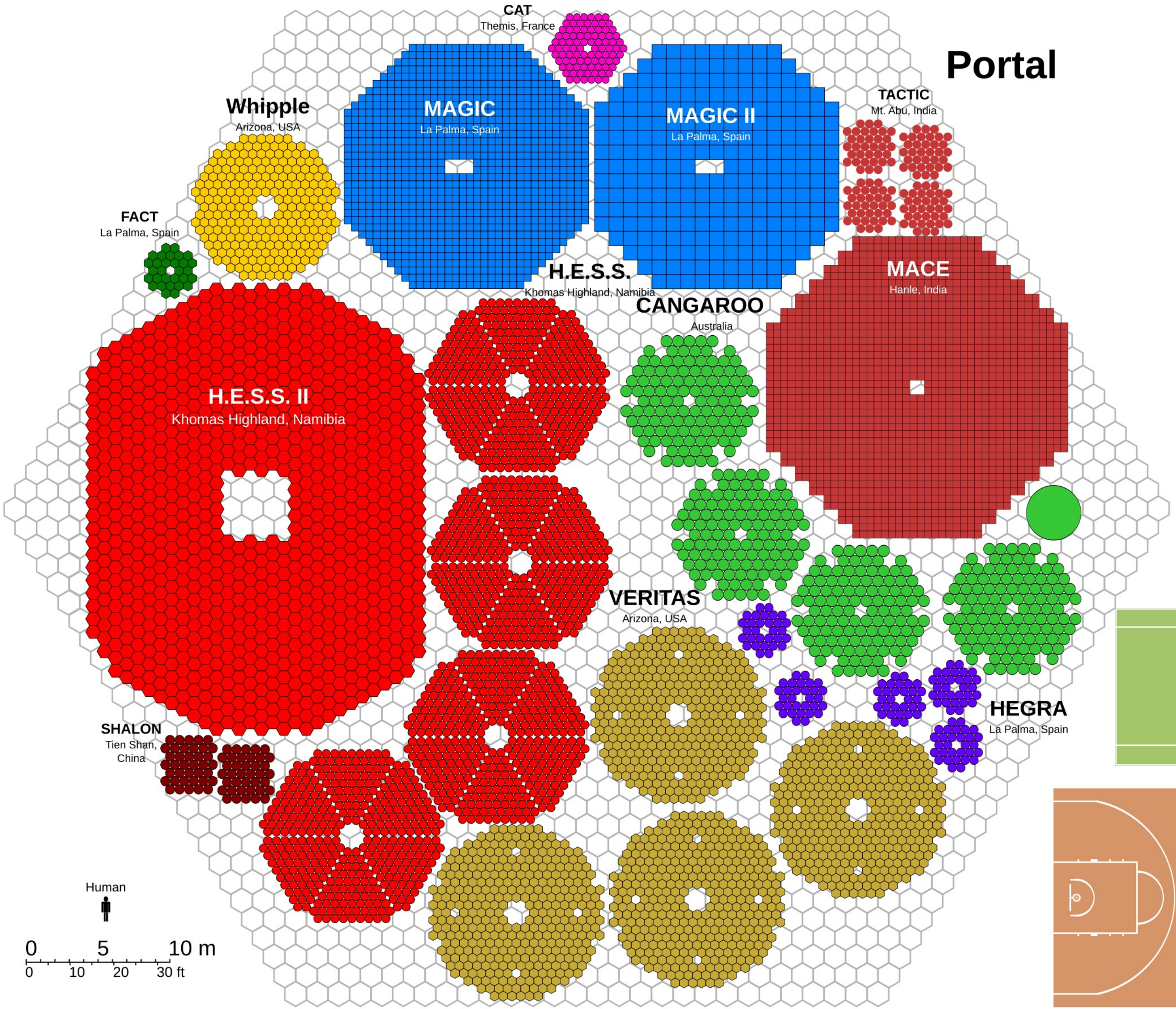
CAT
Themis, France
MAGIC
La Palma, Spain
MAGIC II
La Palma, Spain
Whipple
Arizona, USA
TACTIC
Mt. Abu, India
FACT
La Palma, Spain
H.E.S.S.
Khomas Highland, Namibia
CANGAROO
Australia
MACE
Hanle, India
H.E.S.S. II
Khomas Highland, Namibia
VERITAS
Arizona, USA
HEGRA
La Palma, Spain
SHALON
Tien Shan, China
Human
0
5
10 m
0
10
20
30 ft

Portal

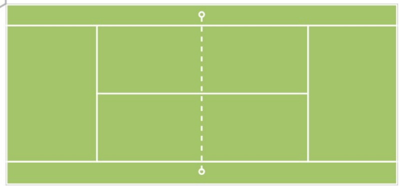

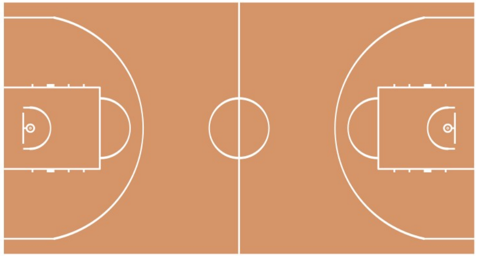

Performance, Sensitivity vs. Energy at 3min

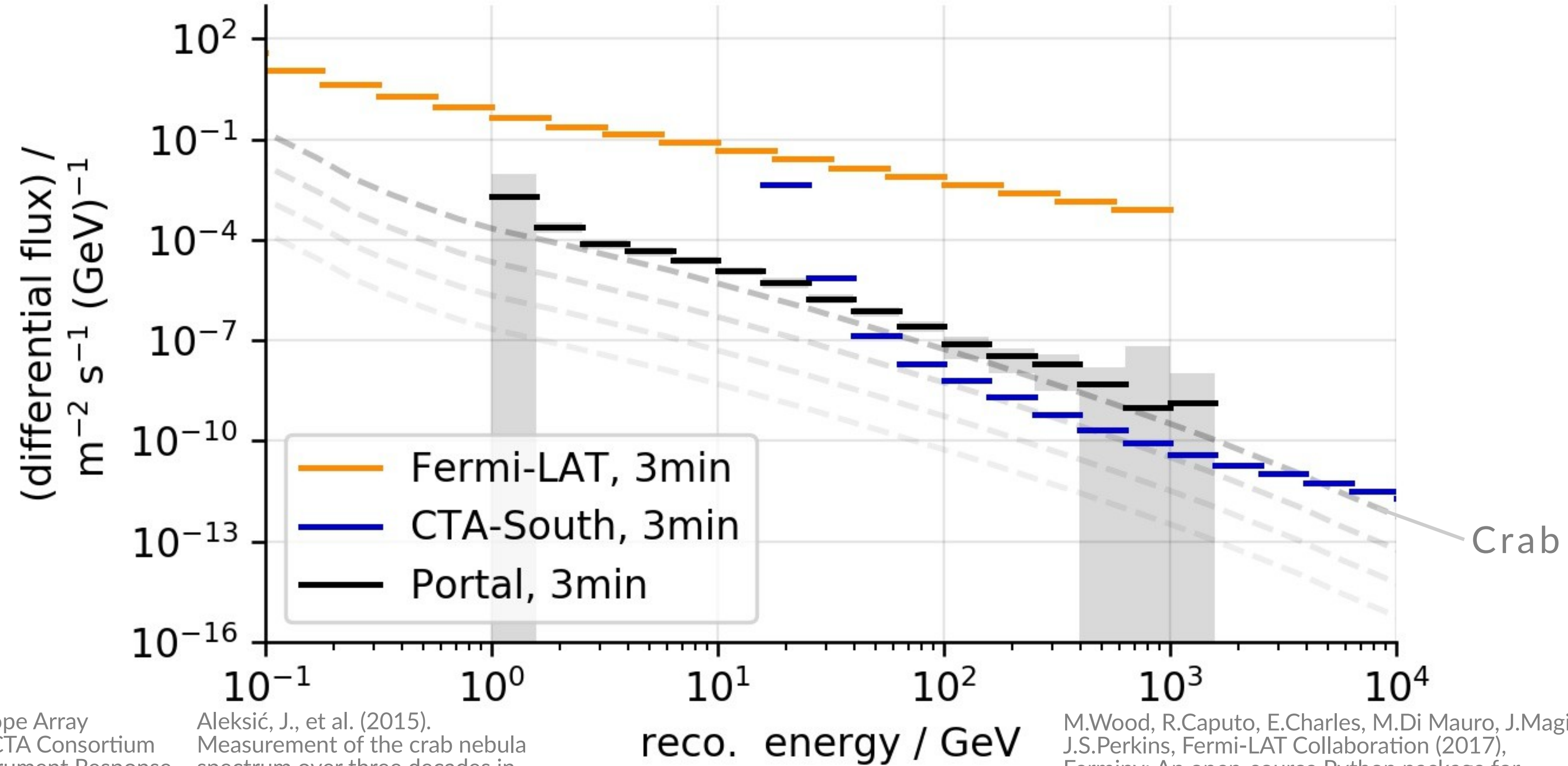

Cherenkov Telescope Array Observatory and CTA Consortium (2021). CTAO Instrument Response Functions - prod5 version v0.1, doi:10.5281/zenodo.5499840

Aleksić, J., et al. (2015). Measurement of the crab nebula spectrum over three decades in energy with the magic telescopes. High Energy Astrophysics, 5:30–38.

M.Wood, R.Caputo, E.Charles, M.Di Mauro, J.Magill, J.S.Perkins, Fermi-LAT Collaboration (2017), Fermipy: An open-source Python package for analysis of Fermi-LAT Data, Proc. 35th ICRC, PoS(ICRC2017)824, IRF: P8R2_SOURCE_V6

Field-of-view

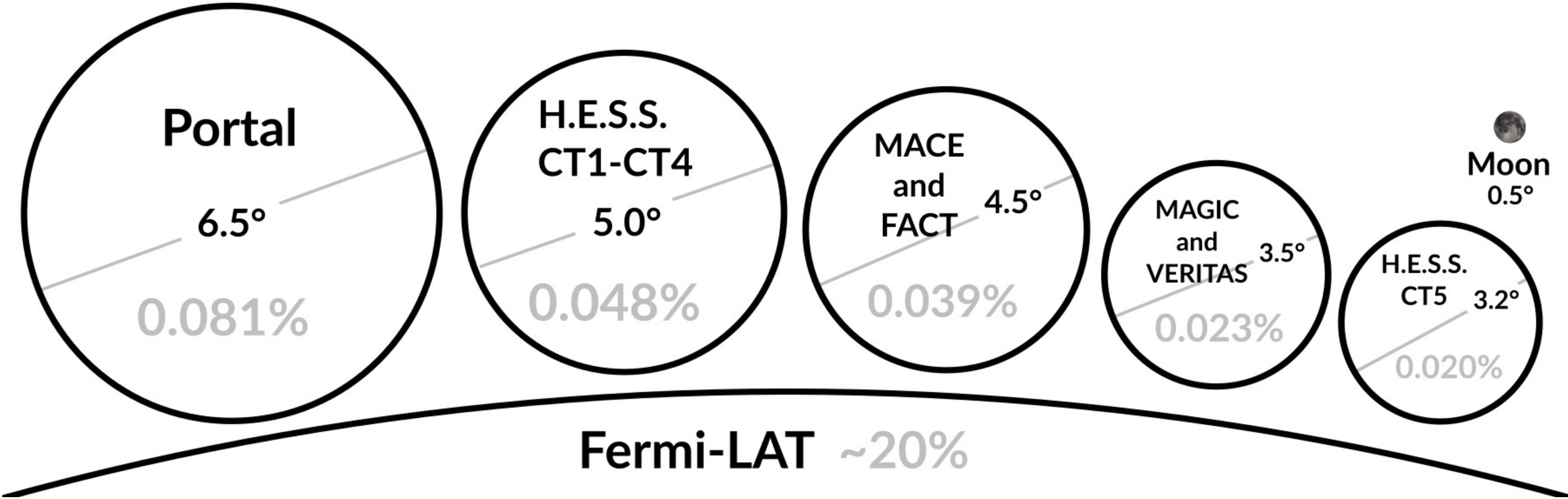

Costs Optics and Electronics

component	unit-costs	demand	cost / 10^6 EUR
Photo-sensors	5×10^5 EUR m^{-2}	115 m^2	57.5
Read-out-electronics	80 EUR $channel^{-1}$	515,023 channels	41.2
Lenses	100 EUR $lens^{-1}$	8,433 lenses	0.9
Mirror-facets	3×10^3 EUR m^{-2}	4174 m^2	12.5
Mirror-facet-actuators	10^3 EUR $facet^{-1}$	2,087 facets	2.1
			114.2

Costs Total

	fraction / %	cost / 10^6 EUR
Optics and electronics	51	114.2
Cable-robot-mount [1]	16	35.8
Central control-system [2]	5	11.2
Project-engineering [2]	5	11.2
Project-management [2]	13	29.1
Site-infrastructure [2]	10	22.4
	100	**223.9**

(1) Civil engineer Spyridon Daglas (2) Adopted from reports by the Eurpean-Southern-Observatory (ESO)